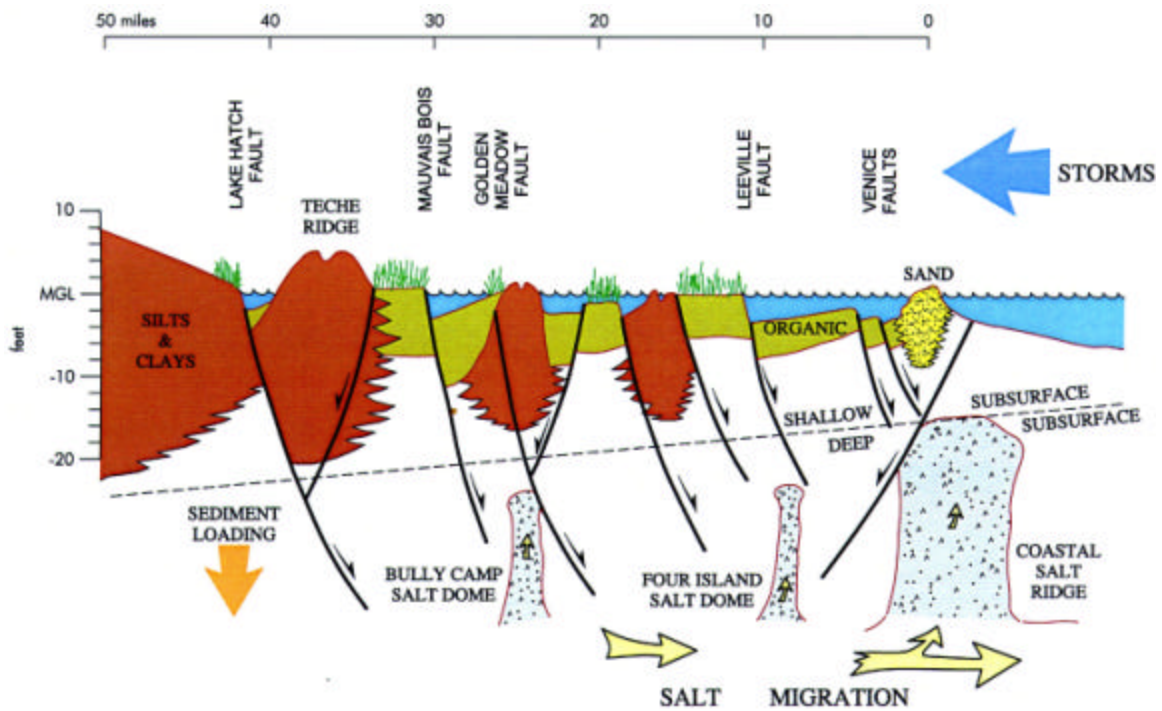


ACTIVE GEOLOGICAL FAULTS AND LAND CHANGE IN SOUTHEASTERN LOUISIANA

A Study of the Contribution of Faulting
to Relative Subsidence Rates, Land Loss, and Resulting Effects
on Flood Control, Navigation, Hurricane Protection
and Coastal Restoration Projects



Contract No. DACW 29-00-C-0034



July 2003

Cover: This diagrammatic north-south section, extending from Thibodaux, Louisiana to the Gulf of Mexico, depicts the subsurface geological processes which cause land submergence in Southeastern Louisiana.

DISCLAIMER

Some of the interpretations and results presented in this report may be controversial. This is to be expected, as the findings challenge a number of conventional concepts and basic assumptions. We recognize the far-reaching implications of these findings, and do not present them lightly. The authors have interpreted the data to the best of their ability, but are not infallible. It is assumed that the research community will rise to the challenge of testing new ideas that depart from convention.

The maps and graphics in this report are not intended for zoning, property and insurance evaluations, engineering design, or similar purposes, but rather are intended to display scientific information. Site-specific geotechnical evaluations and risk assessments are recommended for all projects and land use evaluations within the study area

**ACTIVE GEOLOGICAL FAULTS
AND LAND CHANGE
IN SOUTHEASTERN LOUISIANA**

**A Study of the Contribution of Faulting
to Relative Subsidence Rates, Land Loss, and Resulting Effects
on Flood Control, Navigation, Hurricane Protection
and Coastal Restoration Projects**

Prepared by

Sherwood M. Gagliano, Ph.D.

E. Burton Kemp, III, M.S.

Karen M. Wicker, Ph.D.

and

Kathleen S. Wiltenmuth, M.S., M.S.

Coastal Environments, Inc.

1260 Main Street

Baton Rouge, LA 70802

Prepared for

U. S. Army Corps of Engineers, New Orleans District

7400 Leake Avenue

New Orleans, LA 70118

Contract No. DACW 29-00-C-0034

July 2003

TABLE OF CONTENTS

LIST OF FIGURES	vii
LIST OF TABLES	xix
ACKNOWLEDGMENTS	xxi
SUMMARY	xxiii
INTRODUCTION	1
FAULTS AND FAULT EVENTS	6
PREVIOUS RESEARCH	11
SUBSURFACE GEOLOGY	12
QUATERNARY DEPOSITS AND STRUCTURES	17
Displacement of the Pleistocene	17
Compaction of Holocene Sediments.....	23
SURFACE EXPRESSIONS OF FAULTS	24
Description, Evidence, and Mapping of Surface Faults	28
Stream Alignments and Water Body Shapes	28
Case Studies of Surface Faults.....	43
SPECIAL STUDY AREAS	45
Pontchartrain Basin	45
West Plaquemines Delta Plain (Empire and Bastian Bay Faults).....	54
Mudlumps	61
Delta Front Gravity Slumping	68
Continental Margin Gravity Slumping	68
Middle Barataria Basin	68
Terrebonne Delta Plain	73
The Lake Boudreaux Fault (ET-1).....	77
The Montegut Fault (ET-4).....	77
Isle de St. Jean Charles	84
Fault severance of Bayou Terrebonne and opening of Lake Barré.....	84
Correlation of apparent faults and land loss	87
TRIGGERING MECHANISMS	87
Natural System Succession.....	87
Stage 1. Delta Building: Prehistoric Times (Figure 59)	91

Stage 2. Poised: 1800 A.D. – 1850 A.D. (Figure 60)	93
Stage 3. Early Deterioration: 1850 A.D. – 1900 A.D. (Figure 61).....	94
Stage 4. Intermediate Deterioration: 1900 A.D. – 1950 A.D. (Figure 62).....	96
Stage 5. Advanced Deterioration: 1950 A.D. – 2000 A.D. (Figure 63).....	98
Stage 6. Future: 2000 A.D. – 2050 A.D. (Figure 64).....	99
Summary of Development Sequence	101
Earthquakes and Seiches	103
Earthquakes	103
Vacherie Fault Event (WM – 1).....	106
Other Reported Earthquakes	108
Seiches and Tsunamis	109
Salt Water and Gas Migration along Fault Planes	110
Fluid Withdrawal	112
VERTICAL AND LATERAL MOVEMENT.....	113
Relative Sea Level Rise	113
Tide Gauge Data	114
Sequential Land Leveling	120
NASA-Michoud Benchmarks	120
Mississippi River Line - Chalmette to Venice	123
Bayou Lafourche Line	126
Bayou Petite Caillou Line	129
Comparison of Mississippi River, Bayou Lafourche and Bayou Petite Caillou Lines.....	131
Vertical Movement and Rates of Subsidence and Relative Sea Level Rise for Epoch 2	131
Summary.....	131
Other Processes Contributing to Land Loss and Coastal Erosion.....	138
Reduction of Overbank Flow and Sediment Supply.....	138
Reduction of Organic Matter Build-up and Deterioration of Floating Marshes	139
EFFECTS OF FAULTS	141
Effects on Wetlands	141
Salt Marsh Dieback (Brown Marsh) and Stages of Fault Development	143
Effects on Barrier Islands.....	143
Effects on Ridges and Fastlands	146

Analysis OF Zones.....149
 Land Loss by Analysis Zones149
 Time-Rate Correlations.....149
 Effects of Faults on Coastal Projects152
LAND LOSS ON LARGE FAULT BOUND BLOCKS.....155
FINDINGS AND RECOMMENDATIONS.....161
REFERENCES CITED.....163
APPENDIX A. PREVIOUS RESEARCH175

LIST OF FIGURES

Figure 1. Map of coastal Louisiana showing location of the Deltaic Plain study area and major landforms (after Gagliano and van Beek 1994).	2
Figure 2. Land loss in the Deltaic Plain. Map shows land loss for the period 1956-1990. Graphs show rate of loss in square miles per year and cumulative loss in square miles (Gagliano 1998, adapted from Barras et al. 1994).	3
Figure 3. Factors contributing to relative sea level rise and subsidence in the Louisiana coastal region (after Penland et al. 1988, 1989; adapted from Kolb and Van Lopik 1958:95).	5
Figure 4. Relationship between faults and areas of high land loss in Southeastern Louisiana (after Gagliano 1999).	7
Figure 5. Major structural features of Southeastern Louisiana and adjacent areas (after Saucier 1994). The study area is indicated by the inset box.	8
Figure 6. Southeastern Louisiana structural framework, with major faults and salt domes identified.	9
Figure 7. Cenozoic structure provinces of the Northern Gulf of Mexico and major fault zones of Southeastern Louisiana (structural provinces after Peel et al. 1995; base map with permission of Port Publishing Co., Houston, TX; fault zones reported). Color patterns correspond to those in Figure 6. Note apparent massive slumping of continental slope in the Central Province.	14
Figure 8. North-South cross-section through the Gulf Coast Salt Dome Basin showing stratigraphy and geological structures (after Adams 1997). Extensional section with progressively younger listric faults from north to south. Section also shows inferred basement-salt-decollement surface relationships. Subsurface faults shown in Figure 6 are identified on the section.	15
Figure 9. Segment of north-south megaregional cross-section through Southeastern Louisiana showing stratification and subsurface structure (modified from McBride 1998 and Stover et al. 2001). Location of section shown in Figure 7 as line B.	16

Figure 10. Cross-section of the Raceland Salt Dome, which lies within the Lake Salvador Fault Zone (after P.J. Pickford et al. n.d.). Note the counter-basinward fault, the crestal graben with nested faults and the top of the high pressure zone.18

Figure 11. Relationships between the Lake Washington Salt Dome and regional growth faults (all after P.J. Pickford et al. n.d.). A. Cross-section of dome. The dome is 8.5 mi (13.7 km) in diameter and the top of the salt plug lies 2000 ft (610 m) below the surface. B. Stratigraphic slice showing Empire and Bastian Bay regional growth faults. C. Contours on the plane of the Golden Meadow – Empire Fault at 5000 to 15,000 ft (1524 to 4572 m). Note that the fault plane is coincident with the salt face for several miles.19

Figure 12. Contour map of the bottom of the Pleistocene showing faults and salt domes that were active during and after deposition of the contoured horizon (modified from Sabaté 1968). This work shows that segments of the Golden Meadow, Theriot, Leeville and Venice Faults, as well as nine salt domes, were active during and/or since the beginning of the Pleistocene Period.....20

Figure 13. Depth to the top of the Pleistocene (data from L.D. Britsch 2001). Surface faults exhibiting displacement of the top of the Pleistocene and known subsurface faults are also shown.22

Figure 14. Holocene delta complexes (modified from Frazier 1967 and Weinstein and Gagliano 1985).....25

Figure 15. Sediment pods deposited in subdeltas are often found on the basinward side of growth faults. It is this coupling of deposition and fault movement that results in expansion of the thickness of sedimentary deposits on the downdropped blocks of growth faults (after Curtis and Picou 1978).26

Figure 16. Surface expression of faults.27

Figure 17. Map showing the locations of surface faults, case study areas and special study areas. (See Table 1)29

Figure 18. Common types of faults found in the study area showing linkage between surface features and underlying fault planes. Based on surface and subsurface data.....33

Figure 19. Map showing the relationship between suspected surface and subsurface faults. (See Table 1)	34
Figure 20. Relationship between faults and river courses in Southeastern Louisiana. Base map shows conditions circa 1859-1879 (Excerpt from Mississippi River Commission 1913).	44
Figure 21. Map showing reconstructed landforms and conditions in the Pontchartrain Basin circa 1750 A.D. with known and probable faults (adapted from Saucier 1963).	47
Figure 22. Mississippi River alignments and probable faults that exhibit surface expression in the Pontchartrain Basin. Image from 2000 Coastal Zone TM satellite.	49
Figure 23. LIDAR image showing intersection of the Baton Rouge and West Maurepas Fault Zones. LIDAR data is in DEM format derived from 1999 measurements in USGS format. Data collected for the Louisiana Federal Emergency Management Agency (FEMA) Project-Phase 1.	50
Figure 24. Topographic profiles across Baton Rouge Fault Zone north and northwest of Lake Maurepas. Profiles from LIDAR data. Location shows in Figure 23 LIDAR data is on DEM format from 1999 measurements in USGS format. Data collected for Louisiana FEMA Project-Phase1	51
Figure 25. Baton Rouge Fault system. A. Fault traces from the Mississippi River to Lake Borgne. Displacements have been measured on bridges shown. Reported earthquake occurrences are also shown. B. Drawing showing fault offset in re-built section of Norfolk-Southern Railroad Bridge in eastern Lake Pontchartrain. C. Displacement of beds by south dipping normal fault as recorded on USGS high resolution seismic line from eastern Lake Pontchartrain. Abrupt terminations of shallow reflectors indicate that the fault is within 10 ft (3m) of the lake bottom (after Lopez et al. 1997).	53
Figure 26. Topographic map showing landforms and conditions in the West Plaquemines Deltaic Plain circa 1941-1948. Geomorphic features added. Traces of the Empire (MD-1) and Bastain Bay (MD-2) Faults, which appeared on the surface in the 1970s, are also shown.	55

Figure 27. Aerial image showing West Plaquemines Deltaic Plain in 1998. The Empire (MD-1) and Bastain Bay (MD-2) Faults became active during the 1974 through 1978 period, resulting in massive land submergence. Compare with Figure 26.	56
Figure 28. Aerial view looking north across the Empire (MD-1) and Bastain Bay (MD-2) Faults. Photograph by S.M. Gagliano September 2000.....	57
Figure 29. Section across the Empire Fault showing displacement of near-surface beds. Section based on McCauley auger borings.....	58
Figure 30. Areas exhibiting various degrees of submergence on the down-dropped block of the Empire Fault.	59
Figure 31. Section across the down-dropped block of the Empire Fault showing submergence and tilting. The surface of the down-dropped surface toward the fault scarp as a result of rotation during fault movement. Location of the section is shown in Figure 30.....	60
Figure 32. Photograph of Mr. Pete Hebert’s camp, 2001. The camp was originally built on the bank of Bayou Ferrand in the late 1960s. The camp is located one mile (1.6 km) south of the Bastain Bay Fault Scarp (location shown in Figure 23). The land that the camp was built on is completely submerged and the elevation of the building has been reduced 4 to 4.5 ft (1.2 to 1.4 m) largely as a result of fault movement in the 1970s.	60
Figure 33. Map showing suspected surface and subsurface faults and land loss in the West Plaquemines Delta study area and vicinity.	62
Figure 34. Photographs showing South Pass Mudlumps and drilling operation. A. Aerial view looking north across mudlump island and sands pit with mudlumps. B. Five-foot fault scarp on South Pass Mudlump. C. Core drilling. D. Mud/gas vents, with fault scarp in background. E. Tilted beds with fault trace.	63

Figure 35. Diagrammatic cross-section showing mudlumps, faults and slump features at South Pass and vicinity (after Gagliano and van Beek 1973).....	64
Figure 36. Stratigraphic section and cross-section showing folds and faults, South Pass mudlumps (after Morgan et al. 1968).....	65
Figure 37. Diagrams showing progressive development of folds and faults, South Pass mudlumps (after Morgan et al. 1968).....	66
Figure 38. Mudlump islands at South Pass (after Morgan et al. 1968).....	67
Figure 39. Progressive extrusion of drilling casing from bore hole drilled in South Pass Mudlumps (after Morgan 1961). Figure 34-C shows the coring of this hole in progress and Figure 36 shows BH-B in reference to the stratigraphy and structure of the mudlump fold.....	69
Figure 40. Map and schematic drawing showing fault slumps and other features in the vicinity of the active outlets of the Mississippi River (after Coleman 1976).	70
Figure 41. The weight of sedimentary deposits accumulating at the river mouth depocenters in the coastal area causes salt and shale beds to slide laterally into the deep gulf basin. The salt and shale and associated deposits bulge up along the continental margin and gulf floor. Growth faults in the coastal and shelf areas adjust vertically and laterally to the massive slumping (modified from Winker 1982).....	71
Figure 42. Topographic map showing landforms and conditions in the Middle Barataria Basin, circa 1953-1962. Known and suspect surface faults are shown. Most faults are based on geomorphological evidence.	72
Figure 43. Aerial image of the Middle Barataria Basin in 1998 with locations of suspect surface faults shown.	74
Figure 44. Sequential changes in Bayou Perot and Bayou Rigolets, two ballooned streams in the Middle Barataria Basin, during the period from 1890 to 1998.	75
Figure 45. Satellite image (2000, 1993) showing suspected surface and known subsurface faults in the Terrebonne Deltaic Plain study area.	76
Figure 46. Natural levees, surface expression of suspected faults and breakup areas in the Terrebonne Deltaic Plain study area. Dates signify appearance of fault scarps, break-up areas and ridge severances.	78

Figure 47. Changes in surface expression of the proposed Lake Boudreaux Fault are evident when aerial photographs taken in 1953 (left) and 1998 (right) are compared. First indications of the fault appeared on 1971 aerial photographs and by 1979 a large lake and a zone of altered and deteriorated wetlands had developed east of a well-defined fault scarp.79

Figure 48. Aerial view of the proposed Lake Boudreaux Fault (Fault ET-1) looking southeast from Bayou Grand Caillou. This is a segment of the Boudreaux Fault Zone. The lake in the background resulted from fault displacement, which was first recorded on aerial photographs taken in 1971. Prior to the fault events the marsh was fresh. In 2001, the marsh on the near side of the fault was fresh, while that on the far side was brackish. Photograph by S.M. Gagliano, October 17, 2001.....80

Figure 49. Aerial view of the proposed Lake Boudreaux Fault, looking south along the fault scarp. Note the dead cypress trees in the vicinity of the scarp. Photograph by S.M. Gagliano, October 17, 2001.....80

Figure 50. Section based on borings taken across proposed Lake Boudreaux Fault (ET-1) showing surface elevation, water depths and near-surface stratification. The section shows 3.3 ft (1.0 m) of change in elevation from the marsh surface to the pond bottom and a comparable amount of displacement of the top of the bed identified as “1.” The section is based on data from vibracore and McCauley borings.....81

Figure 51. The proposed Montegut Fault scarp looking north across broken marsh on the down-dropped block of the fault. The town of Montegut, Louisiana can be seen in the background. Photograph by S.M. Gagliano, October 17, 2001.....82

Figure 52. Aerial view of the proposed Montegut Fault. The view is looking north across a large pond and broken marsh on the down-dropped block of the fault. Note the dead cypress trees on the up-thrown block and the flood protection/drainage levee along the back-slope of the Bayou Terrebonne natural levee ridge. The Montegut community is located on the natural levee of Bayou Terrebonne. Photograph by S.M. Gagliano, October 17, 2001.....82

Figure 53. Near-surface geological section across proposed Montegut Fault based on McCauley auger borings.....	83
Figure 54. Looking north along Isle St. Jean Charles. The severed natural levee ridge along the bayou can be seen in the background. Part of the ridge has been submerged as a result of fault movement. Photograph by S.M. Gagliano, October 17, 2001.....	85
Figure 55. Extensive areas of submerged marsh in the vicinity of Isle St. Jean Charles. Photograph by S.M. Gagliano, October 17, 2001.....	85
Figure 56. Comparison of historic maps showing the severance of the natural levees of Bayou Terrebonne and the opening of Lake Barré between 1859-1879 and 1901. The locations of suspect faults have been added to the maps.....	86
Figure 57. Map showing relationship between suspected surface and known subsurface faults, and land loss in the Terrebonne Deltaic Plain study area.....	88
Figure 58. Major features of the Terrebonne Deltaic Plain.....	90
Figure 59. Overlapping lobes of the Teche and Lafourche deltas, Stage 1: prehistoric delta building.	92
Figure 60. Conditions in the Terrebonne Deltaic Plain during the poised stage (1800-1850 A.D.) of the Lafourche Delta cycle. Maximum development of barrier islands and upper deltaic plain fresh swamps and marshes.	94
Figure 61. Conditions in the Terrebonne Deltaic Plain during early deterioration (1850-1900 A.D.) of the Lafourche Delta cycle.	95
Figure 62. Conditions in the Terrebonne Deltaic Plain during the intermediate deterioration stage (1900-1950 A.D.) of the Lafourche Delta cycle.	97
Figure 63. Conditions in the Terrebonne Deltaic Plain during the intermediate deterioration stage (1950-2000 A.D.) of the Lafourche Delta cycle.	99

Figure 64. Projected future conditions in the Terrebonne Deltaic Plain during the transitional stage (2000-2050 A.D.).	100
Figure 65. Map showing the relationship between faults and ridge alignments and relict distributary trends in the Terrebonne Deltaic Plain.	102
Figure 66. Diagrammatic north-south cross-section through the Terrebonne Deltaic Plain from Thibodaux, Louisiana to the Gulf of Mexico. During the active delta building and poised stages of the delta cycle, sediment deposition rates in the alluvial and interdistributary environments are high enough to build and maintain a land surface that is largely above mean gulf level. Location of section shown in Figure 65.	104
Figure 67. Cross-section through the Terrebonne Deltaic Plain after modification by fault and storm events. During the deterioration stages of the cycle fault events reduce the land surface and facilitate invasion of the land by the gulf. Reduction of land elevations in reference to the gulf level is largely due to deep-seated salt and fault movement.	104
Figure 68. Southeastern Louisiana fault zones and earthquakes.	105
Figure 69. Mud vent cone in West Bay area near Venice, Louisiana. James P. Morgan reported that this vent had been active for a least ten years (Morgan per. comm. circa 1960).	111
Figure 70. Water level time series from National Ocean Survey, Grand Isle, LA. Tide gauge between 1947 and 1978. A change in the rate of rise between the period 1947-1962 (Epoch 1), and the period 1962-1978 (Epoch 2) had been found on many of the records from gauges in south Louisiana (after Penland et al. 1989:24).	116
Figure 71. Relative sea level rise based on readings from U.S. Army Corps of Engineers tide gauge stations on Louisiana. Note change in rate of rise between 1947-1961 (Epoch 1) and 1962-1978 (Epoch 2) (after Penland et al. 1989).	117
Figure 72. Elevation and relative sea level changes in the northern Gulf of Mexico region. (Elevation changes after Holdahl and Morrison 1974; RSL rise rates after Penland et al. 1988).	118

Figure 73. Present and future trends of relative sea level rise based on gauge records from coastal Louisiana (after Ramsey and Moslow 1987).	119
Figure 74. Isopleth map of RSL rise rates in coastal Louisiana based on 1962-1982 (Epoch 2) tide gauge data (adapted from Ramsey and Moslow 1987). Locations of sequential land leveling lines are also shown.	120
Figure 75. Locations of re-leveled benchmark data in reference to structural framework.	121
Figure 76. Changes in elevation along Mississippi River natural levees between IHNC Lock and Venice, Louisiana. The graphs show benchmark movement based on four surveys made between 1938 and 1971 (Modified from van Beek et al. 1986, original data from NGS). The negative spikes are correlated with faults as delineated in this study.	124
Figure 77. Changes in rates of vertical movement of re-leveled benchmarks along the Mississippi River natural levees between the IHNC Lock and Venice, Louisiana. The graphs show rates of movement based on four surveys. The scale on the right is adjusted for eustatic sea level rise (0.0075 ft/yr [0.019 cm/yr]). (Data from NGS).	125
Figure 78. Average rate of vertical change (subsidence) and RSL rise for re-leveled benchmarks along Mississippi River natural levees for the 33-year period between 1938 and 1971.....	127
Figure 79. Profiles showing amounts and rates of vertical displacement based on re-leveled benchmarks on a line along the natural levees of Bayou Lafourche from Raceland to the vicinity of Port Fourchon, Louisiana. Data derived from profile by Morton et al. (2002). Original data from NGS. Fault correlations from this study.	128
Figure 80. Profiles showing amount and rates of vertical displacement based on re-leveled benchmarks on a line along the natural levees of Bayou Petite Caillou from Presquille to Cocodrie, Louisiana. Data derived from profile by Morton et al. (2002). Original data from NGS. Fault correlations from this study.	130
Figure 81. Comparison of vertical displacement during Epoch 2 along Mississippi River, Bayou Lafourche and Bayou Petite Caillou lines (for sources Figures 76, 79, and 80).	132

Figure 82. Comparison of rates of subsidence and relative sea level rise during Epoch 2 along the Mississippi River, Bayou Lafourche, and Bayou Petite Caillou lines. For sources see Figures 76, 79 and 80.	133
Figure 83. Rates of relative sea level rise (in ft/yr) from benchmark and tide gauge data for Epoch 2, 1962-1982.	134
Figure 84. Vertical change in elevation from (in ft) benchmark and tide gauge data for Epoch 2, 1692-1982.	135
Figure 85. Comparison of RSL rise rates and wetland sedimentation rates for the Terrebonne Deltaic Plain area. Only in the Atchafalaya River Delta was land building up at rates higher than RSL rise. Wetland sedimentation rates are from DuLaune et al. (1985), and RSL rise rates are based on records from USACE and NGS tide gauges (adapted from Penland et al. 1988).	140
Figure 86. Idealized relationships between sedimentary units and vegetation in fresh marsh. (A - open water, B - ridges and rim and C - interior marsh.	142
Figure 87. Diagrammatic section showing effects of fault movement on root mat and near-surface deposits.	142
Figure 88. Aerial view of proposed Lake Enfermer Fault (BA-15), looking north showing brown marsh on the down-dropped block. The distinctive fault scarp separates unbroken <i>Spartina alterniflora</i> marsh from partially submerged and broken <i>Spartina aeterniflora</i> . marsh (brown marsh). Photograph by S.M. Gagliano March 2001.	144
Figure 89. Stages of fault event in a saline marsh.	145
Figure 90. Effects of subsidence on natural levees and wetlands (modified from H.N. Fisk 1960).	147
Figure 91. Effects of subsidence on ridgeland and fastlands. A. Distributary natural levee corridor, natural conditions. B. Subsided distributary natural levee corridor with forced drainage and storm protection levees (after Gagliano 1990).	148
Figure 92. Fault zones in Southeastern Louisiana.	150
Figure 93. Fault zones and land loss.	151

Figure 94. Comparison of rates of change of process indicators for: A. Total area of barrier islands; B. Area of deltaic plain; and, C. Louisiana oil production. The curves suggest possible relationships between fault events and loss of area of both the barrier islands and the deltaic plain, but also show that oil and gas production peaked during Epoch 2, when land loss and subsidence rates accelerated (barrier island measurements adapted from Williams et al. 1992, deltaic plain measurements adapted from Barras et al. 1994).153

Figure 95. Map showing coastal restoration projects in reference to fault zones.157

Figure 96. Location of coastal restoration projects and HWY 57 alignments in reference to known and suspected faults in the Terrebonne Deltaic Plain area.158

Figure 97. Shore protection feature built across a suspected active fault. Aerial view of proposed Bayou Perot Fault (BA-5) looking north. On the north of the proposed fault is unbroken, brackish, floating marsh. On the down-dropped block the marsh is stressed and broken. A shore protection feature consisting of rip rap was under construction at the time the photograph was taken. Photograph by S.M. Gagliano March 2001.....159

Figure 98. Land loss on mega-fault blocks: 1930-1995160

LIST OF TABLES

Table 1.	Surface Expression of Faults in Southeastern Louisiana (See Figure 17 and 19).....	30
Table 2.	Results of Chorological Analysis of Suspected Surface Fault Signatures.....	35
Table 3.	Stream Segments and Water Bodies Which Appear to be Fault Influenced.	42
Table 4.	Nine Case Studies: Summary of Results.	46
Table 5.	Tide Gauge Data from Southeastern Louisiana.	115
Table 6.	Rates of Relative Sea Level Rise for Three Key Deltaic Plain Tide Gauge Stations and the Pensacola, Florida Reference Station.	136
Table 7.	Correlation of Tide Gauge Stations with Fault Zones. The RSL Rise Rates for Epoch 2 Are Also Given for Each Station.	137
Table 8.	Correlation of Re-Leveled Benchmarks that Exhibit Changes in Rates of Relative Sea Level Rise Between Epoch 1 and 2 with Fault Zones and Segments. Rates of Relative Sea Level Rise for Epoch 2 Are Also Listed.....	138
Table 9.	Area and Rate of Land Loss (sq mi/year) by Fault Zones: 1930-1956/58, 1956/58-1974, 1974-1983 and 1983- 1990 (after Britsch 2001).	152
Table 10.	Location of CWPPRA Projects in Relation to Fault Zones.....	154
Table 11.	Location of State Projects in Relation to Fault Zones.	156

ACKNOWLEDGMENTS

We wish to thank the many individuals who contributed to this study.

At the New Orleans District Corps of Engineers (NODCE), Louis Del Britsch was not only the project manager, but also an active participant in the research. Along with Doug Dillan, he took the vibracores, selected the samples for, and interpreted the results of radiometric dating. He participated in the correlation of borings, provided data on depth to the top of the Pleistocene and in general, provided guidance to the project. Gerard Satterlee, Chief of the Engineering Division, NODCE, provided invaluable guidance from a geotechnical engineering standpoint and general support of the work. Walter Baummy, succeeded Mr. Satterlee as Chief of the Engineering Division and helped bring the project to completion.

Individuals who gave eyewitness accounts of change included Donald Ansardis, Allan Ensminger, William Conway, Duane Crawford, Herman Crawford, Leonard Chauvin, Steve Estoponal, Pete Hebert, Greg Linscombe, Alex Plaisance, Sammy Stipelcovich, John Tesvich and John Woodard. Ed Fike conducted the interviews with eyewitnesses from the Empire-Bastian Bay area.

Report editing and production were done by Yolanda Lynn Charles, Tabitha Mallery, and Margaret Sullivan. Curtis Latolais did much of the cartography and many of the illustrations. Geographic Information System (GIS) analyses were performed by Mark Forsyth, David Alford, Steven Ward and Jason Carr, under the direction of Ms. Lori Cunningham.

Fieldwork, including coring, surveying and sampling was done by Jereme Cramer, Jay Janus, and Paul Moses under the direction of Kathy Wiltenmuth. Juan Lorenzo, Ph.D. Department of Geology and Geophysics at Louisiana State University (LSU) and his students conducted a high-resolution seismic survey down Bayou Lafourche. Edward Overton, Ph.D., LSU's Institute of Environmental Studies, conducted gas chromatography analysis of samples and interpreted the data.

Officers and members of the New Orleans Geological Society (NOGS) assisted the project by providing an opportunity for an oral presentation of preliminary results at one of their meetings. Comments from the audience were of great value in directing focus to important aspects of the research. In addition, a committee was formed to assist in the work. Committee members proved to be seasoned oil and gas industry geologists, who provided very valuable comments, suggestions and information. Members of the committee included: Jack Bryant, Charles Corona, Bob Douglass, Jack Dunlop, Bob Sabaté, and George Rhodes.

Peer review of the manuscript was provided by personnel of the Geology Section of the NOGS and several outside geologists, each of whom has expertise in processes active in coastal Louisiana. The reviewers included Harry Roberts, Ph.D., LSU; Shea Penland, Ph.D., University of New Orleans; Robert Morton, Ph.D., U.S. Geological Survey; Mark Kulp, Ph.D., University of New Orleans, and John Lopez, NODCE. Their comments were very helpful and were greatly appreciated.

Conversion Matrix

<i>mm/yr</i>	<i>cm/yr</i>	<i>m/yr</i>	<i>m/cent</i>	<i>in/yr</i>	<i>ft/yr</i>	<i>ft/cent</i>	
0.004	0.000	0.000	0.00	0.00	0.000	0.0012	<1
0.305	0.030	0.000	0.03	0.01	0.001	0.1	
0.762	0.076	0.001	0.08	0.03	0.003	0.25	
1.524	0.152	0.002	0.15	0.06	0.005	0.5	
2.286	0.229	0.002	0.23	0.09	0.008	.075	
3.048	0.305	0.003	0.30	0.12	0.010	1	1
4.572	0.457	0.005	.046	0.18	0.015	1.5	
5.334	0.533	0.005	0.53	0.21	0.018	1.75	
6.96	0.610	0.006	0.61	0.24	0.020	2	2
6.858	0.686	0.007	0.69	0.27	0.023	2.25	
7.620	0.762	0.008	0.76	0.30	0.025	2.5	
8.382	0.838	0.008	0.84	0.33	0.028	2.75	
9.144	0.914	0.009	0.91	0.36	0.030	2	3
9.906	0.991	0.010	0.99	0.39	0.33	3.25	
10.668	1.067	0.011	1.07	0.42	0.035	3.5	
11.430	1.143	0.011	1.14	0.45	0.038	3.75	
12.192	1.219	0.012	1.22	0.48	0.040	4	4
13.716	1.372	0.014	1.37	0.54	0.045	4.5	
14.478	1.448	0.014	1.45	0.57	0.048	4.75	
15.240	1.524	0.015	1.52	0.60	0.050	5	5
16.764	1.676	0.017	1.68	0.66	0.055	5.5	
18.288	1.829	0.018	1.83	0.72	0.60	6	6
19.812	1.981	0.020	1.98	0.78	0.65	6.5	
21.336	2.134	0.021	2.13	0.84	0.070	7	<7
24.384	2.438	0.024	2.44	0.96	0.080	8	
27.432	2.743	0.027	2.74	1.08	0.090	9	
30.480	3.048	0.030	3.05	1.20	0.100	10	
33.528	3.353	0.034	3.35	1.32	0.110	11	
39.624	3.962	0.040	3.96	1.56	0.130	13	
45.720	4.572	0.046	4.57	1.80	0.150	15	

SUMMARY

A comprehensive study has been conducted of suspected relationships between geological faults and subsidence in Southeastern Louisiana. Results of the work indicate that submergence of lowlands has been one of the major causes of land loss along Louisiana's deltaic coast during the twentieth century. The submergence is the result of compaction/consolidation, sea level rise and faulting, which occur throughout the area and in turn cause saltwater intrusion and accelerated edge erosion. Fault induced (geotechnical) subsidence is caused by sinking of blocks bounded primarily by ancient, deep-seated, east-west trending growth faults. Fault movement occurs in response to interactions among regional, processes which include geosynclinal down-warping, sediment loading, salt movement, gravity slumping, compaction and fluid withdrawal. Surface features on subsiding blocks, including wetlands, natural levee ridges, barrier islands, highway and flood protection levees are affected.

A relationship has been established between surface traces and signatures of fault movement and known subsurface faults and related geological structures. More than one hundred suspected surface fault traces and/or scarps have been identified and evaluated. Typically, the traces occur as linear or broad, arc-shaped segments from 3 to 5 miles (mi) (4.8 to 8.1 kilometers [km]) in length with associated areas of rapid land loss or wetland deterioration ("landloss hotspots") on the down-dropped block. In some instances, relict distributary natural levee ridges that cross the faults have been severed and submerged. The down-dropped blocks are usually tilted toward the fault (within the zone of deformation) and exhibit vertical displacements of 1 to 3.5 feet (ft) (0.3 to 1.1 meters [m]). Based on these relationships, a methodology has been developed for evaluating, dating and quantifying the amount and rate of fault movement and its effects on surface landforms. This methodology provides the first step in risk analysis of hazards related to faults.

Fault movement is often episodic. The periodic movements have not only occurred over and over again for millions of years on a geological time scale, but also have continued to occur during prehistoric, historic and modern times. Episodes of active fault movement are separated by dormant periods or periods when movement persists as slow creep. In the latter instance, sedimentation rates may approximate the rate of fault movement and mask the surface effects. Sediment deprivation results in the opposite effect and accentuates the surface signatures. Along some fault segments the period of activity has been dated. The modern period of fault activity began in the 1960s and continues to the present.

One or more major regional fault event occurred during the period 1964-1980 along the Golden Meadow Fault Zone, which is made up of many fault segments and extends for 130 mi (209.2 km) across the Deltaic Plain of Southeastern Louisiana. Effects of 1964-1980 events are most pronounced along two segments within the Golden Meadow Fault Zone, referred to as the Empire and Bastian Bay Faults, where massive submergence and land loss occurred on down-dropped blocks. Measured vertical displacement along the 3 to 5 mi (4.8 to 8.1 km) fault scarps ranged from a few inches to 3.5 ft (1.1 m). Coastal

marshes were most affected by modern fault movement, but ridges were also severed and down-dropped. Submerged and deteriorated wetland areas of 12,000 to 24,000 acres (ac) (4856 to 9712 hectares [ha]) are associated with these two fault segments. Unraveling the history and changes associated with the Empire and Bastian Bay Fault events provided the key to understanding the relationships among fault movement, subsidence and land loss.

Surface effects of fault movement have occurred, and in some instances appear to be continuing, along other fault zones inland of the Golden Meadow Fault Zone. These include, but are not limited to, the Boudreaux, Penchant, Lake Hatch, Lake Salvador, Thibodaux, Lac des Allemandes, Frenier and Baton Rouge Fault Zones. The highest fault induced land loss is apparently associated with three regional fault related features called the Terrebonne Trough, the Lake Hatch Fault Zone and the Balizé Depression.

The relationship between salt domes and regional faults appears to play a role in activation of faults. The domes typically occur along regional faults. Differential movement between the low-density salt and adjacent sedimentary deposits may have a wedging effect on the faults, initiating brine water and gas movement up fault zones. The water and gas in turn may lubricate the fault plane surfaces and cause instability along fault segments. Brine and gas may also cause vegetation changes at the surface and may indicate areas of active movement or potential movement.

There is abundant evidence of vertical fault displacement of both the base and the top of the Pleistocene deposits. Seismic sections and well logs show vertical displacement along some regional growth faults and activity of salt domes at the base of the Pleistocene. Topographic escarpments, shallow borings and sub-bottom profiles indicate vertical displacement of the top of the Pleistocene deposits in the Lake Pontchartrain area. Amount and rates of modern vertical fault movement have been quantified by using data from tide gauge records, geodetic leveling, movement of bridges and subsided man-made structures.

The findings of the study have direct applications to the planning and design of coastal restoration efforts, including infrastructure elements (flood protection levees, ports and navigation projects and highways). Subsidence and submergence related to fault events cause changes in the distribution of plants and animals (vegetation communities, oyster beds, etc.). Direct associations of *Spartina spp.* dieback (“brown marsh”) and cypress dieback with fault events have been found. The study found that faulting poses a natural hazard in Southeastern Louisiana. The results of the work also provide a basic framework for further evaluating the impacts of faulting.

INTRODUCTION

For 5000 years, land was added to the coast of what is now Southeastern Louisiana by deposition of sediment at the outlets of the Mississippi River. Sediment deposition and related land building processes resulted in the highly dynamic and resource rich Mississippi River Deltaic Plain (Figure 1). During the twentieth century, the long land building process was abruptly reversed. In one hundred years, submergence and erosion have removed the result of 1000 years of deltaic land building (Figure 2). The abruptness and magnitude of this reversal has puzzled scientists and disagreement remains within the scientific community on the relative importance of the processes driving these changes.

The state of Louisiana and the federal government have combined forces to formulate a plan and program for stabilization and restoration of the deteriorating coast.¹ The cost of implementing such a plan is estimated to be \$14 billion (Louisiana Coastal Wetlands Conservation and Restoration Task Force and Wetlands Conservation and Wetlands Authority 1998). An effective stabilization and restoration program cannot be formulated before the causes of coastal deterioration are identified.

Loss of more than 1600 square miles (sq mi) (414,398 ha) of land, most of which was wetland, in coastal Louisiana during the period between 1930 and 1998 is now recognized as a world-class catastrophe. Governor Mike Foster of Louisiana characterized this as “Loss of the Nation’s Wetland” (The Times-Picayune, 2002: B-4). This twentieth century land loss has not been randomly distributed. Analysis of the pattern of loss and changes in rate through time sheds considerable light on the causes. Approximately 46 percent (737 sq mi or 190,493 ha) of the total loss (1620 sq mi or 418,723 ha) has occurred in a triangular area lying south of New Orleans in the Terrebonne and Barataria Basins and Mississippi Birdfoot delta. Subsidence and land loss has dramatically accelerated in this area since the early 1960s. It has been proposed that the primary cause of loss in this triangular area is fault related subsidence (Gagliano and van Beek 1994; Louisiana Coastal Wetlands Conservation and Restoration Task Force and Wetlands Conservation and Wetlands Authority 1998, Gagliano 1999).²

There was a significant acceleration of land loss rates between 1946 and 1965, leading to a peak annual loss rate of 41.8 sq mi (10,826 ha) per year in 1962. The loss rates continued at 25 to 35 sq mi (6475 to 9065 ha) per year through 1990 (Louisiana Coastal Wetlands Conservation and Restoration Task Force and the Wetlands Conservation and

¹ Several plans have now been proposed including the *Coastal Wetlands Planning, Protection and Restoration Act: Louisiana Coastal Wetlands Restoration Plan*. (Louisiana Coastal Wetlands Conservation and Restoration Task Force 1993), known as the CWPPRA Plan, and *Coast 2050: Toward a Sustainable Coastal Louisiana* (Louisiana Coastal Wetlands Conservation and Restoration Task Force and the Wetlands Conservation and Restoration Authority 1998), known as the Coast 2050 Plan.

² A concentration of loss in the Sabine-Calcasieu Basin is largely the result of marine tidal invasion of formerly fresh marsh areas through the Sabine and Calcasieu Ship Channels. In this instance, salt water has killed the marsh grass that builds and sustains root mats, thus exposing underlying organic soils to tidal erosion. Likewise, a concentration of loss east of the Mississippi River is attributed to marine tidal invasion through the Mississippi River Gulf Outlet (MRGO).

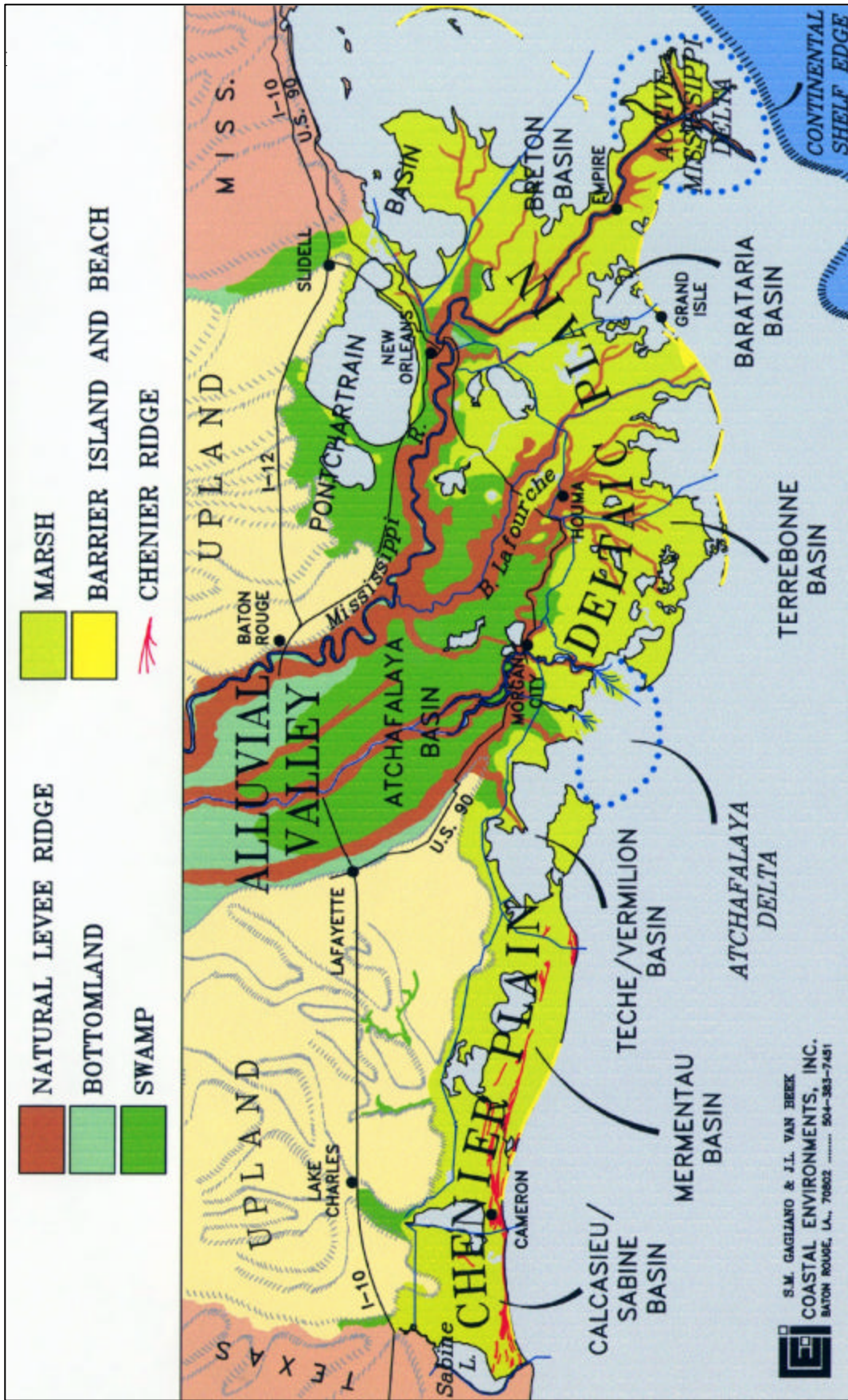


Figure 1. Map of coastal Louisiana showing location of the Deltaic Plain study area and major landforms (after Gagliano and van BEEK 1994).

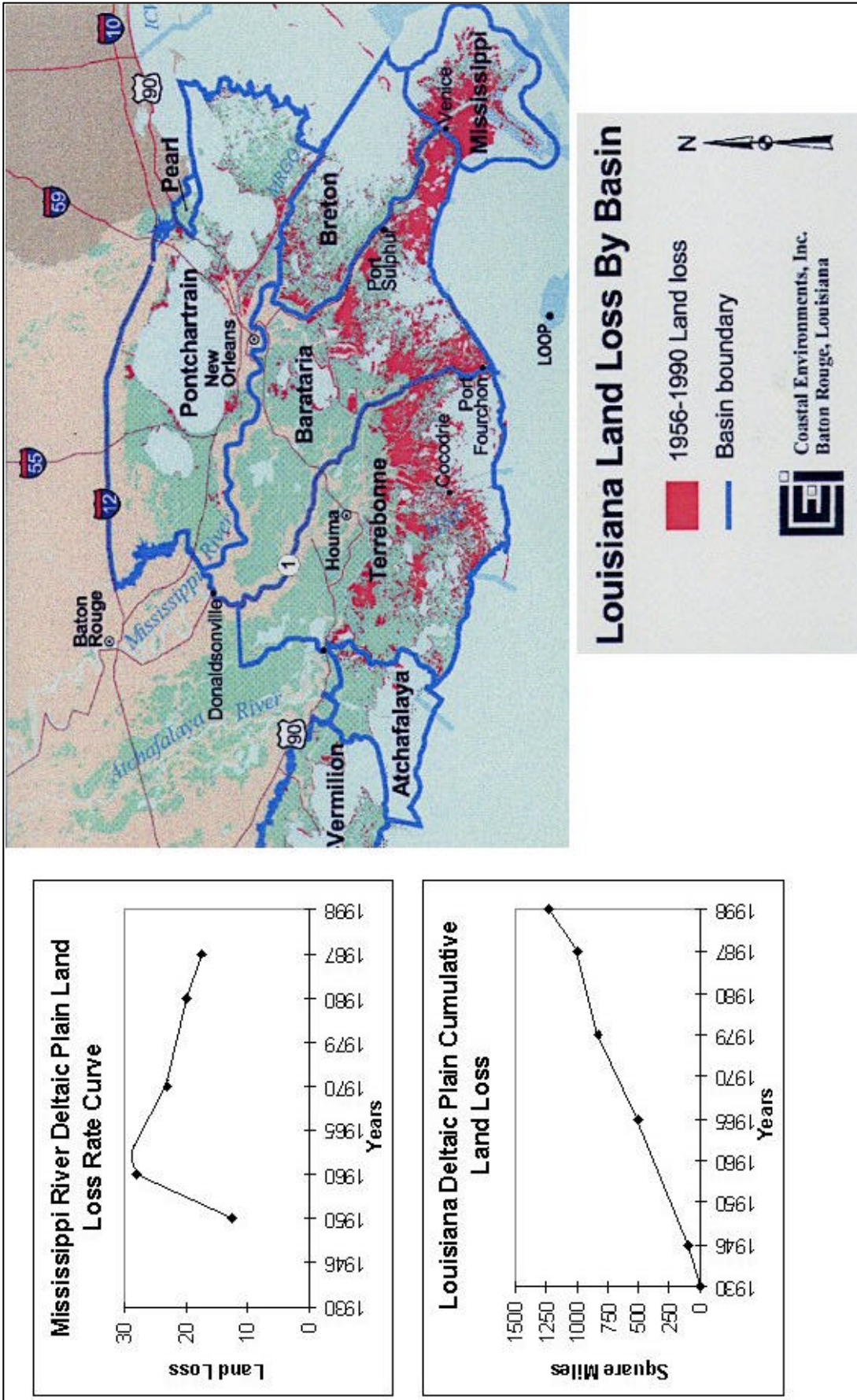


Figure 2. Land loss in the Deltaic Plain. Map shows land loss for the period 1956 - 1990. Graphs show rate of loss in square miles per year and cumulative loss in square miles (Gagliano 1998, adapted from Barras et al. 1994).

Restoration Authority 1998). During the interval of 1990 to 2000, the loss rate declined to 16.4 sq mi (4239 ha) per year (J.A. Barras, per. comm., October 2002

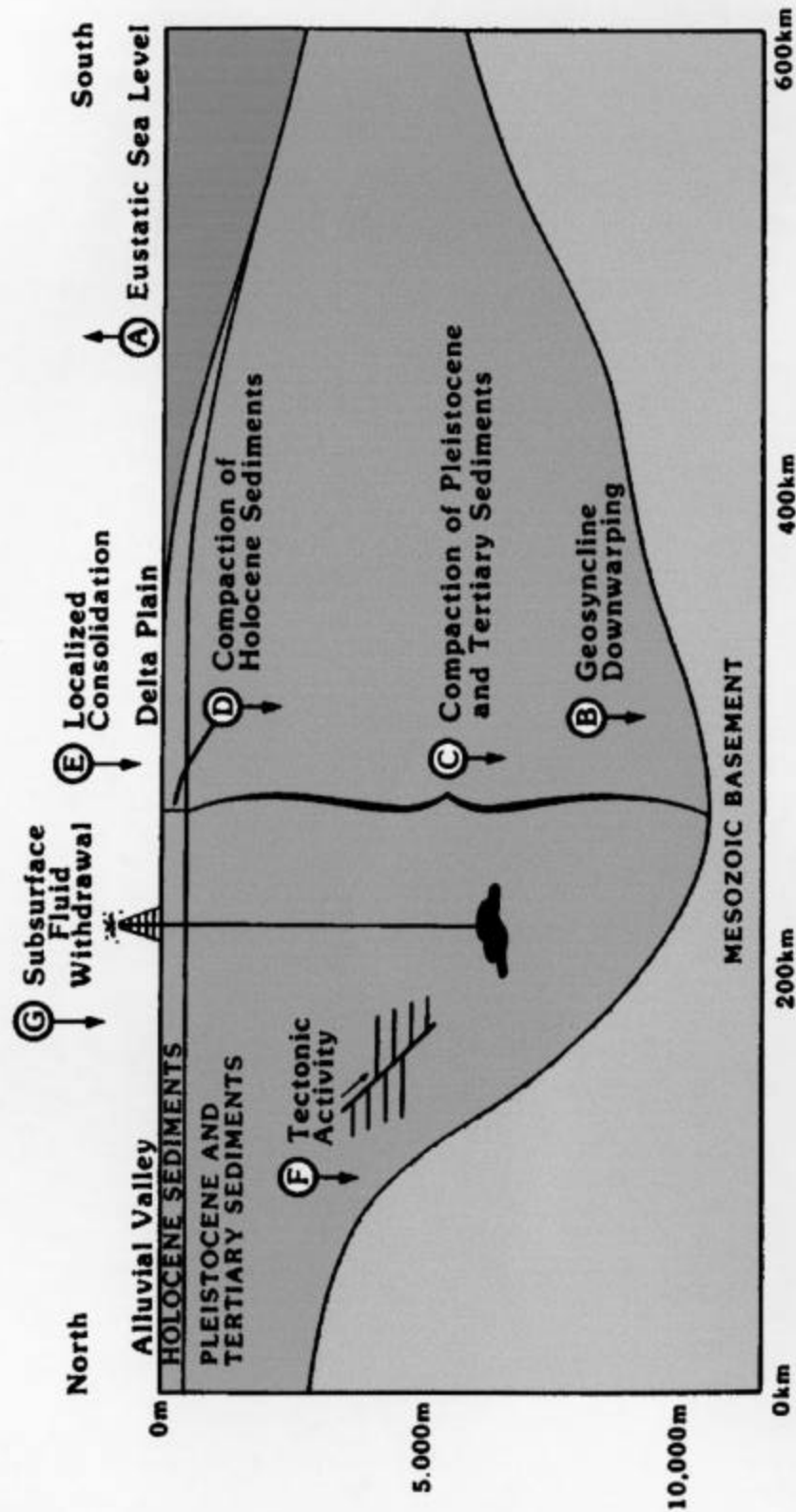
Natural and human processes contributing to this massive landscape change include: 1) shifting of the course of the Mississippi River, 2) flood protection and navigation works, 3) reduction in Mississippi River transported sediment (attributed to tributary dams and channel training), 4) sediment deficit in coastal basins, 5) marine tidal invasion (accelerated by canals dredged for navigation and mineral extraction), 6) herbivory, 7) fire, 8) shore and bank erosion, 9) excavations, 10) coastal storms, 11) drought, 12) world-wide (eustatic) sea level rise and 13) subsidence (Gagliano and van Beek 1994; Penland et al. 1996).

The relative position of the level of the sea and the surface of the land (relative sea level [RSL]) is a critical factor in the land loss problem of coastal Louisiana. An abrupt increase in RSL rise in Southeastern Louisiana began during the twentieth century and continues at present (Penland and Ramsey 1988, 1989). This RSL rise is an apparent major cause of land loss and coastal deterioration.

The RSL rise has two principal components, eustatic sea level rise and subsidence.). Eustatic rise a small of RSL in Southeastern Louisiana accounting for about 0.0075 ft/yr (0.228 cm/yr) in modern decades. Spatial and temporal variations in subsidence rates have been identified in coastal Louisiana (Ramsey and Moslow 1987, Penland et al. 1988). While there is general agreement among researchers on the types of processes causing subsidence, there is considerable disagreement on the relative importance of the processes (Figure 3) in rates of subsidence. Several scenarios have been proposed to explain the variations and apparent correlations with causative processes, as follows:

- 1) Subsidence is caused largely by compaction and de-watering of Holocene sediments. The total thickness, composition, and age of the Holocene deposits are factors in controlling the subsidence rate. Geological faulting may contribute, but is not a major factor.
- 2) Some, if not most, of the twentieth century subsidence in coastal Louisiana is due to mineral extraction including oil, gas and sulphur. In this case the depth of vertical movement may be limited to the depth of the minerals extracted. Mineral extraction could re-activate regional faults, but only to the depth of the extracted minerals.
- 3) Some, if not most, of the twentieth century subsidence is due to fault induced (geotechnical) subsidence. The fault movement is caused by geological processes including crustal down-warping, sediment loading, isostatic adjustment, vertical and lateral (diapiric) movement of salt and shale deposits (at various depths) and gravity slumping.
- 4) A combination of the above.

Factors Contributing to Relative Sea Level Rise and Subsidence



RELATIVE SEA LEVEL : A + B + C + D + E + F + G

SUBSIDENCE :: B + C + D + E + F + G .

Kolb & Van Lopik 1958
Penland et. al. 1989

Figure 3. Factors contributing to relative sea level rise and subsidence in the Louisiana coastal region (after Penland et al. 1988, 1989; adapted from Kolb and Van Lopik 1958:95).

The purpose of this study is to identify near-surface faults in the deltaic plain and to determine the magnitude of movements (Figure 4). Secondary purposes were to determine the nature, distribution, intensity and frequency of fault movement in Southeastern Louisiana and its effect on natural and human-made features in reference to design and construction of infrastructure and coastal restoration projects.

FAULTS AND FAULT EVENTS

Southeastern Louisiana is located in a geological province called the Gulf Coast Salt Basin (Figure 5). The area is underlain by a deep trough in the earth's crust that has been filled, and continues to be filled, by thousands of feet of sedimentary deposits. The basin is riddled by faults and salt domes resulting from processes that formed the trough and vertical and lateral adjustments that accompany accumulation of the sediment within the trough. Salt movement has been a significant factor in the tectonic dynamics of the basin.

One of the work products of this project is a map entitled Southeastern Louisiana Structural Framework, which identifies major fault trends and related structural elements (Figure 6). The basic faults and salt domes depicted on the structural framework map were derived from published sources (See W. E. Wallace, Jr. and Tectonic Map Committee, Gulf Coast Association of Petroleum Geologists, Appendix A). In addition, some of the fault zones and alignments were delineated during the course of this study. The map depicts a framework of faulting to which processes and changes in the Deltaic Plain can be linked.

Movement along faults can be correlated with fault events, which are defined herein as the occurrence of vertical and/or lateral movements along a fault plane that result in land surface displacement. A fault event is a process that has dimensions in time, space and intensity. Fault events may occur within a short period of time and in some instances may be accompanied by localized tremors and/or noise. Such movements and adjustments may also occur over a period of several years. Along some faults, movement may be slow and almost imperceptible, and if no movement is detected over a period of years, the fault is said to be dormant. In Southeastern Louisiana, during modern decades, the vertical movement is relatively small, a few inches to 3.5 ft (1.1 m) or more.³ In the low terrain of the region, the effects of even small amounts of vertical movement are far-reaching. Little data is available on lateral movement.

A fault event is a high-energy process which may cause long-term changes to the landscape that are greater than those resulting from a large hurricane. Fault movement is

³ The maximum vertical displacement of near-surface Holocene beds documented in cores and borings collected during the course of this study was 3.5 ft (1.1 m). Displacements up to 10 ft have been reported for the top of the Pleistocene in the Pontchartrain Basin (Fisk 1944, Saucier 1963, Kolb et al. 1975 and Penland et al. 2001.) Vertical fault displacements of 350 ft (106.7 m) have been reported from the South Pass mudlumps (Morgan et al. 1968).

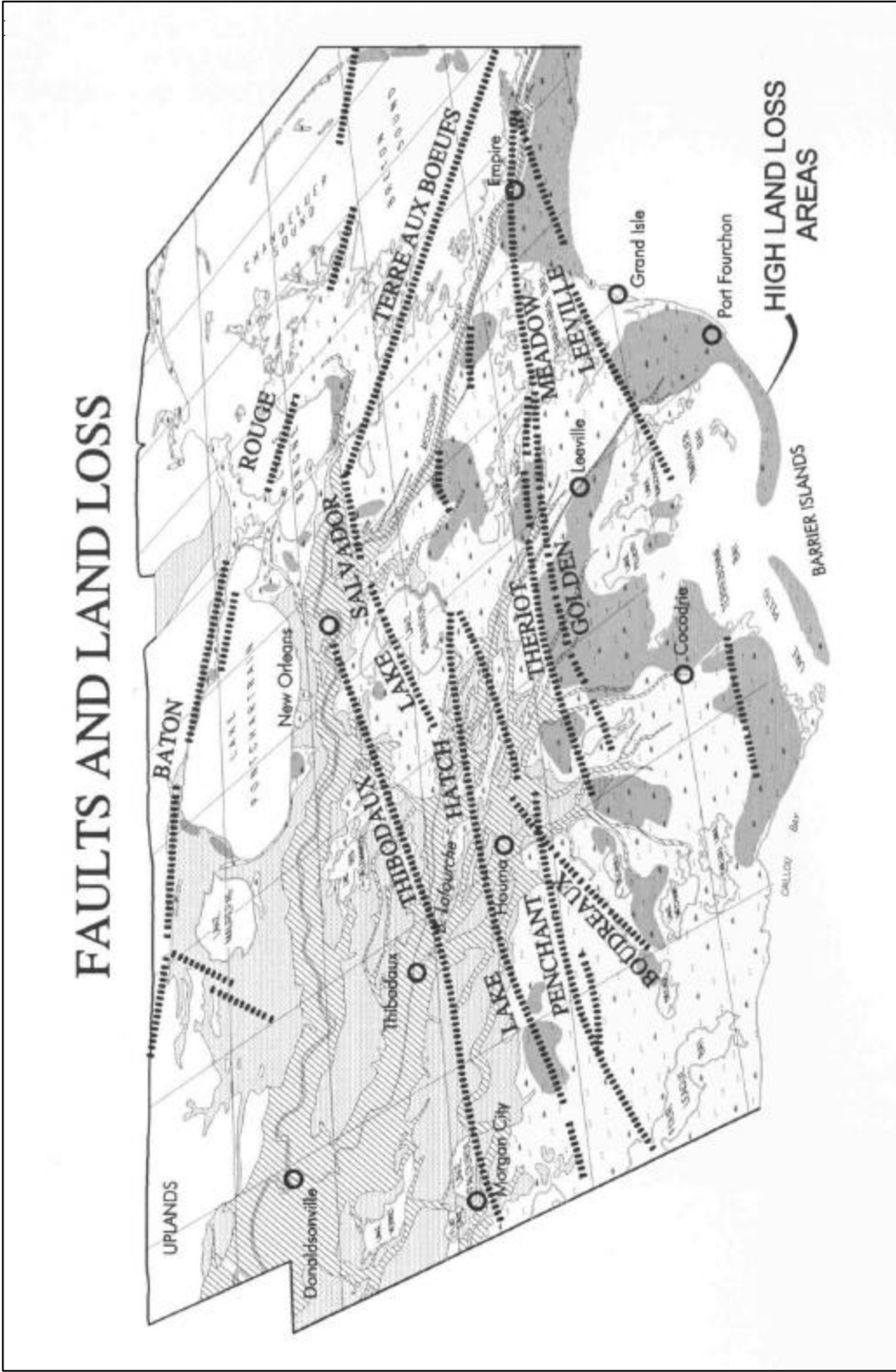


Figure 4. Relationship between faults and areas of high land loss in Southeastern Louisiana (after Gagliano 1999).

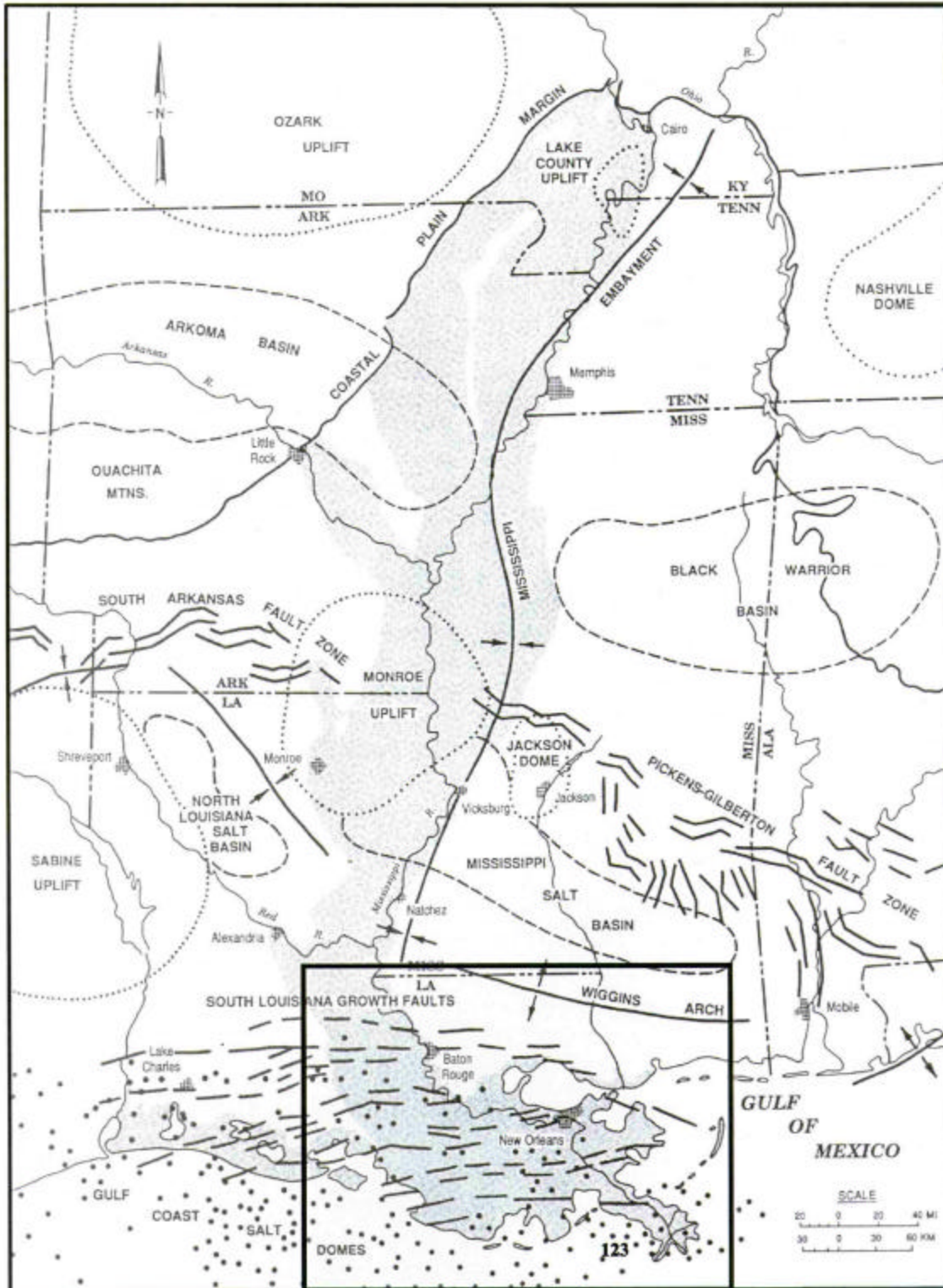


Figure 5. Major structural features of Southeastern Louisiana and adjacent areas (after Saucier 1994). The study area is indicated by the inset box.

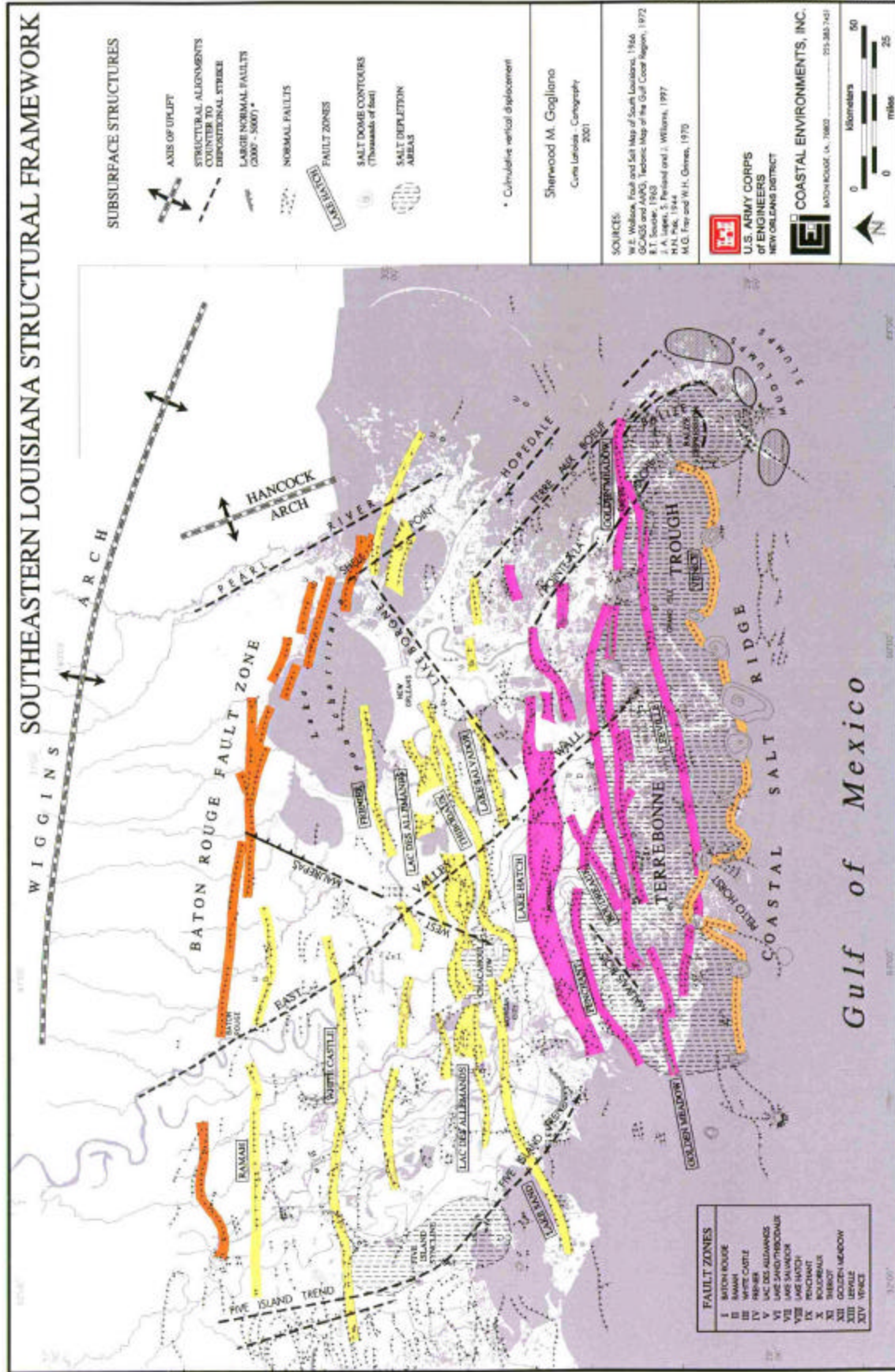


Figure 6. Southeastern Louisiana structural framework, with major faults and salt domes identified.

a driving process that alters the elevation and slope of the terrain, as well as hydrology, water quality and the distribution of plants and animals. Fault events may initiate crevasses, capture the course of a river, submerge natural levee ridges, cause barrier islands to break up and cause lakes and bays to appear. In other words, fault movement may alter the total ecology of natural systems. Fault events may result in large breakup areas that occur within short periods of time, but also may initiate a secondary sequence of changes that can take years to unfold.

Places where wetlands revert to open water are called breakup areas. These areas have also been referred to as “land-loss hot spots.” Marsh breakup and conversion to open water may progress through stages that occur over a long period of time, or during a short time interval, and include submergence of both coastal marshes and ridges. A number of active and previously active breakup areas have been identified, described and analyzed. This approach provides a basis for systematic study, modeling and prediction of future impacts with regard to existing and planned infrastructure and coastal restoration.

Geomorphic changes, as interpreted from historic maps, suggest that modern fault events have resulted in the formation of lakes and bays. Lakes resulting from fault activity are called frangenic lakes. The shapes and trends of fault-induced water bodies are distinctive and can be identified on historic aerial photographs and maps. Data developed during the present study suggest that the inland freshwater lakes, including Lac des Allemands, Lake Cataouatche, Lake Salvador and Lake Lery, formed as a result of pre-1800 fault events along the Lake Salvador, Thibodaux and Lac des Allemands Fault Zones. Geomorphic changes, as interpreted from historic maps suggest that active fault events along the Leeville Fault Zone from the 1850s through the early 1900s may have been the cause of the opening of Terrebonne, Timbalier, Caminada, Barataria, Joe Wise, Bastian, Scofield and Skipjack Bays.

The nineteenth century fault activity was followed by a period when faults in the coastal area were largely dormant. Aerial photographs taken in the 1930s through the 1950s show a relatively stable landscape, particularly in the freshwater wetlands inland from the tidal zone. Low land loss rates, and the presence of only a small number of breakup areas on maps and aerial photographs and an absence of reports of fault activity from the natural scientists conducting research in the area during this time period all provided evidence of this dormancy.

Beginning in the mid-1960s and accelerating in the 1970s, there was another period of active fault events, particularly along the Golden Meadow and Theriot Fault Zones.⁴ The fault activity progressed inland to the Boudreaux, Penchant and Lake Hatch Fault Zones by the mid to late-1970s. Effects of these events are most pronounced along discrete fault traces that are from 3 to 5 mi (4.8 to 8.1 km) long, where fault movement caused massive submergence and land loss on down-dropped blocks. Measured vertical

⁴ The Golden Meadow Fault is a major regional fault system that extends 130 mi (209.2 km) along the Louisiana coast. The zone is from a few miles to 5 mi (8.1 km) or more wide. Two large fault domes fall within the fault alignment. One of these, the Lake Washington Dome is 8.5 mi (13.7 km) in diameter and the fault plane is coincident with the salt face for several miles. One segment of the fault has 2000 to 5000 ft (609.6 to 1524 m) of vertical displacement (Wallace 1966). The Theriot Fault, north of, and trending sub-parallel to the Golden Meadow Fault, also includes two salt domes.

displacement on segments ranges from a few inches to 3.5 ft (1.1 m) or more. The coastal marshes, being more expansive, were most affected by the faulting but ridges were also severed and down-dropped. Evidence of this epoch of fault activity is provided by an increase in land loss rates, the sudden appearance of numerous breakup areas, the appearance of fault traces and scarps, an increase in apparent rate of sea level rise recorded by tide gauges and eyewitness reports of land submergence and the appearance of bays.

This fault movement during the 1960s and 1970s, was the apparent result of massive land submergence and appears to account for a large part of the total land loss that has been recorded in the Mississippi River Deltaic Plain during the twentieth century. Effects of the movement include sinking of ridges, barrier island breakup, salt marsh dieback and advance of the edge of marine tidal conditions into areas that were formerly characterized as fresh, low-energy wetlands. Increased water depth alone can stress plants, alter soils and/or drive plant succession. The gradual introduction of salt water alters the chemistry of the soils and sediments that also causes plant community succession. The latter change causes loss of root mats followed by export of exposed, poorly consolidated organic soils by storm surge return and tidal movement. The secondary effects of fault events of the 1960s and 1970s, have not yet completely unfolded.

The use of the “rate of geomorphic change” as an indicator of fault activity must be tempered by consideration of other processes that cause change. These include hurricanes, floods, droughts, herbivory, man-induced hydrologic change (canal dredging, levee construction) and fluid withdrawal. In this study, other contributing processes were systematically evaluated in the Terrebonne Deltaic Plain (see Triggering Mechanisms, Natural System Succession, of this report) and were generally considered for each of the study areas. It should also be noted that a sequence of land loss occurred in the Chenier Plain that parallels changes in the Deltaic Plain. The study of processes and responses associated with land loss and marsh deterioration in the Chenier Plain was beyond the scope of this study, but faulting also appears to be a contributing factor in that area (Gagliano 1999:10, 39-43).

PREVIOUS RESEARCH

This study builds upon a foundation of more than 100 years of geological research conducted in the region. The century-long exploration for and production of oil and gas in the Gulf Coast Salt Basin has resulted in a vast amount of published and unpublished information regarding the geology of this basin. The Gulf Coast Salt Basin is one of the most intensively explored and most thoroughly known geological provinces on earth. There is a disconcerting disconnect between the level of understanding of fundamental driving geological processes by the petroleum geology community and the community of scientists, engineers and planners engaged in coastal restoration, planning and implementation. Any legitimate future effort to restore or mitigate the effects of faulting should include representatives from the petroleum geology community.

Far fewer publications pertain to surface effects of faults, but this topic has not been completely ignored. The works found to be particularly relevant to the present study are discussed in Appendix A.

SUBSURFACE GEOLOGY

Southeastern Louisiana is diced with innumerable subsurface faults and penetrated by numerous salt domes. The subsurface is in constant motion as a result of interactions between crustal subsidence in response to sediment loading, vertical and lateral (diapiric) movement of buried salt and shale deposits and gravity slumping. Sedimentary beds adjust to these changes by folding, flowing and/or faulting. Faults are the most common form of adjustment. Individual faults move at different times and may go through episodes of activity, slow and imperceptible movement, or dormancy.

The structural pattern, as shown in Figure 6, is dominated by east-west trending growth faults, but several northeast-southwest and northwest-southeast trending faults and/or fracture alignments also occur. These counter-to-depositional strike (CDS) features are not mapped in the subsurface and are only poorly described in the literature, but appear to be important structural elements of the region. Some of the east-west growth faults fade or terminate at their intersection with the CDS features. Also, the throw of the east-west growth faults is often translated to a number of smaller splinter faults at the intersection of basin-bounding CDS features (i.e., Terre aux Boeufs Five Island Trend).

Another major element of the regional structural framework is the Baton Rouge Fault Zone, a basin margin fault system that defines the northern boundary of the Pontchartrain Basin. This fault zone is also the hinge line between areas of sinking to the south and isostatic uplift to the north.⁵

The Coastal Salt Ridge occurs at the southern edge of the Terrebonne Trough, a major salt depletion area that underlies the Terrebonne and Barataria Bay areas. The area overlying the Terrebonne Trough is experiencing the highest subsidence and land loss rates in south Louisiana. The Venice Fault is a counter-basin dipping fault system on the north side of the salt ridge. The Venice Fault is sub-parallel to the shore zone, and is the southern boundary of a subsiding, fault-bound megablock.

Faults and features shown on the structural framework map (See Figure 6) were compared with structural features depicted on published regional cross-sections. A number of researchers have developed cross-sections through the deltaic plain (Murray 1960, Meyerhoff et al. 1968, Worzel and Watkins 1973, Martin 1978, Humphris 1979, Salvador and Buffler 1983, Winker 1984, Salvador 1987, West 1989, Liro 1992 and Fails et al. 1995).

Beginning in the 1990s, a clearer picture of the structural provinces of the offshore gulf and the onshore transition zone began to appear in the literature. This information was the result of intensive seismic surveys, drilling activities and geological modeling techniques related to development of the deep-water oil and gas fields of the gulf. This

⁵ The Baton Rouge Fault Zone is a regional segment of a continental scale structural feature that follows the Early Cretaceous Shelf Margin around the Gulf Coastal Plain from Texas to Florida (See Figure 5). The Florida Escarpment is another regional segment of this feature that continues under the Gulf of Mexico.

explosion of research and data also led to a better understanding of the structures in the Cenozoic section that are driven by gravity and powered by sediment deposition on the shelf and upper slope. Sediment loading and gravity movement cause massive salt displacement that produces diapiric structures, salt withdrawal areas and salt canopies. Seaward gravity spreading and sliding of salt adds to the complexity. It is these processes that are the primary driving force of fault movement, including the surface movement in the deltaic plain. It follows that these continental scale processes are driving landscape level ecological change in coastal Louisiana.

Four structural provinces containing distinctive assemblages of structures have been defined (Peel et al. 1995). One of these, the Eastern Province, extends into the transition zone of Southeastern Louisiana and underlies part of the study area (Figure 7). From a structural standpoint, this province is characterized by a middle-to-late Miocene linked system of extensional and compressional faults (Peel et al. 1995).

Figure 8 illustrates a north-south regional section through the western side of the deltaic plain. This section, constructed by Adams (1997), is based on gravity and seismic data verified by logs and biostratigraphic correlations from wells. It illustrates the relationships between the irregular, fractured surface of the basement rocks, the plastic and mobile Louann Salt beds that overlie the basement, a regional unconformity at the top of the Cretaceous rocks, and the marine and deltaic rock sequences that account for most of the above basement fill.⁶ One of the most striking features of the section is the series of parallel listric faults that dip toward the gulf and extend from the surface or near surface and flatten (“sole out”) at or above the top of the Middle Cretaceous. Only the major regional faults are shown. A correlation has been made between the subsurface faults shown in the section and the alignments of the subsurface faults as shown in Figure 6. The names of the equivalent fault alignments have been added to the Adams section.

In addition to the Adams section, several other regional sections appeared in the literature that utilized seismic data and modeling techniques to a greater extent than previously published sections (Peele et al. 1995, Diegel et al. 1995, McBride 1998 and Stover et al. 2001). Regional faults shown in Figure 6 were correlated with faults depicted in the megaregional section developed by McBride (1998) and further developed and published by Stover et al. (2001) (Figure 9). This north-south section through the salt dome basin is important because it is not a diagrammatic or schematic section; rather, it is drawn from a true image of the stratification and fault planes of the basin constructed from seismic lines and data from deep wells.

The megaregional sections provide a much clearer picture of the driving mechanisms of earth movement in the Gulf Coast Salt Basin and the relative magnitude of the faults involved. Through a technique called “palinspastic reconstructions,” geologists and geophysicists, using sections developed from seismic and well data, and with the aid of

⁶ The Louann Salt was deposited in a shallow hypersaline sea, which occupied a rift valley during Jurassic times. Reconstruction based on volume of displaced salt indicates that the original thickness of the bed was approximately 4000 ft (1219 m) (Robert Sabate, per. comm., October 2002).

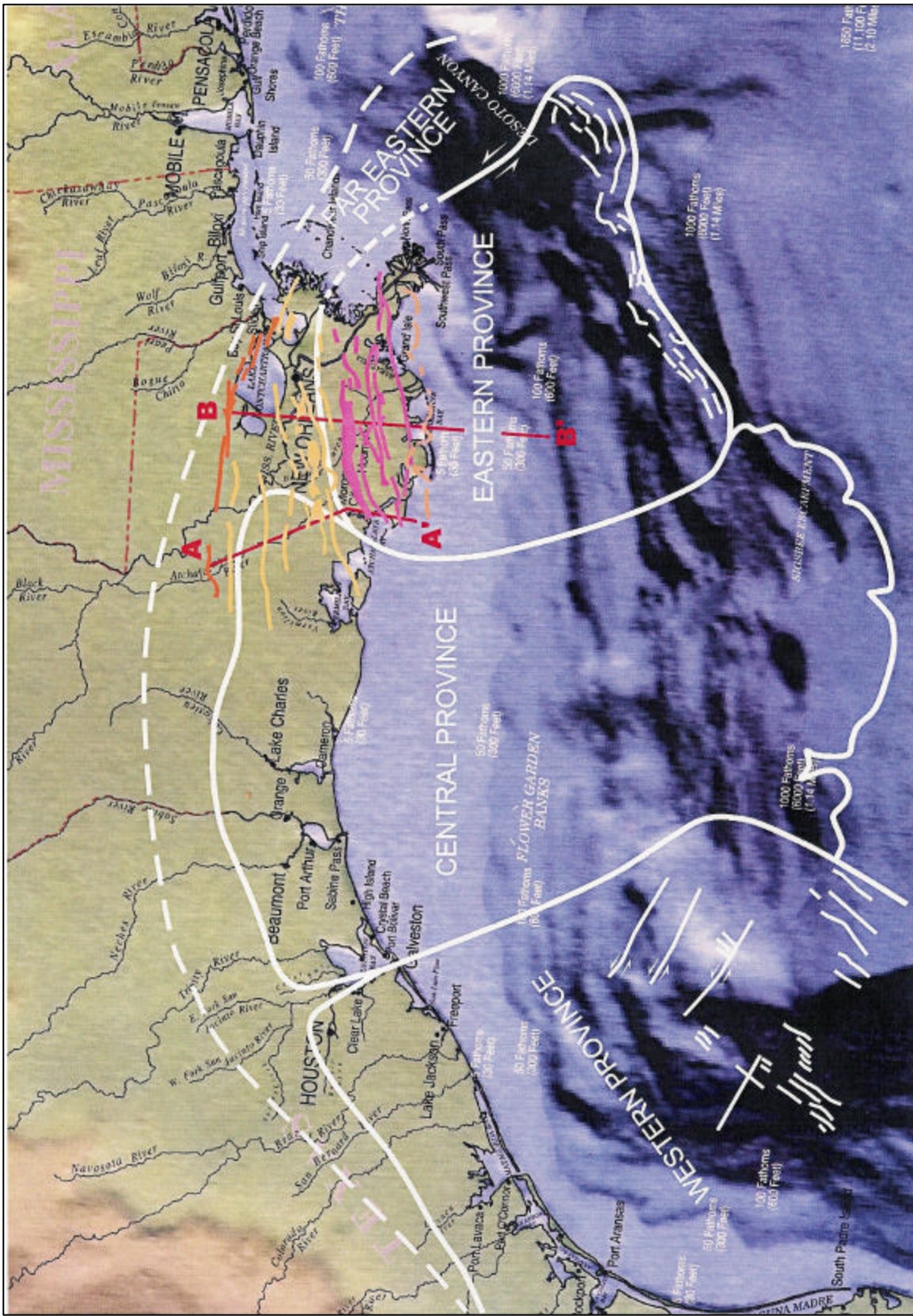


Figure 7. Cenozoic structure provinces of the Northern Gulf of Mexico and major fault zones of Southeastern Louisiana (structural provinces after Peel et al. 1995; base map with permission of Port Publishing Co., Houston, TX; fault zones reported). Color patterns correspond to those in Figure 6. Note apparent massive slumping of continental slope in the Central Province

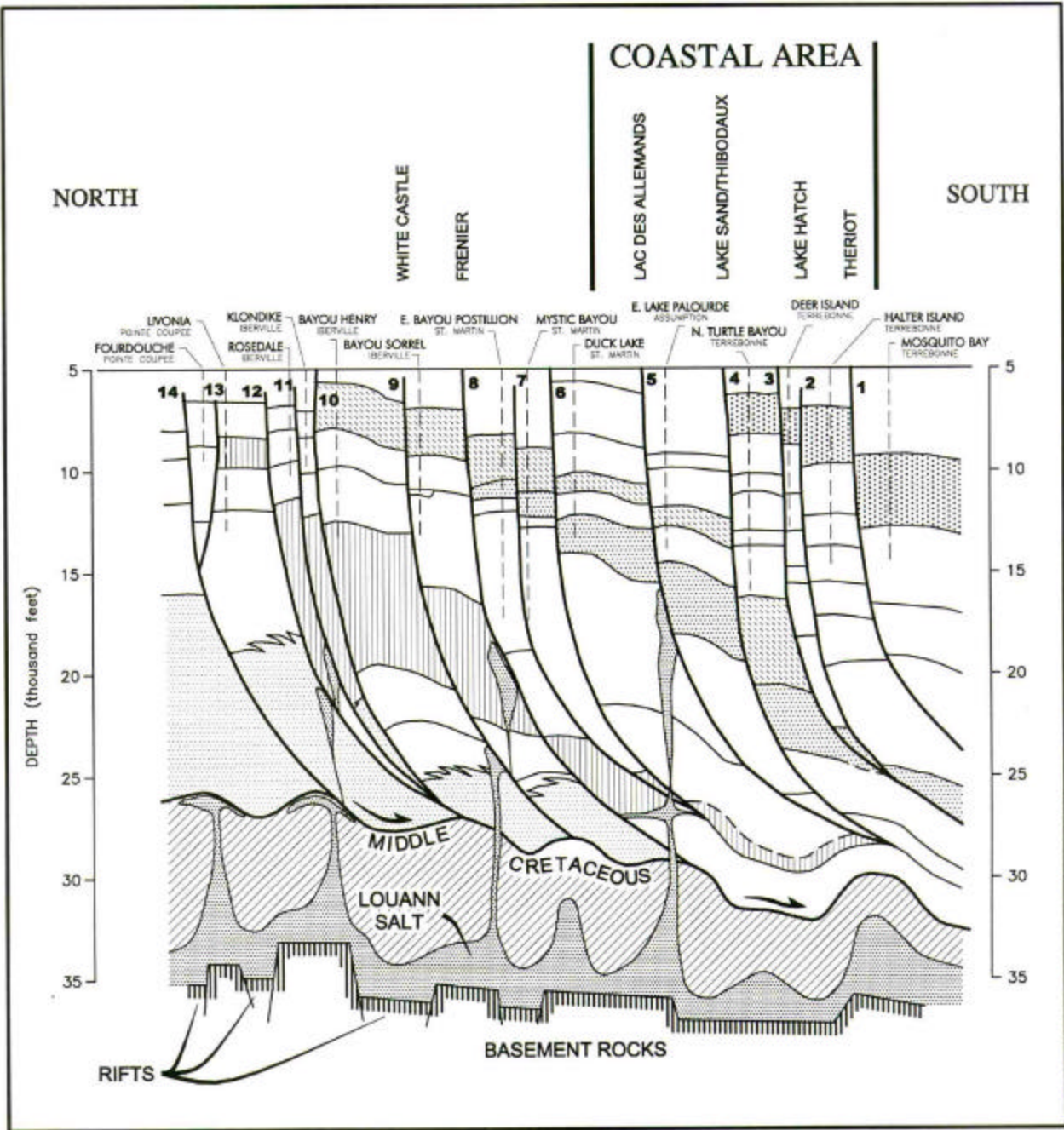


Figure 8. North-South cross-section through the Gulf Coast Salt Dome Basin showing stratigraphy and geological structures (after Adams 1997). Extensional section with progressively younger listric faults from north to south. Section also shows inferred basement-salt-decollement surface relationships. Subsurface faults shown in Figure 6 are identified on the section.

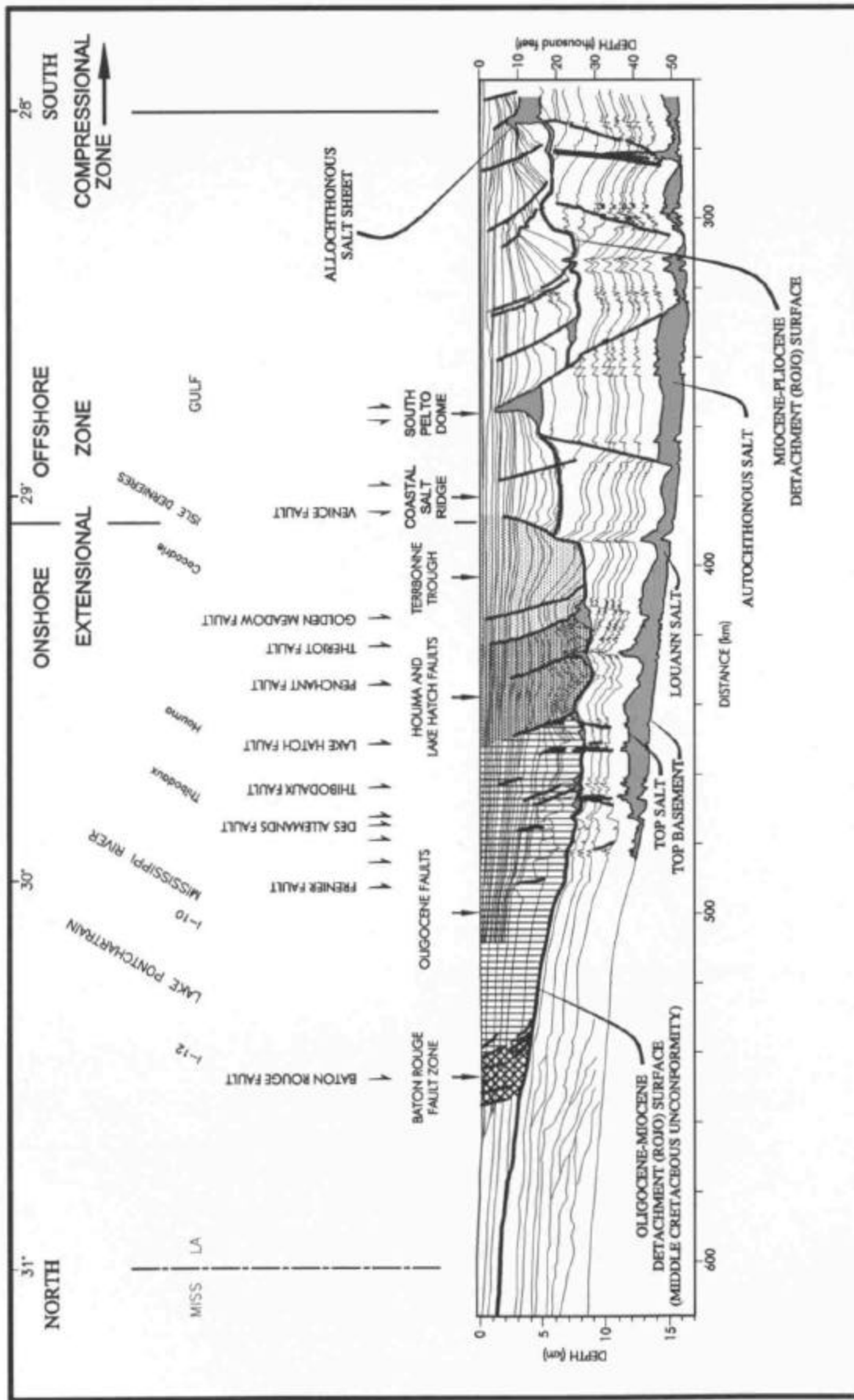


Figure 9. Segment of north-south megaregional cross-section through Southeastern Louisiana showing stratification and subsurface structure (Modified from McBride 1998 and Stover et al. 2001). Location of section shown in Figure 7 as line B.

computer restoration programs, are able to restore the strata and structure to past configurations. By “unpeeling” the section, the history of sequential change and the geological processes are better understood.

As shown on the Stover et al. (2001) section much of the movement in Southeastern Louisiana has been related to specific listric faults that merge into the Oligocene-Miocene detachment surface at depths of 20,000 to 30,000 ft (6096 to 9144 km). These faults are millions of years old and are linked to salt domes and other tectonic features of basin structure.

The area of Southeastern Louisiana where most of the twentieth century land loss has occurred lies within the Terrebonne Trough. As indicated previously this trough is a salt depletion area and part of the extensional zone of an intermediate-sized linked system of extension and compression faults (see Peele et al. 1995 and Stover et al. 2001). The compressional zone lies seaward of the coastal salt ridge (See Figure 9).

Faults and salt domes are intimately related in the study area. The domes are giant salt bubbles that are buoyant because the salt has a lower density than the sand, silt, clay and limestone around them. The domes retain their vertical position as sediment deposited around them accumulates downward in the subsiding basin. The domes tend to rise along fractures and faults, particularly regional listric growth faults. Thus, the major regional faults typically have one or more associated salt domes. Figure 10 is a cross-section of the Raceland Salt Dome, one of several domes that lie along the Lake Salvador Fault Zone. Note that the plane of the regional fault is coincident with the face of the salt. In this instance the fault dips to the north but, most commonly, the regional faults dip to the south.

The giant Lake Washington Dome is a keystone feature where regional faults intersect and merge. The nature of this dome, which is associated with three large faults, Golden Meadow-Empire, Bastian Bay and Leeville, is shown in Figure 11. It should be noted that the Empire Fault is a well-defined segment of the Golden Meadow Fault and the fault plane of this regional fault is coincident with the salt face for several miles.

The relationships between the faults and salt plugs, as illustrated in Figures 10 and 11, suggest that relative movement between the salt and the faults could provide a path for gas and fluid movement upward along the fault plane. This infusion of formation fluids and hydrocarbons in turn may lubricate the fault plane making it more susceptible to movement.

QUATERNARY DEPOSITS AND STRUCTURES

Displacement of the Pleistocene

Evidence of continuity of movement on growth faults is found at both the bottom and the top of the Pleistocene deposits. This is important because: 1) these contacts are distinctive and occur at relatively shallow depths, 2) the deposits are not very old (two

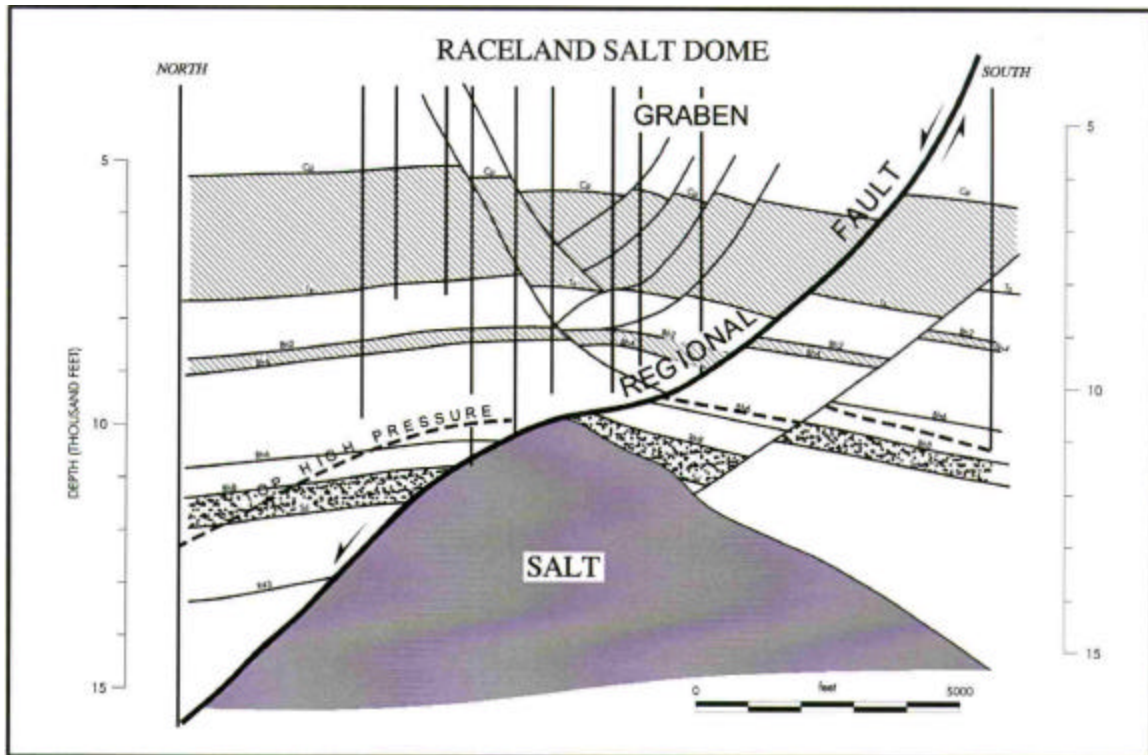


Figure 10. Cross-section of the Raceland Salt Dome, which lies within the Lake Salvador Fault Zone (after P.J. Pickford et al. n.d.). Note the counter-basinward fault, the crestal graben with nested faults and the top of the high pressure zone.

million to 12,000 years old) and 3) the top of the Pleistocene is an important foundation bearing horizon.

Robert W. Sabaté (1968) evaluated the distinctive interglacial contact marking the bottom of the Pleistocene in a zone extending across Southeastern Louisiana (Figure 12). Sabaté found the contact to be 1800 to 4300 ft (549 to 1311 m) below the surface. The base of the Pleistocene is breached by nine salt domes, some of which reach nearly to sea level, while others show sharp relief and are almost completely buried by the Pleistocene. Sabaté (1968:373) states that:

Faults with throws of up to several hundred feet cut many of the structures and influence oil and gas distribution. Many of these faults can be traced downward into the Miocene primary producing measures. Their characteristic downward increase in throw and thicker downthrown blocks qualify them as “growth” or “contemporaneous” faults...

Sabaté’s map (Figure 12) shows evidence of fault movement at the base of the Pleistocene along 80 mi (129 km) of the Golden Meadow Fault Zone. A pronounced graben occurs along the Golden Meadow Fault in the Bayou Lafourche Area. The map shows movement at Point au Fer in the same zone. In addition, the map depicts fault movement along segments of the Leeville Fault, particularly in the vicinity of salt domes

LAKE WASHINGTON SALT DOME

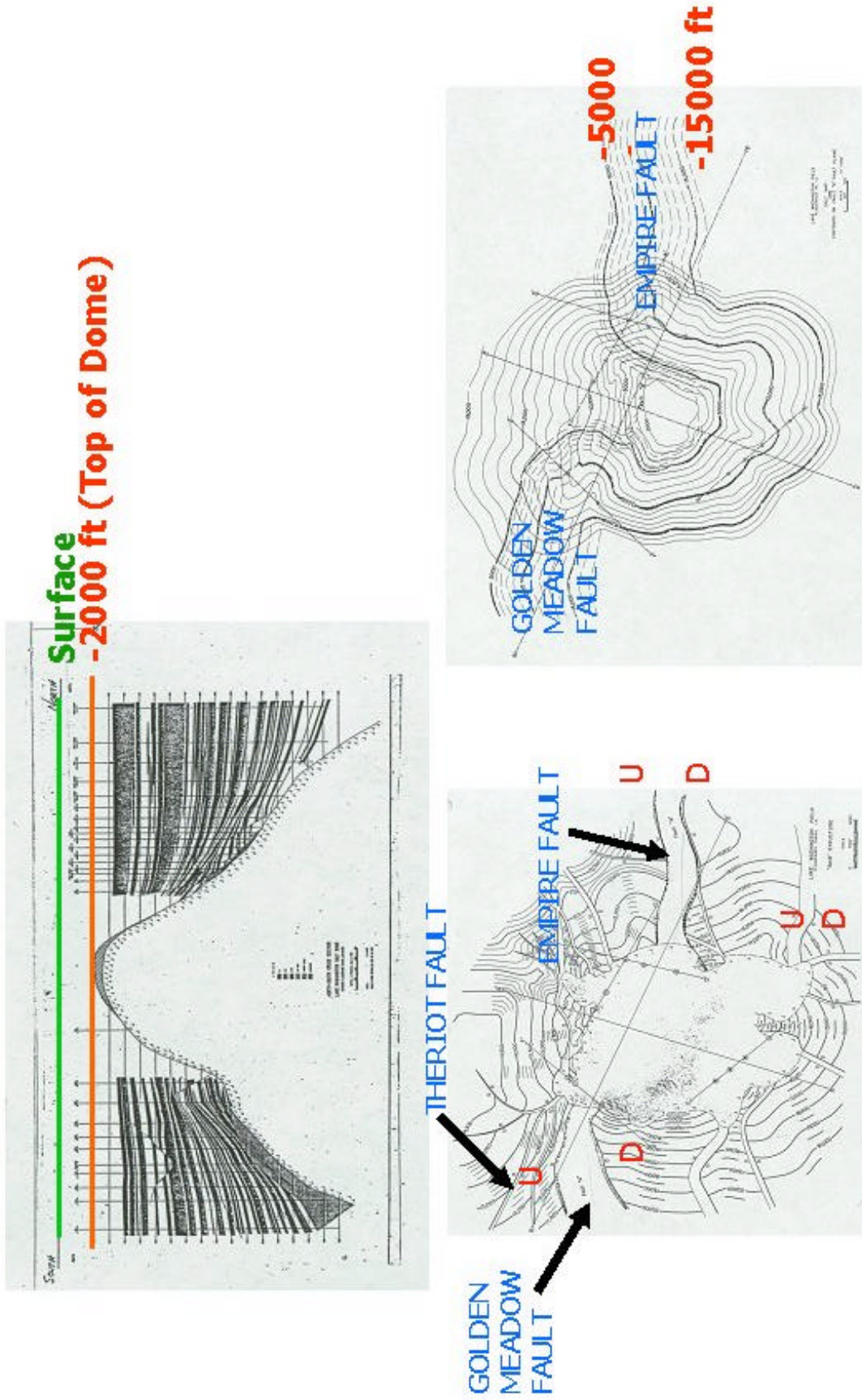


Figure 11. Relationships between the Lake Washington Salt Dome and regional growth faults (all after P.J. Pickford et al. n.d.). A. Cross - section of dome. The dome is 8.5 mi (13.7 km) in diameter and the top of the salt plug lies 2000 ft (610 m) below the surface. B. Stratigraphic slice showing Empire and Bastian Bay regional growth faults. C. Contours on the plane of the Golden Meadow – Empire Fault at 5000 to 15,000 ft (1524 to 4572 m). Note that the fault plane is coincident with the salt face for several miles

and along the Coastal Salt Ridge, where the counter-basin Venice Fault along the north side of the ridge shows movement.

The depth to the top of the Pleistocene, derived from data provided by L.D. Britsch (2001), as shown in Figure 13, is in effect a measure of the thickness of the relatively poorly consolidated sediment that makes up the Holocene wedge. This fill accumulated during the fall, low-stand, rise and relative still-stand of sea level that occurred during and since the last ice age (during approximately the last 25,000 years). Configuration of contours on the top of the Pleistocene suggests fault control. There is a trend of deep holes extending west of Donaldsonville that appears to fall on the down-dropped block of the Frenier Fault. An arc of deep holes extending from Thibodaux to Morgan City appears to be related to the Lake Sands-Thibodaux Fault. A trend of deep holes extending southwest of Houma appears to be related to the Lake Hatch Fault Zone. A long alignment of depressions extends northeast from Four League Bay to Point au Chein overlies segments of the Thibodaux, Golden Meadow and Boudreaux Fault Zones. A general break in contours along the down-dropped block of the Golden Meadow Fault Zone occurs between Bayou Lafourche and Bay Adams.

The East Valley Wall alignment, shown in Figure 13 appears to be a structural feature controlling the general configuration of the late Pleistocene and Holocene courses of the Mississippi River and some of its distributaries. During lower sea level conditions of the last ice age, the river was confined to its trench and alluvial valley. As can be seen in Figure 13, in the area south of the Golden Meadow Fault, the Holocene deposits above the Pleistocene thicken to the east. This thickening suggests that during early stages of the late Pleistocene post-glacial sea level rise, the Mississippi escaped the confines of its trench and alluvial valley and deposited an expanded wedge of sediment to the east.

The geometry of the Holocene deposits in reference to the structural configuration suggest that the East Valley Wall Alignment and the Five Island Trend determined the bounds of the alluvial valley. The modern course of the Mississippi River trunk channel follows the East Valley Wall Alignment from north of Baton Rouge south to its intersection with the Frenier Fault, where it makes a near 90-degree turn to the east for a 20 mi (32.2 km) detour before continuing its journey to the gulf across the east-west regional fault alignments.

It is also noteworthy that the location of the thickest part of the Holocene wedge is underlain by thick Pleistocene deposits (compare Figures 12 and 13). This suggests that the locus of subsidence did not change between Pleistocene and Holocene times, and may be tectonically driven.

Also shown in Figure 13 are the locations of surface and near-surface expressions of fault-modified topography, including scarps, directed stream courses and vertical displacement of shallow beds on the top of the Pleistocene. The linear surface contact between the Pleistocene and Holocene and the attendant sharp breaks in soils, vegetation and topography that occur along the fault scarps and traces along the Baton Rouge and West Maurepas Fault Zones, separating the uplands from the wetlands, provides striking testimony to the role that movement along these faults has played in sculpting the landscape. (See Pontchartrain Basin, Figures 21-24).

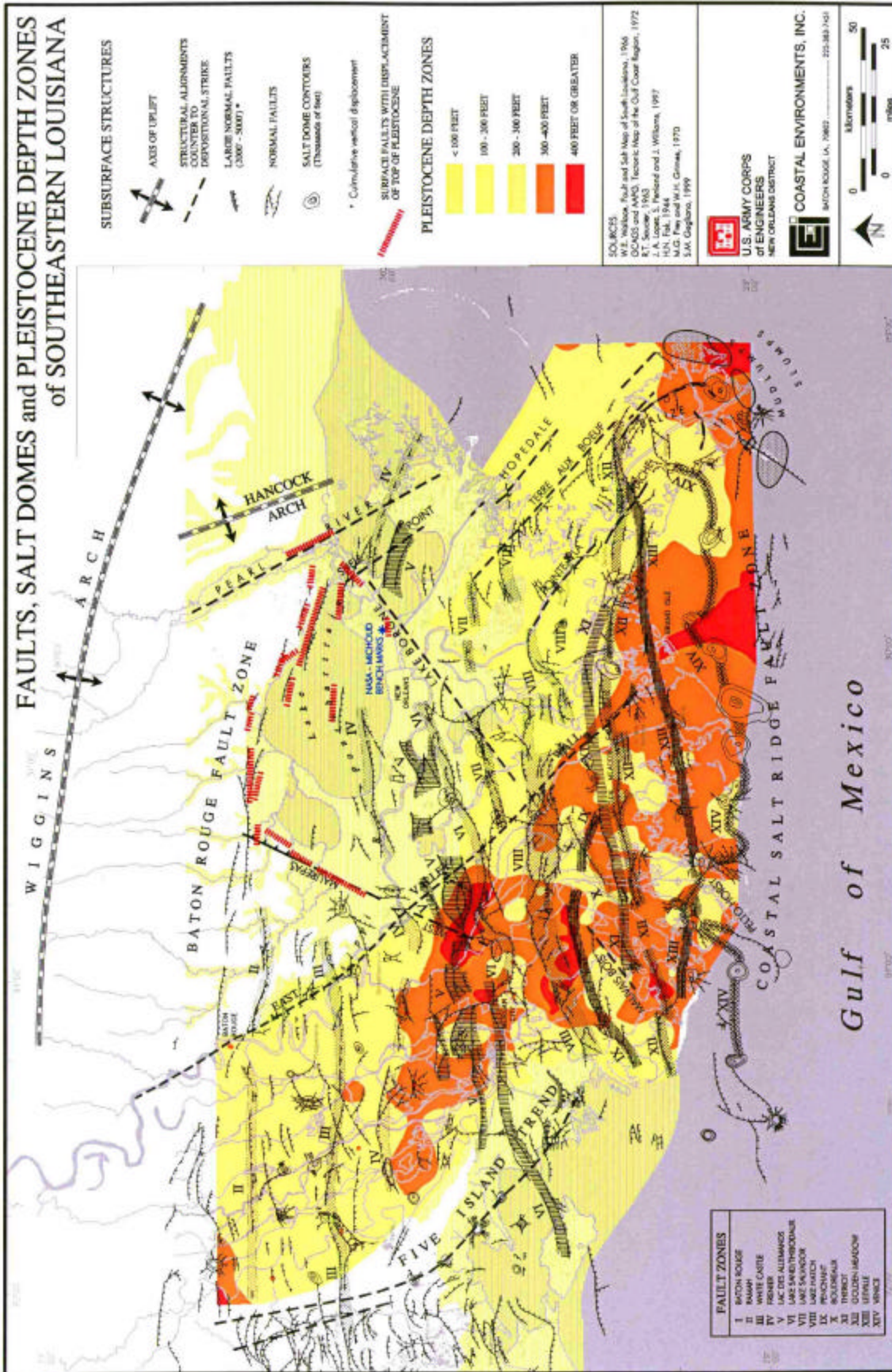


Figure 13. Depth to the top of the Pleistocene (data from L.D. Britsch 2001). Surface faults exhibiting displacement of the top of the Pleistocene and known subsurface faults are also shown.

In general, there are strong indications of fault control of topography on the top of the buried Pleistocene. A detailed investigation of this surface, which was beyond the scope of this study, should be made to verify the apparent correlation and continuity with faults known and identified within the Holocene deposits. Such a study would assist in long-term risk analysis.

Compaction of Holocene Sediments

Consideration was given to two hypotheses for the principal cause of higher subsidence rates in southeastern Louisiana: 1) compaction of poorly consolidated Holocene sediments and 2) movement of growth faults driven by geological processes.

Penland et al. (1994) reported the results of a study of the *Geological Framework, Processes and Rates of Subsidence in the Mississippi River Delta Plain*.⁷ Because of the relevance of this important work to the present study the summary is quoted in its entirety, as follows:

Subsidence is one of the most important processes driving coastal land loss in Louisiana. A direct relationship exists between high rates of subsidence and the high rates of coastal land loss found in the Mississippi River delta plain and its incised valley. The incised-valley of the Mississippi River was infilled with a series of backstepping delta plains composed of subsidence prone sediments during the Holocene transgression. The dominant processes driving the subsidence phenomenon are consolidation, settlement, diagenesis, and faulting. Rates of subsidence are the greatest over the incised valley-fill of the Mississippi River where they measure 0.5 – 1.0 cm/year. Subsidence rates are less than 0.5 cm/year east and west of the incised valley. The primary controls of subsidence are lithology, Holocene thickness, geochemical properties, and position relative to faulting. Subsidence has important implications for the success of coastal restoration projects and the safety of below sea level cities and communities in south Louisiana.

H. Roberts (1995) used radiometric dating of buried organic deposits from an east-west section of core holes to determine subsidence rates across the Central Louisiana coastal plain. The section crossed the buried Pleistocene alluvial valley wall. The data show rates of 0.3 ft/century (9 cm/century) for a shallow area of Holocene sediment fill over the Pleistocene surface increasing to 1.2 ft/century (10.5 cm/century) for an area of thick Holocene fill within the Pleistocene valley, a four fold increase. This section has been cited as an example of the relationship between thickness of Holocene sediments and subsidence rates (Reed 1995). Maps in the Roberts report show a regional fault between the two borings used in the comparison (Roberts 1995). Roberts co-authored a later article (Kuecher et al. 2001) that presented information showing that this is an active fault. It can be concluded from the Roberts report that the differences in deposition and

⁷ The study was part of a larger effort to evaluate the Critical Physical Processes of Wetland Loss, 1988-1994, funded by the U.S. Geological Survey. The project was coordinated by Harry H. Roberts, Ph.D., LSU, Coastal Studies Institute and conducted by a team of scientists from universities in Louisiana.

subsidence rates, as determined from radiometric dates from the two borings, may at least be partially related to movement along this fault.

As previously discussed this present study further examines the relative contributions of compaction and faulting to subsidence. We examined the geometry of the Holocene sediment wedge and contours on both the top and the bottom of the Pleistocene deposits. The data suggest that movement along regional faults and relative movement between salt domes and surrounding sediment continued throughout and after deposition of the Pleistocene. The thickest Holocene section overlies the thickest Pleistocene section. Both overlie the Terrebonne Trough and related listric faults of the extensional zone of the Eastern Province (see Figures 6 and 9). The distribution of surface faults was found to correlate with subsurface faults both in areas of thin and thick Holocene cover.

There is a synergistic relationship between the growth of delta lobes and fault movement. The pattern of prehistoric and historic delta lobes, as delineated by Frazier (1967), that formed during the past 5000 years indicates that faults have influenced the location and trend of trunk channels of the Mississippi River as well as many of its distributaries, and the locations of nodal points of subdelta lobes (Figure 14). Depocenters mark areas of concentrated delta building and sediment deposition. The down-dropped blocks of growth faults create depressions that “attract” distributaries and the distributaries branch into subdeltas that deposit pods of sediment (depocenters). A model developed by Curtis and Picou (1978) shows the relationship between growth faults and depocenters based on depositional sequences that occur repeatedly in the deposits of the Gulf Coast Salt Basin in Louisiana and Texas (Figure 15). The weight of the sediment pods may activate or contribute to the activation of the growth faults causing submergence and subsidence of the delta lobe surface during and after its formation. The subsidence in turn creates a new depression and the cycle repeats.

We conclude from the above, and other data, that compaction and fault movement are interrelated and both may contribute to subsidence. Compaction is a component of subsidence and may be important locally. However, results of this study suggest that vertical movement of faults, which in turn is largely driven by regional tectonic processes, is a major cause of subsidence.

SURFACE EXPRESSIONS OF FAULTS

Recent suspected fault events, as evidenced by surface movement along the Empire, Bastian Bay and Lake Boudreaux Faults, were found early in the study. These events occurred within the last 30 years and resulted in distinctive fault scarps and large breakup areas that occurred within short periods of time. Study of these areas and the fault events that caused them led to identification of distinctive fault-produced geomorphic signatures (Figure 16). These signatures were classified and described and a regional search was made of modern and historic photographs and maps for the telltale indicators of faulting.

Modern suspected fault events were identified using aerial photographs and photo based maps to establish the time of first appearance of associated breakup, fault alignments, fault scarps and other geomorphic signatures. The same techniques were used with older maps and surveys to identify possible historic fault events.

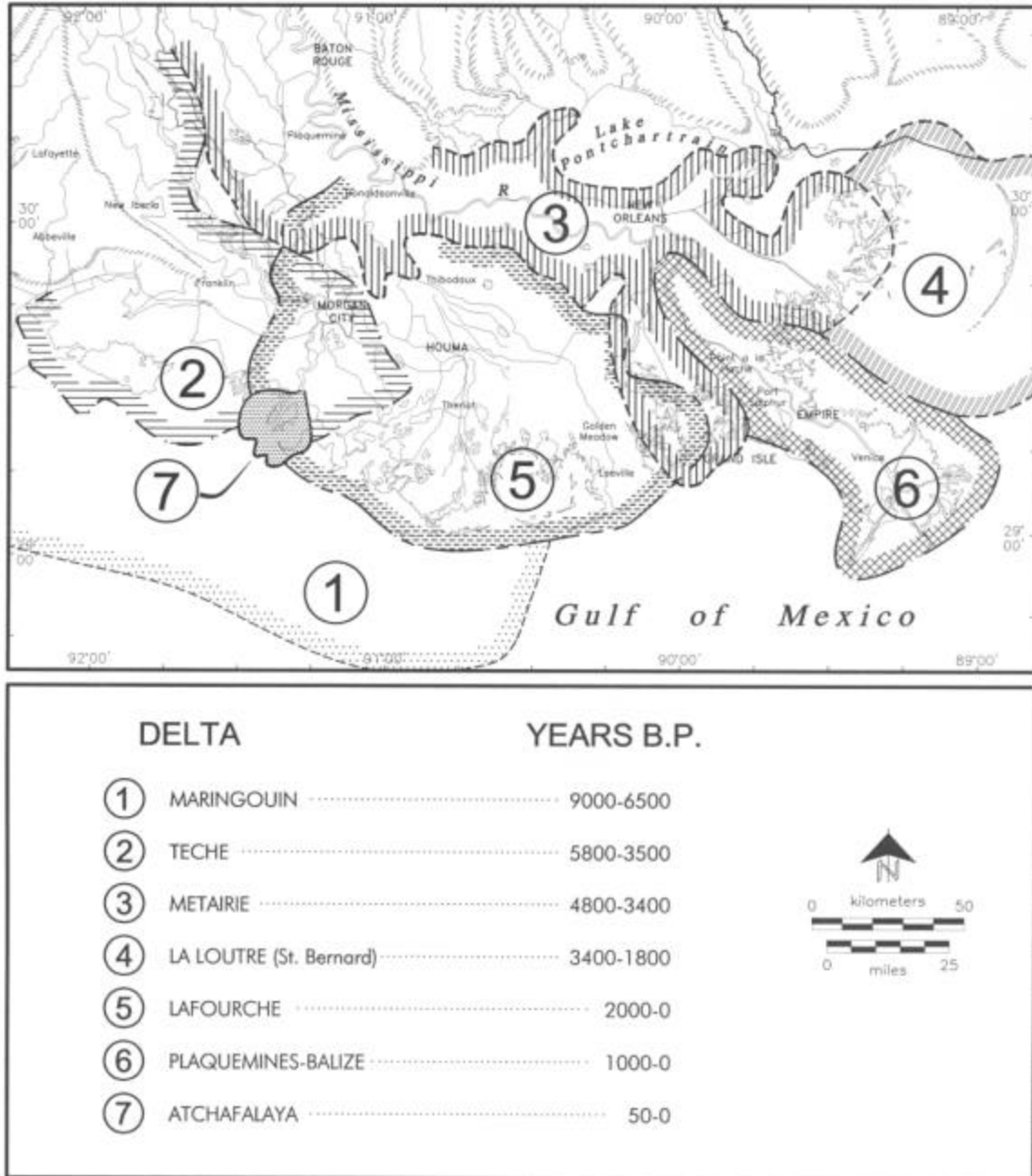


Figure 14. Holocene delta complexes (modified from Frazier 1967 and Weinstein and Gagliano 1985).

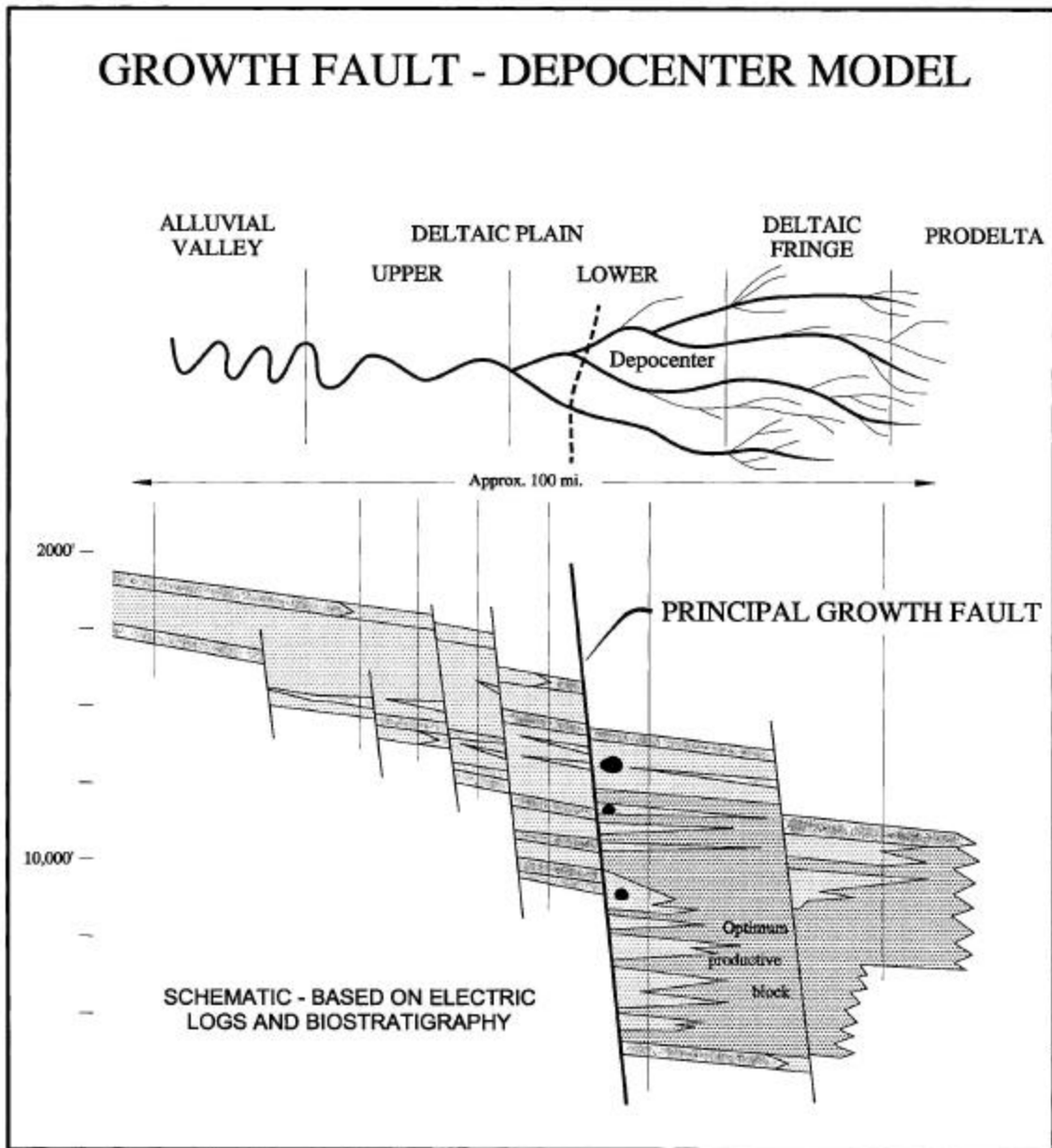
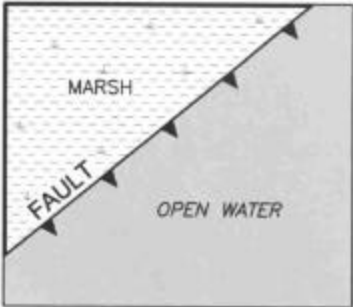


Figure 15. Sediment pods deposited in subdeltas are often found on the basinward side of growth faults. It is this coupling of deposition and fault movement that results in expansion of the thickness of sedimentary deposits on the downdropped blocks of growth faults (after Curtis and Picou 1978).

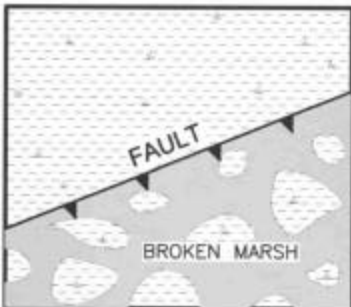
SURFACE EXPRESSION OF FAULTS

DISTINCT TRACES AND SCARPS



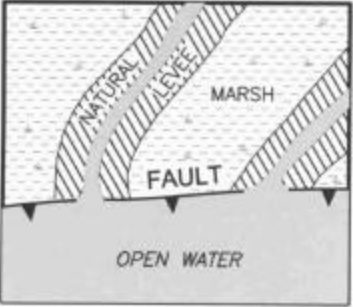
Bayou Long
Empire
Bastian Bay

Lake Boudreaux
Montegut



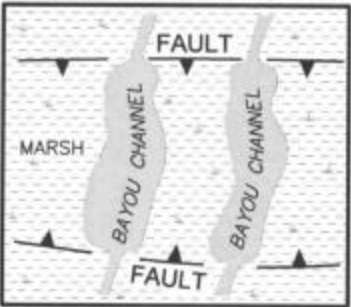
Lake Boudreaux
Montegut
Lake Enfermer

SEVERED RIDGES



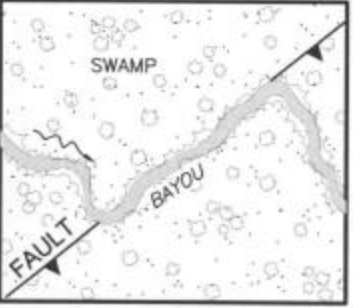
Bastian Bay
Bayou Terrebonne
Empire

BALLOONED CHANNELS



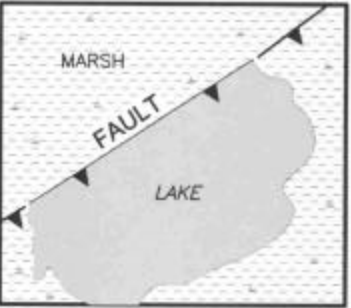
Bayou Perot
Bayou Rigolets
Lake Cheniere

STREAM ALIGNMENT



Amite River
Bayou Penchant
Bayou Barataria

SHORE ALIGNMENT



Lake DeCade
Lake Salvador
Lake Penchant

Figure 16. Surface expression of faults.

A distinction was made between lakes resulting from hurricanes and those that apparently resulted from fault movement. The effects of fault events (primary and secondary) in fresh marsh-swamp environments were studied using GIS comparisons of aerial photographs and vegetation maps published by O'Neil (1949), Chabreck and Linscombe (1978, 1988) and Chabreck et al. (1968). Shifts in vegetation zones were identified from the map comparisons. Stages of fault events were identified from the maps and images, including a brown marsh stage, and to some extent published descriptions, such as the vignette studies of Sasser et al. (1995).

Description, Evidence, and Mapping of Surface Faults

More than 100 apparent surface fault traces and/or scarps have been identified, indexed, classified and evaluated in Southeastern Louisiana. Their distribution is shown in Figure 17 and their nomenclature and characteristics are listed in Table 1.

A basic assumption of the study is that there are linkages between some apparent surface fault traces and scarps and underlying fault planes (Figure 18). A comparison was made between surface expression of faults and known subsurface faults and salt domes (Figure 19). The traces of subsurface faults have been derived from published sources and were originally determined through interpretation of seismic lines and cross-sections across the faults constructed from well data. Most surface traces and scarps can be correlated with known subsurface counterparts and are apparently associated with east-west trending growth faults lying south of the latitude of Baton Rouge. Another group is associated with the Baton Rouge and West Maurepas Faults in the Pontchartrain Basin. Some of the surface traces have no known subsurface counterparts. This suggests deficiencies in the subsurface database (seismic, well control, logs, etc.) and/or that new cracks have appeared as the faults continue to show surface expression as they move upward in the section, or that these traces are not linked to faults.⁸

A summary of the chronological analysis of the suspected surface expressions of faults is presented in Table 2. These data were developed primarily by systematic inspection of the appearance of the surface at locations of suspected faults on maps and aerial images taken at different times. This analysis provides the basis for determining when faults were active and for dating stages of development of fault events.

Stream Alignments and Water Body Shapes

Table 3 lists relationships between regional faults and the alignments of streams and shapes and alignments of water bodies. When the alignments and shapes of geomorphic features are viewed against the backdrop of the fault framework many relationships become apparent. This should not be surprising. Not only does fault movement influence both elevation and slope, fracturing and seepage along the fault planes create conditions that influence drainage patterns.

⁸ For a discussion of how faults change their configuration in response to stress fields and other factors as they move upward in section, the reader is referred to Kattenhorn and Pollard (2001).

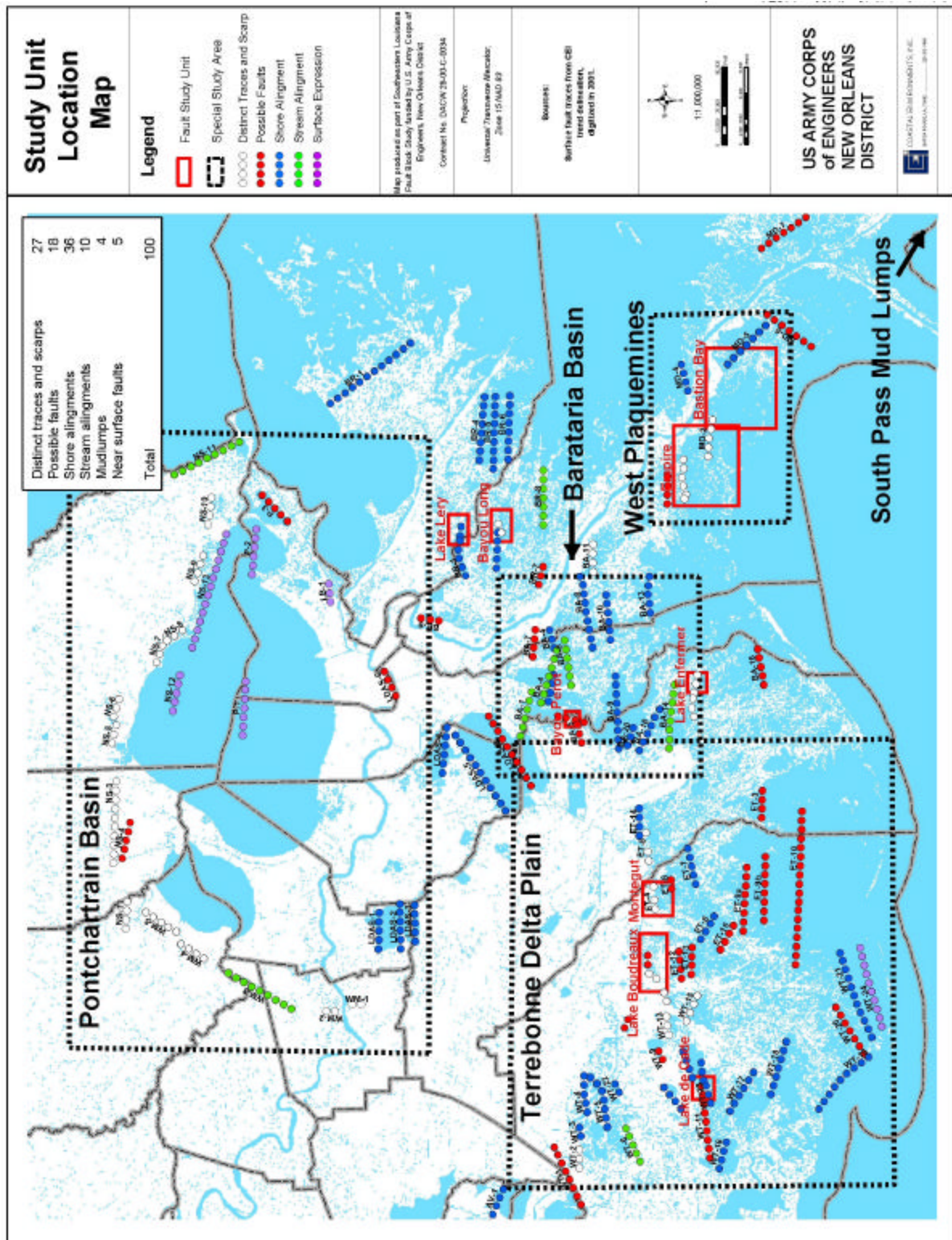


Figure 17. Map showing the locations of surface faults, case study areas and special study areas. (See Table 1).

Table 1. Surface Expression of Faults: Southeastern Louisiana (See Figures 17 and 19).

Index No.	Fault Zone	Name	Distinct Traces & Scarps	Possible Faults	Shore Alignments	Stream alignments	Mud-Lumps	Near-Surface Fault	Hurricane Lake	Totals
North Shore										
NS-1	I	Wadesboro	1							
NS-2	I	Lizard Creek	1							
NS-3	I	Ponchatoula	1							
NS-4	I	Joyce WMG		1						
NS-5	I	Madisonville	1							
NS-6	I	Houltonville	1							
NS-7	I	Lacombe	1							
NS-8	I	St. Tammany WR	1							
NS-9	I	Bayou Liberty	1							
NS-10	I	Weems Island	1							
NS-11	I	Pearl River				1				
NS-12	I	S. Causeway of Mandeville						1		
NS-13	I	Goose Point						1		
Subtotals			9	1	0	1	0	2	0	13
W. Maurepas										
WM-1	Vacherie Dome	Vacherie	1							
WM-2	Vacherie Dome	Gramercy	1							
WM-3	Maurepas	Blind River				1				
WM-4	Maurepas	Denison	1							
WM-5	Maurepas	Clio	1							
Subtotals			4	0	0	1	0		0	5
Pontchartrain										
			0							
P-1	III	Mid Lake Pontchartrain						1		
P-2	III	Pocket (South Point)						1		
P-3	III	Lake Catherine			1					
Subtotals			0	0	1	0	0	2	0	3
Lake Borgne										
LB-1	V	B. Bienvenu						1		
Subtotals			0	0	0	0	0	1	0	1
Biloxi										
BI-1	Pearl River	Lake Eugene	0		1					
Subtotals			0	0	1	0	0		0	1
Atchafalaya/Verret										
AV-1	VI	Lake Palourde	0		1					
Subtotals			0	0	1	0	0		0	1
Des Allemands/Salvador										
LDAS-1	V	Upper Lac Des Allemands			1					
LDAS-2	V	Middle Lac Des Allemands			1					
LDAS-3	V	Lower Lac Des Allemands			1					
LDAS-4	?	Lake Cataouatche			1					
LDAS-5	Lake Borgne	Lake Salvador	0		1					
Subtotal			0	0	5	0	0		0	5

Table 1. Continued.

Index No.	Fault Zone	Name	Distinct Traces & Scarps	Possible Faults	Shore Alignments	Stream alignments	Mud-Lumps	Near-Surface Fault	Hurricane Lake	Totals
Breton										
BR-1	VII	Lake Lery			1					
BR-2	VII/VIII	Grand Lake			1					
BR-3	VIII	Bayou Long	1							
BR-4	VII/VIII	Lake Coquille			1					
BR-5	VII/VIII	Lake Machias			1					
BR-6	VIII	Lake Calibassa			1					
BR-7	VIII	Phoenix							1	
BR-8	?	Oak River				1				
BR-9	Hurricane Lake (?)	Forty Arpent							1	
Subtotal			1	0	5	1	0		2	9
West Terrebonne										
WT-1	VI/VII	Bayou Chene		1						
WT-2	VIII	Black Lake	1							
WT-3	VIII	W. of Hackberry		1						
WT-4	VIII	Lake Blackberry				1				
WT-5	VIII	Orange Grove			1					
WT-6	IX	Penchant Bend				1				
WT-7	IX	Lake Hatch		1						
WT-8	X	Lake Penchant			1					
WT-9	X	Mauvais Bois		1						
WT-10	IX/X	Point Au Fer		1						
WT-11	XI	Lake Long		1						
WT-12	XI	Lake Decade			1					
WT-13	XI	Theriot	1							
WT-14	XI	E. Theriot	1							
WT-15	XI	Falgout Canal		1						
WT-16	XI	Lost Lake			1					
WT-17	?	Lake Mechant			1					
WT-18	XII/XIII	Caillou Lake			1					
WT-19	Pelto Horst ?	Caillou Bay			1					
WT-20	Pelto Horst ?	Pelican Lake			1					
WT-21	Pelto Horst ?	Lake Pelto			1					
WT-22	IX	Long Canal		1						
WT-23	XII	S. Lake DeCade			1					
Subtotal			3	8	10	2	0		0	23

Table 1. Continued.

Index No.	Fault Zone	Name	Distinct Traces & Scarps	Possible Faults	Shore Alignments	Stream alignments	Mud-Lumps	Near-Surface Fault	Hurricane Lake	Totals
<i>East Terrebonne</i>										
ET-1	X	Lake Boudreaux	1							
ET-2	IX	N. Chauvin Basin	1							
ET-3	XIII	Lake Raccourci			1					
ET-4	XI	Montegut	1							
ET-5	XI	Point au Chien	1							
ET-6	XI	East of Wonder Lake		1						
ET-7	XI	Isle Jean St. Charles			1					
ET-8	XII	N. Lower Madison Bay			1					
ET-9a	XII/XIII	Lake Barre		1						
ET-10	XII/XIII	Bayou Terrebonne		1						
ET-11	Hurricane Lake	Wonder Lake							1	
ET-12	XI	Hog Point		1						
ET-13	XI	Lake Gero		1						
ET-14	XI	Bully Camp	1							
ET-15	XI	Pt. Au Chein WMA-N	1							
ET-16	XI	S. Lower Madison Bay	1							
ET-17	XII	S. Lake Barre	1							
<i>Subtotal</i>			4	5	3	0	0		1	13
<i>Barataria</i>										
BA-1	?	N. Bayou Perot				1				
BA-2	?	Bayou des la Fleur				1				
BA-3	VIII	S of B. Dupont			1					
BA-4	VIII	Bayou Dupont				1				
BA-5	VIII	S. Bayou Perot				1				
BA-6	VIII	Bayou Barataria				1				
BA-7	?	Alliance		1						
BA-8	VIII	Round Lake			1					
BA-9	VIII	Little Lake			1					
BA-10	VIII	Roquette Bay			1					
BA-11	VIII	Diamond	1							
BA-12	XI	South of Little Lake	1							
BA-13	XI	Bay Baptiste			1					
BA-14	XII	Bayou Lours	1							
BA-15	XII	Lake Enfermer	1							
BA-16	XIII	Caminada Bay			1					
BA-17	VIII	Sea Deuce			1					
BA-18	XI	John the Fool Bayou			1					
BA-19	VIII	Little Temple		1						
BA-20	XI	Brusle Lake			1					
BA-21	Hurricane Lake	Lac des Isles							1	
<i>Subtotal</i>			4	1	8	5	0	0	0	18

Table 1. Concluded..

Index No.	Fault Zone	Name	Distinct Traces & Scarps	Possible Faults	Shore Alignments	Stream alignments	Mud-Lumps	Near-Surface Fault	Hurricane Lake	Totals
<i>Mississippi Delta</i>										
MD-1	XII	Empire	1							
MD-2	XII	Bastian Bay	1							
MD-3	XI ?	Bay de la Cheniere		1						
MD-4	XII	Bay Denesse			1					
MD-5	Pointe a la Hache	Yellow Cotton Bay			1					
MD-6	XIV	West Bay		1						
MD-7	Balize Loop	Cubits Gap		1						
MD-8	Mudlumps	Southwest Pass					1			
MD-9	Mudlumps	South Pass					1			
MD-10	Mudlumps	Pass a Loutre					1			
MD-11	Mudlumps	Balize Bayou					1			
<i>Subtotals</i>			2	3	2	0	4	0	0	11
TOTALS			27	18	36	10	4	5	3	103
TOTAL NUMBER OF AREAS									103	

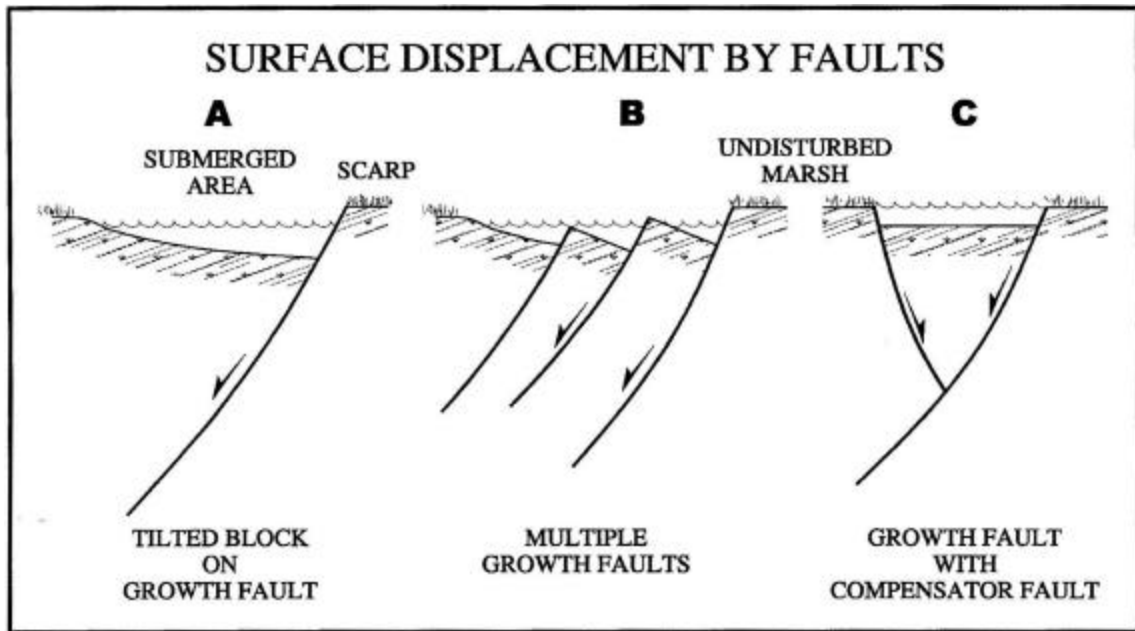


Figure 18. Common types of faults found in the study area showing linkage between surface features and underlying fault planes. Based on surface and subsurface data.

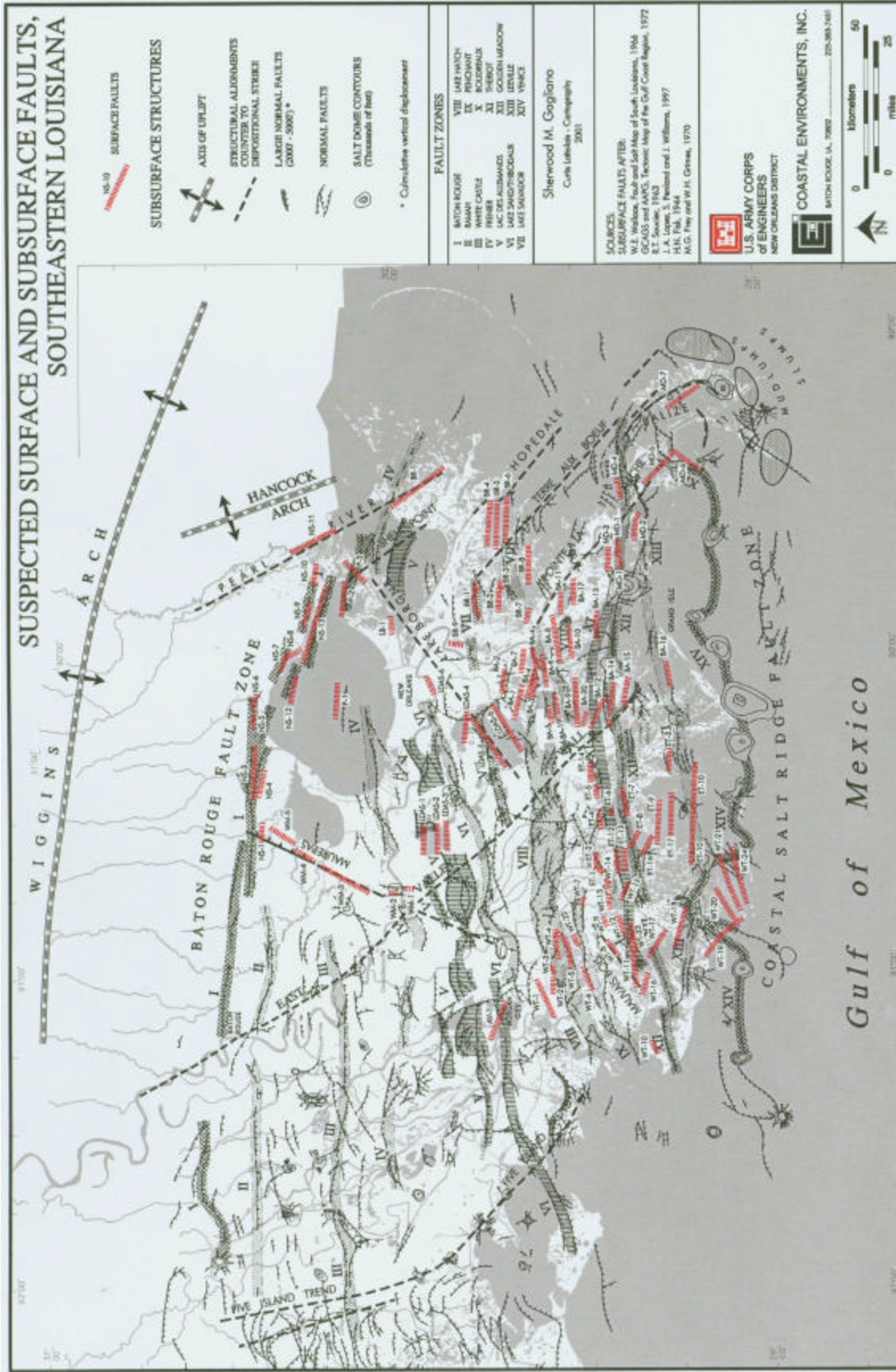


Figure 19. Map showing the relationship between suspected surface and subsurface faults. (See Table 1).

Table 2. Results of Chronological Analysis of Suspected Surface Fault Signatures.

INDEX NO.	FAULT SIG.	1764	1778	1817	1842	1863	1859-79	1915	1930	1932	1933-34*	1945	1949	1950	1955-56**	1962	1963	1964	1965	1966	1967	1971	1972	1976 CIR	1980 CIR	1982 CIR	1990
AV-1	L. Palourde	NSD	SOM	SA OW	SOM	SOM	SA						SD										SA SD		SOM	SOM	SA
BA-1	N. Bayou Perot	NSD	NSD	SD	SOM	SOM	SD						SD BS OW										SA SD BS	SOM	FS SA SD OW BKM	FS SA SD OW BKM	FS
BA-2	Bayou de la Fleur	NSD	NSD	SOM	SOM	SOM	NSD						SD BS										SD BS	SOM	SD BS	SD BS BKM	SD
BA-3	S. of Bayou Dapout	NSD	NSD	SD	SOM	SOM	SD						SD BS										SD BS	SOM	SD BS	SD BS BKM	SD
BA-4	Bayou Dapout	NSD	NSD	NF	SOM	SOM	SD					HU	SD BS										SD BS	SOM	IFT	IFT BKM	IFT?
BA-4a	S. of Bayou Dapout	NSD	SOM	SOM	SOM	SOM	SD						SD										BKM	SOM	SOM	SOM	IFT
BA-5	S. Bayou Perot	NSD	NSD	FS OW	SOM	SOM	SD		PD				SD BS										SD OW	SOM	SOM	SOM	IFT BKM
BA-6	Bayou Barataria	NSD	NSD	SOM	SOM	SOM	SD						SD		BKM								SD	SOM	SOM	SOM	IFT BKM
BA-7	Alliance	NSD	NSD	SOM	SOM	SOM	SD						SD										IFT	SOM	SOM	SOM	IFT BKM
BA-8	Round Lake	NSD	NSD	SOM	NSD	SD	SD SA OW						SA BS OW										IFT SD OW	SOM	SOM	SOM	IFT BKM
BA-9	Little Lake	SOM	NSD	OW SD	NSD	SOM	BS SD						BS SA SD OW										SA OW	SOM	SOM	SOM	SA BKM OW
BA-10	Roquette Bay	NSD	NSD	SOM	NF	SD	SD OW						BS SD										SD BS OW	SD BS OW	SD BS OW	BKM	BKM
BA-11	Diamond	NSD	NSD	SOM	NF	SD	SD						SD					NF					IFT	SOM	SOM	SOM	FT
BA-12	S. of Little Lake	NSD	NSD	SD	NSD	SOM	NF						SD										BKM	FS BKM	FS BKM	FS BKM	BKM
BA-13	Bay Baptiste	NSD	NSD	SOM	FS	NSD	FS SA OW						SA BKM										FS SA	FS SA	FS SA	FS7 SA	FS7 SA
BA-14	B. L'Ours	NSD	NSD	NSD	NSD	SD	SD						SD		LS								SD BKM	SD BKM	SD BKM	SD BKM	SA
BA-15	L. Enfermer	NSD	NSD	NSD	NSD	BS	BS						SD										SA BKM	IFT BKM	IFT BKM	IFT BKM	FS OW

Table 2. Continued

INDEX NO.	FAULT SIG.	1764	1778	1817	1842	1863	1859-79	1915	1930	1932	1933-34*	1945	1949	1950	1955-56**	1962	1963	1964	1965	1966	1967	1971	1972	1976 CIR	1980 CIR	1982 CIR	1990		
BA-16	Camina Bay	NSD	NSD	NSD	NSD	NSD	OW						OW		BKM OW									OW	OW	SOM	OW		
BA-17	Sea Deuce	NSD	NSD	SOM	NF	SD	SD						SD											IFT BKM	SOM	SOM	BKM OW	OW	
BA-18	John the Fool Bayou	NSD	NSD	NSD	NSD	NSD	NSD		SD BS				SD		SD BS BKM									IFT BKM	BKM OW	SOM	SOM	FS OW BKM	OW
BA-19	Little Temple	NSD	NSD	NSD	NSD	NSD	NSD		SA BS OW				SD SA											IFT BKM	SOM	SOM	IFT BKM	SA OW BKM	
BA-20	Brusle Lake	NSD	NSD	NSD	NSD	NSD	NSD						SD SA											SA OW	SOM	SOM	SA OW BKM	SA OW BKM	
BA-21	Lac des L'isle							HU LK																					
BL-1	L. Eugene	NSD	NF	SOM	SOM	SOM	BKM						BKM											SOM	BKM OW	BKM OW	BKM OW	BKM OW	
BR-1	L. Lery	NSD	FNM	SOM	SOM	SOM	HL						HL											SOM	HL	HL	HL	HL	HL
BR-2	L. Petit - Grand L.	NSD	FNM	SOM	SOM	SOM	BS						SD BS OW BKM											SOM	FS BKM SD OW	FS BKM SD OW	FS BKM SD OW	FS BKM SD OW	FS BKM SD OW
BR-3	B. Long (E. of L. Petit)	NSD	FNM	SOM	SOM	SOM	SD						NF BKM											IFS BKM OW	SOM	IFS BKM OW	IFS BKM OW	IFS BKM OW	IFS BKM OW
BR-4	L. Coquille	NSD	OW BKM	SOM	SOM	SOM	BKM						OW BKM											SOM	FS BKM OW	FS BKM OW	FS BKM OW	FS BKM OW	FS BKM OW
BR-5	L. Machias	NSD	OW BKM	SOM	SOM	SOM	BKM						OW BKM											SOM	FS BKM OW	FS BKM OW	FS BKM OW	FS BKM OW	FS BKM OW
BR-6	L. Calibasse	NSD	OW BKM	SOM	SOM	SOM	BKM						OW BKM											SD BKM	SD BKM	SD BKM	SD BKM	SD BKM	SD BKM
BR-7	Phoenix	NSD	NF	SOM	SOM	SOM	TP						BKM											BKM OW	BKM OW	BKM OW	BKM OW	BKM OW	BKM OW
BR-8	Oak River Bay	NSD	OW BKM SA	SOM	SOM	SOM	SD						OW BKM SD											SD BKM	SD BKM	SD BKM	SD BKM	SD BKM	SD BKM
BR-9	Tiger Ridge (Forty Arpent)	NSD	NF	SOM	SOM	SOM	NF						NF																
DAS-1	U. Lac des Allemands	SOM	NSD	SA OW	SOM	SOM	SA						HL OW											SOM	OW	OW	OW	OW	OW

Table 2. Continued

INDEX NO.	FAULT SIG.	1764	1778	1817	1842	1863	1859-79	1915	1930	1932	1933-34*	1945	1949	1950	1955-56**	1962	1963	1964	1965	1966	1967	1971	1972	1976 CIR	1980 CIR	1982 CIR	1990
DAS-2	M. Lac des Allemands	SOM	NSD	SA OW	SOM	SOM	SA						HL OW OW SD BS	BKM OW		SA OW							SA	SA	SOM	IFT BKM OW	OW
DAS-3	L. Lac des Allemands	SOM	NSD	SA OW	SOM	SOM	SA						HL OW OW SD BS	BKM OW		SA OW							SA	SA	SOM	IFT BKM OW BS	OW BS
DAS-4	L. Catawache	NSD	NSD	SA OW	SOM	SOM	SA			SD BS OW		HL SA	HL SA			SA OW							SA	SA	SOM	IFT BKM OW BKM	OW BKM
DAS-5	L. Salvador	NSD	NSD	SA OW	SOM	SOM	SA			SA OW		HL SA	HL SA			SA OW							SA	SA	SOM	IFT BKM OW SA	SA OW
DAS-7	S. Lake Salvador	NSD	NSD	SA OW	SOM	SOM	SA OW					SA OW BS	SA OW BS										OW BKM SD	OW BKM SD	SOM	IFT BKM OW SD	SD OW
DAS-6	Miss. River Bridge	SD	SD	SD	SOM	SOM	SD						SD										SD	SD	SOM	IFT BKM OW SD	SD OW
ET-1	Lake Boudreaux	SOM	SOM	NSD	SOM	SOM	NF						NF		NF									IFT OW	IFT BKM OW SA	SOM SA	OW FS BKM SA
ET-2	N. Chauvin Basin	SOM	SOM	NSD	SOM	SOM	NF						NF		NF									BKM	SOM	SOM	OW BKM
ET-3	L. Raccourci	SOM	SOM	FNM	SOM	SOM	IFT						OW SD BKM											OW	OW	SOM	OW FS BKM SA
ET-4	Montegut	SOM	SOM	FNM	SOM	SOM	NF						NF		NF									IFT BKM	IFT BKM	SOM BKM	OW BS BKM
ET-5	Pt. Au Chien	SOM	SOM	NSD	SOM	SOM	NF						NF		BS OW									BKM BS	BKM BS	SOM BKM	OW SA BKM
ET-6	East of Wonder Lake	SOM	SOM	FNM	SOM	SOM	NF						SD		BM									IFT BKM	IFT BKM	SOM BKM	OW BKM
ET-7	Isle St. Jean Charles	SOM	SOM	NSD	SOM	SOM	NF						SD		BKM									BKM BKM	IFT BKM	SOM BKM	SD BKM
ET-8	Lower Madison Bay	SOM	SOM	NSD	SOM	SOM	NF						BS		IFT (?)									BRN BKM	IFT BKM	SOM BKM	OW BKM
ET-9a	L. Barre	SOM	SOM	FNM	SOM	SOM	NF						BS BKM											BKM BKM	IFT BKM	SOM BKM	SA SA BKM
ET-9b				FNM	SOM	SOM	SD						OW											OW	OW	OW	OW BKM

Table 2. Continued.

INDEX NO.	FAULT SIG.	1764	1778	1817	1842	1863	1859-79	1915	1930	1932	1933-34*	1945	1949	1950	1955-56**	1962	1963	1964	1965	1966	1967	1971	1972	1976 CIR	1980 CIR	1982 CIR	1990	
ET-10	Terrebonne Bay	SOM	SOM	SA OW	SOM	SOM	SA OW				OW								OW				OW SDR					
ET-11	Wonder Lake							HU LK																				
ET-12	Hog Point	SOM	SOM	FNM	SOM	SOM	SA OW						HL SD SA BS										SA SA OW	SA SA OW			BKM SA OW BKM	
ET-13	Lake Gero	SOM	SOM	FNM	SOM	SOM	NF						BS										IFT BKM	BKM BKM			OW BKM	
ET-14	Bully Camp N.-Pt. au Chien WMA	SOM	SOM	NSD	SOM	SOM	NSD						NF										BKM	BKM			BKM OW	
ET-15	S.-Pt au Chien WMA																											
ET-16	S. Lower Madison Bay	SOM	SOM		SOM	SOM	NF						NF										IFT BKM	BKM BS				
ET-17	Empire	NF	NSD	SOM	SD BS	SD BS	SD						SD		NF								IFT BNM	FS FS			FS OW BKM	
MD-2	Bastian Bay	NF	NSD	SOM	SD BS	SD BS	SD BS						SD BS										IFT BNM	FS FS			FS OW BKM	
MD-3	Bay de la Chentiere	NF	NSD	SOM	SD BS	SD BS	SD						SD BS										IFT BNM	FS FS			FS OW BKM	
MD-4	Bay Denesse	SA BKM	NSD	SOM	SOM	SA OW	NF						SA OW										IFT BNM	FS FS			FS OW BKM	
MD-5	Yellow Cotton Bay	SA BKM	SA BKM	SOM	SOM	SA OW	SA OW						NF										BKM BKM	BKM BKM			BKM OW	
MD-6	West Bay	SA BKM	SA BKM	SOM	SOM	SA OW	OW						SD										BKM BKM	BKM BKM			OW BKM	
MD-7	Cubits Gap	NF	SD	SOM	SOM	SA OW	OW						SD										IFT BNM	FS FS			FS OW BKM	
MD-8	Southwest Pass Area	Mud Lump Area																										
MD-9	South Pass Area	Mud Lump Area																										
MD-10	Pass a Loure Area	Mud Lump Area																										
MD-11	Balize Bayou Area	Mud Lump Area																										

Table 2. Continued.

INDEX NO.	FAULT SIG.	1764	1778	1817	1842	1863	1859-79	1915	1930	1932	1933-34*	1945	1949	1950	1955-56**	1962	1963	1964	1965	1966	1967	1971	1972	1976 CIR	1980 CIR	1982 CIR	1990
NS-1	Wadesboro	NSD	NSD	SD	SOM	SOM	SD						NSD SD			SOM						SOM		FT SD	SOM	FS	FS BKM SP SD
NS-2	Lizard Creek	NSD	NSD	NSD	SOM	SOM							NSD			SOM						SOM		SOM	SOM	SD	SD
NS-3	Ponchatoula	SD	SD	SD	SOM	SOM	SD						NSD SD			SOM						SOM		FS	SOM	FS	FS OW SP
NS-4	Joyce WMA	NF	NF	NF	SOM	SOM							NF			SOM						SOM		NF	SOM	NF	OW
NS-5	Madisonville	NSD	SD	NSD	SOM	SOM	SD						NSD SD			SOM						SOM		FT	SOM	FS	FS OW BKM SP
NS-6	Houliouville	NSD	SD	NSD	SOM	SOM	SD						NSD SD			SOM						SOM		FT	SOM	FT	FT SD
NS-7	Lacombe	NSD	SA	SOM	SOM	SOM	SD						SD FS			SOM						SOM		FS	SOM	FS	FS BKM SD OW
NS-8	St. Tammany WR	NSD	NSD	SOM	SOM	SOM	FS						SD FS			SOM						SOM		FS	SOM	FS	FS BKM OW
NS-9	Bayou Liberty	NSD	SD	SOM	SOM	SOM	SD						SD			SOM						SOM		FS	SOM	OW	FS BKM OW
NS-10	Weems Island	NSD	NSD	SOM	SOM	SOM	SD						SD FS			SOM						SOM		FT	SOM	FS	FS BKM OW
NS-11	Pearl River	SD	SD	SOM	SOM	SOM	SD						SD			SOM						SOM		SD	SOM	SD	SD
NS-12	Mandeville (Causeway)	OW	OW	OW	SOM	SOM	OW						OW			SOM						SOM		OW	SOM	OW	OW OS
NS-13	Goose Point	OW	OW	OW	SOM	SOM	OW						OW			SOM						SOM		OW	SOM	OW	OW
P-1	Mid. L. Ponchartrain	OW	OW	OW	SOM	SOM	OW						OW			OW						OW		OW	OW	OW	OW
P-2	Pocket (S. Point)	OW	OW	SOM	SOM	SOM	OW						OW			SOM						SOM		OW	SOM	OW	OW OS (1991- 1996))
P-3	L. St. Catherine	NSD	SA	SOM	SOM	SOM	NF						OW			OW						OW		OW	OW	OW	OW OS SA BKM
WM-1	Vacherie	SOM	SD	NSD	SOM	SOM	NSD						NF			NSD						NSD		SOM	SOM	SD	SD
WM-2	Gramercy	SOM	NSD	NSD	SOM	SOM	NSD						NF			SD						SD		SOM	SOM	IFT	SD

Table 2. Continued.

INDEX NO.	FAULT SIG.	1764	1778	1817	1842	1863	1859-79	1915	1930	1932	1933-34*	1945	1949	1950	1955-56**	1962	1963	1964	1965	1966	1967	1971	1972	1976 CIR	1980 CIR	1982 CIR	1990
WM-3	Blind River	SD	NSD	SD	SOM	SOM	SD						SD										SOM	SD	SD	SD	
WM-4	Denson	SD	NSD	NSD	SOM	SOM	SD						SD										SOM	FT	FT	FT	FS
WM-5	Clio	NSD	NSD	NSD	SOM	SOM	NSD						SD										SOM	FS	FS	OW	SD
WT-1	Bayou Chene	SOM	SOM	NSD	SOM	SOM							BS										SOM	SOM	SOM	SD	
WT-2	Black Lake	SOM	SOM	SD	SOM	SOM	FNM						SD										SOM	SOM	SOM	BKM	
WT-3	W. of L. Hackberry	SOM	SOM	SD	SOM	SOM	NSD						NF					BS					SOM	SOM	SOM	BKM	
WT-4	Lake Hackberry	SOM	SOM	SD	SOM	SOM	SD						SD					BS					SOM	SOM	SOM	BKM	
WT-5	Orange Grove	SOM	SOM	NSD	SOM	SOM	NSD						BS					BS					SOM	SOM	SOM	OW	
WT-6	Penchant Bend	SOM	SOM	FNM	SOM	SOM	SD						SD					SD					SOM	SOM	SOM	BKM	
WT-7	Lake Hatch	SOM	SOM	NSD	SOM	SOM	SD						OW										SOM	SOM	SOM	IFT	
WT-8	Lake Penchant	SOM	SOM	FNM	SOM	SOM	FNM						SA					IFS					SOM	SOM	SOM	OW	
WT-9	Manvais Bois	SOM	SOM	FNM	SOM	SOM	FNM						NF					NF					SOM	SOM	SOM	NF	
WT-10	Pt. Au Fer	SOM	SOM	NSD	SOM	SOM	SD						SD										SOM	BKM	OW	BS	
WT-11	Lake Long	SOM	SOM	NSD	SOM	SOM	FNM						SD										SOM	OW	SOM	BS	
WT-12	Lake De Cade	SOM	SOM	FNM	SOM	SOM	BS						SA					FS					SOM	SA	OW	FS	
WT-13	Theriot	SOM	SOM	FNM	SOM	SOM	FNM						NF					NF					FS	FS	OW	BS	
WT-14	E. Theriot	SOM	SOM	NSD	SOM	SOM	FNM						NF					BKM					IFT	IFT	IFT	IFT	
WT-15	Falgout Canal	SOM	SOM	SD	SOM	SOM	SD						NF										OW	OW	OW	OW	

Table 2. Concluded.

INDEX NO.	FAULT SIG.	1764	1778	1817	1842	1863	1859-79	1915	1930	1932	1933-34*	1945	1949	1950	1955-56**	1962	1963	1964	1965	1966	1967	1971	1972	1976 CIR	1980 CIR	1982 CIR	1990
WT-16	Lost Lake	SOM	SOM	SD	SOM	SOM	SA						SA OW										FS SA	SOM	SA	SOM	FS SA OW BKM BS
WT-17	L. Mechant	SOM	SOM	FNM	SOM	SOM	SA						SA OW SD					BKM OW					IFT SA	SOM	SA	OW SOM	OW BKM
WT-18	Caillou Lake	SOM	SOM	SD	SOM	SOM	SA						SA										BKM OW	SOM	FS	SD OW	FS
WT-19	Caillou Bay	SOM	SOM	FNM	SOM	SOM	W						FS SA										FS SA	SOM	SA	OW SOM	FS SA OW
WT-20	Pelican Lake	SOM	SOM	SA	SOM	SOM	SD						OW										FS BKM SA SA OW	SOM	SA	OW SOM	FS BKM OW SA
WT-21	Lake Pelto	SOM	SOM	SA	SOM	SOM	SA						OW										FS BKM OW	SOM	FS	OW SOM	FS OW BKM
WT-22	Long Canal	SOM	SOM	NSD	SOM	SOM	FNM						NF										BKM	SOM	SOM	OW BKM	SA OW BKM
WT-23	S. Lake De Cade	SOM	SOM	NSD	SOM	SOM	FNM						SD BS										SD BKM	SOM	BKM	OW BKM	SA OW BKM
WT-24	Pelto Dome	SOM	SOM	SA	SOM	SOM	SA						OW										OW	OW	OW	OW	OW

* US&GS T & H Charts

** Annamann & Tobin Aerial Photo Mosaics

BS - Ballooned Stream
 BKM - Broken Marsh
 BNM - Brown Marsh
 FNM - Feature Not Mapped
 FS - Fault Scarp
 FT - Fault Trace

HU - Hurricanes
 HL - Historic Lake
 IFT - Incipient Fault Trace
 LO - Lake Offset
 LK - Lake
 NF - No Fault

NLL - Notched Natural Levee
 NSD - Not Sufficient Detail
 OS - Offset Structure
 PD - Ponds
 SA - Shoreline Alignment
 SD - Stream Diversion

SDR - Severed Distributary Ridge
 SOM - Site Off Map
 SP - Swamps
 TP - Trembling Prairie

Table 3. Stream Segment and Water Bodies Which Appear to be Fault Influenced.

Fault	Case Studies	Mississippi River Channel & Tributaries (Active and Relict)	Lake & Bays
I Baton Rouge			Some lobes of Lake Pontchartrain
II Ramah		2. Miss. R., Longwood Bend	
		3. Miss. R., Plaquemine Bend	Lake Maurepas
III White Castle		4. Miss. R., St. Gabriel Bend	
		5. Miss. R., Dorceyville Bend	
IV Frenier		7. Miss. R., St. James to Wallace Reach a. B. Teche, New Iberia Bend	
		8. Miss. R., Laplace to Luling	
V Lac Des Allemands		9. Miss. R., St. Rose to Kenner b. B. Teche Franklin Bend	Lac Des Allemands
		10. Miss. R., Kenner to Avondale	
VI Lake Sand/Thibodaux		11. Miss. R., Avondale to Carrolton Bend	Lake Palourde
		Metairie-Sauvage Relict Miss. R. Course c. B. Cypremort Relict Miss. R. Course	
		12. Miss. R., Caernaveron to English Turn j Bayou Terre aux Boeufs Relict Dist.	
VII Lake Salvador	BR-1 Lake Lery		Lake Salvador
		14. Miss. R., Live Oak to Myrtle Grove	
VII Lake Hatch	BA-5 Bayou Perot BR-2 Bayou Long	g. Teche-Miss. Relict Course h. Bayou Barataria Bend, Relict Dist.	Lake Petit Grand Lake
		15. Miss. R., Myrtle Grove to Port Sulphur	
		16. Miss. R., Empire to Triumph	
IX Penchant			
X Boudreaux	ET-1 Lake Boudreaux	f. B. Mauvais Bois, Relict Miss. Dist.	
XI Theriot	Et-4 Montegut WT-12 Lake de Cade (& WT-31)		Little Lake (Lower) Lake de Cade
XII Golden Meadow	MD-1 Empire MD-2 Bastian Bay BA-15 Lake Enfermer		
XIII Leeville		17. Miss. R., Fort Bend Bayou Terrebonne Bend & Severance	Bay Joe Wise Bastian Bay Shell Island Bay Scofield Bay Skipjack Bay English Bay Bay Jacquin Cyprien Bay Caminada Bay
East Valley		1. Miss. R., B. Sara to Solitude Pt. 6. Miss. R., Burnside to St. James	
West Maurepas		Amite River Bend Blind Rive alignment	Lake Maurepas
Lake Borgne			Lake Salvador
Terre aux Boeuf		h. B. Terre aux Boeuf, Relict Miss. R., Dist.	
Pointe a La Hache		12. Miss. R., Reach - Live Oak to Myrtle Grove 13. Miss. R. Reach - Myrtle Grove to Port Sulphur	

Throughout the Quaternary (and long before) the trunk channel of the Mississippi River and its major distributaries in the lower valley and deltaic plain have been influenced by faults. These streams generally cut across the structural grain of the region. The modern course of the Mississippi River, for example, climbs down a stairway of fault blocks, many of which slope into the faults. The fault planes and backslope direct the location of the channel.

Figure 20 shows interpreted relationships between bends and reaches of the Mississippi River from north of Baton Rouge to the gulf. Reaches one and six follow the East Valley Wall Alignment. The acute bends at two through five occur where the river channel crosses regional faults. At Reach seven, the Mississippi makes an almost 90-degree turn to the east and takes a 20 mi (32.1 km) detour before swinging back to the south and continuing its journey to the gulf. Reach seven (the German Coast) follows the Frenier Fault. Reaches nine and eleven also follow fault zones and the reverse bend at English Turn (Bend 11). Reaches twelve through fourteen are long, straight reaches controlled by the Pointe La Hache alignment. The acute bend at Fort Jackson and Fort St. Phillips appears to be controlled by the convergence of the Empire and Bastian Bay Faults.

Also shown in Figure 20, are segments of relict Mississippi River distributaries that appear to have been fault controlled when the distributaries were active (see Table 3). Places where the river channel intersects a fault at a bend are prone to levee breaks and bank slumps (Fisk 1944 and Saucier 1963).

CASE STUDIES OF SURFACE FAULTS

Nine of the suspected surface faults were selected for site-specific field study, which included shallow borings across apparent fault scarps and traces (See Figure 17). Study of the faults included analysis of historic and modern maps and aerial images, field sampling across the fault scarps and traces (vegetation, salinity, temperature and elevation/depth) and shallow borings. Borings were made with a vibracorer and a McCauley auger.⁹ The borings were logged and correlated. Radiometric dating of selected vibracore samples was done to facilitate correlation and to determine subsidence rates.

A “gas sniffing” technique used for oil and gas prospecting was tested at several of the case study sites. Mud samples were taken in selected surface fault locales and gas chromatograph runs were made on the samples in the laboratory yielding positive identification of hydrocarbons in some samples. Edward B. Overton, Ph.D., LSU, Institute of Environmental Studies did the sample analysis and interpretation. Results indicate that this will be a useful technique in future evaluation of potential for fault movement.

⁹ While the vibracore technique allows collection of relatively large, continuous samples in a protective aluminum tube that can be transported to the laboratory for analysis, there is an inherent problem in the coring process that compacts soft deposits. Adjustments for compaction were made, but in a number of cases vertical control of samples was also maintained by use of the McCauley auger. In this auguring technique, samples are taken and logged in 1 ft (0.3 m) intervals in the field, so the maximum error from compaction is less than 1 ft (0.3 m).

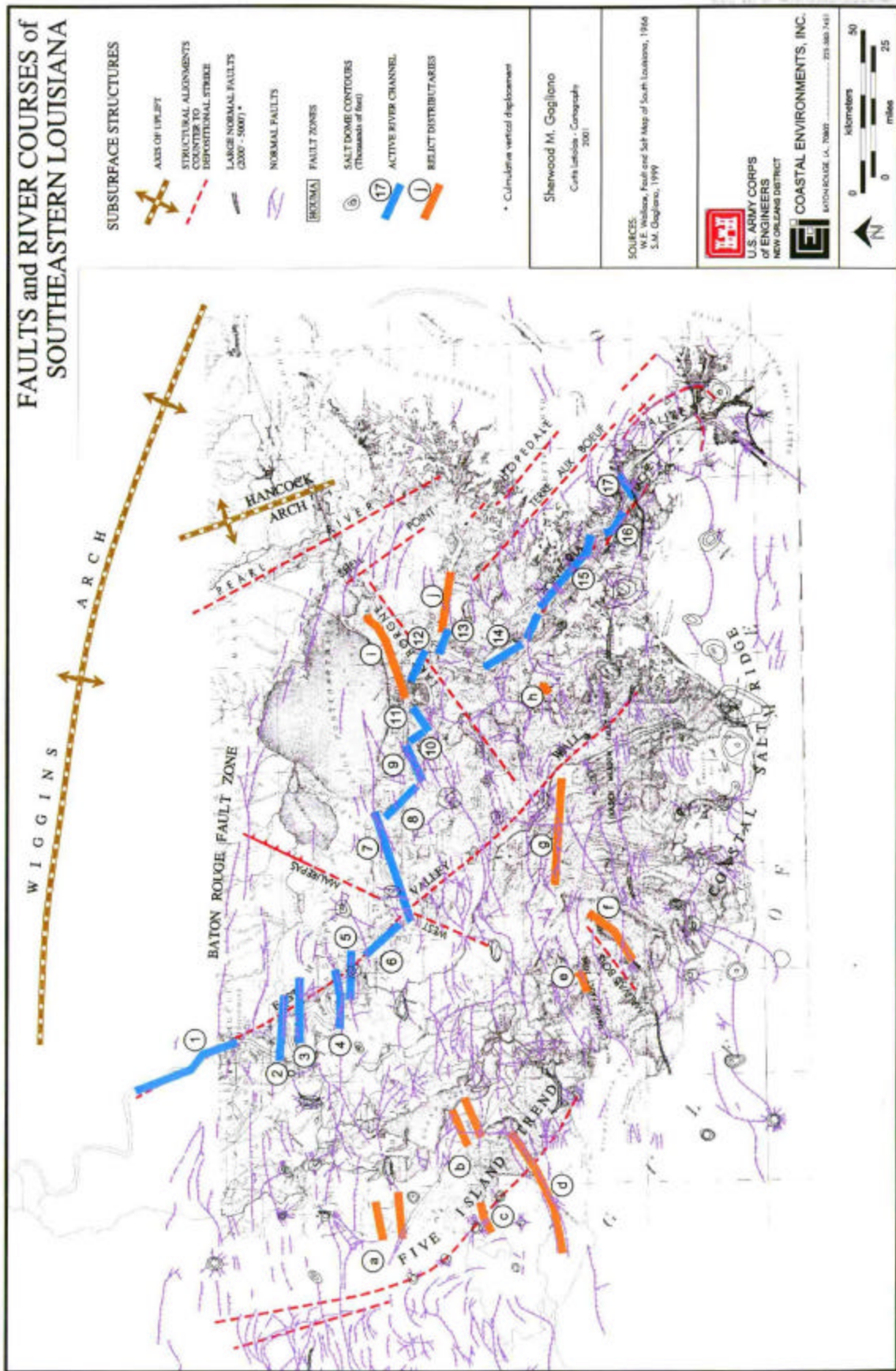


Figure 20. Relationship between faults and river courses in Southeastern Louisiana. Base map shows conditions circa 1859-1879 (Excerpt from Mississippi River Commission 1913).

A high-resolution seismic profile was run along a segment of the Bayou Lafourche corridor, in the vicinity of the Golden Meadow Fault Zone. Juan Lorenzo, Ph.D. a faculty member in the Department of Geology and Geophysics at LSU, ran the seismic profile with the help of his students. No indication of a fault plane was found in the seismic record. However, it should be noted that the line was run during the early stages of the study and definitive surface signatures of faulting had not been recognized or mapped in the area. In short, we missed the fault. The methodology is sound and should be applied to future work. A description of the test run and the results are reported in a separate technical report.

Some characteristics of the nine case study sites are listed in Table 4. Seven of the nine suspected faults showed measurable vertical displacement of near-surface beds, as well as distinctive surface. It was concluded that three of the fault events were also determined to have been active during either prehistoric or historic times. Bayou Perot appears to be still active. Geomorphological evidence suggests that Lake Lery is the result of a pre-1800 fault event and the fault has been dormant since the event. The Lake Enfermer and Bayou Long Faults exhibit salt marsh dieback or brown marsh on the downthrown block. A brown marsh stage has been identified with fault events at Empire and Bastian Bay. Movement on one fault (Lake Boudreaux) has resulted in hydrologic and water chemistry changes that have caused dieback of cypress trees in addition to impacts to shrub-scrub and freshwater marsh communities.

Regional faults move along one fault plane or several closely spaced planes at depth. However, the surface does not break uniformly in response to the fault movement. Typically the traces and scarps occur as linear segments from 3 to 5 mi (4.8 to 8.1 km) in length along fault trends and have associated areas of rapid land loss or wetland deterioration on the down-dropped block (wetland breakup areas). In some instances, relict distributary natural levee ridges that cross the faults have been severed and submerged. The down-dropped blocks also are typically tilted into the fault in the zone of deformation and exhibit vertical displacement of 1 to 3.5 ft (0.3 to 1.1 m). Some fault planes dip to the Gulf Salt Dome Basin, while others dip in a counter-basin direction.

SPECIAL STUDY AREAS

Five areas were selected for special study where suspected fault events were evaluated chronologically in reference to geomorphological change, resulting from natural and anthropogenic processes (See Figure 17). The analyses revealed temporal and spatial patterns. The more detailed evaluations also led to a better understanding of the inter-relationships of depositional, erosional and fault processes and the secondary consequences of fault events (i.e., changes in elevation, slope, hydrology, water chemistry, vegetation communities, etc.) A summary of the characteristics and findings of each of the study areas follows.

Pontchartrain Basin

It has been reported in the literature that faults have influenced the shape and formation of landforms bordering Lakes Pontchartrain and Maurepas and that the origin of the lakes may at least in part be fault induced (Fisk 1944, Saucier 1963, and Lopez 1991). Figure 21 shows the paleogeography of the Pontchartrain Basin, circa 1750 A. D., along with locations of known and suspected surface fault traces, scarps and alignments. The

Table 4. Nine Case Studies: Summary of Results.

Index No.	Fault Segment	Regional Subsurface Fault	Fault Zone	Date of Scarp/Trace Appearance	Duration of Fault Event in Years	Length of Scarp/Trace in Miles	Apparent Surface Displacement* in Feet	Vertical Offset of Near-surface Beds (Vibracores) in Feet	Vertical Offset of Near-surface Beds (McCauley) in Feet	Comments on Core Data	Vegetation Response and Comments
MD-1	Empire	Golden Meadow	F	1976-78	2 - 4	4.8	2.9 - 3.3	1.2 - 3.5	3.5	Offset decreases upward	Brown Marsh & Submergence
MD-3	Bastian Bay	Leeville	F	1974-75	1 - 4	4.6	4.0	0.6	0.5		Brown marsh & Submergence
ET-1	Lake Boudreaux	Mauvais Bois	E	1972-83	11	3.5	2.5 - 3.3	0.2 - 2.0	0.2 - 1.3	Offset decreases upward	Fresh-to-brackish Cypress-dieback Submergence
ET-4	Montegut	Theriot	E	1972-80	8	4.5	1.8 - 3.4	2.0 - 4.0	1.5 - 4.8	Offset decreases up in vibracores increase up in McCauley	Fresh to brackish Breakup & Submergence
WT-12	Lake De Cade	Juncture	E	Historic		4.9	No data	1.1 - 2.7	No data	Offset	Submergence
WT-31		Theriot & Mauvais Bois		Re-activated						Decreases upward	Breakup
BA-15	Lake Enfermer	Golden Meadow	F	1980 - Present		5.3	No data	0.2 - 1.2	No data	Offset increases upward	Brown marsh & Breakup on downthrown block
BA-5	Bayou Perot	Houma	E	Active 1980 - Present		2.3	No data	No apparent movement	No data	Minimal Change	Fresh-to-intermediate Breakup on downthrown block
BR-2	Bayou Long	Houma	D	Historic Re-activated 1982 - Present		1	0.8	1.1	No data	Minimal Change	Brown marsh & Breakup on downthrown block
BR-1	Lake Lery	Lake Salvador	D	Pre-1812 Dormant	NA	8.5	Natural levee sag - 1.0 lake depth	Fan faults 1.3 - 5.0	0.5 - 2.2	Fan faults Offset decrease up	Historic submergence

* Marsh floor to water bottom.

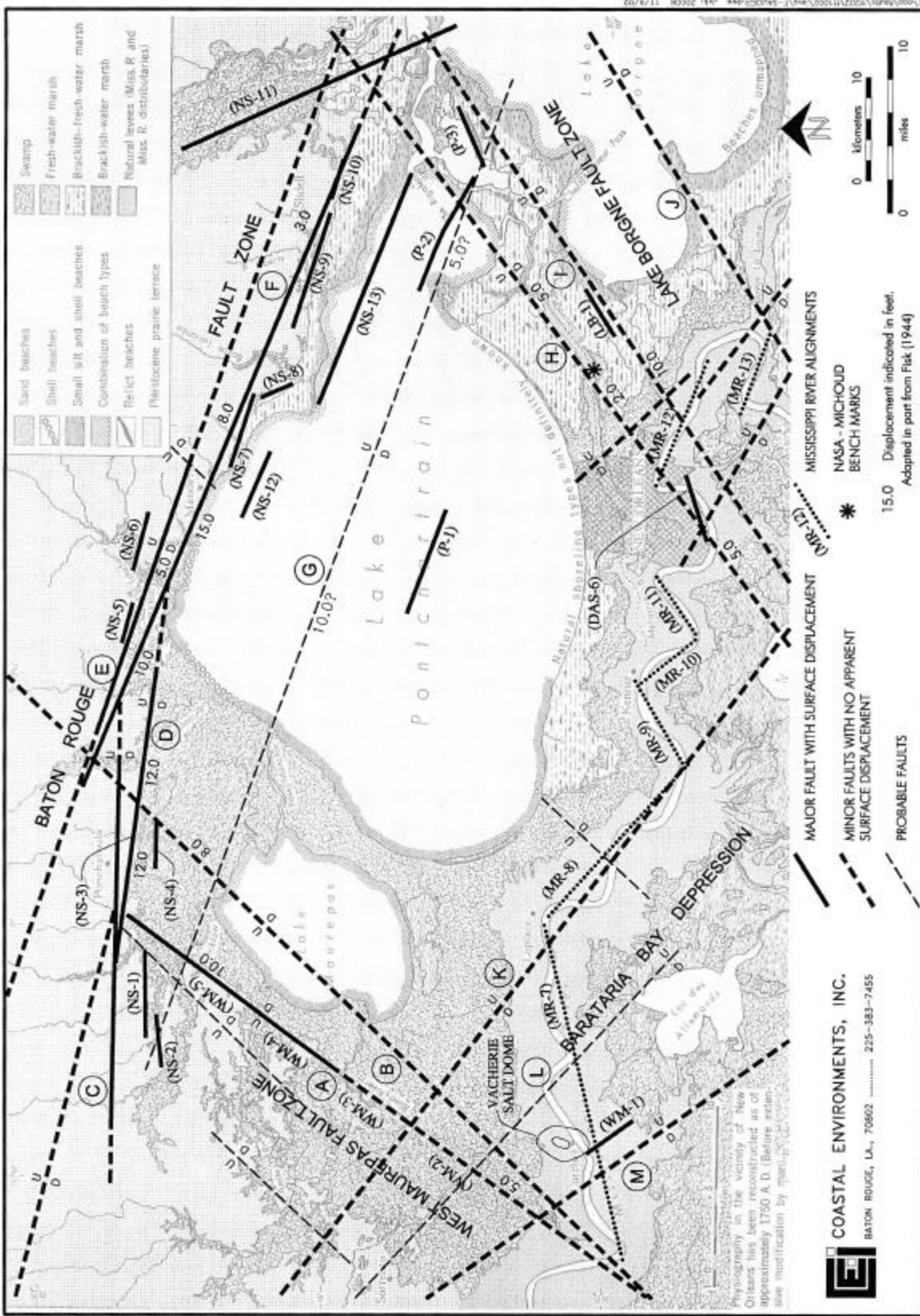


Figure 21. Map showing reconstructed landforms and conditions in the Pontchartrain Basin circa 1750 A.D. with known and probable faults (adapted from Saucier 1963).

Pontchartrain Basin is boxed in by four major fault alignments: 1) the Baton Rouge Fault Zone, 2) the West Maurepas Alignment, 3) the Lake Borgne Fault Zone and 4) alignment “K” of Saucier (1963). Alignment “K” trends northwest-southeast and is defined by a series of reaches along the Mississippi River, which appear to be fault controlled (MR-8, MR-10, MR-12 and MR-13). Faults “H” and “I,” also defined by Saucier, are parallel to the Lake Borgne Fault Zone, as designated by Fisk (1944).

Figure 22 is a Coastal Zone thematic TM satellite image of the Pontchartrain Basin taken in 2000. The surface traces and scarps of suspect and proven surface faults are shown on the image. The relationships between the landforms and the faults around the western and northern margins of Lakes Maurepas and Pontchartrain are clearly discernable on the image. The West Maurepas Fault is not delineated on maps of subsurface faults compiled by petroleum geologists, but the geomorphological evidence is compelling, and this appears to be an important structural element of the region.

Fault segments along some of the regional northwest-southeast trending alignments in the lake where near-surface movement has been reported in the literature are shown on the image and are identified by index numbers. These are NS-7, the Madisonville Point Fault; NS-12, the Causeway Fault; NS-13, the Goose Point Fault; and P-2, the South Point Fault.

Figure 23 is a Light Imaging Detection and Ranging (LIDAR) image of an area north and west of Lake Maurepas. The image shows the area of intersection of the Baton Rouge and West Maurepas Fault Zones. Fault scarps and fractures are well defined by changes in elevation and drainage patterns. There appears to be a previously unrecognized southwest-northeast trend lying between the southernmost faults in the Baton Rouge Zone (NS-1) and the West Maurepas Faults (WM-3, WM-4 and WM-5). Examination of the image at higher resolution revealed that in addition to the well-defined faults, there is a complex fracture pattern in the area. The morphology of the scarp WM-5 suggests that it was coincident with a shoreline and reworked by waves and currents. Based on the geomorphology this reworking appears to have occurred after the fault scarp had formed. Conditions favorable for a shoreline existed in this area about 4000 to 5000 years before present (YBP). If this interpretation proves to be correct, it would indicate that the fault scarp WM-5 has been relatively dormant since it was re-shaped by shore processes.

Figure 24 shows two north-south topographic profiles across faults. The profiles were derived from the LIDAR data. Profile A-A' crosses five well-defined fault scarps. The cumulative vertical displacement apparently resulting from the faults along this profile is 25 ft (7.6 m). The profile suggests rebound and back-sloping on one of the faults.

Profile B-B', which follows Highway I-55, is also shown in Figure 24. This profile crosses three or more stair-step scarps along the Prairie Terrace edge. The total vertical displacement across these three scarps is 24 ft (7.3 m). This profile also exhibits back-sloping on the upthrown-block of one of the faults.

Lake Maurepas is located on a down-dropped block bounded on the north by the Baton Rouge Fault Zone (Faults NS-1, NS-3 and others) and on the west by the Maurepas Fault Zone (Faults WM-2, WM-4 and WM-5). The shape of the lake suggests fault origin. Based on geomorphic and archaeological data, Saucier (1963:58-65) showed that Lake

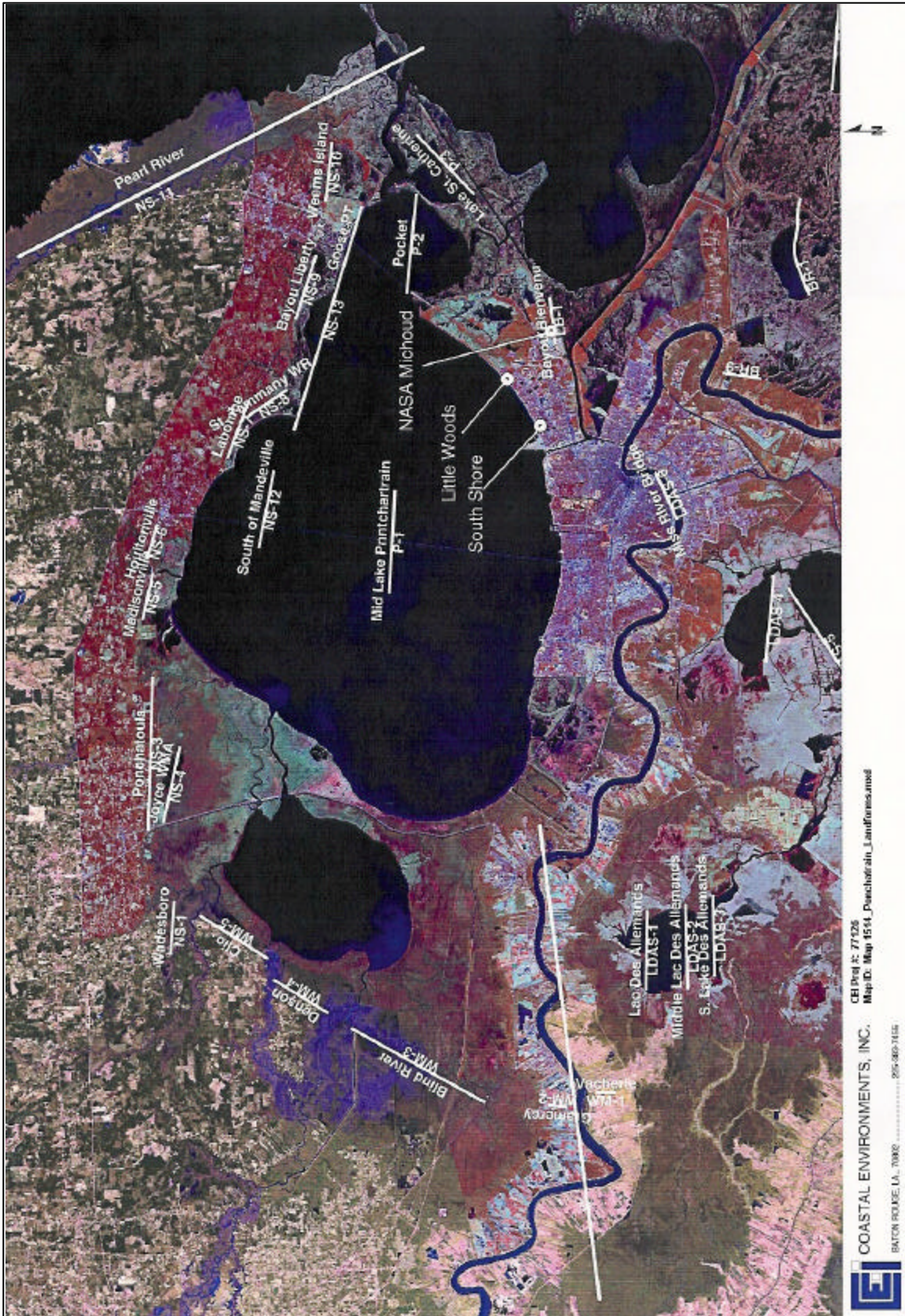


Figure 22. Mississippi River alignments and probable faults that exhibit surface expression in the Pontchartrain Basin. Composite image from 1993 and 2000 Coastal Zone TM satellite.

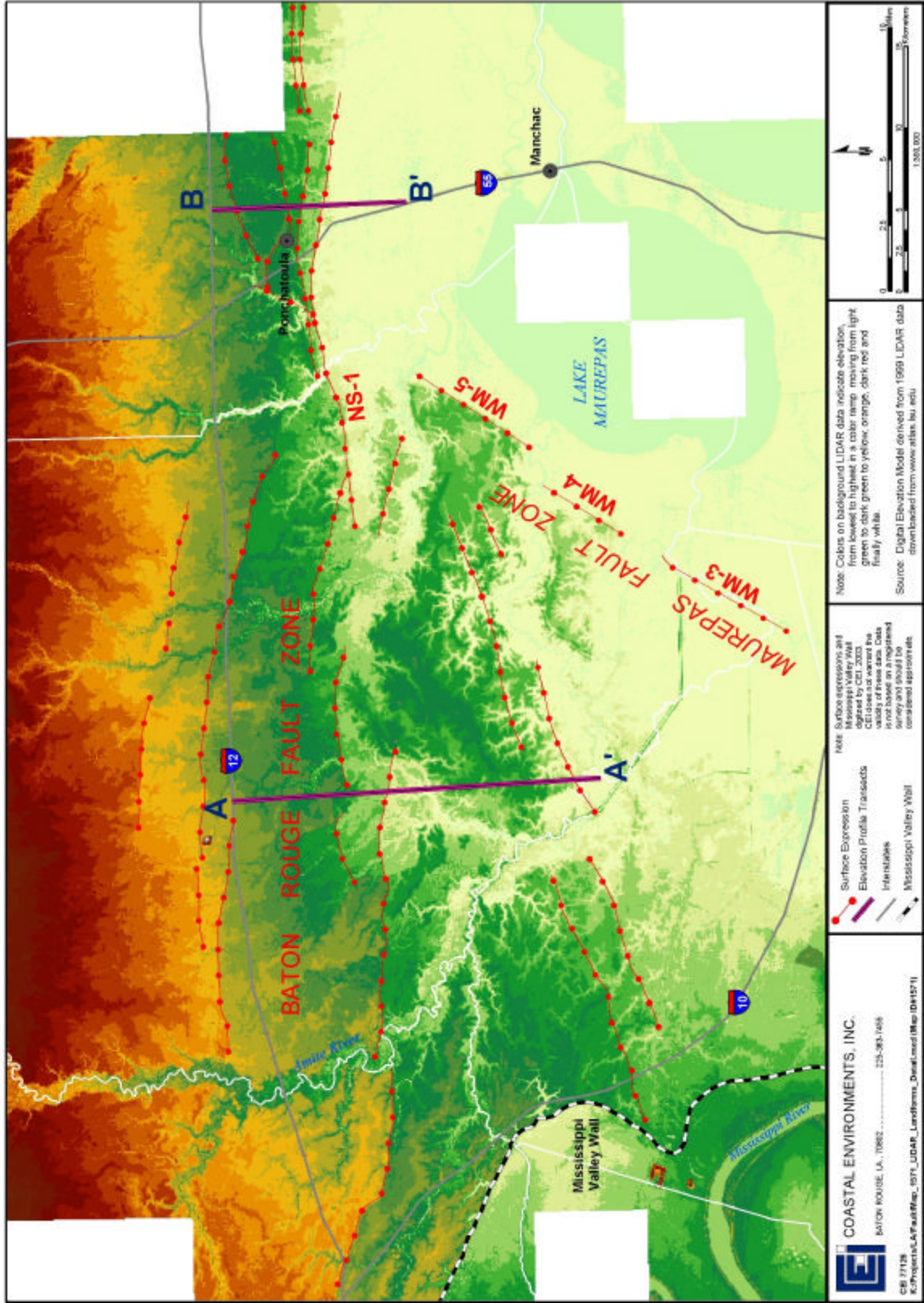


Figure 23. LIDAR image showing intersection of the Baton Rouge and West Maurepas Fault Zones. LIDAR data is in DEM format derived from 1999 measurements in USGS format. Data collected for the Louisiana Federal Emergency Management Agency (FEMA) Project-Phase 1.

Maurepas formed between 3500 to 2800 YBP, but offered no explanation for its formation. Saucier's interpretation of the age of the lake coupled with its shape, and its location in reference to the Baton Rouge and Maurepas fault trends suggest that Lake Maurepas was the result of one, or several prehistoric fault events.¹⁰

Movements along fault segments within the Baton Rouge Fault Zone have occurred periodically, if not continuously, from at least the Middle Wisconsin Stage (Farmdalian) of the Pleistocene (30,000 YBP) to the present. Virtually all surface faults in the Pontchartrain Basin exhibit displacement of the top of the Pleistocene. These faults extend into the subsurface to a minimum depth of 20,000 ft (6096 m) have a dip of 45 to 65 degrees from the horizontal and are presently active with relative offsets of 0.0083 ft per year (2.54 mm per year) (Penland et al. 2001).

Lopez and his associates (Lopez 1991, Lopez et al. 1997) used offsets of bridge structures that cross faults underlying Lake Pontchartrain to measure fault movement (Figure 25). They documented rates of movement of 0.008 to 0.033 ft per year (0.25 to 1.00 cm per year). It has not been determined whether these rates are episodic or continuous.

The Goose Point Fault (NS-13), as shown in Figure 22, is one of the faults that apparently caused some of the bridge displacement. This fault has been identified on a high resolution seismic line west of the Highway 11 and I10 bridges (Lopez et al. 1997) (Figure 25 A and 25 C). The seismic image shows displacement of reflectors by the fault to within 10 ft (3m) of the lake bottom. The image also shows displacement of shallow reflectors to a depth of more than 140 ft (42.7 m). This is through the Holocene wedge and well into the Pleistocene deposits. The image shows expansion of the section on the down-dropped block of the fault to at least 140 ft (42.7 m), indicating continuous or episodic movement during the Pleistocene and the Holocene.

Shallow seismic sections and cross-sections based on geological borings and showing shallow displacement along faults under Lake Pontchartrain have been reported and illustrated by other researchers (Fisk 1944:Plate 17, Kolb et al. 1975:Plates 13, 38 and 39, Penland et al. 2001).

Lopez and his associates also reported that minor "apparent earthquake activity" has been documented for the region encompassing the Baton Rouge Fault System. While the Baton Rouge Fault has long been regarded as the most active fault in southeastern Louisiana, inspection of the regional megasection and other subsurface data suggests that growth faults south of the latitude of New Orleans are much larger in terms of cumulative vertical displacement.

In summary, not only is evidence of surface expression of faults in the Lake Pontchartrain area well documented in the literature, but Pleistocene and Holocene movement has also been verified by data from borings, seismic lines and bridge displacements. There are numerous, recorded instances of small earthquakes which may be associated with movement on some of these faults. It should also be noted that surface

¹⁰ Archaeological data was used in this study to date landforms and to bracket the probable dates of fault events. The geoarchaeological methodology utilized was pioneered by McIntire (1958), and further developed by Saucier (1963), Weinstein and Gagliano (1985), Gagliano (1984), and others.

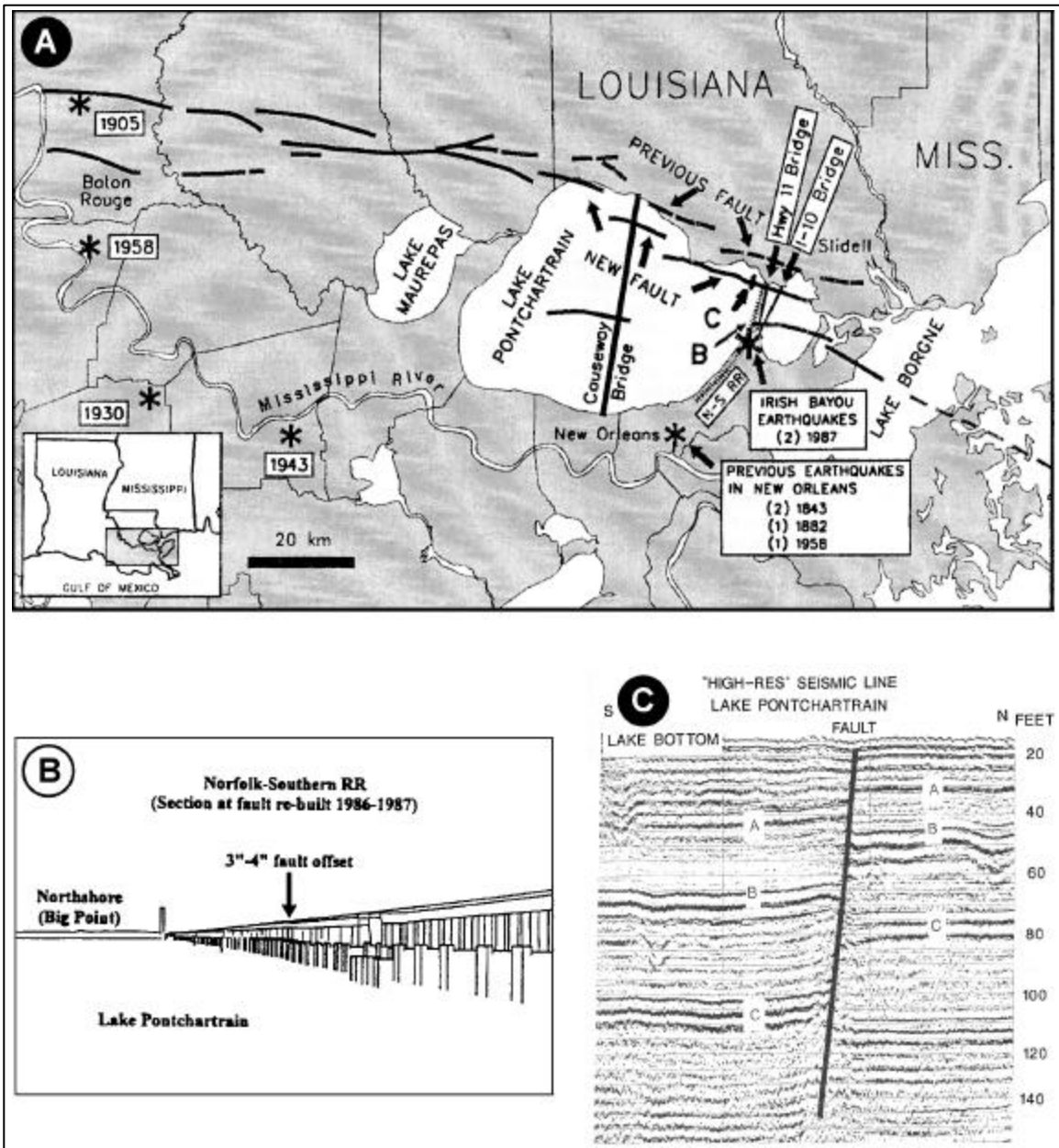


Figure 25. Baton Rouge Fault system. A. Fault traces from the Mississippi River to Lake Borgne. Displacements have been measured on bridges shown. Reported earthquake occurrences are also shown. B. Drawing showing fault offset in re-built section of Norfolk-Southern Railroad Bridge in eastern Lake Pontchartrain. C. Displacement of beds by south dipping normal fault as recorded on USGS high resolution seismic line from eastern Lake Pontchartrain. Abrupt terminations of shallow reflectors indicate that the fault is within 10 ft (3 m) of the lake bottom (after Lopeze et al. 1997).

expression of faults at the top of the Pleistocene in most of the Pontchartrain Basin is not masked by Holocene sediments and marsh grass root mats, and therefore, the full extent of vertical displacement and slope change is revealed.

West Plaquemines Delta Plain (Empire and Bastian Bay Faults)

The area west of the Mississippi River in the vicinity of Empire and Buras, Louisiana was chosen for special study because of conspicuous surface fault scarps in the marsh. The Empire and Bastian Bay Fault events unfolded in this study area during the 1970s. They represent what appear to be the largest modern fault events that have occurred in coastal Louisiana (Figures 26 and 27). The Empire and Bastian Bay Faults are the Rosetta Stones for deciphering modern and historic fault events in Southeastern Louisiana. The development of these two faults is well documented on maps, aerial photographs and by eyewitness accounts (Figure 28).

The Empire Fault has a scarp that is 4.8 mi (7.7 km) long, an apparent maximum vertical displacement of 3.5 ft (1.1 m), and an affected area of approximately 12,000 ac (4856 ha) (Figures 29 through 31). Measurements indicate that approximately 31.2 million cu yds (24 million cu m) of fill would be required to restore the area of land that has reverted to open water as a result of the Empire Fault event.

The Bastian Bay Fault created a new coastal bay and detached a beach complex from its headland to form a barrier island during the 1974 through 1978 period (See Figures 26-28). Landform geometry was completely changed and a large area of marsh was submerged and subjected to erosion. The fault segment is 4.6 mi (7.4 km) long and affects an area of approximately 24,100 ac (9752 ha). In 1998, 23,600 ac (9550 ha) of the affected area was open water. The measured water depth at the scarp was 3.5 ft (1.1 m). Offset measured in near-surface beds from a cored section was only 0.5 ft (15.2 cm) and 0.75 ft (22.9 cm), but measurements of land sinking under a camp indicate 3.0 to 3.5 ft (0.9 to 1.1 m) of submergence. Prior to the fault event the area was occupied by saline marsh.

Eyewitnesses to the Empire and Bastian Bay Fault events include scientists, oyster fishermen and camp owners. Numerous camps that were built on land are now located in large open water bodies or have been abandoned as the land upon which they were built has been completely submerged (Figure 32). One account that is well documented indicates that the land surface under the camp sank 3 to 3.5 ft (0.9 to 1.1 m) (Pete Hebert, per. comm., 2001). Oysters now grow on the submerged marsh surface. The fault events have unfolded in several stages and have initiated a geomorphic/environmental succession. The water bodies resulting from these fault events are shown on the Official State Map of Louisiana (2000 ed.). The areas occupied by broken marsh and open water on the 2000 map were shown as land on the 1950 edition.



Figure 26. Topographic map showing landforms and conditions in the West Plaquemines Deltaic Plain circa 1941 - 1948. Geomorphic features added. Traces of the Empire (MD-1) and Bastian Bay (MD-2) Faults, which appeared on the surface in the 1970s, are also shown.

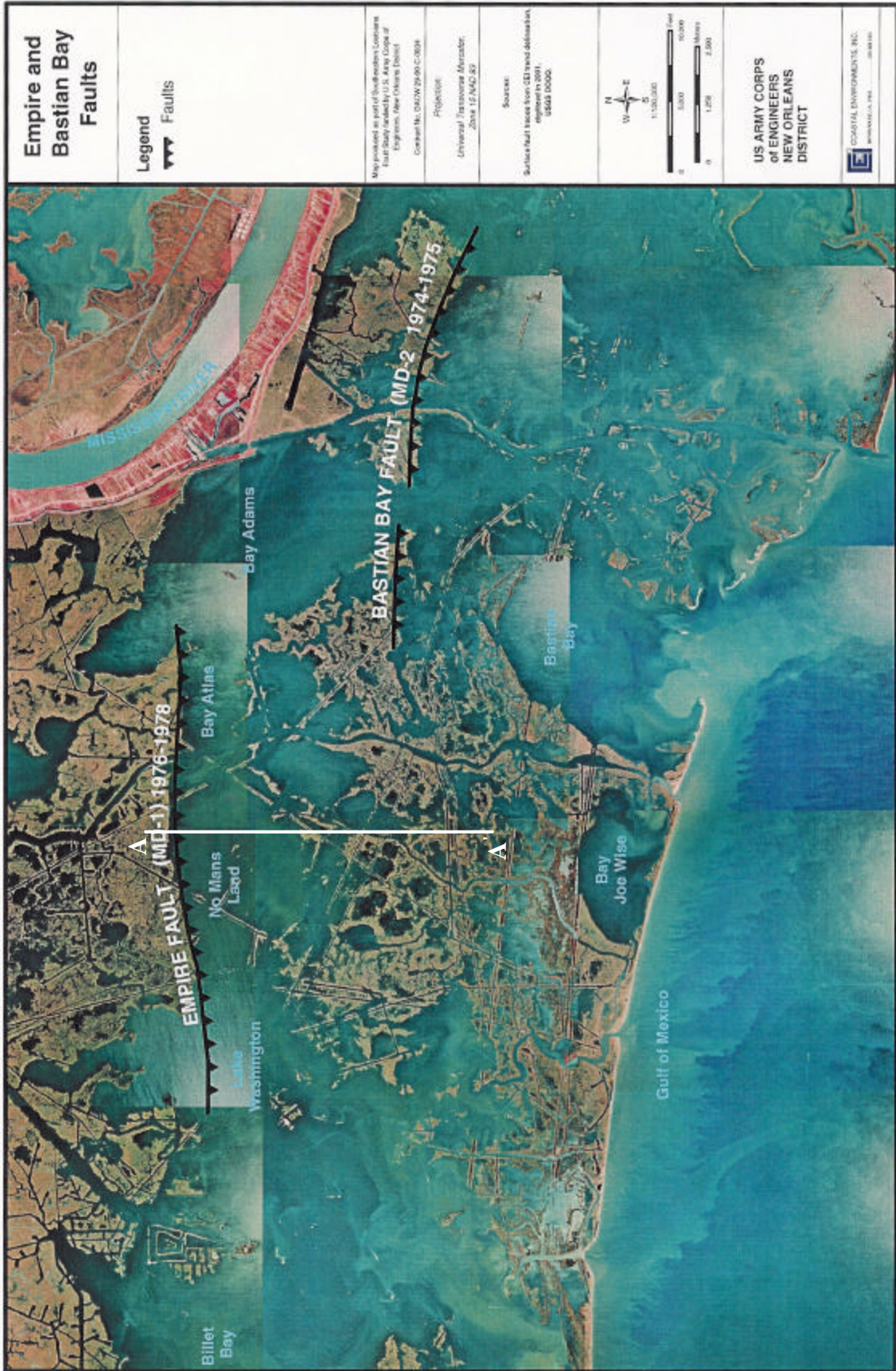


Figure 27. Aerial image showing West Plaquemines Deltaic Plain in 1998. The Empire (MD - 1) and Bastian Bay (MD - 2) Faults became active during the 1974 through 1978 period, resulting in massive land submergence. Compare with Figure 26.



Figure 28. Aerial view looking north across the Empire (MD - 1) and Bastian Bay (MD - 2) Faults. Photograph by S.M. Gagliano, September 2000.

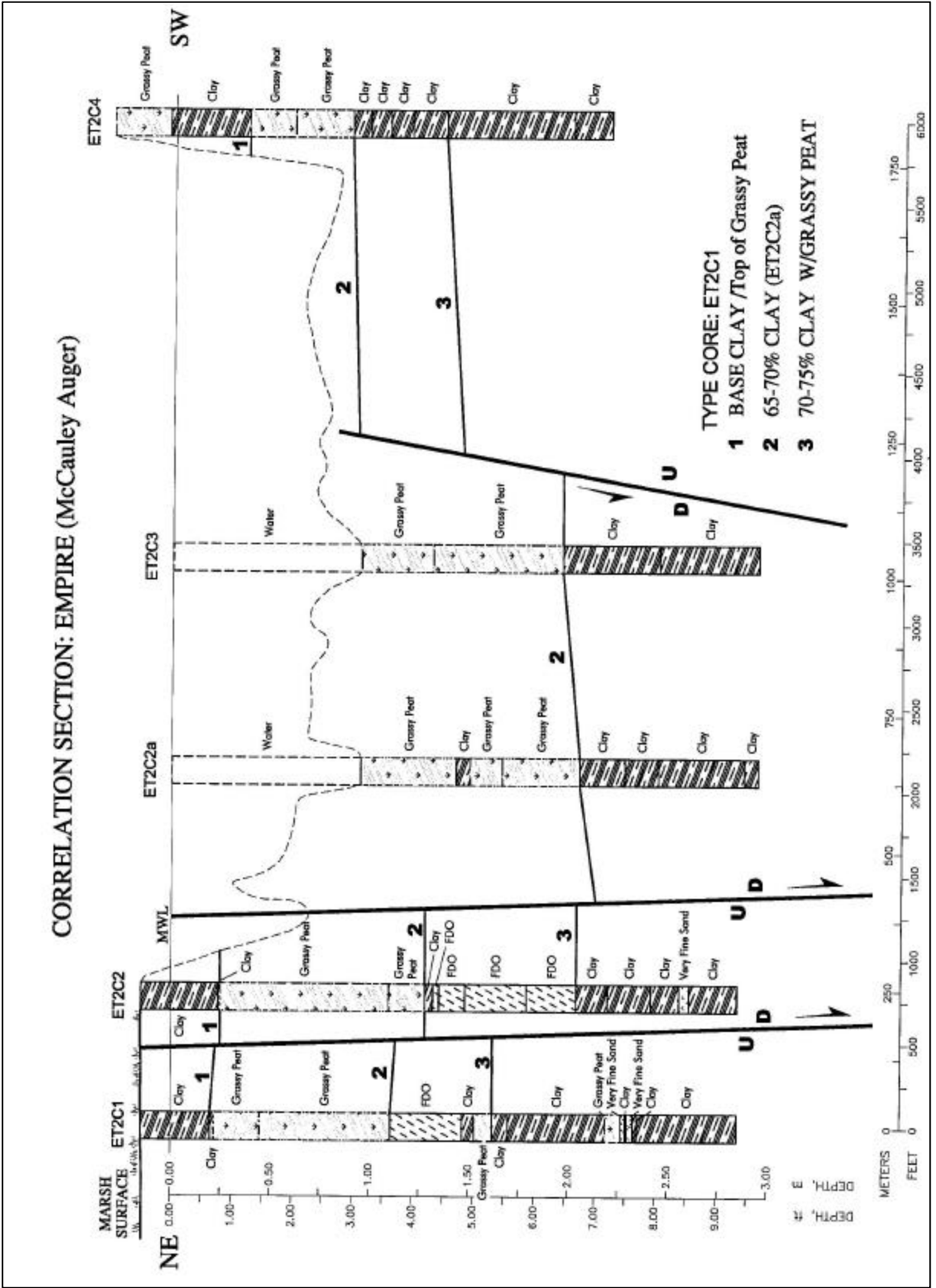


Figure 29. Section across the Empire Fault showing displacement of near - surface beds. Section based on McCauley auger borings by CEI in 2001.

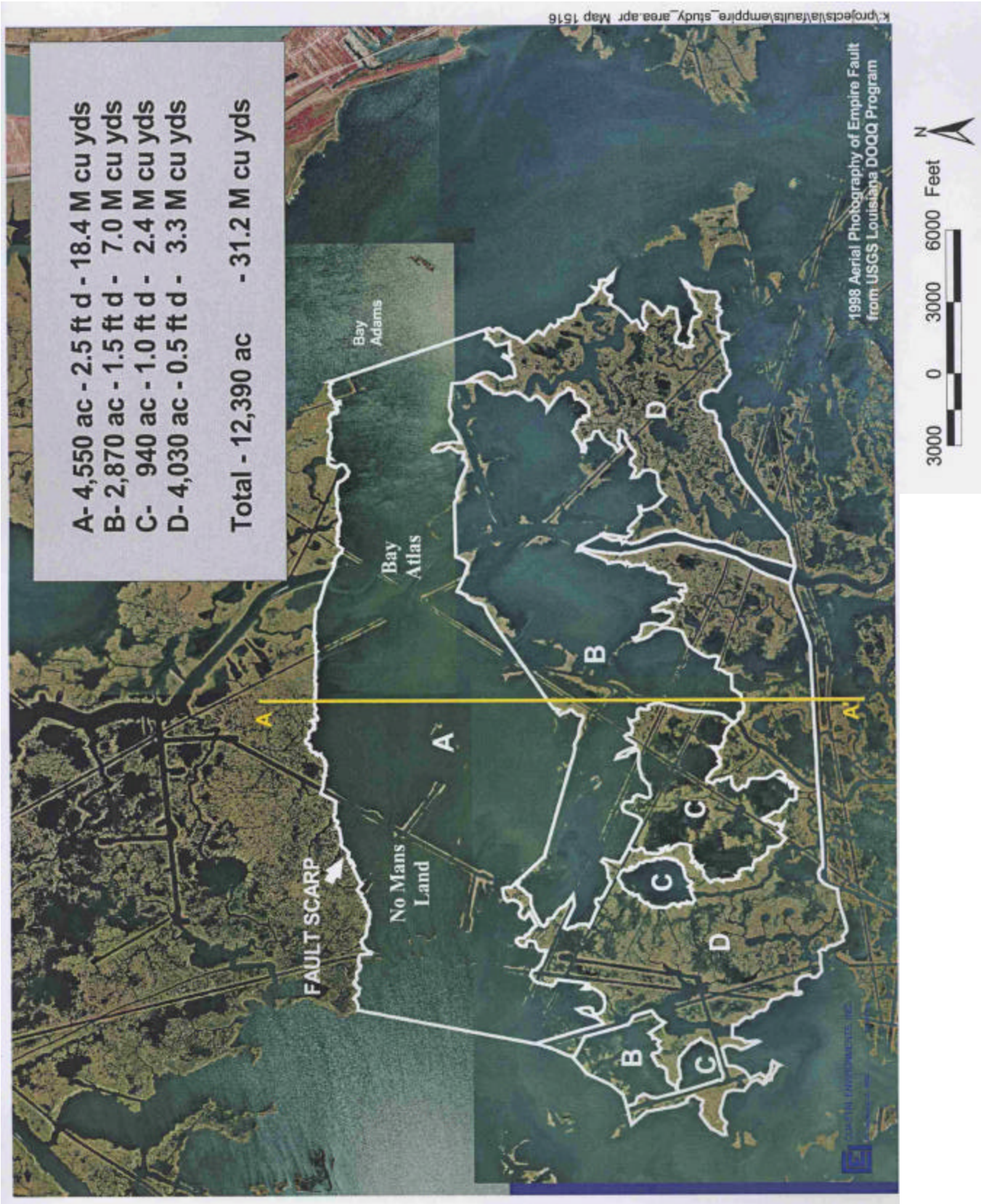


Figure 30. Areas exhibiting various degrees of submergence on the down - dropped block of the Empire Fault.

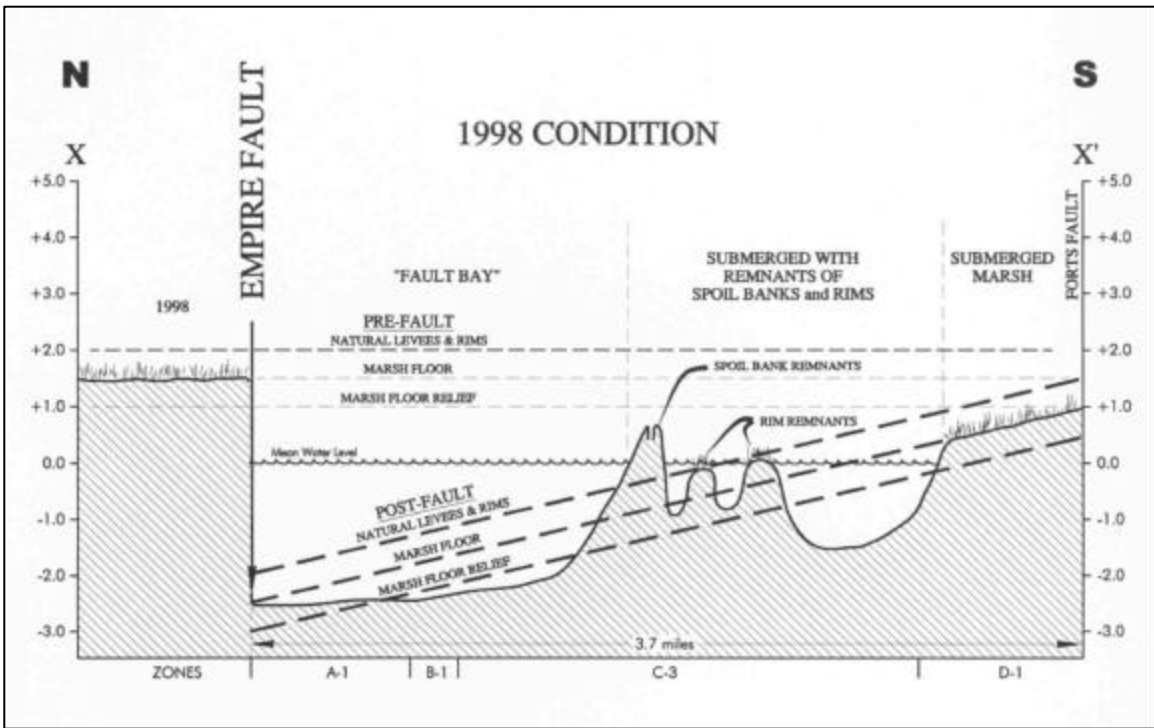


Figure 31. Section across the of the down-dropped the down-dropped block of the Empire Fault showing submergence and tilting. The surface of the down-dropped surface toward the fault scarp as a result of rotation during fault movement. Location of the section is shown in Figure 30.

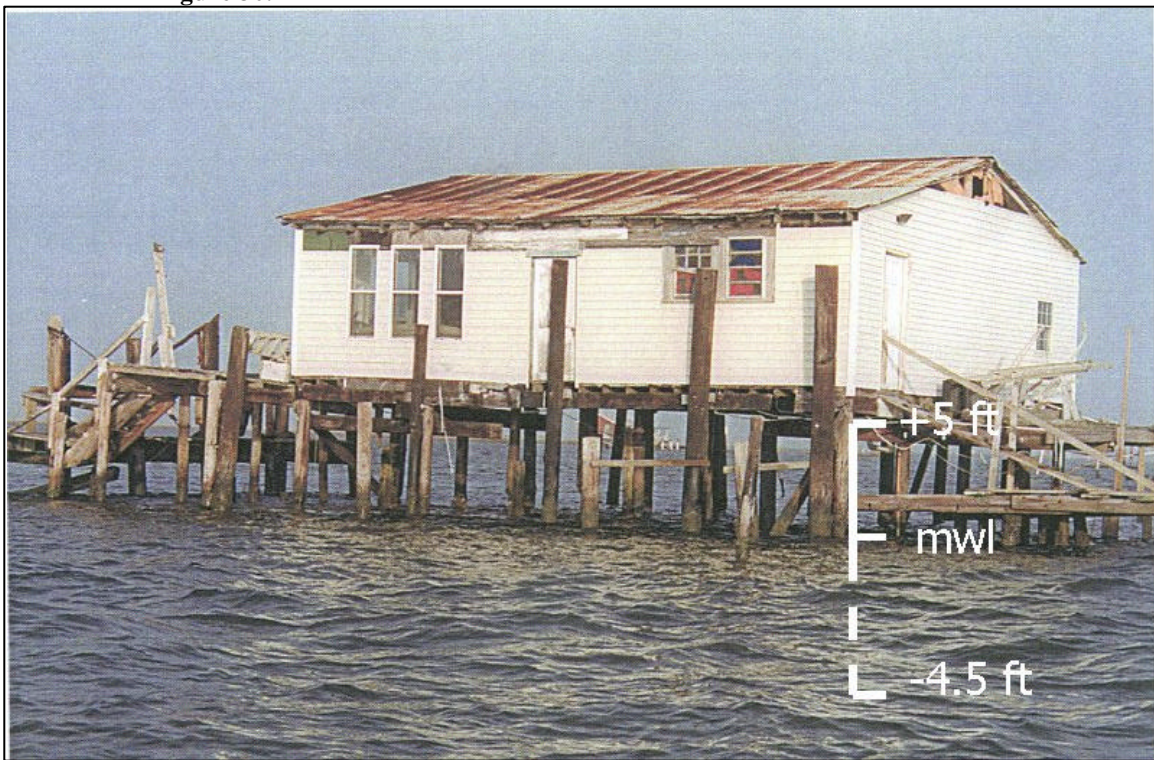


Figure 32. Photograph of Mr. Pete Hebert's camp, 2001. The camp was originally built on the bank of Bayou Ferrand in the late 1960s. The camp is located one mile (1.6 km) south of the Bastain Bay Fault Scarp (location shown in Figure 26). The land that the camp was built on is completely submerged and the elevation of the building has been reduced 4 to 4.5 ft (1.2 to 1.4 m) largely as a result of fault movement in the 1970s.

In the West Plaquemines Deltaic Plain area, we also found that natural levee ridges that cross active faults have been severed and submerged.¹¹ Gulf beaches have been separated from barrier islands by fault events. Large-scale land submergence has occurred on down-dropped fault blocks. Modern fault events have completely altered the landscape and hydrology of this area.

Figure 33 shows the relationship of surface expressions along the Empire and Bastian Bay Faults with known subsurface faults and salt domes as well as land loss in the West Plaquemines study area and vicinity.

Mudlumps

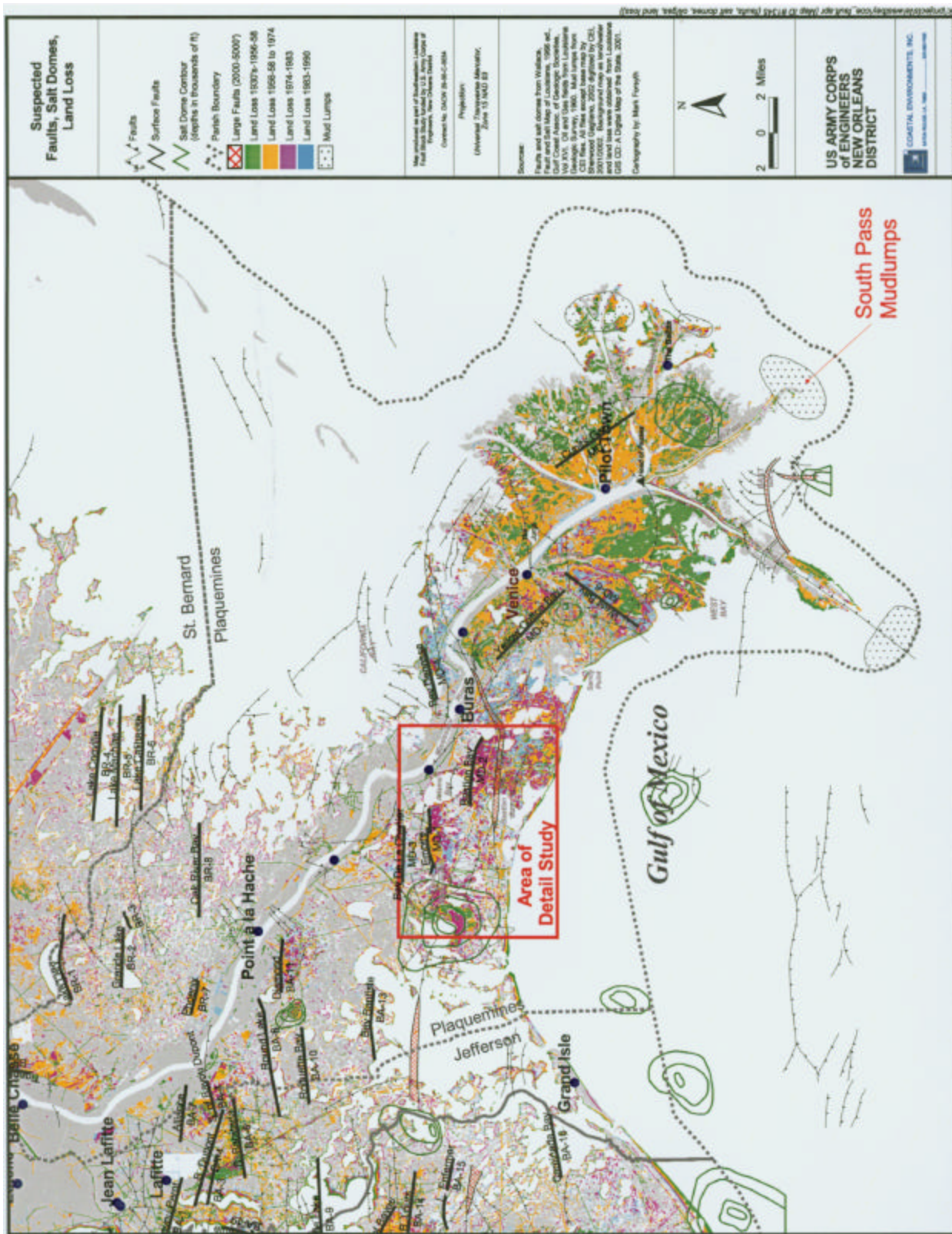
Another example of neotectonic activity is found in the mudlump phenomenon that has been documented at the mouths of the major Mississippi River distributaries of Southwest Pass, South Pass, Pass a Loutre and Balize Bayou. (See Figure 33 for location of mudlumps). The “Birdfoot” portion of the delta has extended beyond the continental shelf edge into deep water and as a result has built a thick sedimentary platform. Here a zone of diapiric clay structures, faults and massive gravity slumps has developed along the sloping front of the delta (Morgan et al. 1968, Gagliano and van Beek 1973, Coleman et al. 1980). Figure 34 shows photographs of surface features of one of the South Pass mudlumps taken at the time of drilling operations conducted by the Coastal Studies Institute of LSU in 1959-1960.¹² The extruded clay and the fault planes are evident on the surface. The fault scarp that can be seen in photographs Figures 34B and 34D had more than 5.0 ft (1.5 m) of vertical displacement. The fault planes are often well defined in the soft sediment and exhibit slickensides and striations. Small vents along surface traces of the fault emit methane gas and brine water.

Data obtained from continuous cores and borings taken at the mouth of South Pass indicate that the weight of bar sands building progressively seaward caused underlying unstable prodelta and shelf clays to squeeze up into furrows or folds (Figures 35 through 37). At the base of the folds is a zone of algal reef deposits and strand plain sands found in the borings at depths of 500 to 600 ft (152.4 to 182.8 m) (Figure 36). The abrupt change in lithology from soft, poorly consolidated clay to coarse, granular material of the Algal Reef Zone at the base of Clay Unit III constitutes the glide plane upon which the folds move and is also the base of the faults. As the bar advanced, the folds became asymmetrical and faults developed along the inclined axial planes of the folds. The folds ruptured and squeezed to the surface to form mudlump islands (Figure 38).

A string of casing was left in one of the borings that penetrated a well-defined fold within one of the South Pass mudlumps. After the project was completed, the site was

¹¹ Artifacts and radiocarbon dates from prehistoric Native American archaeological sites situated on these relict distributary natural levee ridges have been used to establish the time when the distributaries were active (Gagliano and Weinstein 1979, Gagliano 1984.)

¹² A comprehensive study of the mudlumps at the mouth of South Pass was conducted by staff geologists of the Coastal Studies Institute, Louisiana State University in the early 1960s under the direction of Dr. James P. Morgan. The senior author of the present paper participated in that study and was a co-author of resulting publications.



SOUTH PASS MUDLUMPS

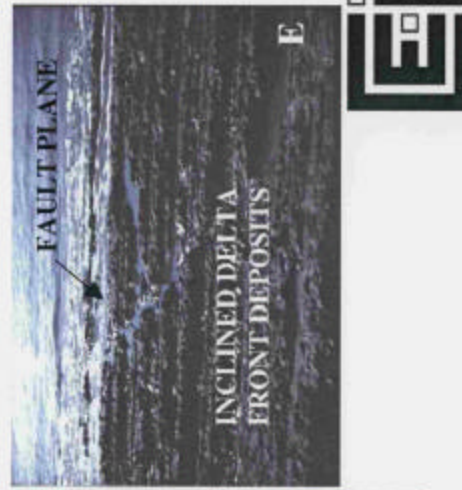
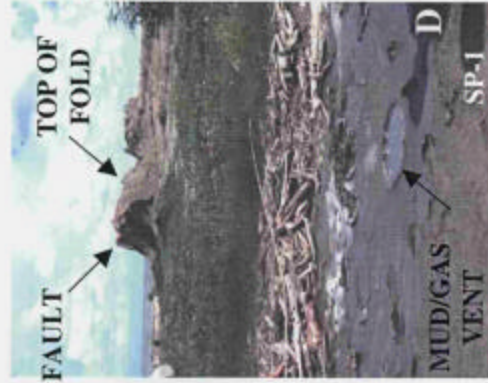
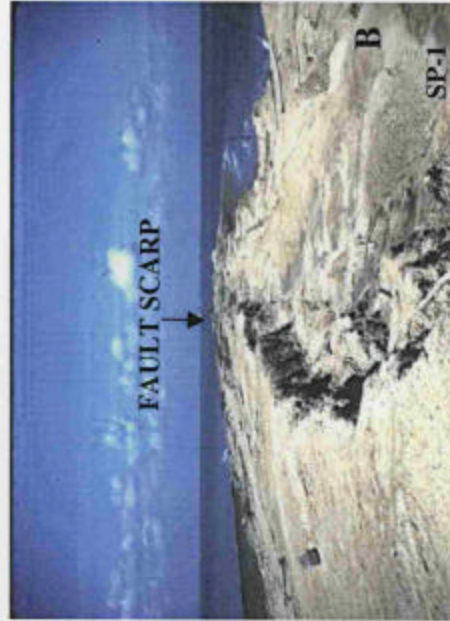


Figure 34. Photographs showing South Pass mudlumps and drilling operation. A. Aerial view looking north across mudlump island and sands spit with mudlumps. B. Five-foot fault scarp on South Pass mudlump. C. Core drilling. D. Mud/gas vents, with fault scarp in background. E. Tilted beds with fault trace.

SOUTH PASS MUDLUMPS

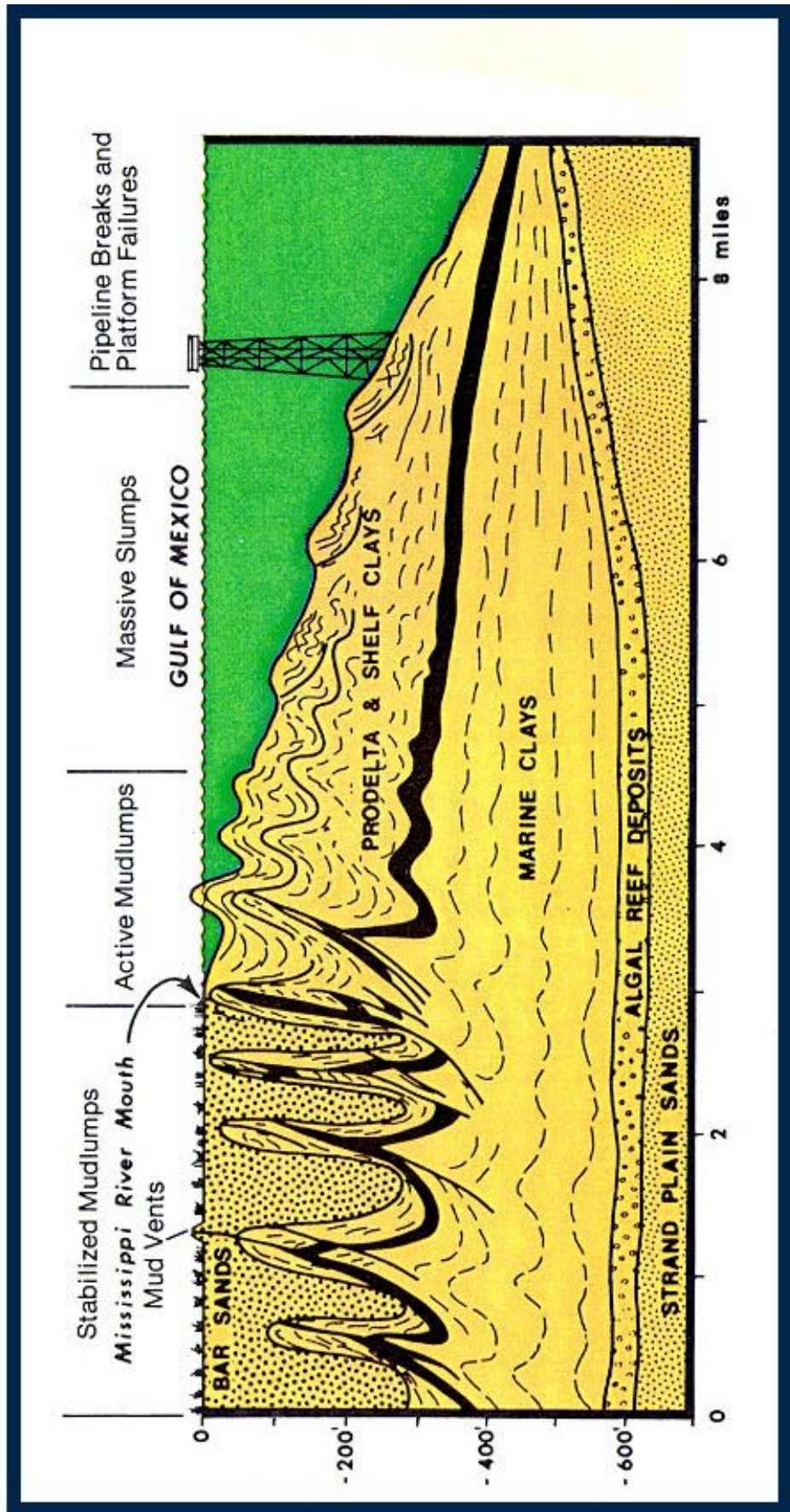


Figure 35. Diagrammatic cross-section showing mudlumps, faults and slump features at South Pass and vicinity (after Gagliano and van Beek 1973).

SOUTH PASS MUDDLUMPS

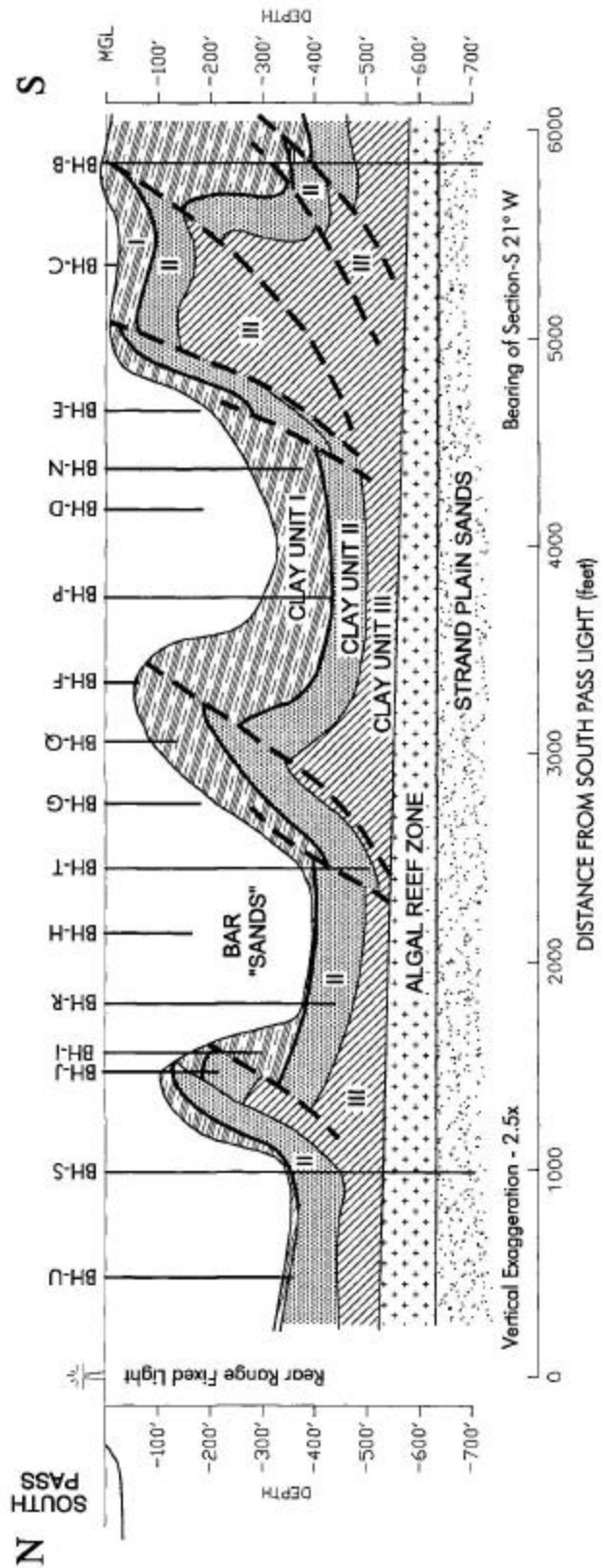
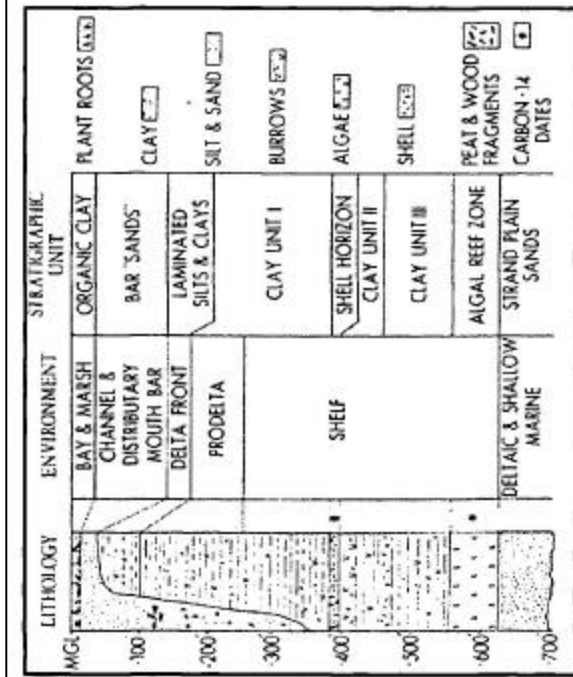


Figure 36. Stratigraphic section and cross - section showing folds and faults, South Pass mudlumps (after Morgan et al. 1968).

SOUTH PASS MUDLUMPS

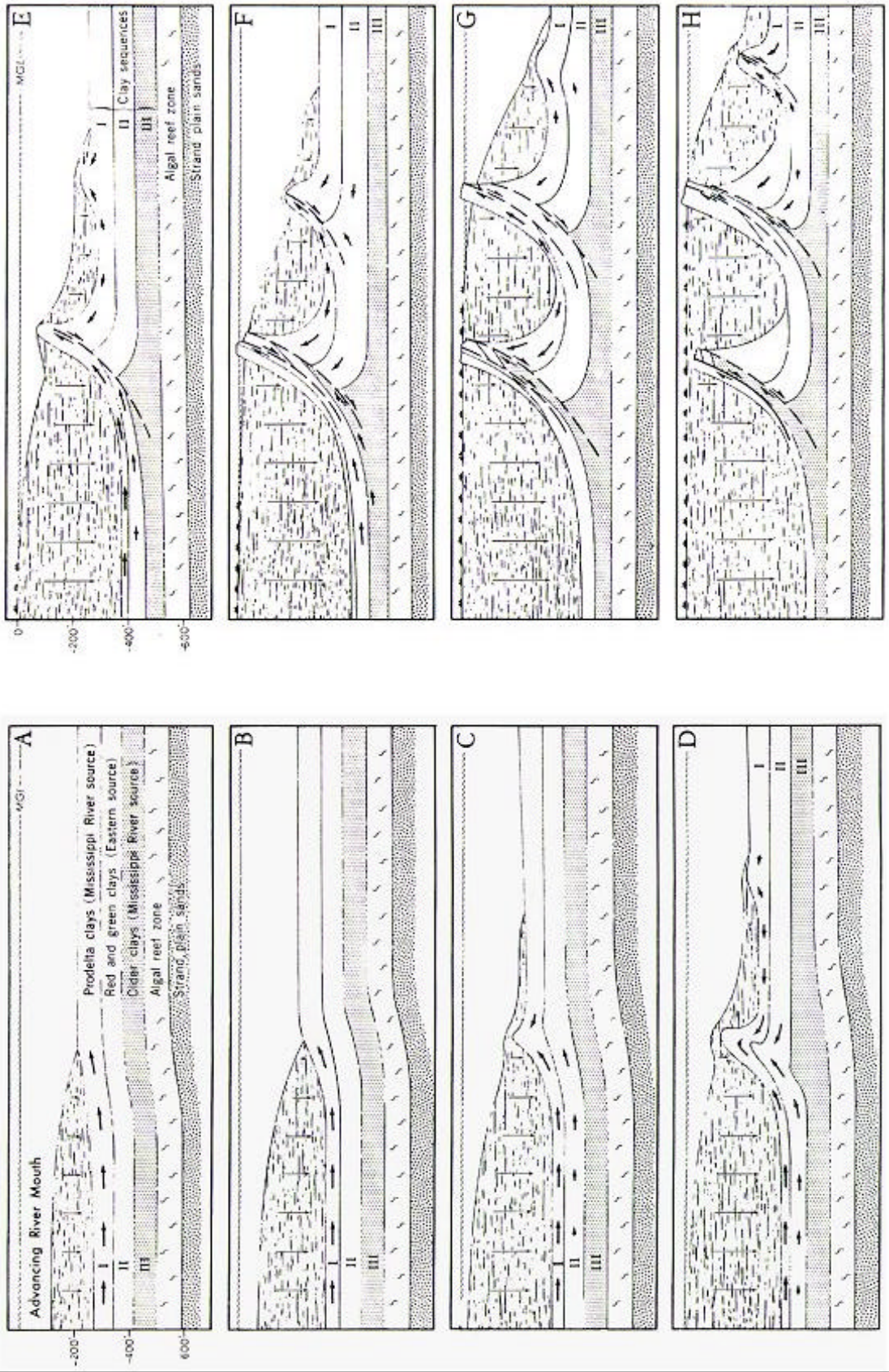


Figure 37. Diagrams showing progressive development of folds and faults, South Pass mudlumps (after Morgan et al. 1968).

SOUTH PASS MUDLUMPS

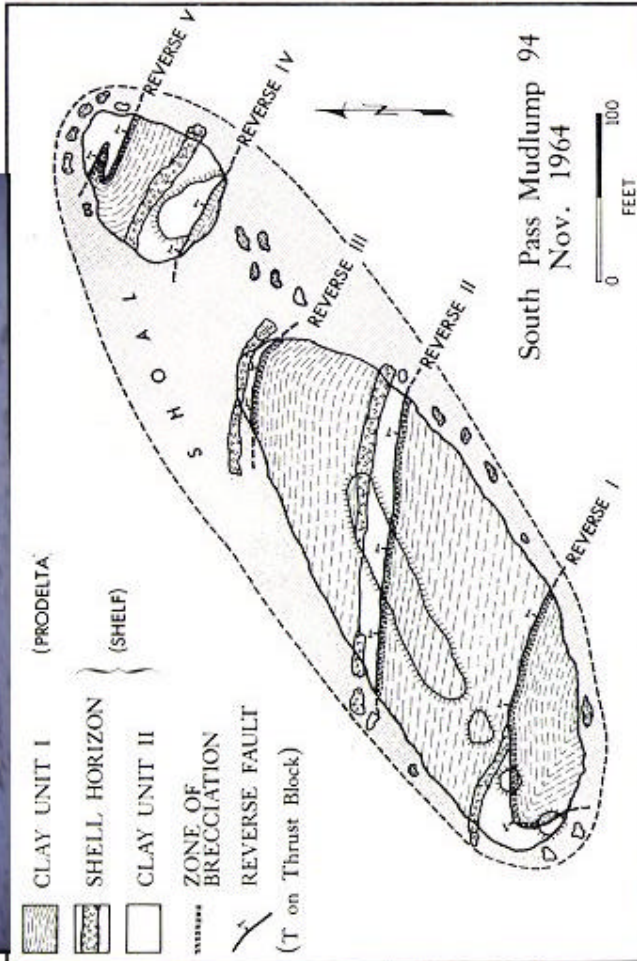
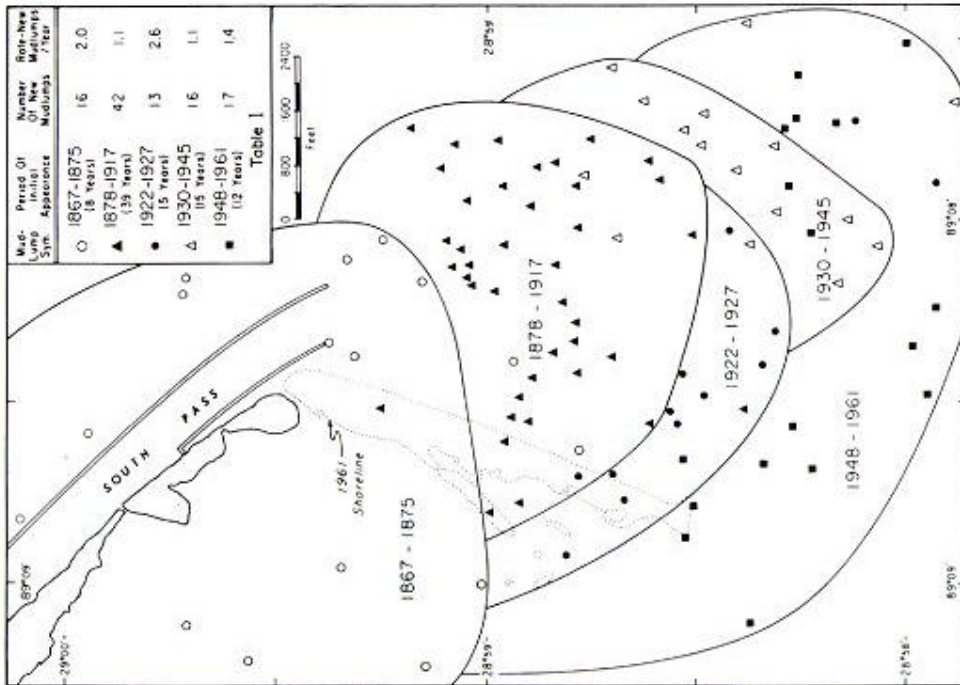


Figure 38. Mudlump islands at South Pass (after Morgan et al. 1968).

periodically revisited and it was found that the casing was gradually being extruded, providing evidence of the continuing movement of the fold and an associated axial plane fault. Figure 39 shows the increase in length and angle of tilt of the extruded casing over a period of 11 years.

It should be noted that the mudlump phenomenon occurs within Holocene sediments and is driven by sediment loading and gravity slumping, and not deep-seated tectonic processes.

Delta Front Gravity Slumping

J. M. Coleman (1976) and others have documented and studied massive slumps, mudflows and related gravity induced earth movement along the delta front (Figure 40). As discussed previously, sediment is deposited in subdeltas and at major distributary outlets. These areas are called depocenters and each is underlain by a sediment pod composed of sands, silts and clay (See Figure 15). The depocenters are generally located on the down-dropped side of regional growth faults, probably because fault movement has created a depression or hole. Through time the cumulative weight of the sediment pods on top of a thick underlying section of relatively soft sediment upsets the equilibrium of the near-shore and continental shelf area and massive landslides occur.

Hurricanes are known to trigger slumping along the delta front. The slumps in turn have caused pipeline breaks and the toppling of drilling platforms.

Continental Margin Gravity Slumping

Continental margin gravity slumping is one of the mechanisms proposed by geologists to account for massive growth faults and diapiric salt and shale movement in the Louisiana coastal region (Winker 1982). This is depocenter loading, growth fault movement, mudlump movement and delta front slumping on a grand scale. Great blocks of sediment literally slide into the deeper waters of the gulf (Figure 41). At the ends of these slides, sediment is pushed and distorted and may bulge up to form salt and clay diapiric structures. In the deep gulf, diapiric structures form the traps that are now producing large volumes of oil and natural gas.

Middle Barataria Basin

The interdistributary area lying between the Mississippi River and Bayou Lafourche is one of the largest and most biologically productive estuarine basins along the Louisiana coast (see Figures 1 and 17). The hydrologic axis of this estuary crosses three east-west growth fault trends: 1) Golden Meadow, 2) Theriot and 3) Lake Hatch (see Figures 6 and 42). The Lake Hatch Fault System branches into three components within the area.

The mosaic of USGS topographic maps in Figure 42 shows the Middle Barataria Basin circa 1953-1962. Annotations added to the map indicate relict Mississippi River distributaries and prehistoric archaeological sites that are located on the distributary natural levee ridges and lake shores. Also shown are probable fault traces and scarps,

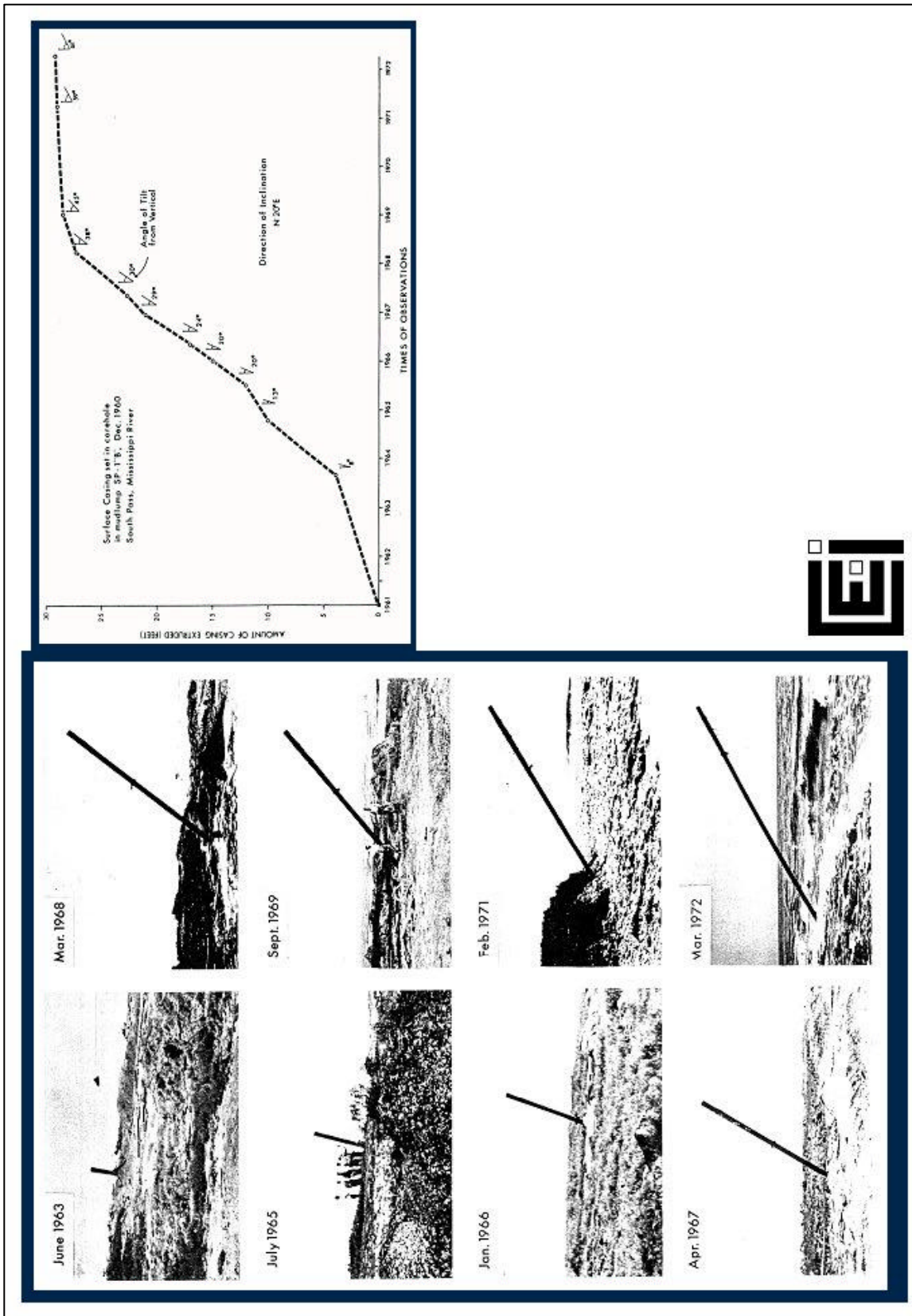


Figure 39. Progressive extrusion of drilling casing from bore hole drilled in South Pass mudlumps (after Morgan 1961). Figure 34 - C shows the coring of this hole in progress and Figure 36 shows BH - B in reference to the stratigraphy and structure of the mudlump fold.

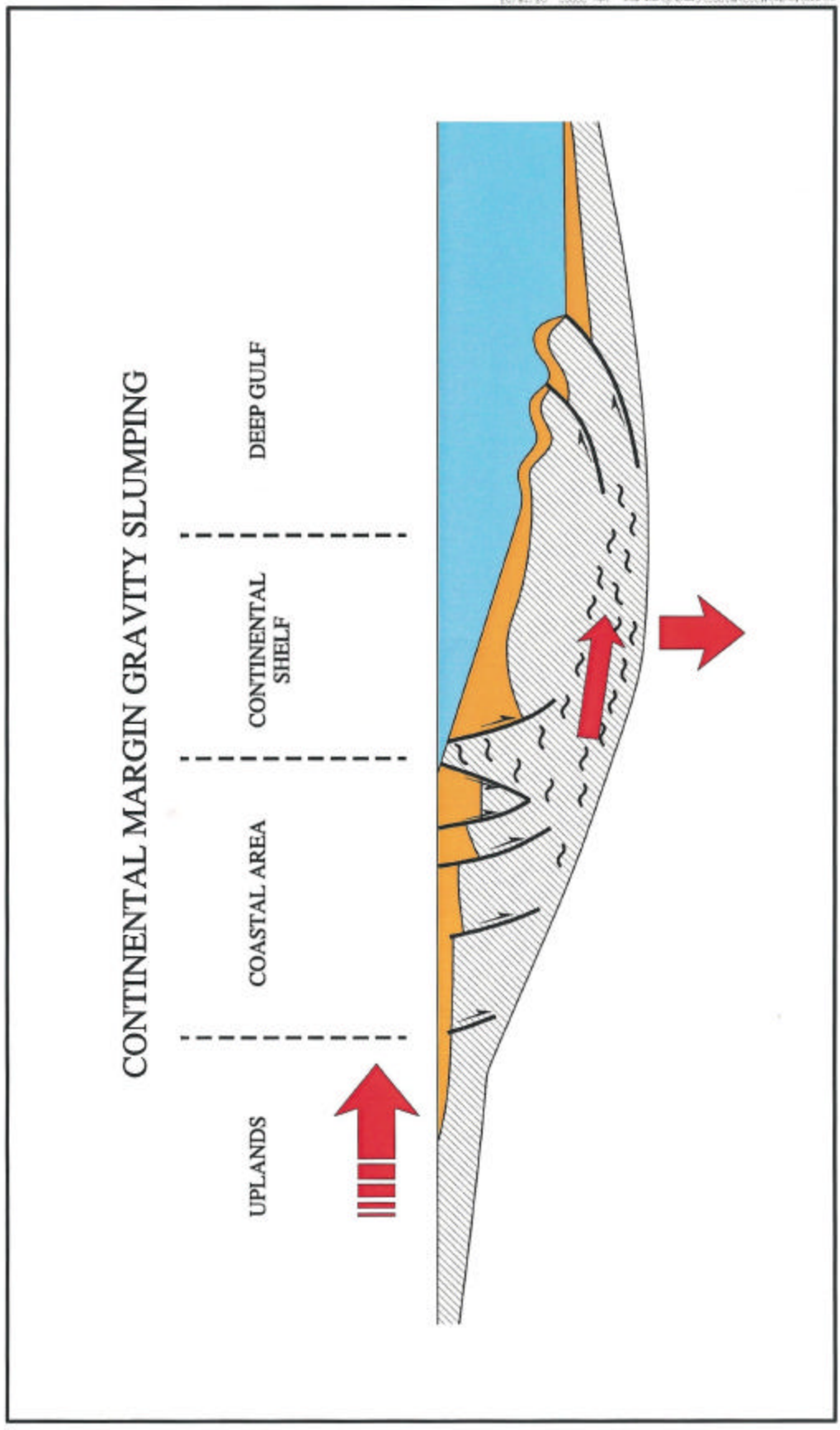


Figure 41. The weight of sedimentary deposits accumulating at the river mouth depocenters in the coastal area causes salt and shale beds to slide laterally into the deep gulf basin. The salt and shale and associated deposits bulge up along the continental margin and gulf floor. Growth faults in the coastal and shelf areas adjust vertically and laterally to the massive slumping (modified from Winker 1982).

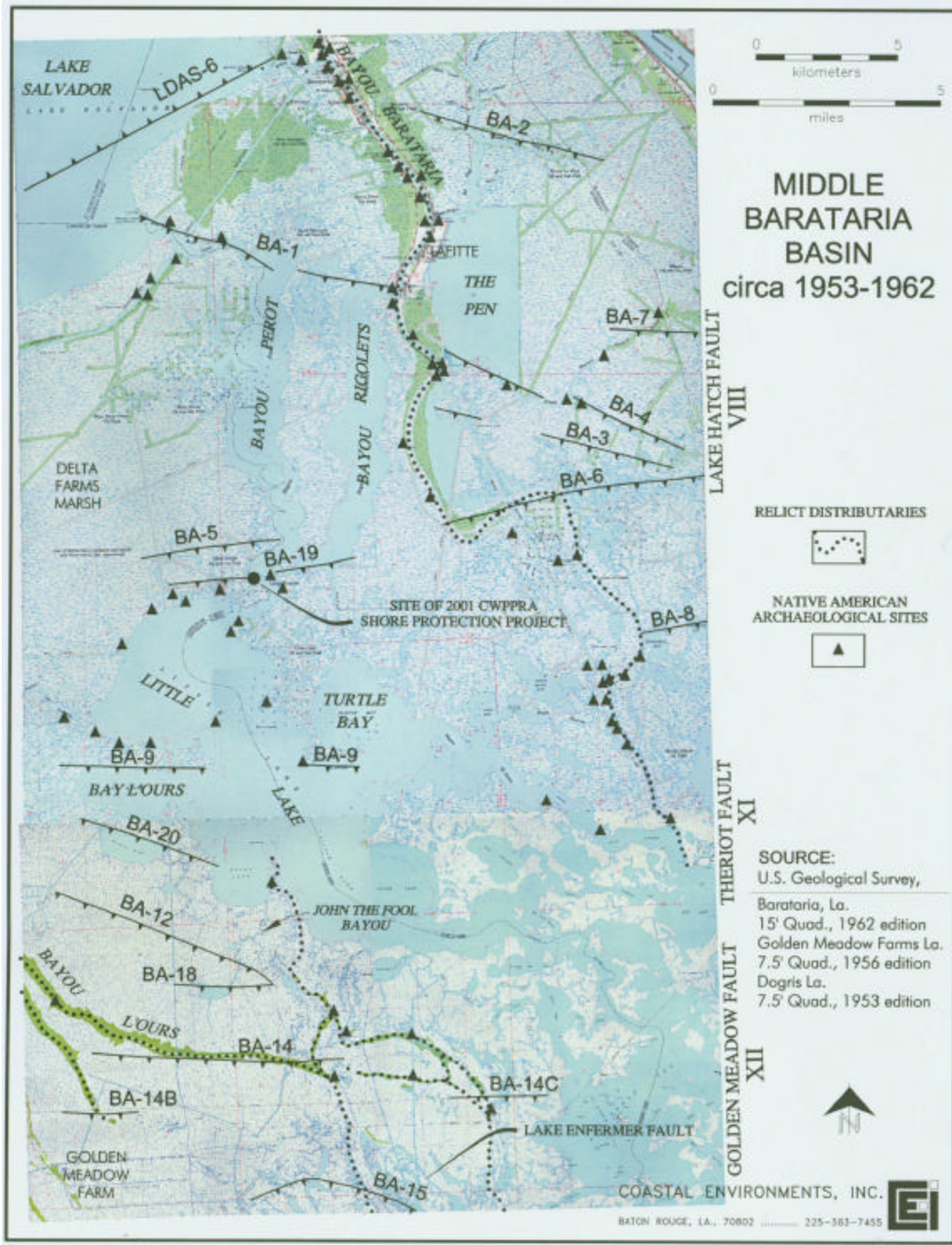


Figure 42. Topographic map showing landforms and conditions in the Middle Barataria Basin, circa 1953-1962. Known and suspect surface faults are shown. Most faults are based on geomorphological evidence.

delineated on the basis of distinctive geomorphological signatures. These included alignments of streams, alignments of lakes and lakeshores, natural levee sags and, particularly, two large ballooned streams, Bayou Perot and Bayou Rigolets.

It appears that fault segments BA-5A and BA-6 have exerted a strong influence on landforms in this area. Bayou Barataria, a Mississippi River distributary which was active between 3500 and 2000 YBP (Frazier 1967:308), makes a right angle turn and a detour of 3 mi (4.9 km) where it encounters this apparent fault. There are indications (marsh breakup and shore calving) that the South Bayou Perot Fault (BA-5) is presently active.

A comparison of 1953-1962 conditions shown in Figure 42 with the 1998 image of the Middle Barataria Basin shown in Figure 43 reveals the extent of deterioration and land loss that occurred. There is also geomorphic evidence for movement along the Lake Hatch, Theriot and Golden Meadow Faults during this interval. Large breakup areas developed south of Little Lake (BA-20), Bayou L'Ours (BA-14) and Lake Enfermer (BA-15) Faults. The Lake Enfermer Fault scarp did not become evident until about 1981. Inspection of land loss maps for the 1990-2000 interval recently completed by the National Wetlands Research Center of the U.S. Geological Survey indicates that the Lake Enfermer Fault continued to be active during this interval.

Map evidence indicates that rapid bank retreat along Bayou Perot and Bayou Rigolets (Figure 44), which is associated with the ballooning process, took place during two intervals. The first was between 1890 and 1932, and the second was between 1953-1962 and 1998. There was relatively little expansion of the ballooned streams between 1932 and 1953-1962. This suggests two periods of activity within the Lake Hatch Fault Zone, preceded by, and separated by, periods of relative dormancy.

The Barataria estuary crosses three east-west trending fault systems. Each zone exhibits evidence of historic activity. There have been periods of fault dormancy and several dormant faults have become re-activated. Changes in slope and elevation have resulted in an acceleration of the inland march of the fresh/non-fresh marsh boundary within the Barataria Basin.

Terrebonne Delta Plain

This large relict subdelta was chosen for study because of the high rates of land loss that occurred here during modern decades and because north-south relict distributaries and interdistributary basins overlie and cross east-west trending growth faults (See Figures 1 and 17). In Figure 45 is a mosaic of 1993 and 2000 satellite images of the Terrebonne Deltaic Plain study area. Suspected fault traces and scarps are shown on the image. The influence of the faults on landforms can be seen at many locations.

Experience gained in the analysis of the other regional basins was used in the Terrebonne study area. Based on this experience, in addition to delineating and indexing apparent surface faults, adjacent affected wetland areas were also delineated and indexed for systematic chronological evaluation. Thirty-five known and suspected surface faults and

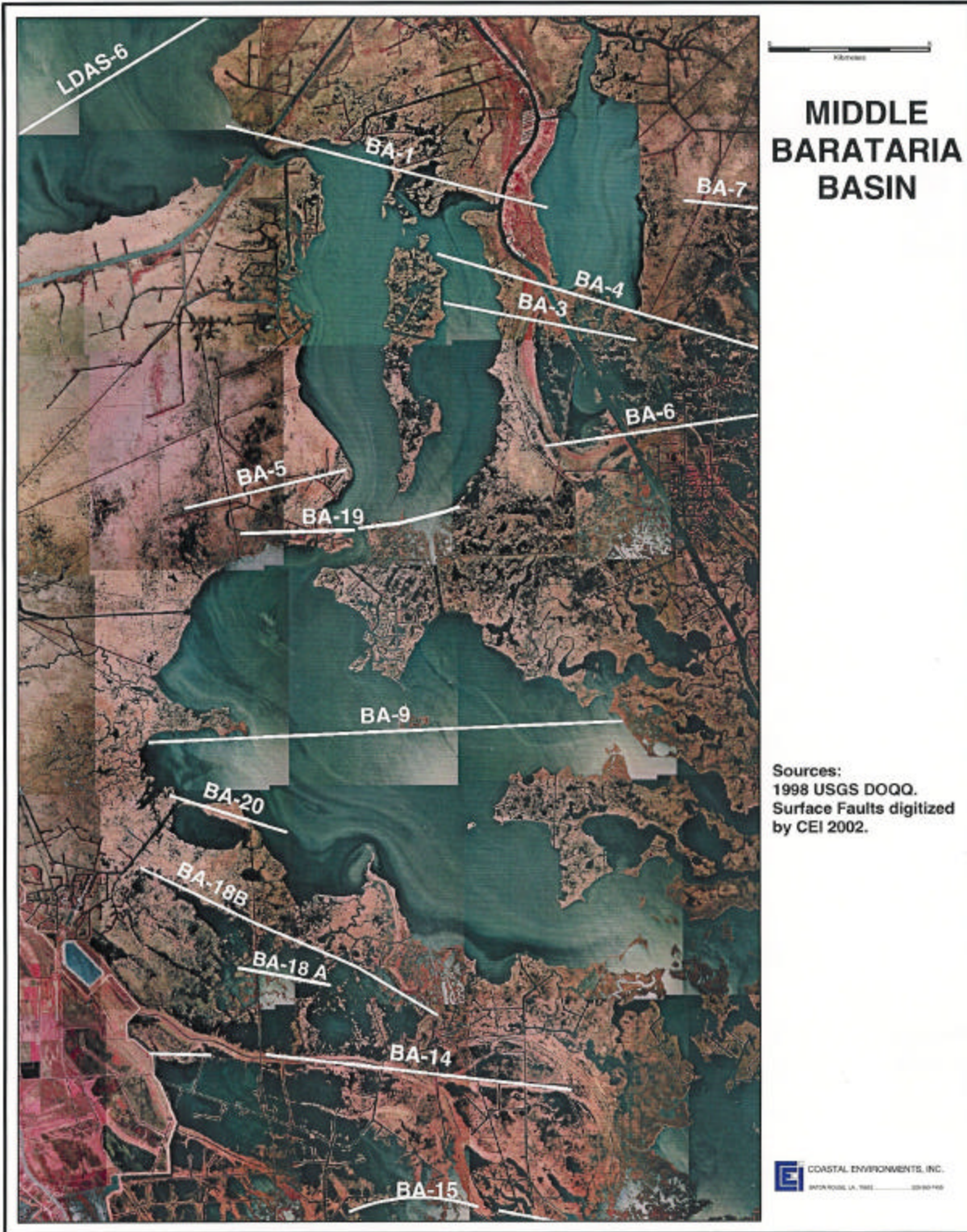


Figure 43. Aerial image of the Middle Barataria Basin in 1998 with locations of suspect surface faults shown.

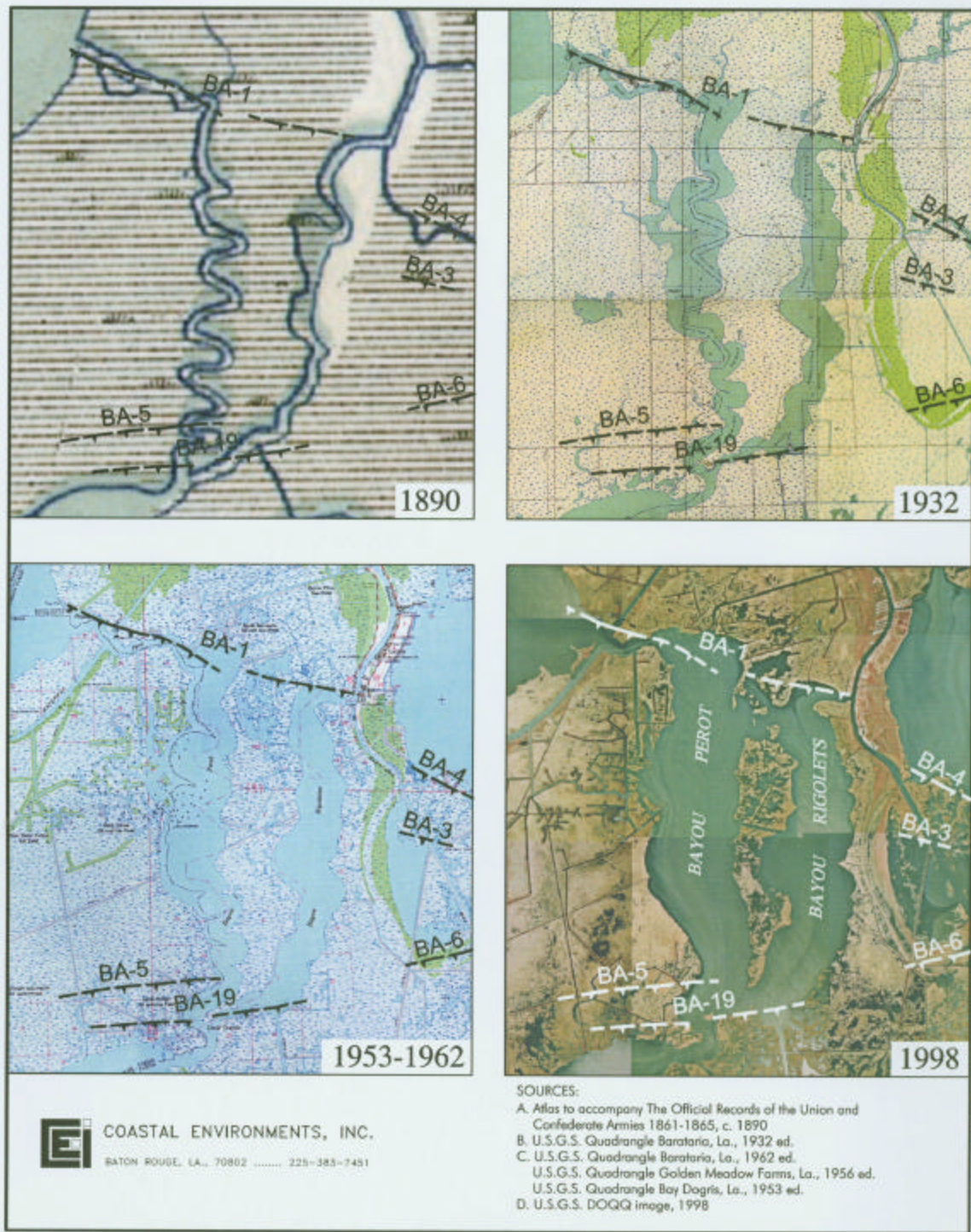


Figure 44. Sequential changes in Bayou Perot and Bayou Rigolets, two ballooned streams in the Middle Barataria Basin, during the period from 1890 to 1998.

32 breakup areas were identified and studied (Figure 46).¹¹ Field studies were conducted at the suspected Lake Boudreaux (ET-1) and Montegut (ET-4) Fault locales and eight suspected fault-breakup areas were studied in detail. This analysis technique provided a basis for specific conclusions regarding relationships between fault activity and landscape changes.

The Lake Boudreaux Fault (ET-1)

Surface expressions of the proposed Lake Boudreaux Fault first appeared on an aerial photograph taken in 1971. As illustrated in Figure 47, prior to the fault event the area consisted of unbroken fresh marsh with scattered stands of cypress trees. The fault event not only created an open water area, but also completely altered the hydrology and water chemistry. Figures 48 and 49 show aerial views of the shallow lake and dieback of cypress trees apparently caused by the Lake Boudreaux Fault event.

A geological section across the fault, based on shallow borings, is shown in Figure 50. The maximum depth of the water body on the down-dropped block of the fault is approximately 3 ft (0.9 m). The maximum vertical displacement documented by the borings is 2.0 ft (0.6 m) (See Table 4).

The Montegut Fault (ET-4)

A very distinctive east-west trending fault scarp is present in the marshes lying between Bayous Terrebonne, St. Jean Charles and Pointe au Chein southeast of the community of Montegut, Louisiana (Figure 51). Along most of its length the scarp is defined by a marsh-open water interface. The photograph (Figure 52) shows the nature of the scarp and the down-dropped block. As can be seen in photograph, the fault appears to run under the natural levee ridges of Bayou Terrebonne, but the effects of fault movement on the natural levees are masked by a flood protection levee and forced drainage district. Field inspection confirmed that there are multiple, closely spaced parallel faults just south of the scarp that is visible from the air.

A profile drawn from cores taken across the fault scarp is shown in Figure 53. While there is only a 2.5 ft (0.8 m) variation from the marsh floor to the adjacent water body, the borings show 4.5 ft (1.4 m) of vertical displacement of near-surface sedimentary beds.

The interior marshes south of the proposed Montegut Fault have largely reverted to open water with scattered marsh remnants and spoil banks. It is apparent from these extant landforms that submergence has generally been less than 2 ft (0.6 m), but it has, nevertheless, affected a large area.

It is also of interest that Wonder Lake, which lies just south of the proposed Montegut Fault, and which formed during the 1915 hurricane, remained virtually unchanged for more than half a century after its formation. However, it has now been engulfed by submergence of the interior marshes around the lake. Only remnants of the rim marking the lake's ragged outline remain to indicate the position of the former shore. Sasser et al. (1995:257) noted this

¹¹ The methodology and results of the systematic evaluation of the breakup areas is presented in a report by Gagliano et al. 2002, entitled Geological characterization of potential receiving areas for the central and eastern Terrebonne basin freshwater delivery project.

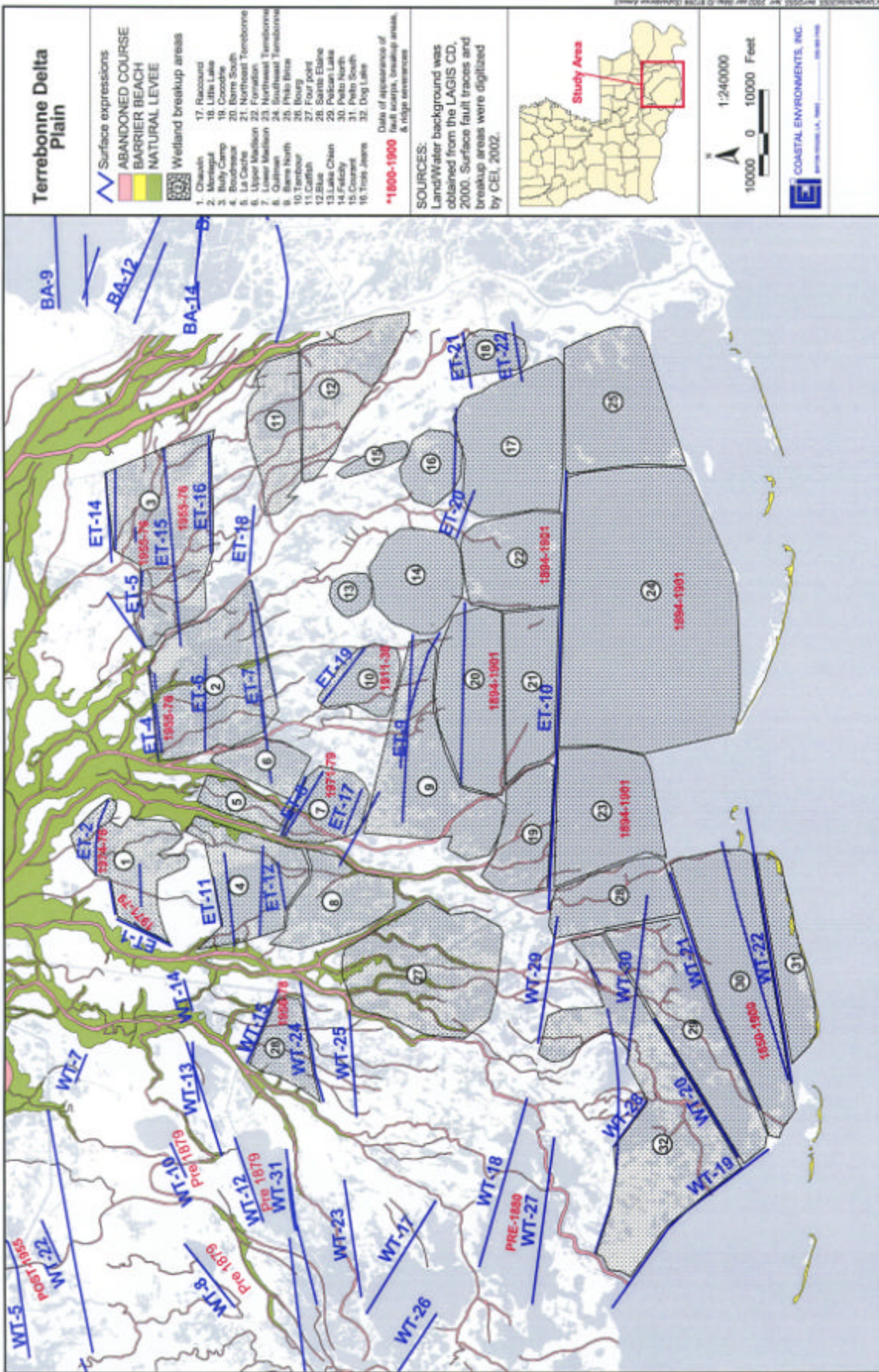


Figure 46. Natural levees, surface expression of suspected faults and breakup areas in the Terrebonne Deltaic Plain study area. Dates signify appearance of fault scarps, break - up areas and ridge severances.

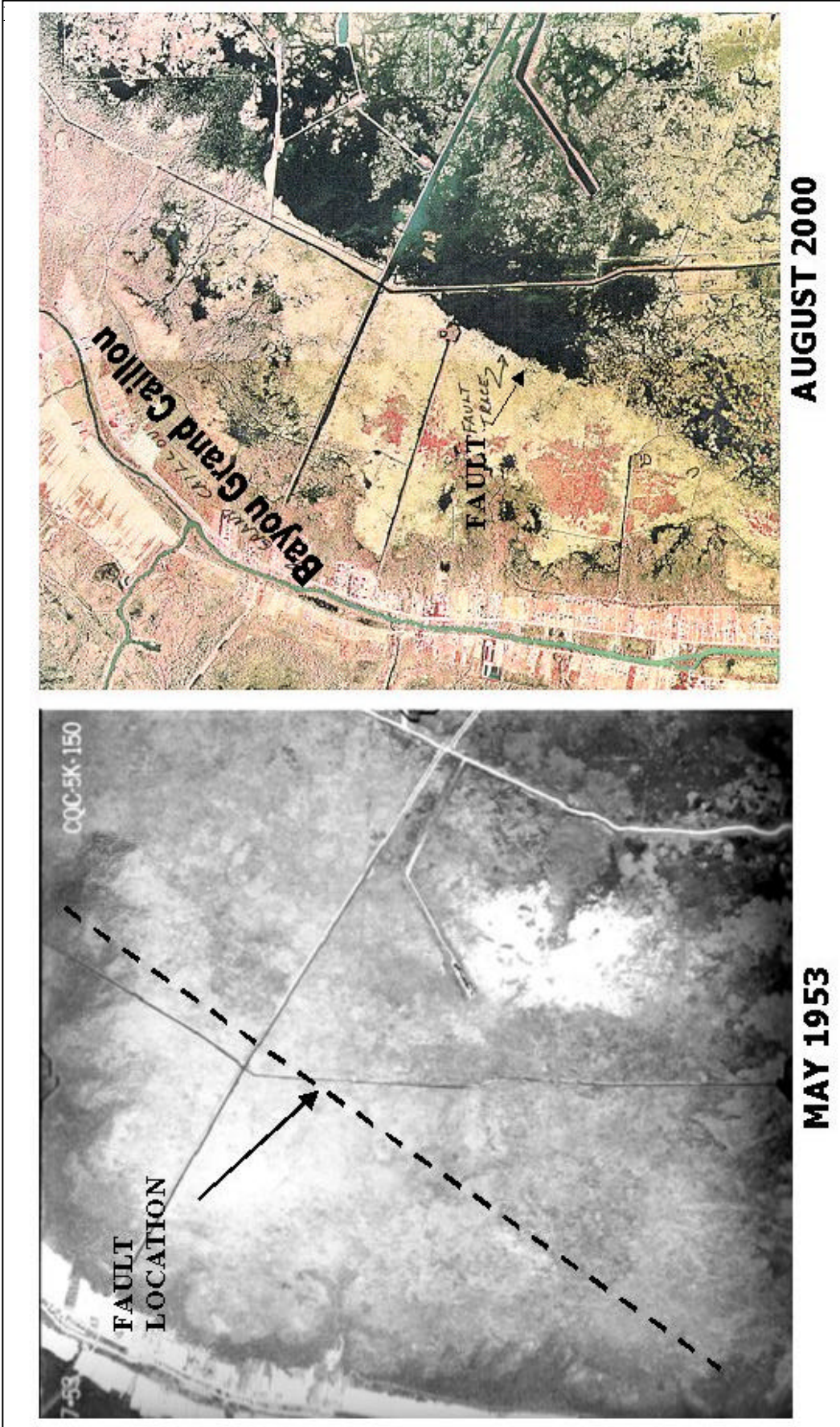


Figure 47. Changes in surface expression of the proposed Lake Boudreaux Fault are evident when aerial photographs taken in 1953 (left) and 2000 (right) are compared. First indications of the fault appeared on 1971 aerial photographs and by 1979 a large lake and a zone of altered and deteriorated wetlands had developed east of a well - defined fault scarp.



Figure 48. Aerial view of the proposed Lake Boudreaux Fault (Fault ET-1) looking southeast from Bayou Grand Caillou. This is a segment of the Boudreaux Fault Zone. The lake in the background resulted from fault displacement, which was first recorded on aerial photographs taken in 1971. Prior to the fault events the marsh was fresh. In 2001, the marsh on the near side of the fault was fresh, while that on the far side was brackish. Photograph by S.M. Gagliano, October 17, 2001.

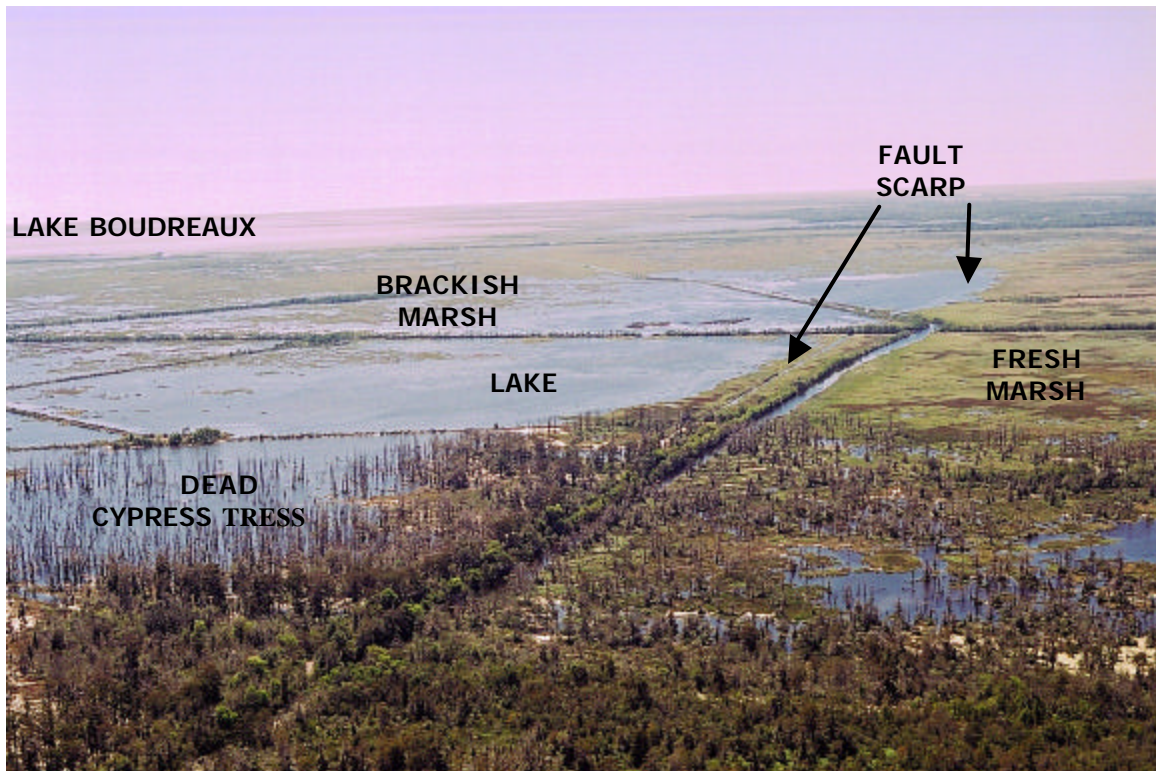
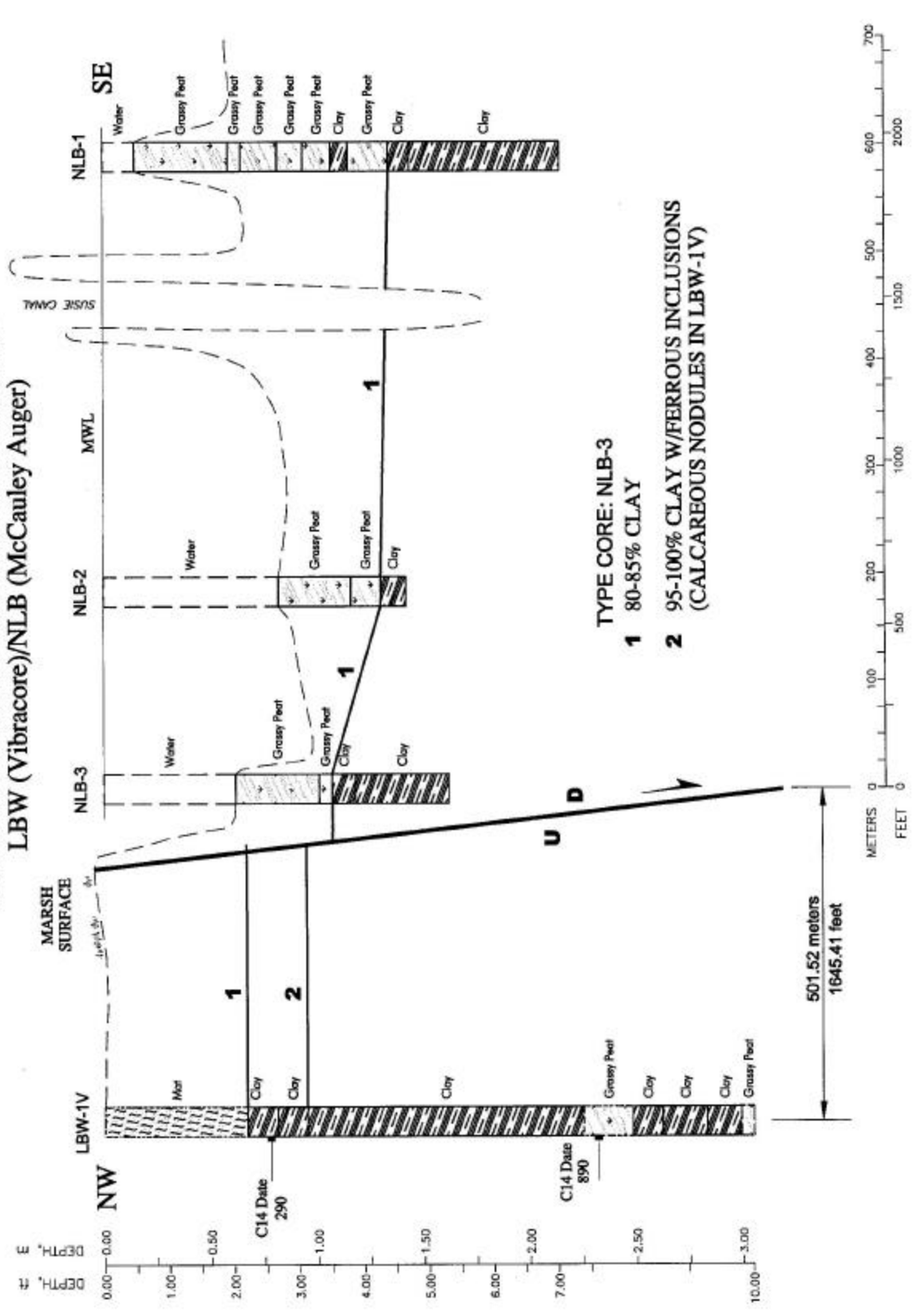


Figure 49. Aerial view of the proposed Lake Boudreaux Fault, looking south along the fault scarp. Note the dead cypress trees in the vicinity of the scarp. Photograph by S.M. Gagliano, October 17, 2001.

**CORRELATION SECTION: LAKE BOUDREAUX
LBW (Vibrocure)/NLB (McCauley Auger)**



- TYPE CORE: NLB-3**
- 1** 80-85% CLAY
 - 2** 95-100% CLAY W/FERROUS INCLUSIONS (CALCAREOUS NODULES IN LBW-1V)

Figure 50. Section based on borings taken across suspected Lake Boudreaux Fault (ET-1) showing surface elevation, water depths and near - surface stratification. The section shows 3.3 ft (1.0 m) of change in elevation from the marsh surface to the pond bottom and a 1.8 ft (0.55 m) of displacement of the top of the bed identified as '1.' The section is based on data from vibrocure and McCauley borings by CEI in 2001.



Figure 51. The proposed Montegut Fault scarp looking north across broken marsh on the down-dropped block of the fault. The town of Montegut, Louisiana can be seen in the background. Photograph by S.M. Gagliano, October 17, 2001.

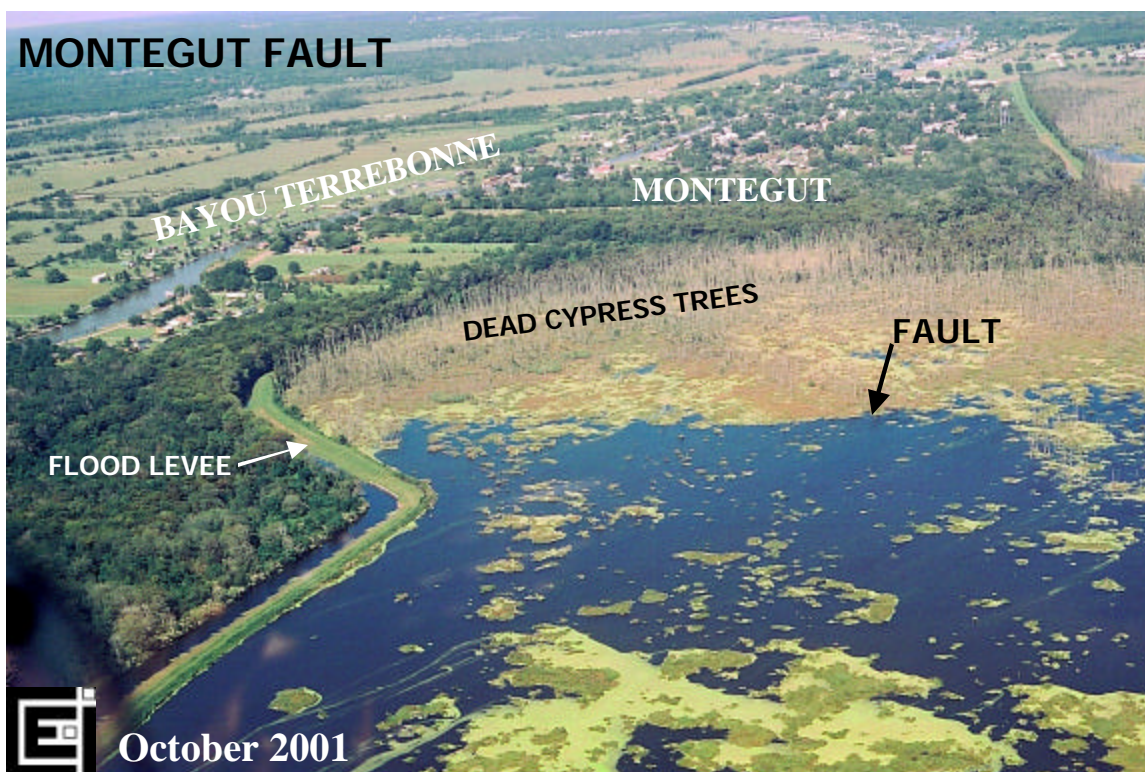


Figure 52. Aerial view of the proposed Montegut Fault. The view is looking north across a large pond and broken marsh on the down-dropped block of the fault. Note the dead cypress trees on the up-thrown block and the flood protection/drainage levee along the back-slope of the Bayou Terrebonne natural levee ridge. The Montegut community is located on the natural levee of Bayou Terrebonne. Photograph by S.M. Gagliano, October 17, 2001.

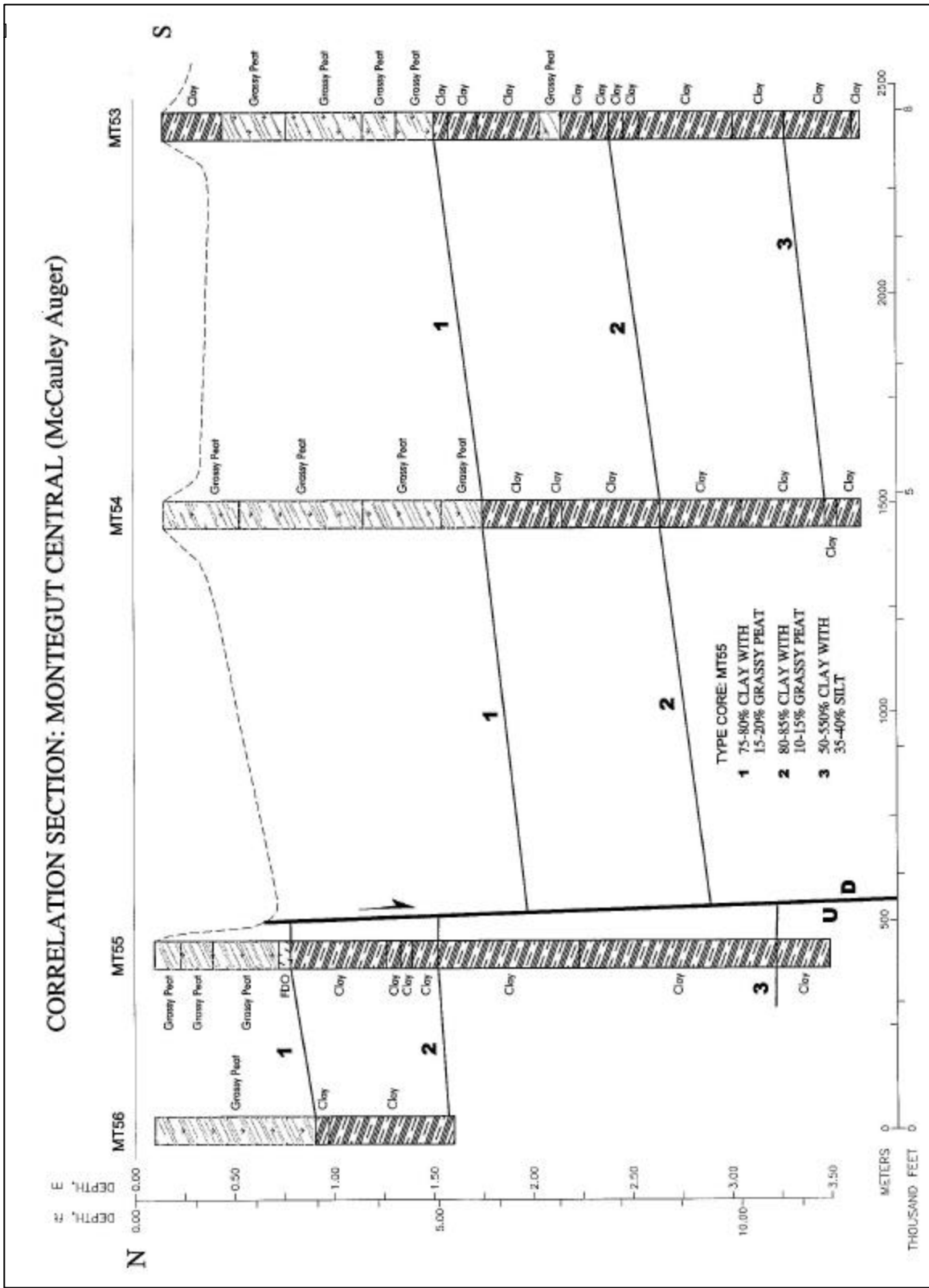


Figure 53. Near - surface geological section across proposed Montegut Fault based on McCauley auger borings by CEI in 2001.

same phenomenon in reference to a small isolated lake in fresh floating marsh south of Little Lake in the Bayou L'Ours area of Lafourche Parish. Here, interior marshes around a small lake at the end of John the Fool Bayou became submerged, apparently as the result of a modern fault event, leaving only the rim of the old lake above mean water level.

Isle de St. Jean Charles

Natural levee ridges that trend north-south and cross east-west trending faults can be seen in Figure 45 and 46. The relict distributary natural levees are draped across the faults. The pattern of the distributaries appears to have been influenced by the pre-existing faults. Ridges along the major distributaries Bayou DuLarge, Bayou Grand Caillou, Bayou Petit Caillou, Bayou Terrebonne and Bayou Lafourche are relatively high, and while they have been reduced in elevation and width (where not enclosed by forced drainage levees), they have not been completely submerged by fault movement. Some lesser relict natural levees, however, have been clipped and down-dropped by faults. Minor relict distributary natural levees are clipped at the Montegut and Pointe au Chein segments of the Theriot Fault. A part of the Bayou St. Jean Charles ridge has been down-dropped and submerged leaving the Isle de St. Jean Charles community stranded and isolated in an interior marsh area that has progressively reverted to open water since the mid-1950s (Figure 54). Ring levees have been built around part of the island to protect the community from flooding but submergence continues to occur.¹²

Figure 55 is an aerial view showing the extensive inundation of interior marsh in the vicinity of Isle de St. Jean Charles. This area lies within the core of the Terrebonne Trough and has been greatly affected by subsidence.

Fault severance of Bayou Terrebonne and opening of Lake Barré

An excellent example of severed natural levee ridges occurs in Terrebonne Bay, where the Natural levees along Bayou Terrebonne have been cut off and submerged by a segment of the Leeville Fault System. Excerpts from a series of three historic maps are shown in Figure 56. Changes from map to map indicate that each was drawn from "new", and presumably current information. Map "B" was not simply redrawn from map "A" and map "C" not redrawn from map "B."

Archaeological sites located along the natural levees of Bayou Terrebonne indicate that the stream was an active distributary of the Mississippi River during the interval from 1300 to 1000 YBP (Weinstein and Gagliano 1985). There was an apparent deflection of the course of Bayou Terrebonne by a fault when the bayou was an active Mississippi River distributary. Figure 56 presents historic evidence of the severance and down-

¹² The island community had a reported population of 277 people, many of whom were decedents of a band of Biloxi-Chitimacha-Choctaw Indians. The Corps of Engineers has developed a relocation plan for the island residents. At a public hearing in June 2002, Albert Naquin, Chief of the community, advised that the community consider the relocation alternative. Later in the same year the island was hard hit by hurricanes Isadore (September 25th) and Lili (October 3rd) and Chief Naquin again advised the residents to move.



Figure 54. Looking north along Isle de St. Jean Charles. The severed natural levee ridge along the bayou can be seen in the background. Part of the ridge has been submerged as a result of fault movement. Photograph by S.M. Gagliano, October 17, 2001.

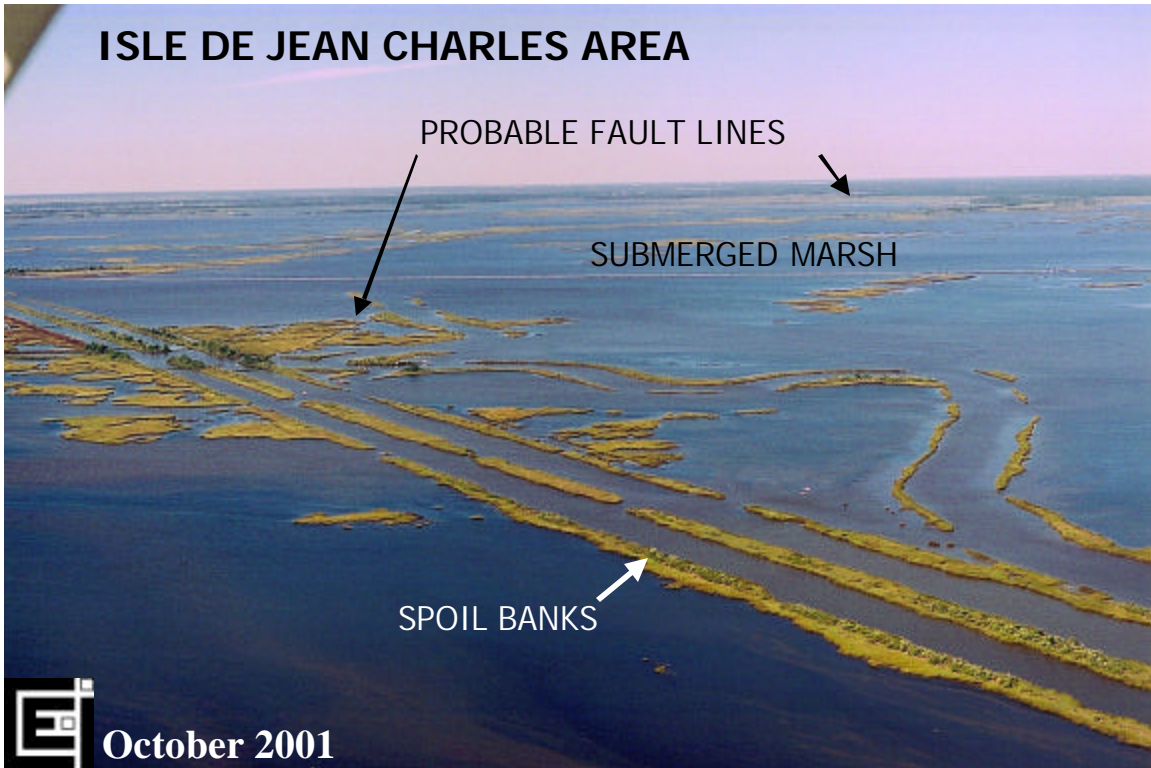


Figure 55. Extensive areas of submerged marsh in the vicinity of Isle de St. Jean Charles. Photograph by S.M. Gagliano, October 17, 2001.

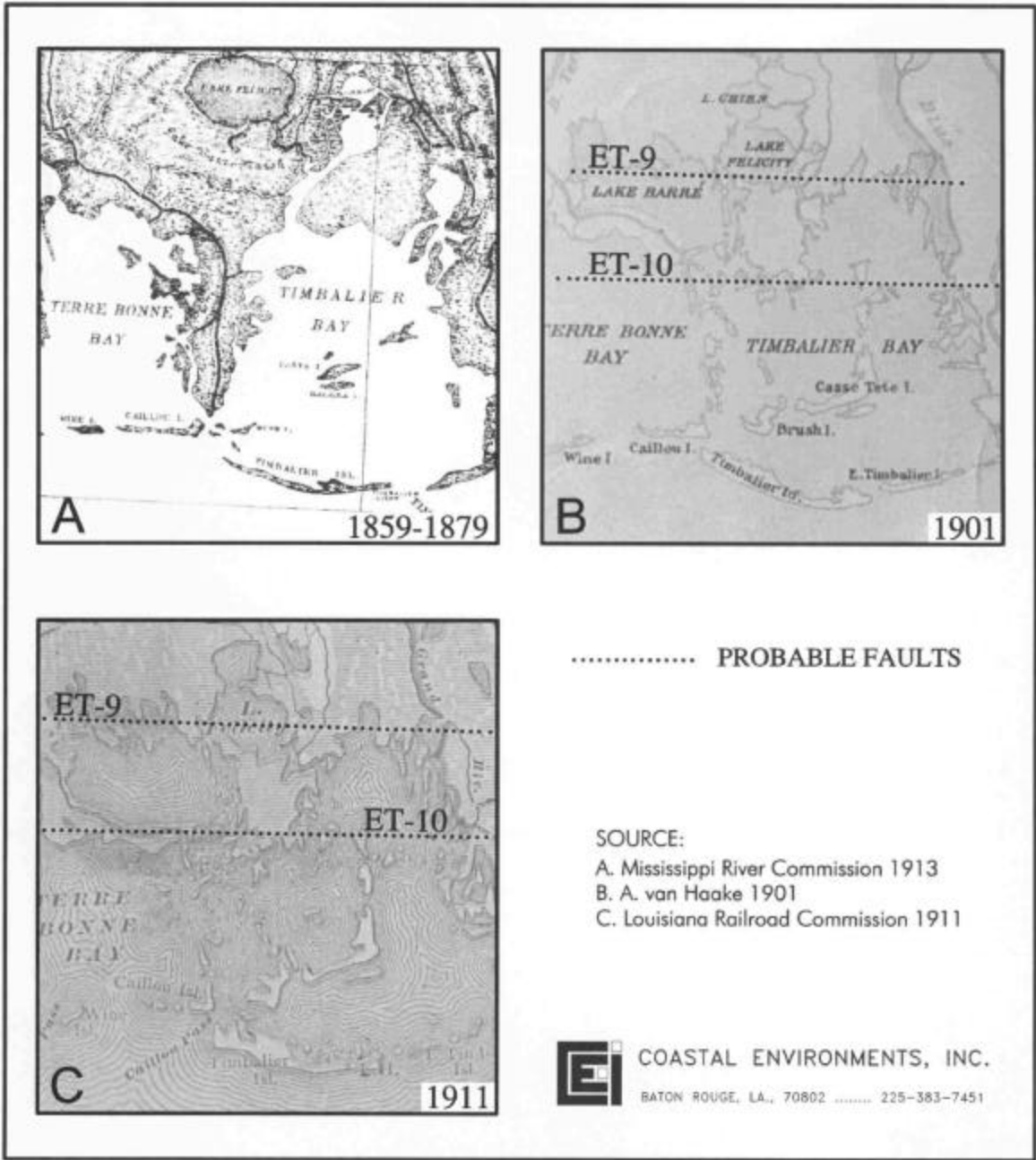


Figure 56. Comparison of historic maps showing the severance of the natural levees of Bayou Terrebonne and the opening of Lake Barré between 1859-1879 and 1901. The locations of suspect faults have been added to the maps.

dropping of the natural levees along Bayou Terrebonne between 1859-79 and 1901. The 1859-79 map shows that Bayou Terrebonne extended almost to Caillou Island.¹³

The maps also show the opening of Lake Barré. On the 1859-79 map the area lying between Lake Felicity and the then “Bayou Terre Bonne” ridge is shown on the map as marsh and bears the name “Lake Barré Marsh.” On the 1901 map this same area is shown as a water body with the name “Lake Barré.” The rapid conversion of the Lake Barré marsh to a lake qualifies as a turn of century “land loss hot spots.”

There was relatively little change in the remnant marsh islands between 1901 and 1911.

Correlation of apparent faults and land loss

A three-way correlation is made in Figure 57 between known subsurface faults and suspect surface faults identified from geomorphic signatures and areas of high land loss during the period from the 1930s to the 1990s.

The correlation between suspect surface and known subsurface faults is evident. In most instances where suspect surface faults do not have a direct subsurface counterpart, they conform to trends of major regional faults or occur within complex fault patterns around salt domes or other features such as the Pelto Horst. Particularly evident is the correlation between land loss and faults in the Penchant Basin (Lake Hatch Fault Zone) and the zone through the communities of Golden Meadow, Galliano, Montegut, Chauvin, and Dulac (Theriot and Golden Meadow Faults).

Occurrence of relatively high natural levee ridges in the immediate area of Houma, masks the effects of subsidence during the time interval covered by the land loss data. That is, while elevations of the ridges may have been reduced by fault events during modern decades, because of the height of the ridges the land did not revert to water. It should also be noted that historic fault events along the coast occurred prior to the interval covered by the land loss data.

TRIGGERING MECHANISMS

Natural and anthropogenic processes that could initiate local and/or regional fault events were considered. These included sediment loading, hydrocarbon extraction (fluid withdrawal), flood and storm water loading, earthquakes, seiches and upward movement of salt water and gasses along fault planes.

Natural System Succession

The interplay between sediment loading and fault movement is fundamental to the understanding of past and the prediction future fault events in Southeastern Louisiana.

¹³ The historic condition of Bayou Terrebonne was described by the late U. S. Senator Allen Ellender of Terrebonne Parish who related the story of how his family drove cattle down the natural levee ridges and waded them across a shallow stretch of water to Caillou Island, where they were left to graze (Senator Allen Ellender, per. comm. circa 1971).

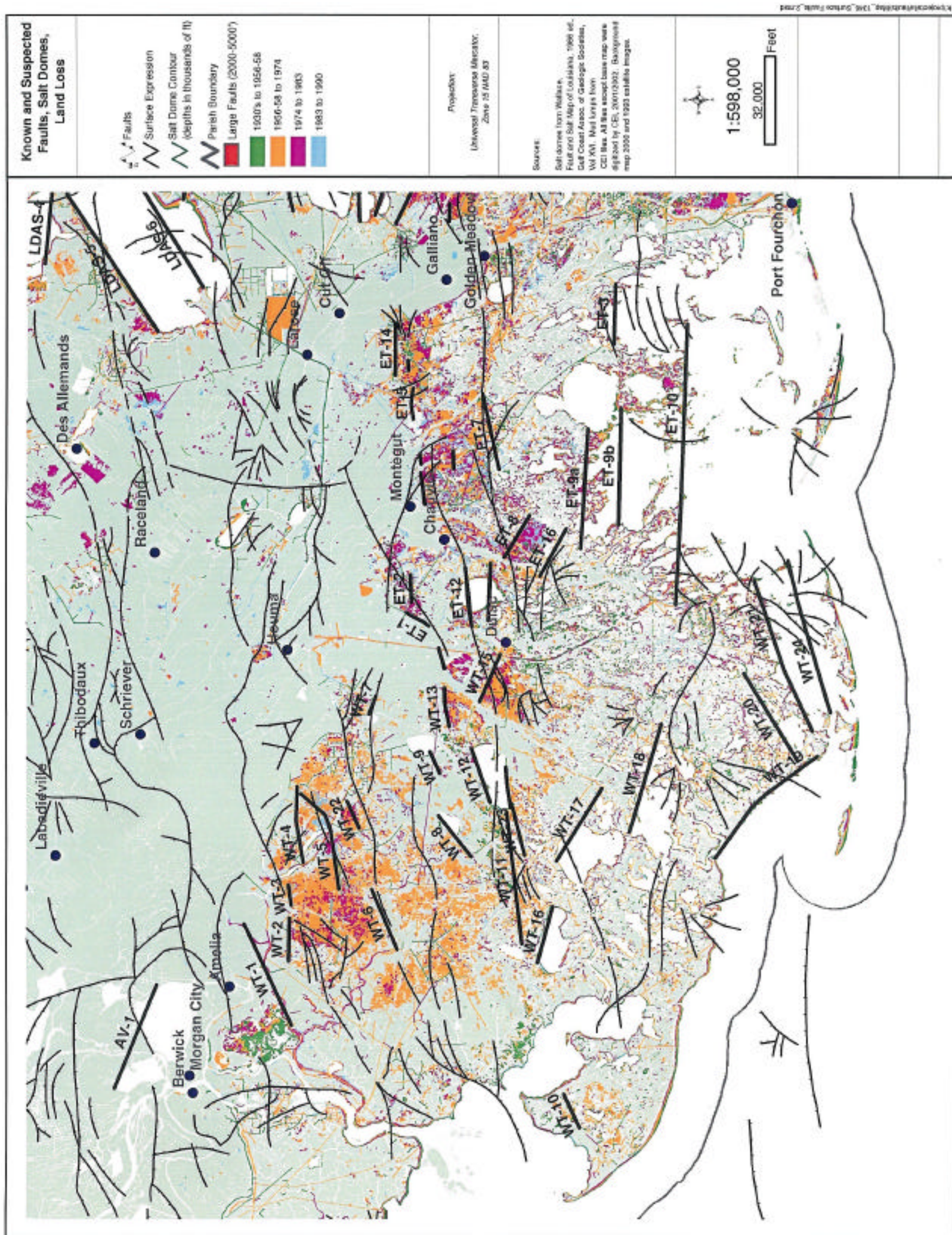


Figure 57. Map showing relationship between suspected surface and known subsurface faults, and land loss in the Terrebonne Deltaic Plain study area.

To further understand these interactions a study of successive growth and deterioration of the Lafourche Delta lobe, the dominant feature of the Terrebonne Deltaic Plain (see Figures 1, 14 and 17), was conducted. Six chronological stages of delta development were defined and analyzed. Tracing the development and change of the landforms and environmental conditions of the ridges and basins through time in reference to the underlying structural features revealed a remarkable interplay between sedimentary processes, geological structural movement and cyclic delta system growth and deterioration.

The foundation and landform framework of the Terrebonne area is the product of Teche-Mississippi delta building during the interval from 4500 to 3500 YBP (see Figure 14). After the Teche-Mississippi cycle ended, there was a 1000-year period when an upstream diversion shifted most of the Mississippi flow to a new course and initiated delta building in the St. Bernard Delta, with little if any inflow continuing into the Terrebonne area.

During this interval, Red River discharge and fresh water from the entire Atchafalaya and Verret Basins entered the Terrebonne area. After the 1000-year hiatus, Mississippi River sediment laden water was again introduced into the Terrebonne area via an ancestral Bayou Lafourche. This was the beginning of the Lafourche-Mississippi Delta cycle, which progressed from an initial stage of building around and over the older Teche Delta marshes to building out into the open waters of the gulf.

The Lafourche-Mississippi Delta was in a declining condition at the end of the nineteenth century but was still receiving 10 to 15 percent of the total flow of the Mississippi River. After a severe flood in 1903, which inundated agricultural land along the natural levees of Bayou Lafourche, a dam was built across the head of the bayou at Donaldsonville, thus cutting off all flow from the parent river. Since being cut off from the Mississippi, the Lafourche Delta has passed through several stages of deterioration. Although humans have occupied the area throughout both the Teche and Lafourche-Mississippi cycles of delta building, as well as the deterioration stages, they have only been a factor in altering the processes that drive the system for about the past 250 years.

The major geomorphic features of the area are shown in Figure 58. The Teche Ridge consists of a pair of natural levees that flank the relict master channel of the Teche-Mississippi Delta System. This Teche channel once carried the full flow of the Mississippi River. Likewise, the Lafourche Ridge is made up of the natural levees along the master channel of the Lafourche-Mississippi Delta, but this channel never carried full flow of the river system because there were several other branches that remained active throughout its history.

The branching distributaries of the Lafourche-Mississippi Delta System fan out from the City of Thibodaux, break up into a braided pattern in the Fields Basin, cut through the Teche Ridge, and then spread into a broad fan that reaches out toward the gulf. The nodal points, where the channels branch, are identified on the map. The relict natural levee ridges trend from north to south and cross the regional faults, which trend east-west. Two island chains form the seaward margin of the Terrebonne Delta. Each island

A sequential analysis of geological change, driving processes and resulting environmental succession of the study area has been conducted as a basis for predicting future conditions. A synthesis of this analysis is presented in six stages. The first stage summarizes two prehistoric episodes of delta building. Stages 2 through 5 are largely post-delta building stages covered in 50-year increments. The final episode, Stage 6 presents probable future conditions with the caveat that future conditions depend to some extent on human intervention (or non-intervention). A discussion of each of these stages follows.

Stage 1. Delta Building: Prehistoric Times (Figure 59)

System – The active Teche-Mississippi Delta (4500 – 3500 YBP) and the Lafourche-Mississippi Delta (2000 – 100 YPB) developed sequentially with overlapping landforms.

River Supply – The Teche Delta was fed from the west via the Teche-Mississippi, which peaked at 100 percent Mississippi system flow and diminished to 5 percent. The Teche Delta was cut off from Mississippi flow about 3500 years ago as the result of an upstream diversion which directed the master river to the east side of its alluvial valley. The eastern side remained dominant for about 1000 years during which time the old Teche Delta received fresh water not only from its own catchment area but also from the entire Atchafalaya and Verret Basins lying to the north. It also received flow and some sediment from the Red River, which was not directly linked to the Mississippi during this time. About 2000 years ago, a branch channel developed from the eastern course trunk channel of the Mississippi into the Terrebonne deltaic plain area via Bayou Lafourche and several lesser distributaries. River flow into the Lafourche Delta peaked at about 50 percent and diminished to 15 percent during this stage. Many abandoned Teche distributaries were re-occupied and continued to receive flow during the active life of the Lafourche Delta. Distributary channels delivered large volumes of river water, bedload, suspended sediment and dissolved solids into the system. In addition, the area continued to receive fresh water from the Atchafalaya and Verret Basins.

Hurricanes – There are no data on prehistoric storms.

Fault events – The Penchant graben directed the Teche-Mississippi trunk channel, and influenced the position of nodes of the Lafourche Delta. Faults of the Mauvais Bois System severed Teche distributaries, initiated a transgression at the end of the Teche delta building stage. The Golden Meadow Fault influenced bends and branches of the distributary channels. The Lake Caillou Fault influenced the position of bends and distributaries. The Salvador Fault influenced lacustrine delta building into the western end of Lake Salvador.

Sea level – Sea level was relatively stable.

Upper Deltaic Plain – The Upper Deltaic Plain covered three-quarters of the total area of the system. Natural levee ridges became higher, broader and longer (extending seaward). Bottomland hardwood forests developed on natural levee ridges. Cypress swamps and fresh marshes occupied large freshwater basins. Water flow in these basins was sluggish. Native American settlements were located on natural levees.

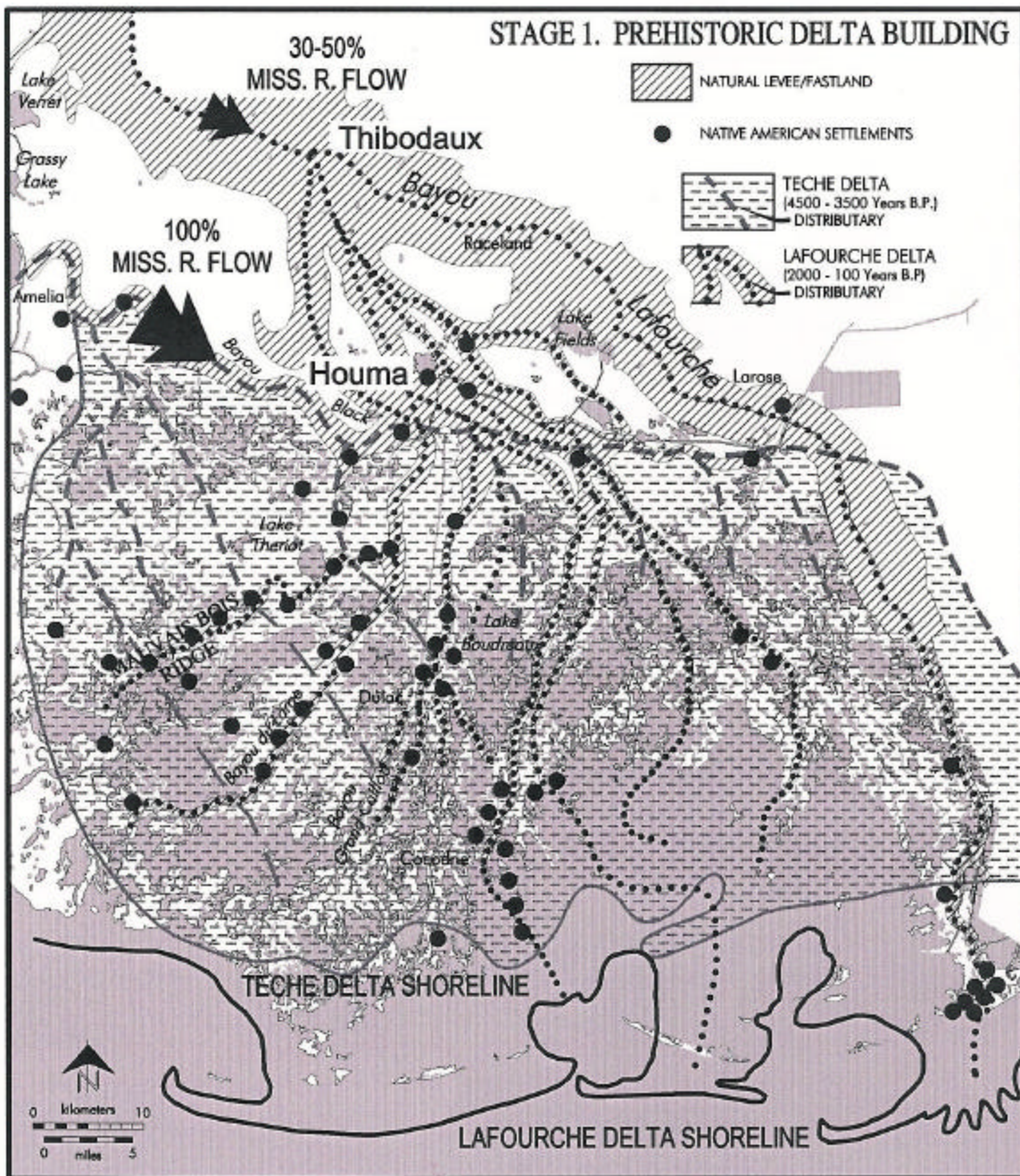


Figure 59. Overlapping lobes of the Teche and Lafourche deltas, Stage 1: prehistoric delta building.

Lower Deltaic Plain – The Lower Deltaic Plain encompassed one-fourth of the total area. Delta building overshadowed subsidence. Active distributaries extended into the gulf (prograding shore zone). There were beach ridge complexes at major distributary outlets and muddy islands and bars at others, as beaches and spits formed at the outlets of abandoned distributaries. Barrier island chains started to develop. Bays and tidal inlets were small with oyster reefs restricted to the small bays.

Stage 2. Poised: 1800 A.D. – 1850 A.D. (Figure 60)

System – The system was in the early abandoned stage of the delta cycle.

River supply – Mississippi River flow delivered by Bayou Lafourche diminished from 20 percent to 15 percent during this stage. The supply of supplemental fresh water from the Atchafalaya and Verret Basins continued. River water was distributed broadly through active and abandoned distributaries and over-bank flow.

Hurricanes - Seventeen hurricanes developed in the Gulf of Mexico region and five struck the New Orleans area. There is no information of hurricane activity in eastern Terrebonne Parish.

Fault events – Fault events probably created Lake Caillou, Lake Boudreaux and Lake Felicity. Fault events separated the Dernier Islands from headlands through creation of ancestral Lake Pelto. Lake Caillou first appears on maps during this period. Lake Boudreaux and Lake Felicity may pre-date this period.

Upper Deltaic Plain – The Upper Deltaic Plain covered two-thirds of the total delta area. Minor distributaries were closed at their heads (later re-opened for navigation) and only major channels remained active. Aggradation continued only on natural levees of major channels. Fresh marshes and swamps reached maximum development. Fresh marsh vegetation invaded open water bodies and channels, and the marsh was continuous and unbroken with a strong resilient root mat.

Accretion of marshes kept pace with subsidence but ridges started to diminish in elevation and width. Occasional lakes were formed by fault events. Hardwood forests on the natural levees were cleared for agriculture and cypress swamps were logged. The Barataria Canal was dug through the ridges and the channels of some relict distributaries channels that had silted. As a result they were re-opened.

Lower Deltaic Plain – The Lower Deltaic Plain occupied one-third of the total Terrebonne Delta area. The tidal zone was narrow but expanding. Bays began to form as a result of hurricanes and fault events.

Progradation and bar building occurred only at the mouth of Bayou Lafourche.

Barrier islands increased in size and elevation as sand was liberated by waves and redistributed by long-shore drift, storm waves and wind. Barrier islands reached maximum size, elevation and continuity early in this period, but some deterioration may have begun as a result of the Caillou and Pelto Fault events. Passes became constricted, thus controlling water exchange between the estuary and gulf. Oyster reefs expanded with enlargement of bays. The Southwest Canal was dug across Bayou Lafourche at Leeville.

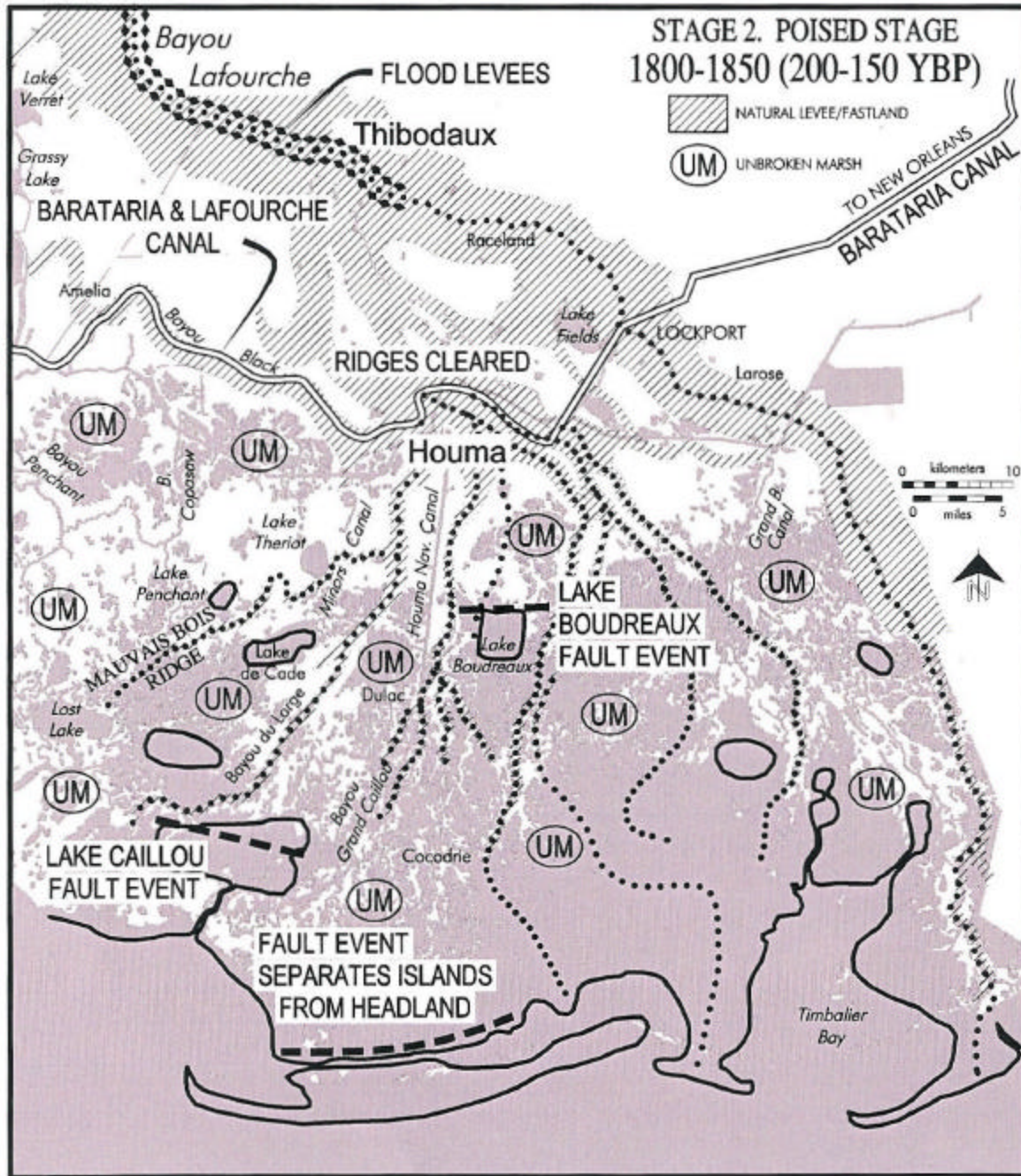


Figure 60. Conditions in the Terrebonne Deltaic Plain during the poised stage (1800-1850 A.D.) of the Lafourche Delta cycle. Maximum development of barrier islands and upper deltaic plain fresh swamps and marshes.

Stage 3. Early Deterioration: 1850 A.D. – 1900 A.D. (Figure 61).

System – The system was an abandoned delta, stage 2. This was a period of intensive deterioration in the Lower Deltaic Plain. The Upper Deltaic Plain remained in a poised condition.

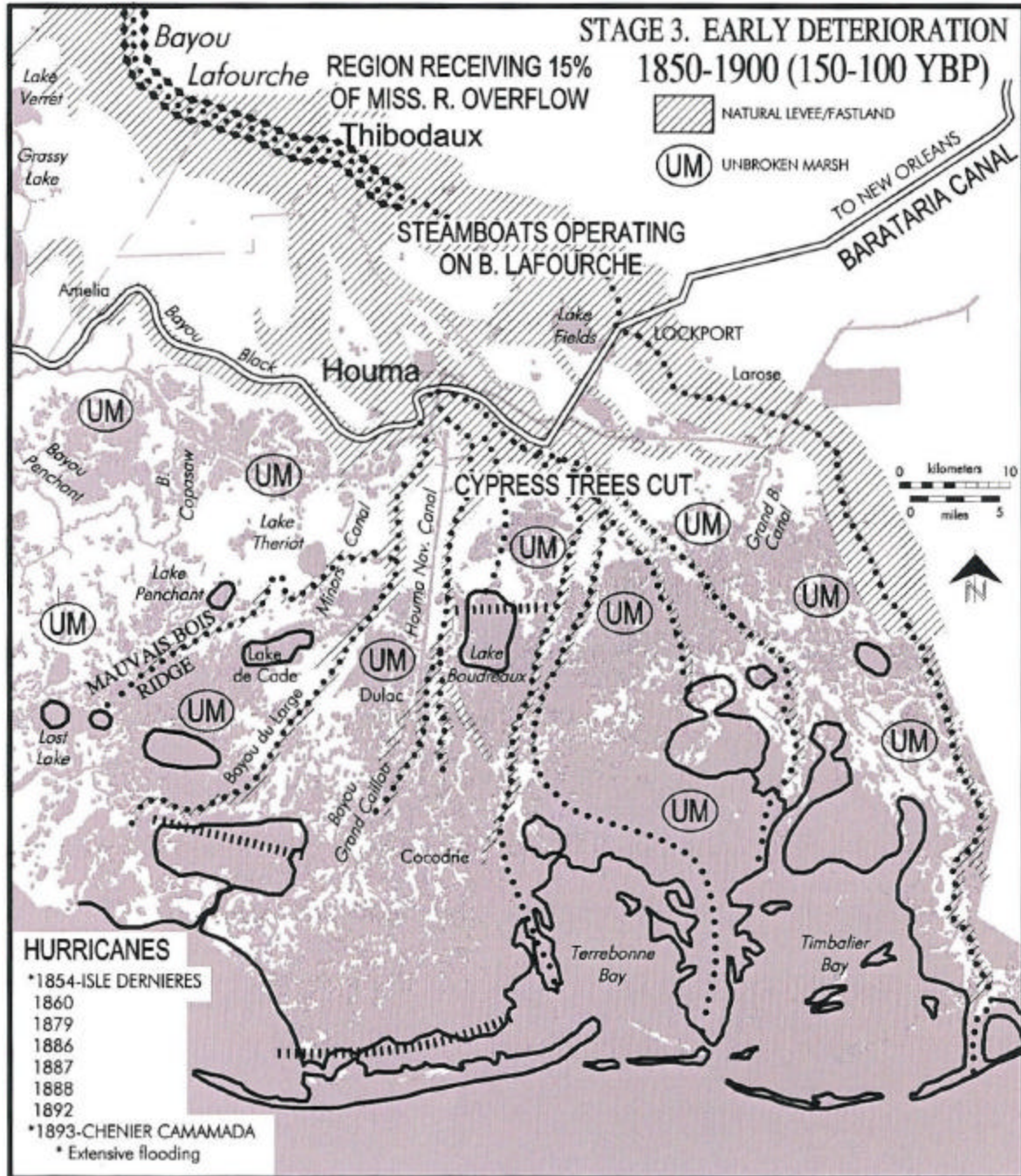


Figure 61. Conditions in the Terrebonne Deltaic Plain during early deterioration (1850-1900 A.D.) of the Lafourche Delta cycle.

River Supply – Fifteen percent of Mississippi River flow entered the area via Bayou Lafourche and through abandoned channels and over-bank flow. The Terrebonne area continued to receive supplemental fresh water from the Atchafalaya and Verret Basins.

Hurricanes – This was a period of intensive hurricane activity. The Last Island storm of August 1856 drowned hundreds of people and had a severe impact on the Dernier Island chain. A series of very destructive storms had great impact on the Chenier Caminada

community and lower Lafourche area in 1892 and 1893. The 1893 hurricane claimed almost 800 lives in and around Caminada.

Fault events - This was a period of active faulting in the Lower Deltaic Plain, resulting in expansion of the bays. Bayou Terrebonne was severed at the end of this stage or the beginning of the next (1894-1901). Lake Barre opened, as did bays south of Lake Felicity.

Upper Deltaic Plain – The Upper Deltaic Plain covered two-thirds of the total area. Fresh marshes remained unbroken and continuous. These marshes were self-mending against minor storm and fault breaks. Natural levees decreased in elevation and width but remained prominent. Flood levees were built along Bayou Lafourche to a point below Thibodaux for the protection of crops grown on natural levee ridges. Steamboats were operating on Bayou Lafourche. Navigation improvements were made to natural channels and the canal network was deepened and expanded.

Lower Deltaic Plain – The Lower Deltaic Plain covered one-third of the total area. Lower reaches of distributary channels were kept open by tidal action. Storms and fault events enlarged the bays. The size and elevation of the barrier islands started to diminish in response to fault movement. Natural levees began to slowly lose elevation and width as a result of subsidence.

Stage 4. Intermediate Deterioration: 1900 A.D. – 1950 A.D.
(Figure 62).

System – The system was estuarine-marine. Rapid deterioration of the Lower Deltaic Plain continued and the Upper Deltaic Plain began to show symptoms of deterioration.

River supply – A dam was constructed across Bayou Lafourche at Donaldsonville, Louisiana in 1904, and flood levees along the river were improved. Virtually all Mississippi River flow was cut off from the study area.

Hurricanes – Six hurricanes affected the area during this period. The storm of 1909 claimed the lives of 300 people on Grand Isle and Chenier Caminada. Two hurricanes occurred one month apart in 1915; one of which was the most severe storm ever recorded along the Louisiana coast up to that time. The 1915 storm had unusually high tides and caused the death of an additional 300 inhabitants. Wonder Lake and other bays were created by storms during this period.

Fault events – A second Pelto Fault event enlarged Lake Pelto and further separated the Dernier Barrier Islands from the headland. Lake Tambour was formed. There was an expansion of the bays as a result of fault events followed by severe hurricanes.

Sea level – Sea level was relatively stable.

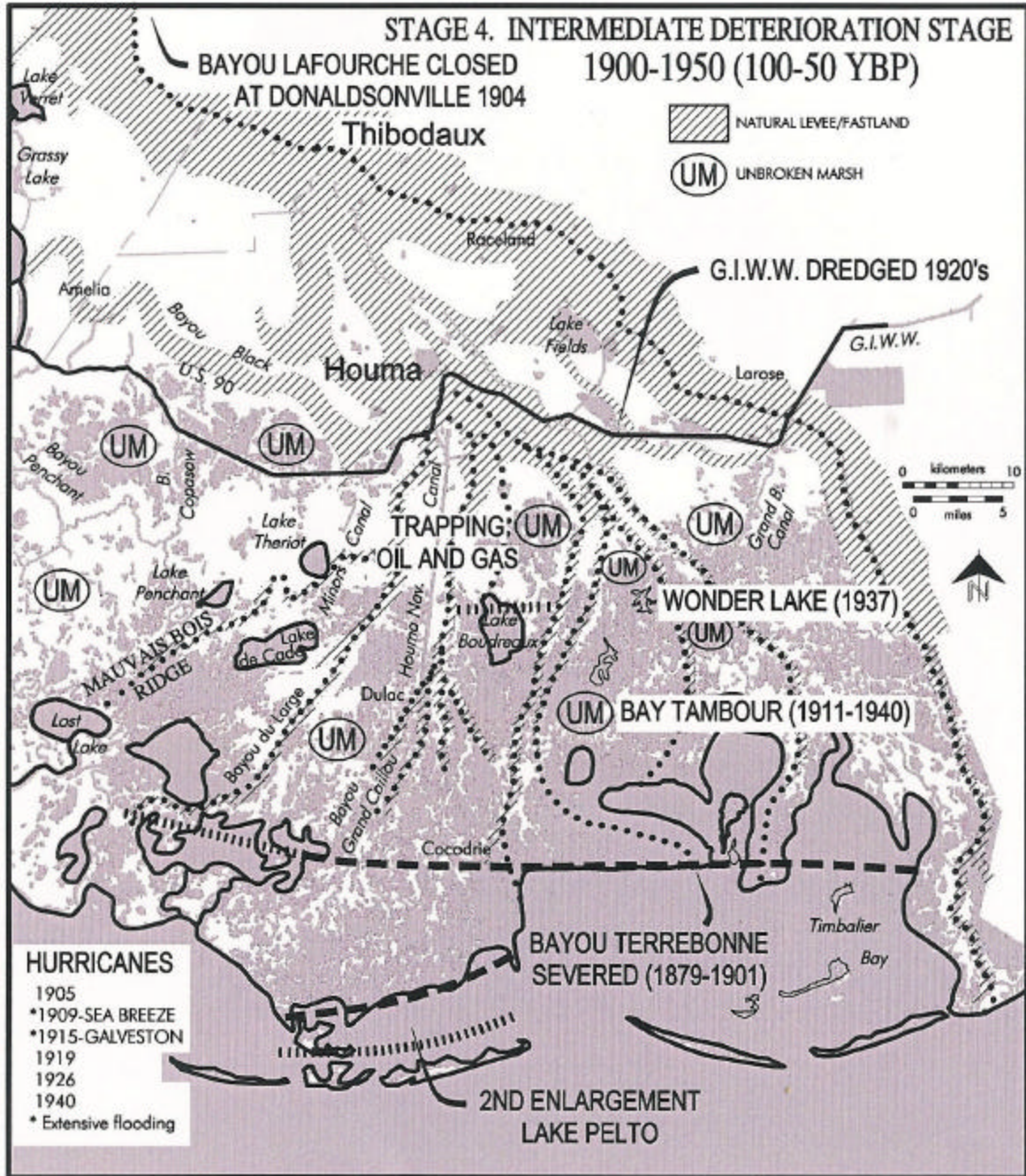


Figure 62. Conditions in the Terrebonne Deltaic Plain during the intermediate deterioration stage (1900-1950 A.D.) of the Lafourche Delta cycle.

Upper Deltaic Plain – The Upper Deltaic Plain occupied one-half of the area. The black water dominated Upper Deltaic Plain marshes remained largely unbroken and continuous. They had become a black water system that no longer received sediment and dissolved solids from river water. Marsh root mat accretion continued to remain the primary defense against subsidence. The root fabric mats were self-mending against minor storm and fault breaks but were becoming increasingly separated from the

substrate and, therefore, more fragile. Natural levees continued to decrease in elevation and width.

The Gulf Intracoastal Waterway (GIWW) was dug through this area around 1925. The extensive network of drilling rig access canals and long pipeline canals was started and grew geometrically during this stage.

Muskrat trapping was at its peak. Trainasses were dug and marsh vegetation was burned seasonally to facilitate access to the traps and to improve grass conditions for muskrats.

Lower Deltaic Plain – The Lower Deltaic Plain encompassed half of the total area. This was a period of continued deterioration of the Lower Deltaic Plain. Subsidence became a dominant process. Major hurricanes pounded the coastal area, particularly early in this period. Barrier islands deteriorated and bays and tidal channels expanded rapidly. Areas favorable for oyster growth expanded. There was an accelerated inland advance of the fresh-non-fresh line (e.g., leading edge of marine tidal processes). Reef building continued in the bays.

Stage 5. Advanced Deterioration: 1950 A.D. – 2000 A.D.
(Figure 63).

System – The abandoned delta system was estuarine-marine. The abandoned delta totally collapsed and was replaced by a marine dominated system.

River supply – The Atchafalaya River water began entering the Houma Navigation Canal (HNC) via the GIWW about 1950. Atchafalaya water inflow through this route was accelerated after the construction of the Bayou Chene, Boeuf, Black Navigation Project. This water carries clay and dissolved solids, but no silt and sand bedload.

Hurricanes – Ten hurricanes occurred during this interval. The storms of 1965, 1974, 1985 and 1992 were particularly damaging.

Fault events – Movement along the Golden Meadow Fault Zone caused massive breakup of marsh in the Upper Deltaic Plain.

Sea level – The rate of rise of worldwide sea level became measurable in the 1980s.

Upper Deltaic Plain – The Upper Deltaic Plain covers one-third of the area. The HNC was dug through the area around 1965. The network of oil and gas canals expanded rapidly and peaked about 1965. There has been extensive breakup and submergence of the fresh marshes as a result of fault events, primarily along the Theriot Fault Zone. Weakened flotant grass mats were torn open and large fragments of mats were exported by hurricanes during this period. Return storm surge and subsequent tidal movement also exported organic soils left exposed by the breaching of the mats. The marshes have been reduced in areal extent. The root mats are in a fragile condition and are no longer self-healing as a result of increasing water depth beneath the flotant. Accretion in the subsided areas can no longer keep pace with subsidence.

Lower Deltaic Plain – The Lower Deltaic Plain encompassed two-thirds of the area. During this period the barrier islands collapsed, and tidal passes expanded in size. Some barrier island restoration efforts were undertaken in this area during the last 10 years.

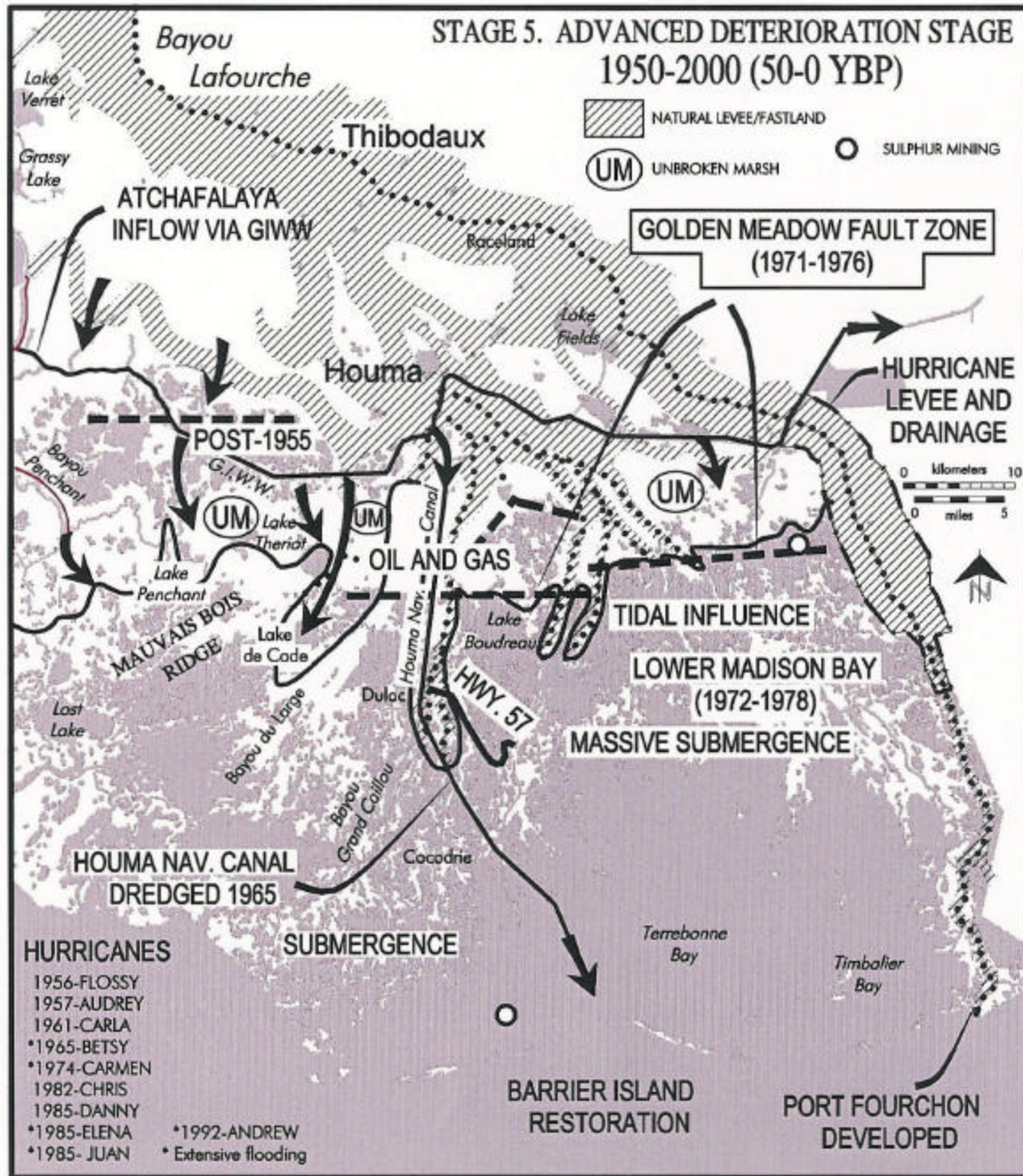


Figure 63. Conditions in the Terrebonne Deltaic Plain during the intermediate deterioration stage (1950-2000 A.D.) of the Lafourche Delta cycle.

The bays continued to expand at the expense of the tidal marshes, with a corresponding expansion of favorable conditions for oysters. The inland line of marine tidal conditions reached the Golden Meadow Fault line.

Stage 6. Future: 2000 A.D. – 2050 A.D. (Figure 64).

System – The system was marine with a narrow shore zone. The shore zone will continue to move inland and will stabilize along fault lines and at the heads of the interdistributary

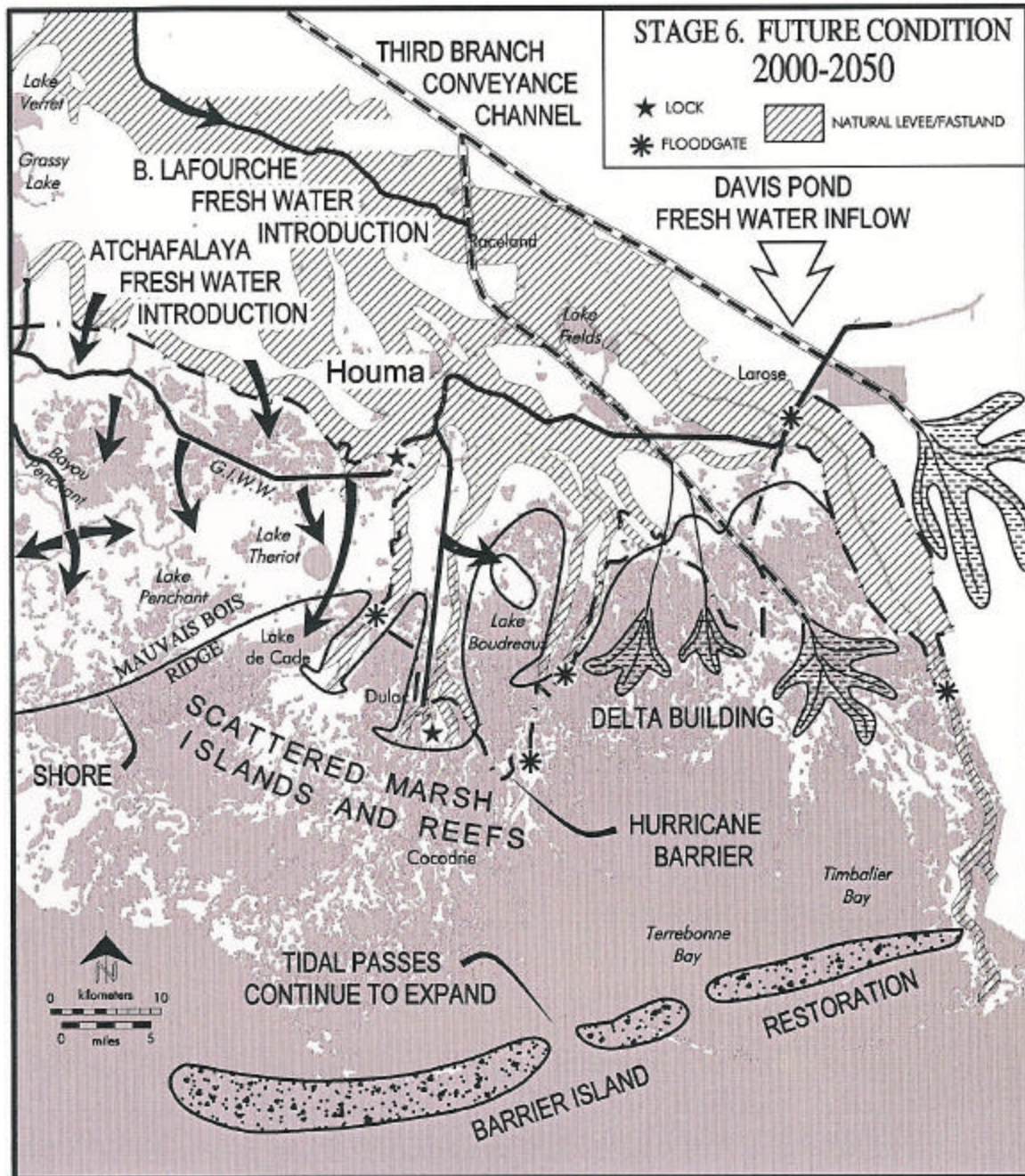


Figure 64. Projected future conditions in the Terrebonne Deltaic Plain during the transitional stage (2000-2050 A.D.).

basins. The proposed Third Delta Conveyance Channel of the Coast 2050 plan would convert the eastern part of the area to an active delta.

River supply – Atchafalaya River water will continue to enter the HNC through the GIWW and discharge may increase. Minor amounts of river water may enter the St. Louis Canal/North Bully Camp area via the GIWW from Davis Pond and/or the proposed Bayou Lafourche freshwater introduction projects. Water from the latter source will be more sediment and nutrient enriched than water from the former.

Hurricanes – Future hurricane events will heavily impact remnants of marsh above the Golden Meadow Fault line, as well as the remaining tidal marsh islands.

Fault Events – Fault events will continue to unfold in the submerged zones. Subsidence and submergence will continue. Further subsidence may occur between the fault zones.

Sea Level – The level of the world's oceans is predicted to rise 0.67 ft (20.42 cm) or more during the next 50 years as a result of global warming.

Upper Deltaic Plain – A shore zone will stabilize along the Mauvais Bois ridge and the Golden Meadow Fault line or at the ridges immediately north of it. Lakes created by fault events will expand into a continuous open bay. Organic rich soils will continue to be exported. Shore zone erosion will rework coarser sediment in the ridges into small barrier islands.

Lower Deltaic Plain – Further deepening of the newly created water bodies will occur along with a corresponding increase in cross-sectional area of tidal channels.

The sand budget of the barrier islands is already depleted, and the base level has been lowered. Without massive sand introduction, the islands will revert to discontinuous shoals. If the islands are further restored with supplemental sand they will be separated from the inner shore zone by 40 to 45 mi (64.4 to 72.4 km) of open bay-sound environment with scattered remnants of tidal marsh, shoals and oyster reefs. The scattered marsh islands that remain will gradually be lost to subsidence and edge erosion. Oyster reefs will continue to proliferate.

The success of hurricane protection barriers, levees and related locks and flood gates will depend upon the effectiveness of the engineering designs of these projects. However, the elevation of all features within the areas of proposed protection will continue to subside and most will be below mean gulf level within 50 years.

Summary of Development Sequence

Tracing the development and change of the landforms and environmental conditions of the ridges and basins through time in reference to the underlying structural features reveals a remarkable interplay among sedimentary processes, geological structural movement and delta system growth and deterioration. It can be seen in Figure 65 that the topographic grain of the natural levee ridges and interdistributary basins cuts across the strike of the major growth faults and grabens of the study area at near right angles. The southwest-northeast strike of the Boudreaux Fault system is an exception, trending diagonally under the ridges and basins. The location and movement of major faults has affected the course of distributaries during their formation (Figure 65). The course of the Teche-Mississippi trunk channel follows the Golden Meadow Fault zone and the nodal points of the Lafourche delta are located at places where the distributaries cross faults. A series of fault events created bays and severed distributaries in the Lower Deltaic Plain, followed by a wave of similar events that resulted in submergence of large areas of interior marsh.

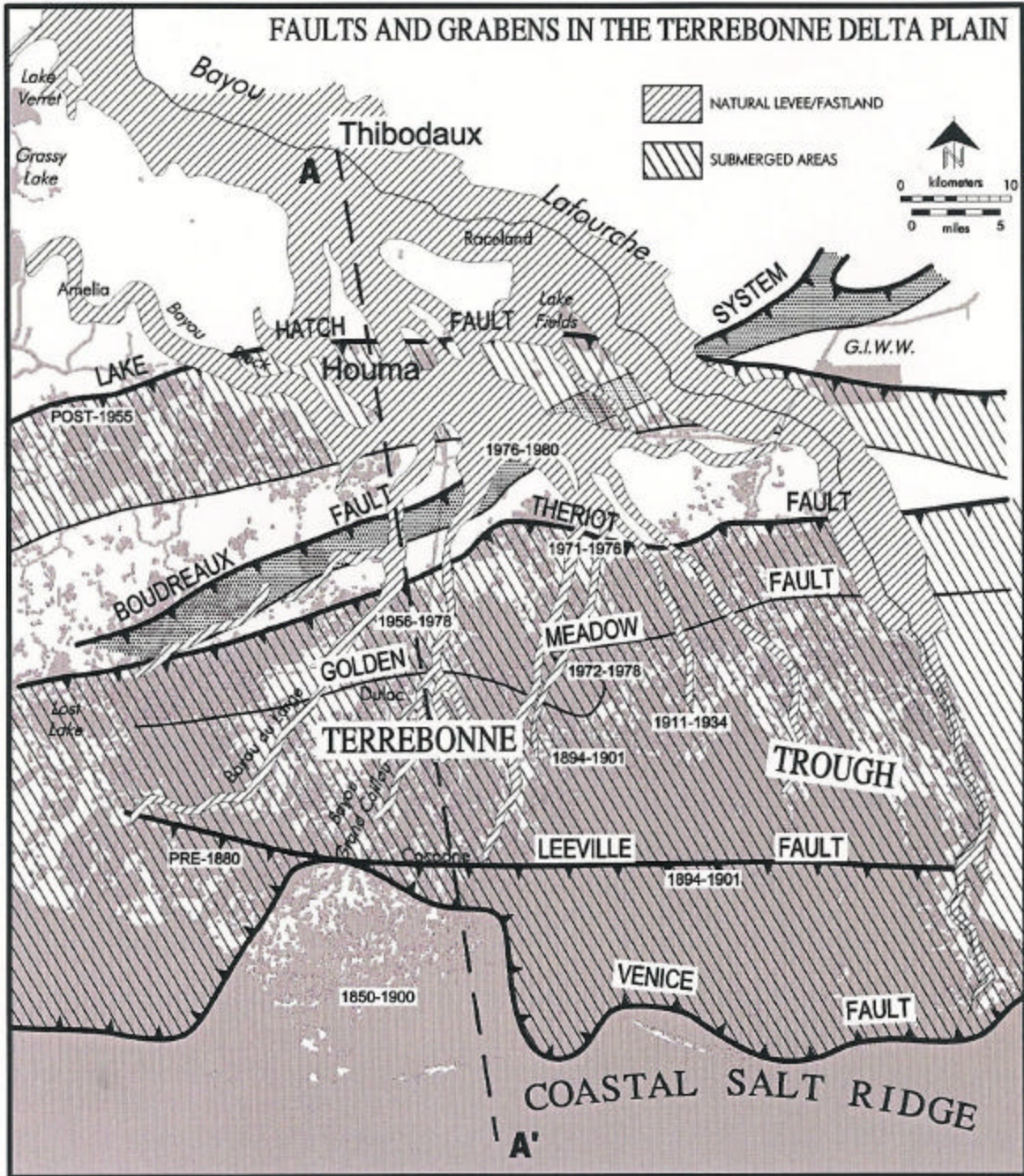


Figure 65. Map showing the relationship between faults and ridge alignments and relict distributary trends in the Terrebonne Deltaic Plain.

Secondary effects, or feedbacks, include: 1) lowering of base levels of the barrier islands, which accelerated their deterioration, 2) hydrologic change, which caused the opening of coastal bays and associated increase in cross-sectional area of the tidal inlets and 3) the inland movement of the leading edge of marine tidal influence (fresh/non-fresh marsh boundary).

The fault movements driving these changes occurred both in prehistoric and historic times, and therefore, are not a result of human activity. The surface fault movements are

also associated with deep-seated growth faults that have been active for millions of years. The vegetation changes (die-back of cypress trees, *Spartina sp.*, and other fresh, brackish and saline plants) is largely a response to fault events, severe storms, droughts, floods and other driving processes. Vegetation is only a positive land building or maintenance factor in fresh, low energy, continuous unbroken marsh-dominated environments of the Upper Deltaic Plain, where it may expand its boundaries, and aggrade (accrete) at a rate equal to, or faster than, subsidence. However, for this to occur these areas require a strong framework of ridges encompassing a low energy hydrologic regime and freshwater input/retention.

This sequential analysis of geological change, driving process and resulting environmental succession also demonstrates that the delta building processes of the Mississippi River are sufficient to overcome subsidence, but high volume flow and bedload are necessary (Figure 66). Flow through re-occupied channels and over-bank flow will sustain Upper Deltaic Plain marshes as long as the skeletal framework remains intact and the separation of the floating root mat from underlying mineral deposits is not too large.

Figure 67 depicts faults and related structures that underlie the ridges and basins of the study area. Sediment loading over the growth faults by the Teche and Lafourche Delta lobes created a condition of instability. Development of extensive fresh floating marshes indicates that for a long time after the cessation of inflow of sediment charged water through the distributary network fault movement and related subsidence was slow and imperceptible. This condition persisted until the early to mid-1960s when a regional fault event occurred. At the time of the fault event the skeletal framework of ridges had been reduced to the level of the marsh surface or below, and the floating root mat had become separated from the substrate over large areas. A network of canals had also been dug throughout the area for navigation and oil and gas development. When the fault event or events occurred the marshes were in a precarious balance. The fault event initiated rapid hydrologic changes including a marine tidal invasion. The breakup was further accelerated by hurricanes which ruptured the marsh mat and broke it into pieces. Individual pieces or floats were exported by return storm surge.

Earthquakes and Seiches

Earthquakes

Earthquakes are caused by the release of energy associated with plate adjustments. Fracturing and faulting of the earth's crust relieves the stress. Earthquakes are not a phenomenon that most people associate with Louisiana. However, earthquakes have been recorded, either by personal testimony or actually measured by monitoring devices in Louisiana since the early 1800s. The locations of reported earthquakes have been plotted in reference to fault zone and the tectonic framework of Southeastern Louisiana in Figure 68.

The most famous historic earthquake to hit the central United States was the New Madrid Earthquake of 1811 and 1812. This earthquake, actually a series of quakes, was centered

DELTA BUILDING OVERWHELMS SUBSIDENCE AND STORM IMPACTS

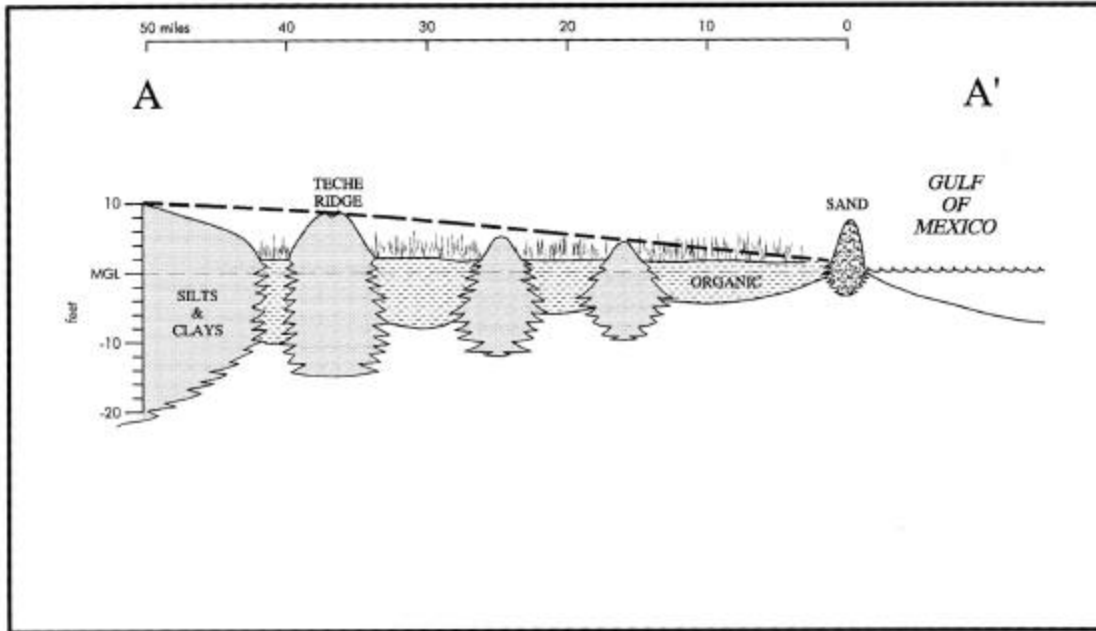


Figure 66. Diagrammatic north-south cross-section through the Terrebonne Deltaic Plain from Thibodaux, Louisiana to the Gulf of Mexico. During the active delta building and poised stages of the delta cycle, sediment deposition rates in the alluvial and interdistributary environments are high enough to build and maintain a land surface that is largely above mean gulf level. Location of section shown in Figure 65.

FAULT INDUCED SUBSIDENCE AND STORM IMPACTS CAUSE THE SEA TO INVADE THE LAND

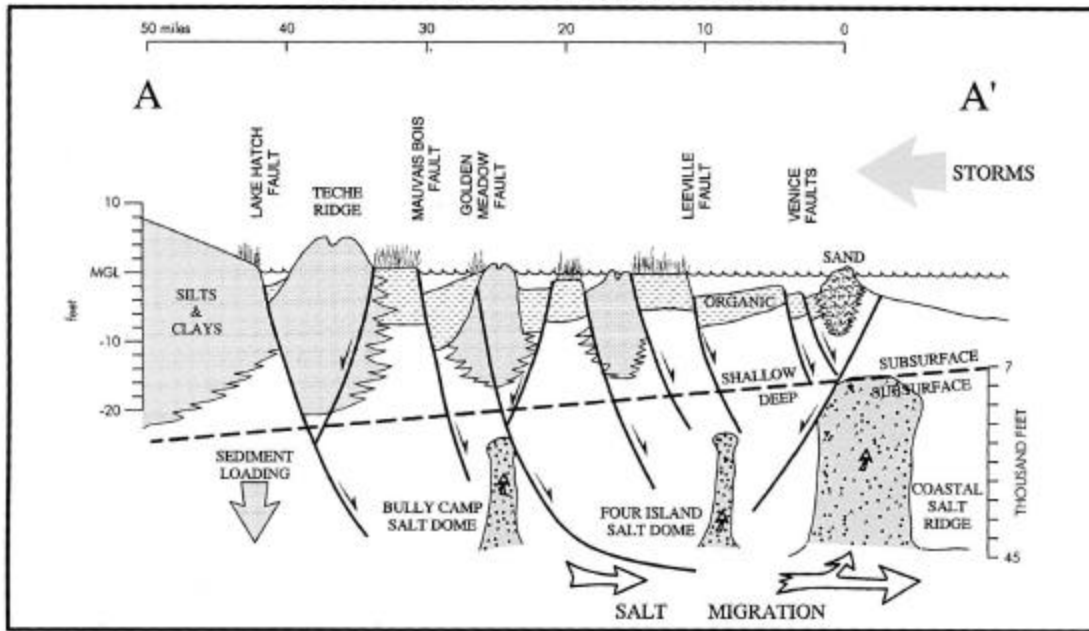


Figure 67 Cross-section through the Terrebonne Deltaic Plain after modification by fault and storm events. During the deterioration stages of the cycle fault events reduce the land surface and facilitate invasion of the land by the gulf. Reduction of land elevations in reference to the gulf level is largely due to deep-seated salt and fault movement.

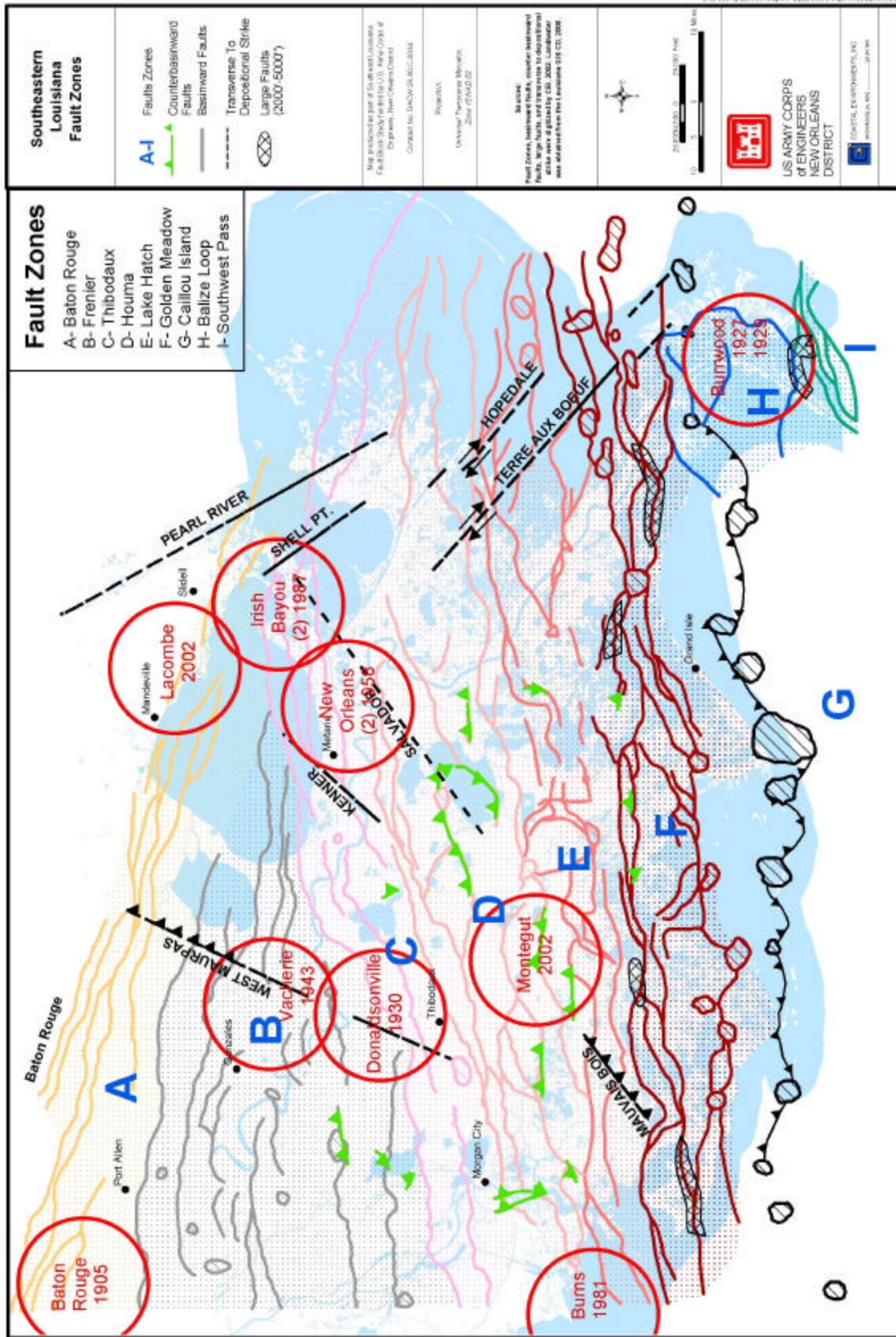


Figure 68. Southeastern Louisiana fault zones and earthquakes.

in New Madrid, Missouri. The area continues to respond to these movements and is now referred to as the New Madrid seismic zone. Meloy and Zimmerman (1997) concluded that the presence of wrench faults does not increase the seismic risk to Louisiana from the New Madrid seismic zone. However, the New Madrid seismic zone remains the area most likely to produce earthquakes that could have damaging effects to buildings and other structures in the northeastern and central portions of Louisiana (Stevenson and McCulloh 2001).

The New Madrid earthquake of 1811, estimated as a magnitude 7.8 on the Richter scale, rang church bells 1000 mi (1609 km) away in Boston, Massachusetts. The isoseismal lines for that quake extended into northeastern Louisiana and central Mississippi. The largest of the series of events on February 7, 1812, was apparently felt in New Orleans and reported as a slow oscillatory motion, rather than strong shaking (Moniteur de la Louisiane, February 11, 1812). About 84 years later, on Halloween 1895, the New Madrid area shook again. That earthquake was felt in 23 states, an area exceeding a million square miles (2,589,986 sq km).

But not all earthquakes are of epic proportions. Earthquakes and shocks in the central or eastern United States affect larger areas than the California earthquake events (Central United States Earthquake Consortium, 2002 http://www.cusec.org/S_zones/NMSZ/nmsz_home.html).

Geologic province makes the difference. The hard, brittle rocks along an active plate margin, like California, respond differently from the expansive strata of the central region, and the softer sediments of Louisiana. Earthquakes in California are not felt over such great distances as those in the central part of the country. The “softer” sedimentary basins of Louisiana and much of the northern Gulf Coast, seem to dampen the surface effects of earthquakes. Also, the thick organic soils, densely vegetated ground surfaces and pockets of biogenic/natural gas tend to further dampen and muffle the transmission of energy to the surface.

Even though Louisiana does not have many dramatic surface earthquake effects, this does not mean that nothing is happening at depth. An earthquake centered in Napoleonville, a small town about 60 mi (96.5 km) west of New Orleans, occurred in October 1930. This earthquake had a magnitude of 4.2 Mfa, Intensity VI, and is still the strongest quake ever recorded in Louisiana. Chimneys were damaged, windows were broken, and plaster walls cracked at White Castle, a small town just north of Napoleonville. People rushed into the streets (USGS, National Earthquake Information Center web site 6/19/2002 http://neic.usgs.gov/neis/eqlists/USA/1930_10_19.html). In December of 1927 and again in July of 1929, a slight earthquake was felt in Burrwood, about 82 mi (131.9 km) southeast of New Orleans.

Vacherie Fault Event (WM – 1)

Perhaps the most thorough investigation of the surface effects of a fault event in South Louisiana was that of H.N. Fisk (1943) in the instance of the 1943 Vacherie Fault and earth-tremor. The event was thoroughly documented by Fisk. The fault was mapped and 17 borings were made.

Fisk (1943) reported that during the period of April 12-15, 1943, a fault event occurred on the west bank of the Mississippi River opposite river mile 920.25 on the Waguespack Planting Company's Laura Plantation, in irregular section 20, T. 12 S., R. 17 E. near Vacherie, Louisiana. The disturbed area extended almost a mile in a south-southeasterly direction from a point about 1200 ft (365.8 m) on the landside of the flood levee. The fault was defined by a mile-long zone of parallel, open cracks and offset in *en echelon* fashion. The downthrown side of the displacement was to the west. The fissures in the earth had a maximum depth of 6 ft (1.8 m) and width of 6 in (15.24 cm). The maximum vertical displacement was 8 in (20.32 cm), but it was more typically a few inches. At the extreme ends of the fault, the cracks exhibited no apparent displacement, but the maximum displacement occurred in the central area of the fault. The displacement was sufficient to disrupt drainage. The fissure followed the natural levee of a relict crevasse distributary.

At 2:00 AM, April 12, 1943, there was a slight earthquake and a fissure appeared with an observed displacement of 3 in (7.62 cm). The fissure gradually extended and at 12:50 AM, April 13, a second slight shock was felt. The fissure continued to extend. It crossed an existing railroad track and embankment. These were down warped for a distance of 125 ft (38.1 m) and it was necessary to raise the rails 2 in (5.08 cm) where the fault intersected the embankment. The fissure continued to extend until April 15. Observations were continued until April 29 but no further movement occurred.

The fault was situated on the southeast flank of the Vacherie Salt Dome. At the time of the fault event, the dome was producing oil from several wells and a new prospect well was being drilled (George Echols' Realty Operators No. 1) within 1500 ft (457.2 m) of the fault. This well was drilled to a depth of 8792 ft (2679.8 m) and was shut down on April 11, 1943, when it hit a sand bearing salt water under a pressure of 2000 lbs per sq in. The well was later plugged with cement.

Fisk (1943:34-36) concluded that the dominant cause of the fault was subsidence of surface sediments over an inactive subsurface fault line located on the flank of the Vacherie Salt Dome. Specifically, the cause of the subsidence was believed to be compaction of subsurface sand and gravel bodies along the inactive fault caused by vibrations set up in the Echols' well while the sands were under increased pressure during crest stage in the river rather than by deep-seated movement of the fault.

A check of seismographic records at the Loyola seismograph station did not reveal any deep-seated event. The borings revealed that the faulting resulted from stresses deeper than 75 ft (22.8 m) beneath the surface, and were not caused by superficial compaction of beds. The straightness of the fault line was believed to be an indication that it was related to an older inactive fault. The borings indicated a sag in the underlying Pleistocene sediments. This indicated that adjustments have taken place along the Vacherie Fault Zone in the past and that "...the present faulting is probably a recurrence of adjustment to subsurface inequalities along the same line" (Fisk 1943). However, Fisk felt that the growth pattern of the fissures and the displacements were related to the Echols' well disturbance and not to some deep-seated movement.

Fisk (1943) noted that the position of the Vacherie crevasse, directly parallel with the sag in Pleistocene sediments, was suggestive that prehistoric crevassing of the river followed a zone of weakness along the fault. He stated that should faulting reoccur, there was a possibility that the flood protection levee would be endangered.

Fisk showed the fault as a radial fault extending out from the Vacherie Salt Dome. In a map in the 1944 report, Fisk shows a regional northwest-southeast alignment that extends through the Vacherie Fault. In the context of the present study, the Vacherie Salt Dome is located near a critical intersection of the Frenier regional growth fault, the West Maurepas Alignment and the East Valley Wall Alignment, the latter being roughly equivalent to Fisk's northwest-southeast regional alignment.

Other Reported Earthquakes

In 1927, and again in 1929, slight earthquakes were reported in Burrwood, Louisiana. From the areas studied in this report, it seems that the surface evidence for recent faults appears in the late 1950s through mid-1970s. Earthquake data are largely lacking in the coastal regions of Terrebonne, Lafourche, Jefferson, Plaquemines and St. Bernard Parishes, the only notable exceptions being the 1927 and 1929 earthquakes reported near the mouth of the river. Perhaps this is due in some small part to the historically sparse population of these remote coastal areas.

More recently, in February of 1981, there was an earthquake recorded in the vicinity of Burns, a coastal community south of Morgan City. There were also several earthquakes reported from areas outside of the study area within the state, the latest was in 1994. However, one event in 1987, shook the area around Irish Bayou in eastern New Orleans between Lake Pontchartrain and Lake Borgne. This event was thought to be possibly related to the fault activity that had been occurring in Lake Pontchartrain. Lopez (1991) documented the evidence of two separate faults in the lake through observations of offsets in two vehicular bridges and a railroad bridge. Historically, repairs had been made to the 1883 wooden railroad bridge for many years as a part of routine maintenance. A new concrete railroad bridge was built in 1996.

The southern fault crosses the railroad bridge about a mile from the south shore of the lake. This portion of the trestle was undergoing repairs between 1986-87. When this southern section of the railroad bridge was examined in 1996, it showed an offset in the rails of 3 to 4 in (7.5-10 cm). The offsets on the railroad trestle are slightly more than the offset on the car bridges. The variation in the amount of offset from east to west along the fault could be interpreted as episodic movement along the fault as Lopez et al. (1997) concluded, or it might be related to the zone of deformation associated with one fault that is episodic. That is, the epicenter of fault movement might have been nearer the railroad bridge than to the car bridges, even with episodic movement along the fault.

The northern fault crosses near the north shore of the lake. In 1991, an inspection of the old wooden trestle on the northern end of the lake showed several inches of offset but there was no bend in the rails. By 1996, the steel track was offset by 2 in (5 cm). This clearly documents 2 in (5 cm) of movement in a 6-year period. High resolution seismic data capable of imaging beds approximately 1 ft (0.3 m) in thickness, from the vicinity of

Big Point on the north shore of Lake Pontchartrain, show expansion of marker events across the fault. The offset in reflectors show slight thickening between all of the upthrown and downthrown reflectors in the 150-ft (45.7 m) depth converted time slice across the fault. The events are thought to correlate with Pleistocene and Recent age sediments (Lopez et al.1997).

Correlations of specific earthquakes to specific faults has rarely happened due to the fortuitous circumstances of having recording equipment and seismic data in an area that experiences an earthquake. Such was the case in 1983, near Lake Charles, Louisiana. The Louisiana Geological Survey recorded and correlated an earthquake to movement along a regional growth fault (Louisiana Geological Survey 2001).

It seems unlikely that the earthquakes in the coastal regions of Louisiana are directly related to mid-continent plate shifting episodes. However, modern earthquakes in the mid-continent area are thought to be the result of the reactivation of buried ancient faults that are being squeezed by the present-day movement of tectonic plates (USGS, National Earthquake Information Center http://neic.usgs.gov/neis/bulletin/neic_fnbk.html June 20, 2002). Perhaps the processes are similar.

Seiches and Tsunamis

Seiches are oscillations in enclosed bodies of water caused by earthquakes or trimmers. (<http://www.cityofseattle.net/projectimpact/pages/pioverview/regionalhazards/tsunami.htm>). In coastal Louisiana, seiches are generally caused by seismic waves that are associated with earthquakes. These earthquake-generated waves can be felt in restricted bayous and lakes. Tsunamis are large waves generated by submarine earthquakes caused by plate adjustments and faulting and other large-scale disturbances to the ocean water surface such as meteor/asteroid impacts. On March 18, 1952 an apparent tsunami damaged the jetty at Southwest Pass, displacing 180 concrete blocks (Chief of Engineers U.S. Army Corps of Engineers, 1952:PT.744).

The Prince William Sound, Alaska earthquake, with a magnitude of 8.3, of March 27, 1964 generated tsunamis and seiches that were felt globally. There were reports of long-period surface waves that set up seiches or periodic oscillations of the surface of closed bodies of water in the Gulf Coast region. The effects of the seiches were noticed in the rivers and bayous of the New Orleans area where considerable damage was done to many boats and barges, which slammed against piers or were torn from their moorings. Most accounts indicate that water oscillations had peak-to-peak amplitude of approximately 6 ft (1.8 m) with a period of oscillation on the order of 5 seconds. The Amite River, east of Baton Rouge, had peak-to-peak oscillations on the order of 4 ft (1.2 m) for a duration of 20 minutes. In Baton Rouge, the water in swimming pools, including the pool on the fourth floor of the Capital House Hotel, was disturbed. Water disturbances “were not particularly noticeable” along the Mississippi River (Baton Rouge Morning Advocate, Mar. 28, 1964). There were reports, however, of boats breaking from their moorings in Venice, Louisiana.

On November 3, 2002, a 7.9 magnitude earthquake centered about 90 mi (144.8 km) south of Fairbanks, Alaska, caused oscillations in water bodies in Southeastern Louisiana

(Burdeau 2002 a,b). The earthquake was shallow, and centered about 6 mi (9.6 km) underground on the Denali Fault in Alaska. Sail boats in a marina in Mandeville, Louisiana were reported to have bobbed and broken from their moorings. Water in ponds and pools in the New Orleans area was reported to splash about over a 30-minute period. A minor earthquake was reported in Montegut, Louisiana, by local residents (Bob Jones, per. comm. 2002). It is noteworthy that the effects in south Louisiana were similar to those of the Prince William Sound, Alaska earthquake of March 27, 1964.

Salt Water and Gas Migration along Fault Planes

Kuecher (1994) and Kuecher et al. (2001) reported results of electromagnetic measurements conducted along the natural levees of Bayou du Large and Bayou Grand Caillou where they cross both the Lake Hatch and Golden Meadow Fault Zones. Conductivity anomalies were found across the Lake Hatch Fault at two locations indicating that it is a non-sealing and/or active fault zone. Active faults may be either sealed or non-sealing depending on a number of factors including the nature of the sediments, the nature of their formation fluids and the differential pressures juxtaposed across the fault plane. In contrast, the Golden Meadow Fault appeared to be a sealed and/or inactive zone (Kuecher et al. 2001: 87-91).

A recent paper by Aminzadeh and Connolly (2002) summarized the identification and use of “gas clouds and chimneys” recorded on seismic records, as an important tool in the search for oil and gas in the Gulf of Mexico. Gas migrating up-section towards the surface from traps and source beds can be identified by the computer, imaged in horizontal and vertical slices, and tied to original seismic sections. The gas moves upward along faults. A distinction can be made from the seismic images between sealing and leaking or non-sealing faults. Aminzadeh and Connolly (2002) have also established relationships between subsurface “canopies and clouds” of gas and surface seeps.

Vents and cones that emit water, gas and mud have been reported from the lower Mississippi Delta where they are associated with mudlumps and faults (See Figure 34D). James P. Morgan (per. comm. circa. 1960) periodically visited a large mud/gas vent in the West Bay area over a 20-year period (Figure 69). Local hunters and fishermen attributed the vent to a shallow seismic boring, but this was not verified. Morgan reported that the vent belched flammable gas, salt water and mud over the ten years of his observations.

Morton et al. (2002) cite an obscure reference (Troutman 1956) to surficial gas seeps that led to the discovery of the Lirette field in 1937. Morton et al. (2002) suggest that these seeps were the result of vertical mitigation of fluids along deep fault planes that intersected subsurface gas from Miocene reservoir at depths from 5,500 to 12,000 ft (1676 to 3658 m).



Figure 69. Mud vent cone in West Bay area near Venice, Louisiana. James P. Morgan reported that this vent had been active for at least 10 years (Morgan per. comm. ,circa 1960).

During the course of the fieldwork conducted in conjunction with this study, attention was directed toward finding surface evidence of salt water, temperature changes and gas migration along fault finding planes. No conspicuous cones or vents were found outside of the Active Mississippi Delta. Steve Estiponal (per. comm., 2002), a licensed land surveyor, informed us of a brine water seep located along the back slope of the Mississippi River natural levee in Chalmette, Louisiana. Estiponal reported that the seep had been active for a number of years, but is no longer active. Salinity/temperature profiles were run across surface fault traces and scarps and through water bodies in the vicinity of suspected faults. Several of these profiles have positive gradients toward the fault scarps and traces, suggesting vertical saltwater migration.¹⁴ Gas chromatographs of soil samples taken at some of the surface faults indicated the presence of hydrocarbons (Ed Overton per. comm., 2002).

Wedging of fault planes as a result of relative movement between salt domes and surrounding beds may create opportunities for hydrocarbon, gas and brine releases. Water and gas migration may serve to lubricate fault planes and may be a precursor to movement.

¹⁴ A salinity profile taken by CEI in October 2001 at Montegut showed an increased gradient toward the fault.

Fluid Withdrawal

Fluid withdrawal is believed to cause localized subsidence, and undoubtedly some subsidence has occurred as a result of removal of shallow hydrocarbons, gas and produced water. White and Tremblay (1995), Morton et al. (2000 and Morton et al. (2001) have reported an apparent correlation between surface fault traces and scarps and marsh loss in southeast Texas and related this to fluid withdrawal.

R. A. Morton, N. A. Busteri and M. D. Krobin (2002) have made correlations between subsidence and withdrawal of hydrocarbons and produced water at locations along the Lake Hatch and Golden Meadow Faults in Terrebonne Parish, Louisiana. They have correlated production figures and pressure reduction data from individual oil and gas fields with land loss and measurements of vertical surface movement measurements derived from re-leveling of benchmarks. From this research Morton et al. (2002) concluded that fluid withdrawal may have re-activated growth faults and may be the primary cause of subsidence in the area studied.

Morton et al. (2002) concluded that fluid withdrawal is the principal cause of subsidence and if faults play a role, they have been re-activated by “stress related to fluid withdrawal.” Part of the supporting evidence for the theory of subsidence and fault movement induced by fluid withdrawal is that the rise and fall of annual land loss rates in coastal Louisiana approximately correlates with the increase and decrease of oil and gas production. Land loss peaked when mineral production peaked. It follows, if these apparent correlations can be proven, that as oil and gas resources are depleted land loss will decline.

Extrapolation of these findings across the Deltaic Plain should be done with caution. Production from the fields studied by Morton et al. (2002) is fluid driven, and fluids refill pore space as withdrawal occurs. The locations of most of the fields in Southeastern Louisiana, including those along the Lake Hatch and Golden Meadow Fault Zones, are on down-dropped fault blocks, and therefore, are not an independent variable in reference to fault movement. That is the locations of the oil and gas accumulations are related to faults that were active before modern oil and gas production began. The faults moved before and during fluid withdrawal and may continue to move after fluid withdrawal is discontinued. It should also be noted that fault movement is apparently occurring in a number of areas throughout the Deltaic Plain where there is little if any fluid withdrawal. Morton et al. (2002) gave little consideration to other tectonic processes acting in the region. While fluid withdrawal may contribute to some areas of local subsidence, it does not explain fault events that have occurred in coastal Louisiana throughout geological, prehistoric, historic and modern times.

The present study found evidence of episodic fault activity along deep-seated regional faults during the Pleistocene and early and middle Holocene periods. Evidence was also found of historic fault movement in the late 1800s and early 1900s, all of which pre-date oil and gas withdrawal in the coastal zone. Faults located in the Pontchartrain Basin, with demonstrable prehistoric, historic and modern vertical movement, have little or no associated oil and gas production. Further, there is abundant evidence, documented in the

geological literature, that sediment loading coupled with deep-seated tectonic movements are the primary driving processes of growth fault movement. Whether or not oil and gas activity is the triggering mechanism for movement along major faults remains unresolved but certainly warrants further research.

VERTICAL AND LATERAL MOVEMENT

Virtually the entire Mississippi River Deltaic Plain lies within a structural “expansion area” cut by listric growth faults. The very nature of this fault movement results in lateral displacement of the surface. Mudlumps display lateral movement and *en echelon* faults suggest lateral movement. Small horizontal displacements of bridges that cross Lake Pontchartrain have been documented. The present study focuses on the vertical components of fault movement; so further discussion of the lateral movement will be reserved for a later day.

Apparent vertical displacements of near-surface Holocene beds at the nine case study locations ranged from a few tenths of a foot to a maximum of 3.5 ft (1.1 m). Depths of associated water bodies that apparently formed as a result of fault movement at the case study locales are similar, but deeper. Some bottom erosion undoubtedly occurs after the water bodies initially form as a result of fault events. The difference in bottom depth and displacement of beds is a reflection of the age of the water body and the extent of bottom scour.

It should again be noted that vertical displacement of the top of the Pleistocene along some faults is 10 ft (3.0 m) or more.

Relative Sea Level Rise

If fault bound blocks along the coast are sinking and are being inundated by the sea, it becomes important to determine the rate of change between the elevation of the land and the level of the sea, the combined effect of which is defined as relative sea level (RSL) rise. Subsidence is a component of RSL rise and is the difference between the rate of sea level rise and the total apparent sea level rise.

As the level of the sea is rising everywhere on earth, the first aspect of the problem is to determine the rate of this eustatic rise. The literature dealing with eustatic rise is voluminous and an in-depth review of the topic is beyond the scope of the present work, but published study findings indicate that current average eustatic sea level rise rate is about 0.0049 ft/yr (0.149 cm/yr) (Wigley and Raper 1992).¹⁵ The rate of sea level rise has been low but has increased during the past 50 years. A reasonable estimate is that the level of the world’s oceans will increase 0.67 ft (20.4 cm) over the next 50 years and 1.53 ft (46.6 cm) during the next century.

¹⁵ In the present report four measurements are considered to be important in characterizing subsidence and relative sea level. The first is the total amount of vertical movement. The second is the period of record. The third is the rate of change derived from one and two above. The fourth is the eustatic rate of change for the Northern Gulf of Mexico. Most measurements in this report are reported on the English system in order to facilitate direct application to engineering problems.

Several methods have been used for measuring RSL rise and subsidence. These include: 1) measuring change in elevation of surfaces upon which human structures (prehistoric Native American village sites, lighthouses, forts, roads, etc.) were built, 2) radiometric dating of buried peat deposits, 3) measuring changes in water level from tidal gauge records and 4) measuring changes in land elevations by re-leveling of benchmarks. The following discussion will focus on the latter two methods.

Tide Gauge Data

Shea Penland, Tom F. Moslow, Karen E. Ramsey, and their colleagues, in an important series of studies and papers, have grappled with problems related to causes, effects, and rates of RSL rise in south Louisiana (Ramsey and Moslow 1987, Penland et al. 1988, Penland et al. 1989, Ramsey and Penland 1989, Nakashima and Loudon 1989, Penland and Ramsey 1990). The team conducted a comprehensive study of historical water level records from 78 tide gauge stations and 342-line mi (550.3 km) of geodetic leveling data from south Louisiana and adjacent areas of the northern Gulf of Mexico region for the period 1942-1982 (Table 5).

Figure 70 shows a typical water level time series from the Grand Isle gauge, as analyzed by Penland et al. (1989). Water levels generally “climb the gauge” through time. The records from each station were analyzed to determine the rise rate for the entire period of record as well as for two twenty-year time epochs. Epoch 1 included the period 1942 – 1962 and Epoch 2, the period 1962 – 1982 (Figure 71).¹⁶ Records from many south Louisiana stations showed a distinctive increase in rate of rise during Epoch 2.

Gauge records from the northern Gulf of Mexico, from Cameron, Louisiana to Cedar Key, Florida, were analyzed. Most records indicated a relative rise in the level of the sea through time, but as shown in Figure 72, the rates of relative rise also varied from east to west, with the lowest rates being along the coasts of Florida, Alabama and Mississippi and the highest being along the deltaic plain of Louisiana.

Land leveling data indicate that the Florida Panhandle has remained relatively stable and for this reason the tide gauge records from Pensacola were selected as the best measure of eustatic sea level change for the northern Gulf of Mexico region. Thus, the rate of 0.0075 ft/yr (0.228 cm/yr), as determined from the Pensacola record, was used by the Penland et al. (1989) team as a correction factor in adjusting RSL rise rates to subsidence rates and vice versa. The same correction method and factor are also used in this paper.

This change differences in RSL rise rates are most pronounced in three areas, the South Shore–Little Woods area in the eastern end of Lake Pontchartrain, the deltaic plain west of the Mississippi River, and the Mermentau River area in the Chenier Plain; the first two of which are in the present study area. Differential fault movement provides an explanation for these differences. Further, the records suggest that the rate of movement on faults in the three areas has increased during the 1962-1982 interval.

¹⁶ The twenty-year periods were selected by Penland et al. (1989) to average out effects of astronomical tidal cycles.

Table 5. Tide gauge data from Southeastern Louisiana.

Station Name	Record Period		Epoch 1		Epoch 2		Entire Record		Increase in Rate of Change			
	cm/yr	in/yr	ft/yr	cm/yr	in/yr	ft/yr	cm/yr	in/yr	ft/yr	cm/yr/Epoch	in/yr/Epoch	ft/yr/Epoch
Calumette*	0.380	0.150	0.012	2.640	1.039	0.087	1.770	0.697	0.058	2.26	0.890	0.074
Eugene Island*	0.790	0.311	0.026	1.640	0.646	0.054	1.610	0.634	0.053	0.85	0.335	0.028
Eugene Island**	0.950	0.374		2.170	0.854	0.071	1.190	0.469				
Morgan City*	0.010	0.004	0.000	2.140	0.843	0.070	1.340	0.528	0.044	2.13	0.839	0.070
Greenwood*	-0.080	-0.031	-0.003	2.310	0.909	0.076	1.260	0.496	0.041	2.39	0.941	0.078
Houma*	0.070	0.028	0.002	1.940	0.764	0.064	1.310	0.516	0.043	1.87	0.000	0.000
Bayou Lafourche at Leeville (#32)*		0.000		1.220	0.480	0.040	0.740	0.291	0.024			
Leeville****							0.770	0.303	0.026			
B. Lafourche at Golden Meadow (#31)*		0.449	0.037	1.800	0.709	0.059	2.330	0.917	0.075		0.000	0.000
Grand Isle* (Bayou Rigaud)	1.140	0.449		1.800	0.709	0.059	1.300	0.512	0.043	0.66	0.260	0.022
Grand Isle (#33) *	1.140	0.449		1.800	0.709	0.059	1.300	0.512	0.043		0.000	0.000
Grand Isle**	0.300	0.118		1.920	0.756	0.063	1.030	0.406	0.034			
Grand Isle****							1.060	0.417	0.035			
Cocodrie		0.240	0.020	0.840	0.331	0.020	0.600	0.236	0.020	0.23	0.091	0.008
B. Petit Caillou (26) Port Eads*	0.610	0.240		0.840	0.331	0.028	1.280	0.504	0.042			
South Shore*	0.010	0.004	0.000	1.410	0.555	0.046	1.000	0.394	0.033	1.4	0.000	0.000
Little Woods*	0.770	0.303	0.025	2.160	0.850	0.071	1.090	0.429	0.036	1.39	0.000	0.000
West End*				0.150	0.059	0.005	0.430	0.169	0.014	0.15	0.547	0.046
Frenier*	0.150	0.059	0.005	0.230	0.091	0.008	0.380	0.150	0.012	0.08	0.031	0.003
Mandeville*	0.220	0.087	0.007	0.750	0.295	0.025	0.480	0.189	0.016	0.53	0.000	0.000
B. des Allensands (29)				0.080	0.031	0.003	0.380	0.150	0.012	0.08	0.209	0.017
Catfish Lake***				1.280		0.107					0.031	0.003

* After Penland et al. 1988, primary data from Corps of Engineers.

** After Penland et al. 1988, primary data from NOS.

*** After Sasser et al. 2002, primary data from Corps of Engineers.

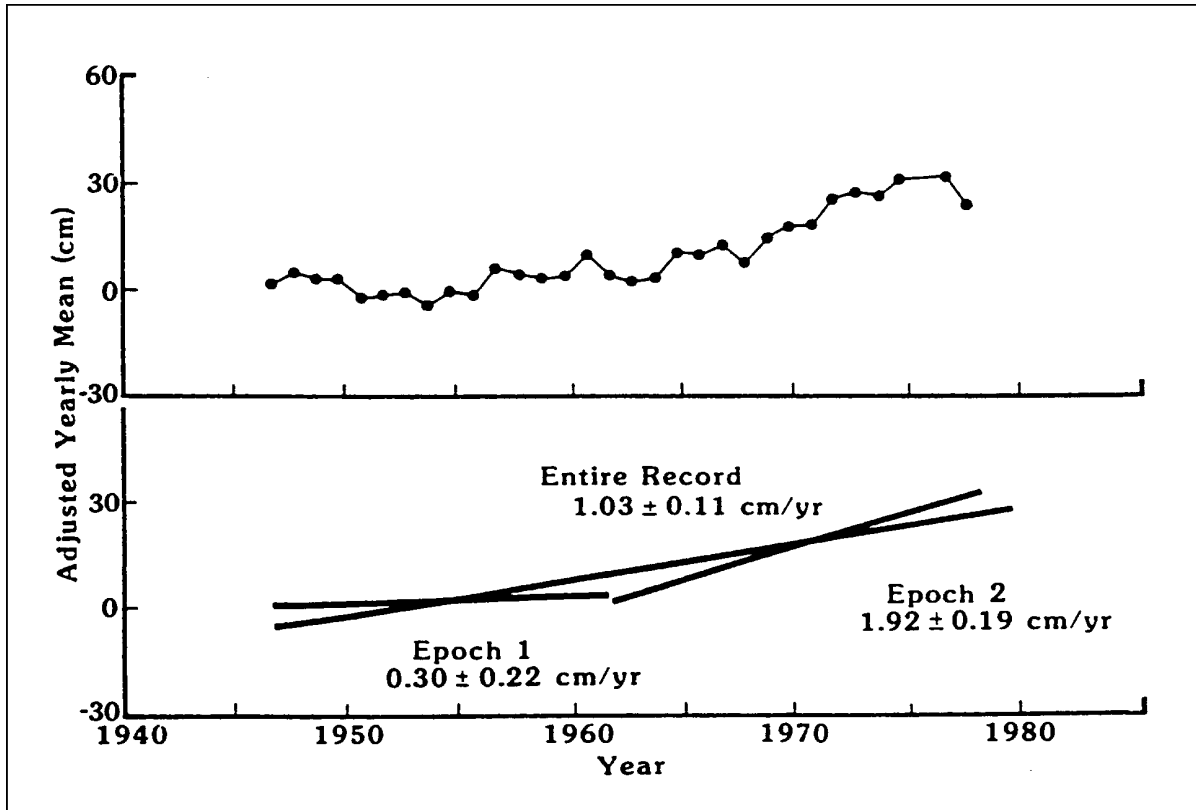


Figure 70. Water level time series from National Ocean Survey, Grand Isle, LA. Tide gauge between 1947 and 1978. A change in the rate of rise between the period 1947-1962 (Epoch 1), and the period 1962-1978 (Epoch 2) had been found on many of the records from gauges in south Louisiana (after Penland et al. 1989:24).

The statewide sea level rise rate was calculated to be 0.015 ft/yr (0.457 cm/yr) for the 1942-1962 period and 0.0367 ft/yr (1.117 cm/yr) for the 1962-1982 period (Figure 73). The RSL rise rate was found to be 3.2 times greater in the second 20-year epoch.

Ramsey and Moslow (1987) grouped the gauge data into seven hydrographic basins (See Figure 71). The data show great variations both temporally and spatially throughout coastal Louisiana. Using average values for the entire period of record (1942 through 1982), rates of rise of 0.0328 to 0.0394 ft/yr (0.498 to 1.198 cm/yr) were found in the areas immediately along the Louisiana coast. The RSL rise in the southwest portion of the deltaic plain was determined to be 0.0591 to 0.0623 ft/yr (1.800 to 1.897 cm/yr). In most cases, there was a pronounced decrease in rate landward.

Ramsey and Moslow (1987) determined the “compactional subsidence” rate by subtracting the isostatic rate of rise of 0.0075 ft/yr (0.228 cm/yr), as determined from the Pensacola, Florida tide gauge record. From this analysis, the authors concluded that approximately 80 percent of the observed RSL rise in Louisiana was attributable to compactional subsidence. They also concluded that compaction and loading account for the spatial variation in rate.

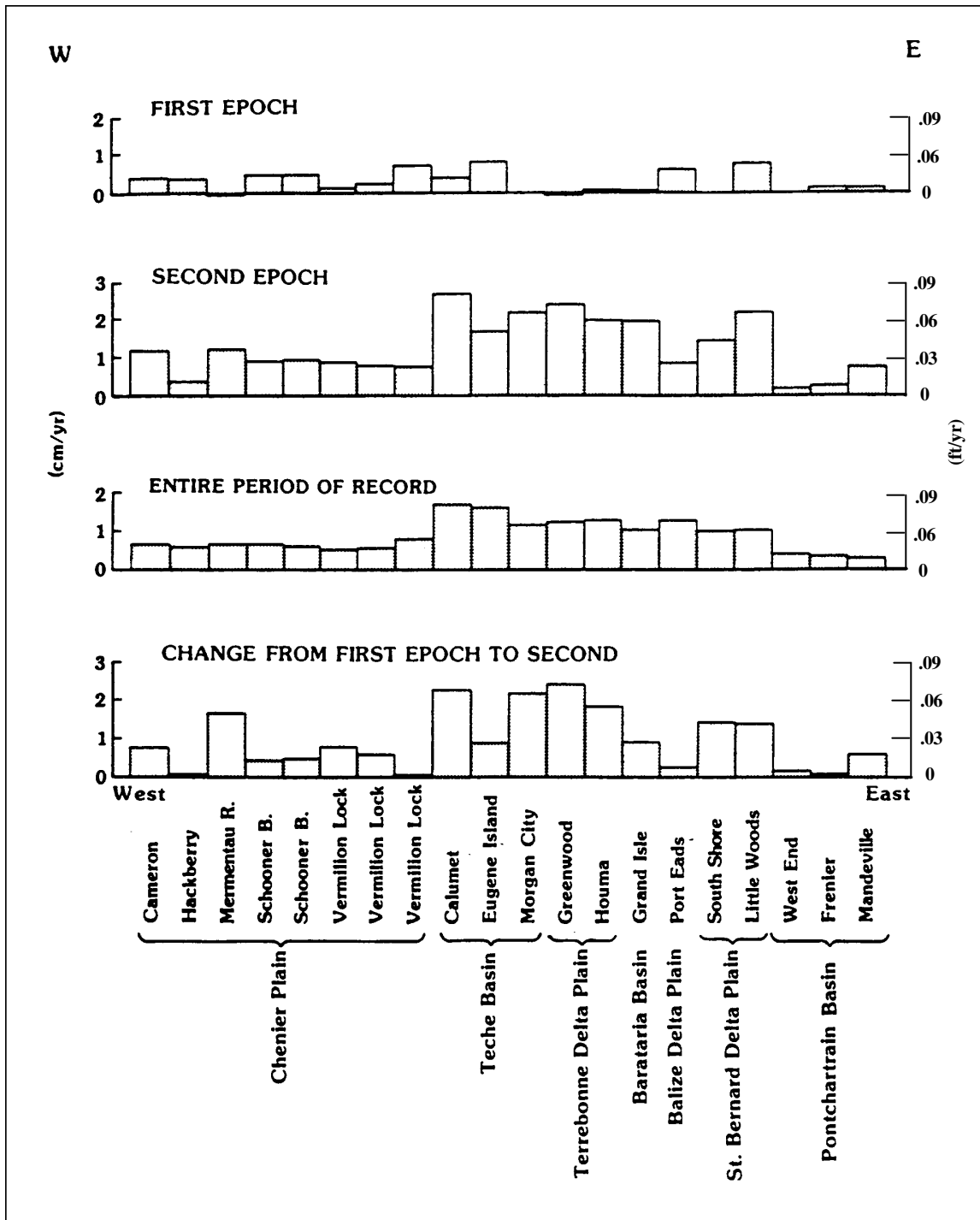


Figure 71. Relative sea level rise based on readings from U.S. Army Corps of Engineers tide gauge stations on Louisiana. Note change in rate of rise between 1947-1961 (Epoch 1) and 1962-1978 (Epoch 2) (after Penland et al. 1989).

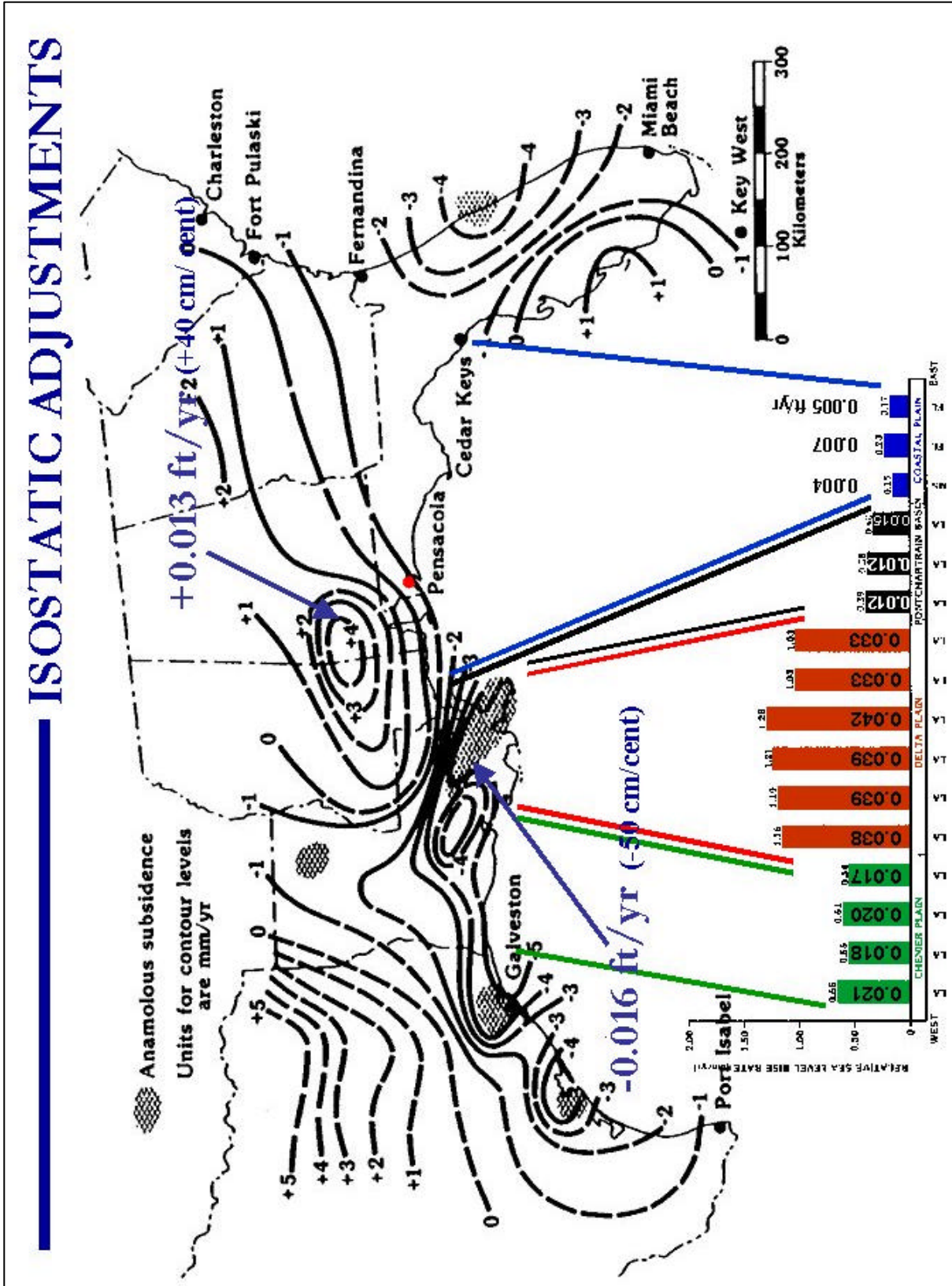


Figure 72. Elevation and relative sea level changes in the northern Gulf of Mexico region. (Elevation changes after Holdahl and Morrison 1974; RSL rise rates after Penland et al. 1988).

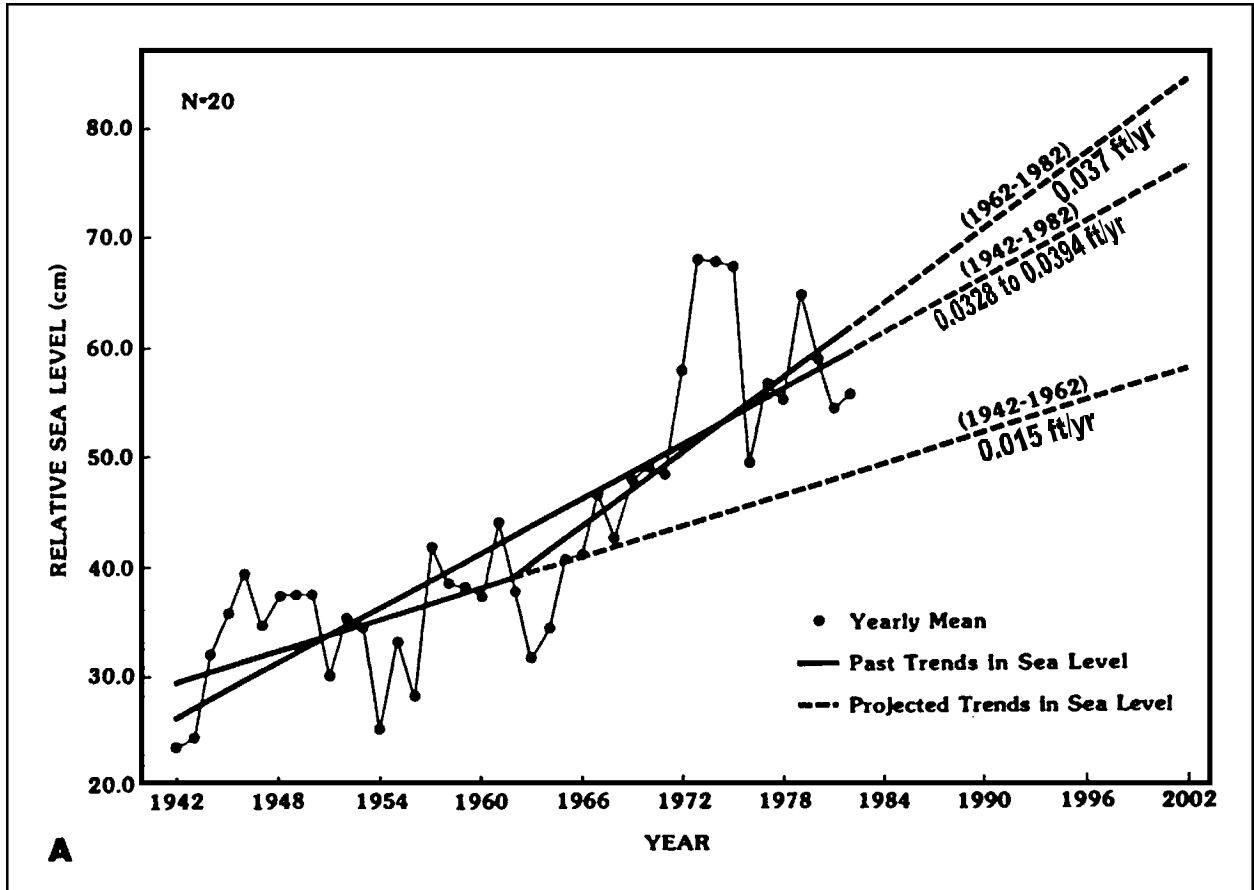


Figure 73. Present and future trends of RSL rise based on gauge records from coastal Louisiana (after Ramsey and Moslow 1987).

Figure 74 depicts a map showing contours of equal rates of RSL rise for Epoch 2 adapted from Ramsey and Moslow (1987). The map shows a large area of high RSL rise rates south of the Theriot-Golden Meadow Fault Systems. A local area of high rates occurs along the south shore of the eastern end of Lake Pontchartrain. There are no reported subsurface faults in this area, but the high rates fall along the trend of Frenier Fault Zone, and in the vicinity of faults in Lake Pontchartrain, where movement has been documented by Lopez et al. (1997) and others.

The implications of the Ramsey and Moslow (1987) map are far reaching. Do rates of RSL rise in the Terrebonne area meet the reality test? The rate of 0.08 ft/yr (2.44 cm/yr) equals 2 ft (60.96 cm) of vertical change during twenty years. During the twenty years from 1962-1982 did the RSL rise rate in the Barataria Basin exceed the rate in the Balize Delta area, where, historically, RSL rise rates have been reported to be the highest in region? Are the rates of rise lower along natural levee ridges than in interdistributary basin areas as depicted on the Ramsey and Moslow (1987) map?

Findings of the present study and results of other recent fault studies provide partial answers to these questions. See Table 5 for presents a summary of tide gauge data from various sources.

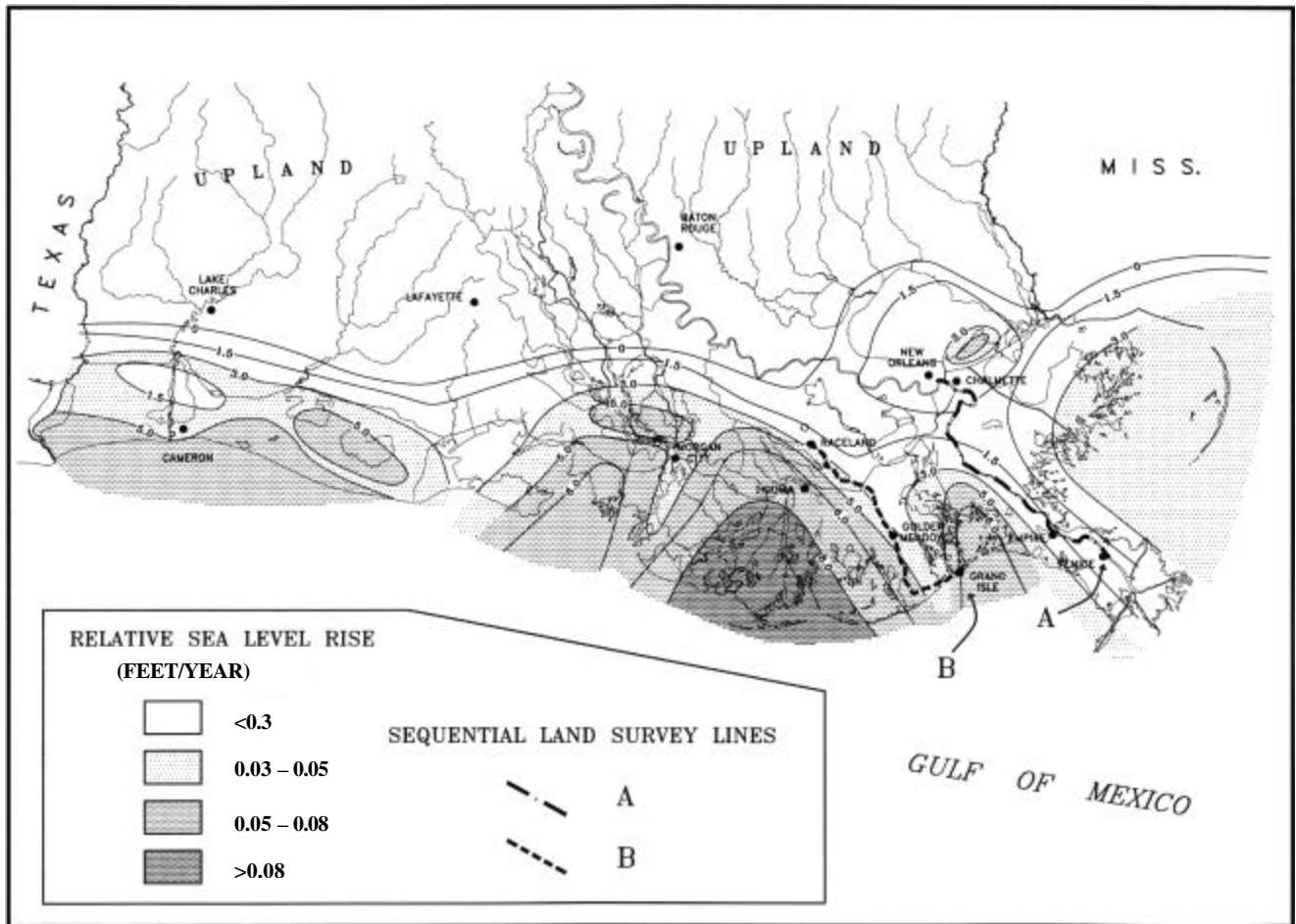


Figure 74. Isopleth map of RSL rise rates in coastal Louisiana based on 1962-1982 (Epoch 2) tide gauge data (adapted from Ramsey and Moslow 1987). Locations of sequential land leveling lines are also shown.

Sequential Land Leveling

An analysis has been conducted of four data sets derived from repetitive benchmarks. The first data set is from benchmarks at the NASA-Michoud Facility located in eastern New Orleans (Figure 75). Three additional sets are from lines of benchmarks along highways that follow natural levee ridges along the Mississippi River from New Orleans to Venice, along Bayou Lafourche from Raceland to the bend in LA Highway 1 near Port Fourchon, and along Bayou Petite Caillou from the Presquille Isle Bridge to Cocodrie. Along each line, graphs were plotted showing the amount of vertical displacement and the average rate of vertical movement (velocity) for the periods between surveys.

NASA-Michoud Benchmarks

In 1986, D. B. Zilkoski and S. M. Reese, Jr. published the results of a study of subsidence in the eastern New Orleans area based on analysis of geodetic leveling data. They reported that during 1984 and 1985 the National Geodetic Survey (NGS) conducted a major re-leveling of vertical control networks in the vicinity of New Orleans. This was

the third re-leveling, as the network was previously surveyed in 1951-55 and 1964. In addition, several leveling lines of this network were re-leveled in 1969, 1971 and 1977.

Zilkoski and Reese (1986) selected three of the re-leveling networks (1951-55, 1964 and 1984-85) for comparison. They found that overall subsidence in the eastern New Orleans area for the total period of record (1951–1984) in the amount of 0.82 ft to 0.98 ft (249 to 298 mm) was common.

The elevations were carried from a benchmark at Biloxi, Mississippi which was assumed to be stable. The elevation was carried to Benchmark J92 in northeastern Orleans Parish. Comparison with the 1938 elevation indicated that benchmark J-92 subsided only 0.13 ft (40 mm) between 1938 and 1977. This is a rate of 0.0045 ft/yr (1.37 mm/yr).

Plots showed that elevation differences varied considerably from benchmark to benchmark and from epoch to epoch. Zilkoski and Reese (1986) offered no specific explanation, but noted that many factors contribute to the movement. They called particular attention to the NASA – Michoud area (Figure 75) where there are four deep-well benchmarks (Benchmarks 284 – 287). Three of the four (284, 285 and 286) were leveled in both 1964 and 1985. These three benchmarks are set on top of deep-casement wells ranging in depth from 569 to 590 ft (173.4 to 179.8 m). The benchmarks were assumed to be stable because of the depth of the casings. However, Zilkoski and Reese (1986) found that the benchmarks appeared to have subsided a significant amount between 1964 and 1985, as follows:

<u>Benchmark</u>	<u>Vertical Change</u>		<u>Rate</u>	
284	-0.76 ft	(-231.4 mm)	-0.036 ft/yr	(-10.97 mm/yr)
285	-0.74 ft	(-214.6 mm)	-0.034 ft/yr	(-10.36 mm/yr)
287	-0.89 ft	(-269.8 mm)	-0.042 ft/y	(-12.80 mm/yr)
Average	-0.78 ft	(-238.6 mm)	-0.037 ft/yr	(-11.28 mm/yr)

Zilkoski and Reese (1986) do not provide information on the original purpose of the casements upon which the benchmarks were set. It is not known at this time whether the wells were drilled for a water supply at the NASA - Michoud facility or if there was some other fluid withdrawal that may have contributed to the anomalous subsidence rate. However, the benchmarks were selected because of their depth, which was well below the base of Holocene deposits in the area and into or below the Pleistocene.

Records from the South Shore and Little Woods tide gauges, which are in the general vicinity of the NASA – Michoud benchmarks, also show anomalous increases in RSL rise in the same order of magnitude and for corresponding periods of record (Ramsey and Moslow 1987, Penland et al. 1989, see also Figure 74 of this report). The NASA – Michoud location falls along the Frenier Fault Zone of this report. H. N. Fisk (1944:Plate 17) illustrated a profile based on borings, which was in the general vicinity of the NASA – Michoud facility, and which showed a displacement of approximately 10 ft (3.1 m) of the top of the Pleistocene. There are several lines of converging evidence which suggest fault movement in this eastern New Orleans area during the 1964 – 1985 interval.

Mississippi River Line - Chalmette to Venice

P.C. Howard and S.M. Gagliano (in van Beek et al. 1986) studied subsidence in Plaquemines Parish, including the Mississippi River from New Orleans to its mouth. A review of the geological literature disclosed subsidence estimates for the Balize Delta (Active Mississippi River Delta) area ranged from 0.04 to 0.14 ft/year (1.22 to 4.27 cm/year). From the published estimates, Howard concluded that the minimum value of subsidence was 4 ft/century (1.2 m/century). It should be noted that “subsidence” as used by Howard is equivalent to RSL rise as used herein. A re-evaluation of the original sources during the course of this work verifies Howard’s findings.

Howard also evaluated data from NGS vertical benchmark surveys along the Mississippi River natural levees between the Inner Harbor Navigation Canal (IHNC) lock and Venice, Louisiana. Figure 76 shows vertical movement along this line for three intervals, 1938 to 1951, 1951 to 1964, and 1964 to 1971. The line cuts across the east-west trending regional growth faults and appears to show vertical displacement and changes in slope through time. The data suggest activity on six or more faults.

When this benchmark data set is analyzed within the context of the tectonic framework model, the vertical movements have new meaning. Inspection of the section shows that all but three of the 34 benchmarks exhibit measurable lowering during the 33-year period from 1938 – 1971 (van Beek et al. 1986).

The amount of vertical movement of individual benchmarks varies through time. Negative spikes along the correlation lines identify probable faults, most of which correlate with known subsurface faults shown in Figure 6. Five probable faults are made conspicuous by sharp variations in amounts of vertical displacement. The three most prominent are correlated with the Bayou des la Fleur and Diamond segments of the Lake Hatch Fault Zone, and an unnamed segment of the Lake Borgne Fault Zone.

The direction of slope of the correlation lines in areas between faults suggests that three of the faults are downthrown to the basin, while two appear to have counter-basin dip. Apparent rise in land elevation has been recorded at a few of the benchmarks. This can be attributed to either survey error or possibly to rebound of up-thrown blocks adjacent to fault scarps. The Empire and Bastian Bay segments of the Golden Meadow Fault Zone show indications of positive rebound movement after the 1964 survey.

Figure 77 shows subsidence rates and relative sea level rise rates for each of the benchmarks through time. The NGS elevations do not include the effect of sea level rise, as the benchmark elevations are carried in along survey networks that are referenced to stable benchmarks. To determine the rate of relative sea level rise an adjustment must be added for the rate of eustatic rise. The relative sea level scale on the right has been adjusted by 0.0075 ft/year (2.286 mm/yr) (the rate at Pensacola, Florida) to correct for eustatic sea level rise. With the exception of four points, the amount of vertical movement during the 1938 – 1951 and 1951-1964 intervals, totaling 26 years, was relatively small. The average vertical velocity for the two intervals, respectively, was -0.023 and -0.016 ft/yr (-7.010 and -4.877 mm/yr). In contrast, the rate of downward

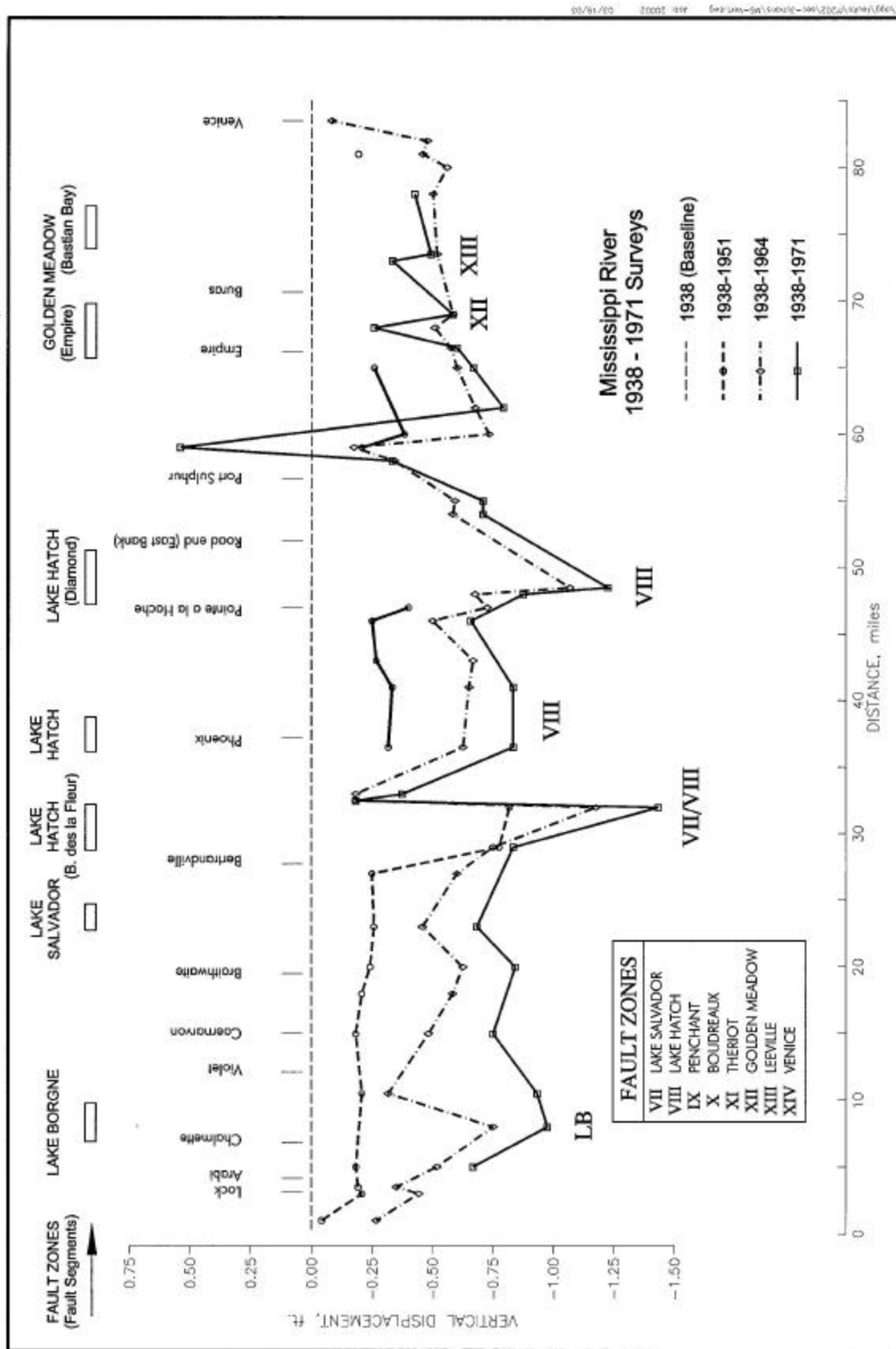


Figure 76. Changes in elevation along Mississippi River natural levees between IHNC Lock and Venice, Louisiana. The graphs show benchmark movement based on four surveys made between 1938 and 1971 (Modified from van Beek et al. 1986, original data from NGS). The negative spikes are correlated with faults as delineated in this study.

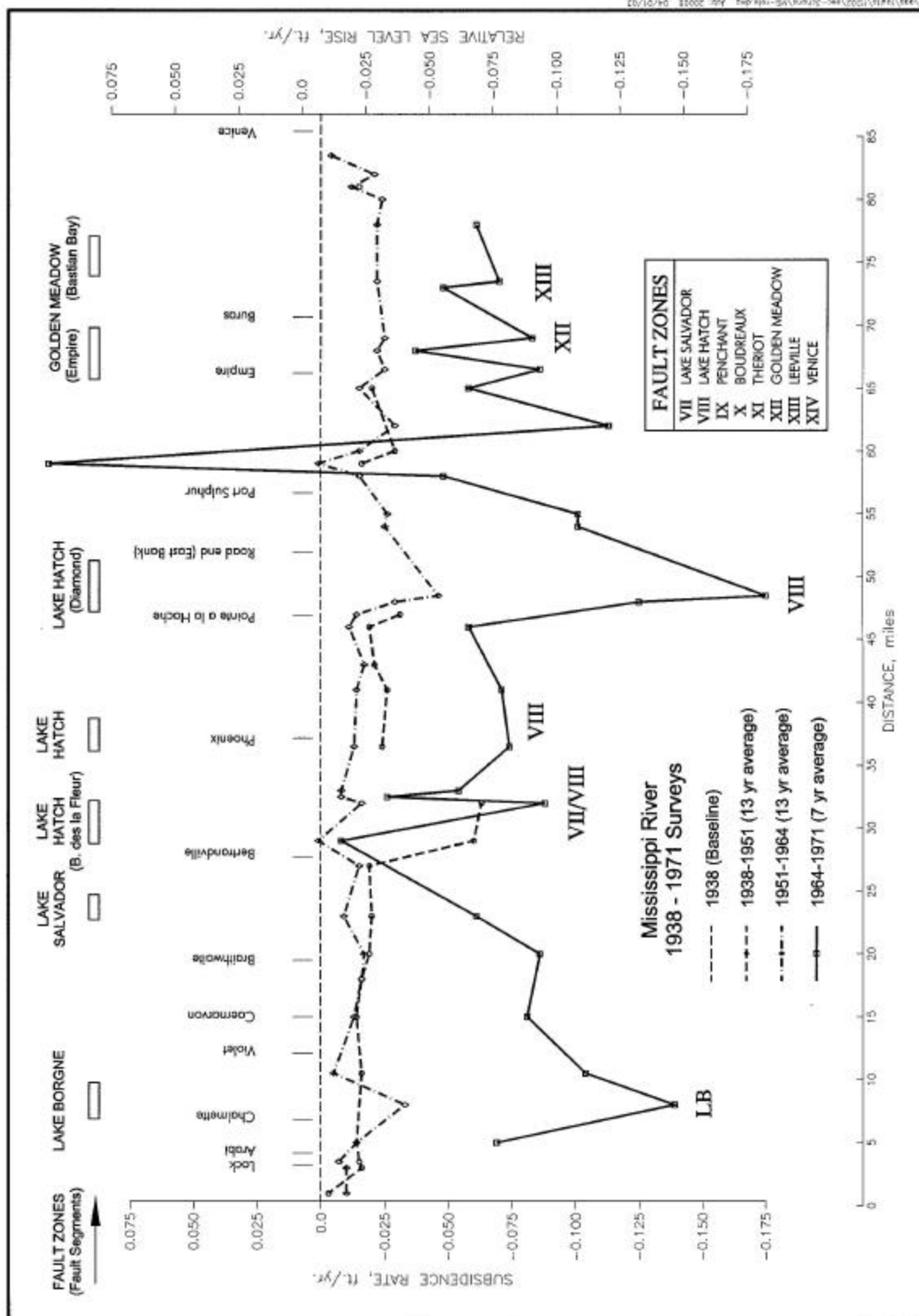


Figure 77. Changes in rates of vertical movement of re-leveled benchmarks along the Mississippi River natural levees between the IHNC Lock and Venice, Louisiana. The graphs show rates of movement based on four surveys. The scale on the right is adjusted for eustatic sea level rise (0.0075 ft/yr [0.019 cm/yr]). (Data from NGS).

movement at all but three points greatly accelerated during the 1964 – 1971 interval, with an average rate of -0.071 ft/yr (-21.641 mm/yr).

The rate curves (Figure 77) indicate that some movement had occurred on the Lake Borgne Fault between 1951 and 1964, but the rate increased significantly between 1964 and 1971. At the Bayou des la Fleur segment of the Lake Hatch Fault Zone, the rate of movement was high during the 1938 – 1951 interval, but increased during the 1964 – 1971 interval. The Diamond segment of the Lake Hatch Fault Zone was moving during the 1951 – 1964 interval, but greatly accelerated during the 1964 – 1971 period. Finally, rates were only significant on the Empire and Bastian Bay Fault segments during the 1964 – 1971 interval.

Figure 78 shows average rates of vertical change and RSL rise of the entire 33-year period of record along the Mississippi River Line. An average rate of subsidence, discounting the rebound peaks and the large faults, for the section is 0.02 ft/yr (0.05 cm/yr), with a corresponding relative sea level rise rate of 0.03 ft/yr (0.076 cm/yr). The average rate for the two largest faults is 0.04 ft/yr (0.10 cm/yr) for subsidence and 0.045 ft/yr (0.114 cm/yr) for RSL rise.

Bayou Lafourche Line

Ramsey and Moslow (1987) and Penland et al. (1988) also used sequential land leveling data to measure subsidence. The most important section that they studied follows the natural levee ridges along Bayou Lafourche. Ramsey and Moslow (1987:1682) illustrated a section showing rates of land movement for the period 1965 – 1982 and extending from Raceland to Grand Isle, Louisiana. Kuecher (1994) correlated the location of NGS benchmarks showing spikes along the Lafourche section with locations of the Golden Meadow and Lake Hatch Fault traces. He concluded that pronounced negative spikes occur immediately on the down-dropped sides of the fault traces.

Morton et al. (2002:Figure 11) re-evaluated and plotted NGS benchmark data along the Lafourche Line for the period 1965 - 1982. They utilized a larger number of data points than Penland et al. (1988) and made adjustments in the data. They plotted a profile showing adjusted offset and made correlations with subsurface faults and oil and gas fields. They reconfirmed the correlations of negative spikes with the Lake Hatch and Golden Meadow Faults made by Kuecher (1994).

In this paper we have used the data set from the Morton et al. (2002) Bayou Lafourche line, but have re-plotted the numbers at a different scale for comparative purposes. We have also calculated rates of vertical change from the Morton et al. (2002) Bayou Lafourche profile for comparison with the Mississippi River line and other data sets.

The re-plotted Morton et al. (2002) data from the Bayou Lafourche line is shown in Figure 79. The figure shows both a vertical displacement profile and a rate of displacement profile. As along the Mississippi River line, there are pronounced negative spikes that are interpreted as faults. There are eight probable faults along the Lafourche line. These are correlated with the Lake Hatch Fault Zone (2), the Theriot Fault Zone (1),

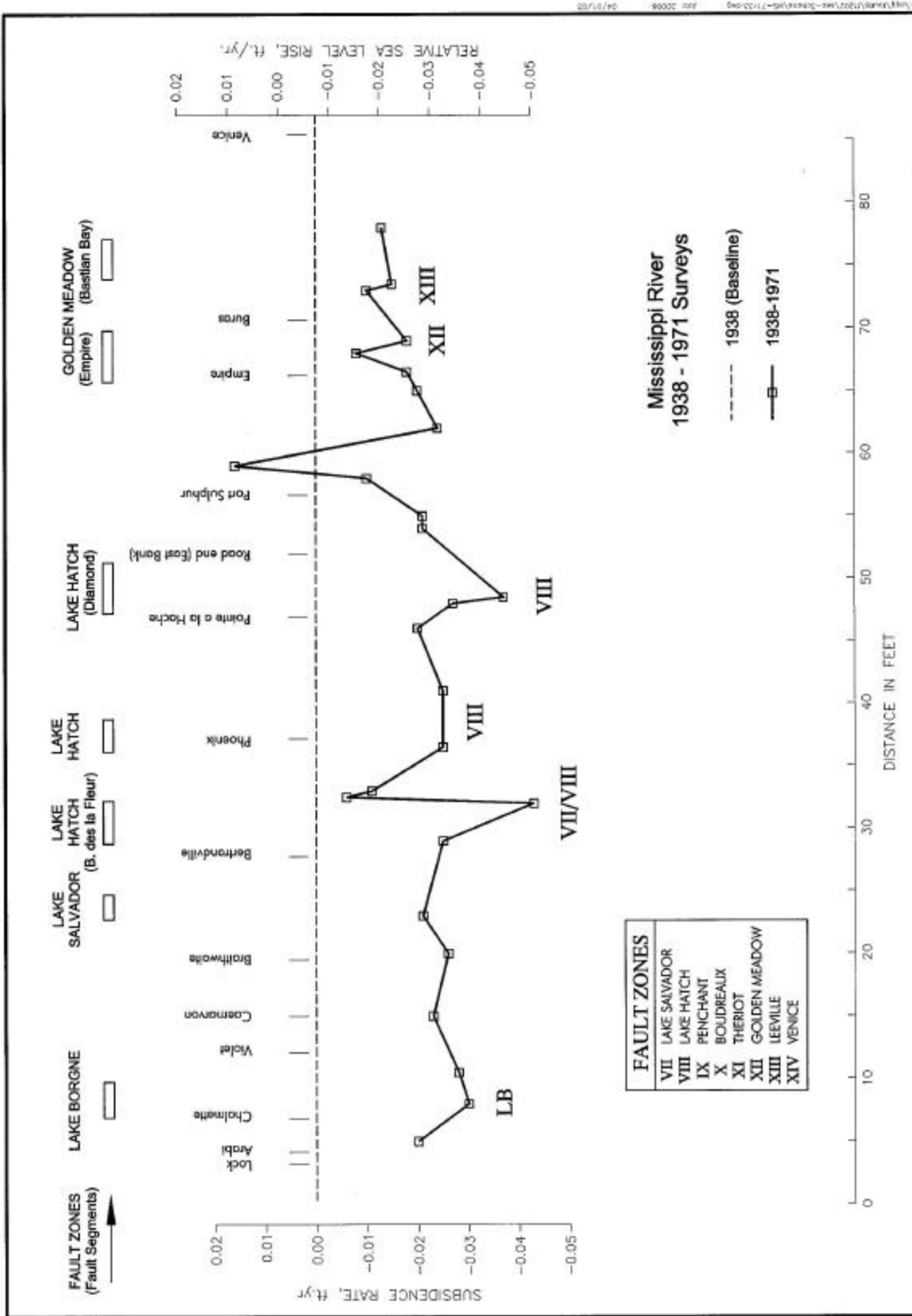


Figure 78. Average rate of vertical change (subsidence) and RSL rise for re - l eveled benchmarks along Mississippi River natural levees for the 33-year period between 1938 and 1971.

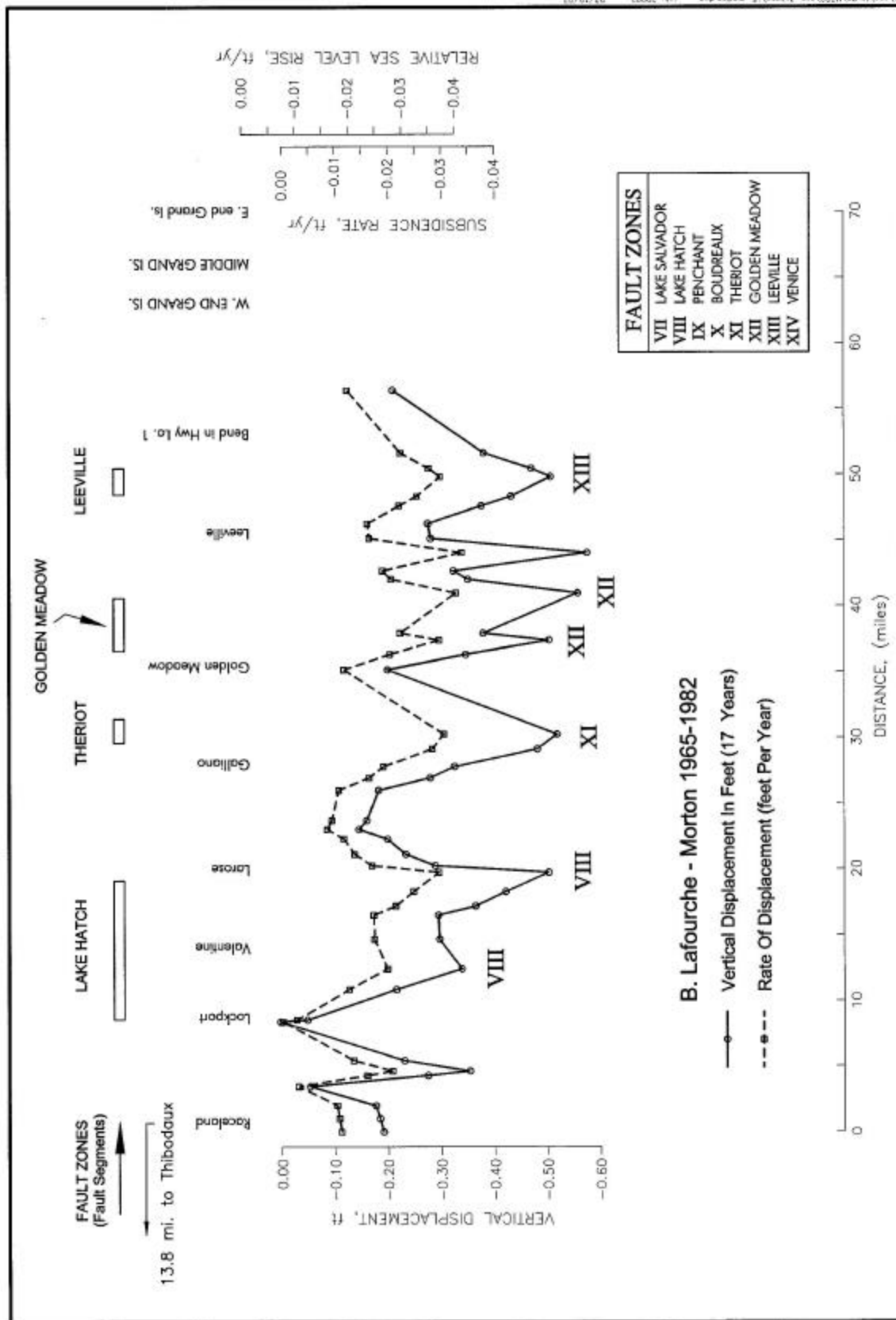


Figure 79. Profiles showing amounts and rates of vertical displacement based on re - leveled benchmarks on a line along the natural levees of Bayou Lafourche from Raceland to the vicinity of Port Fourchon, Louisiana. Data derived from profile by Morton et al. (2002). Original data from NGS. Fault correlations from this study.

the Golden Meadow Fault Zone (2) and the Leeville Fault Zone (1). Two spikes do not appear to be related to known subsurface faults.

This Bayou Lafourche section exhibits a general down-to-the basin increase in subsidence, with a general reduction of the surface from approximately -0.2 to -0.3 ft (-60.96 to -91.44 mm) for the 17-year period of record. A line of best fit through the negative spikes ranges from approximately -0.4 to -0.5 ft (-121.92 to -152.4 mm) of vertical displacement. The maximum rate of vertical displacement is 0.035 ft/yr (10.668 mm/yr) and the average rate for the apparent faults is 0.036 ft/yr (10.973 mm/yr). The rates of vertical displacement along the line are remarkably uniform.

In addition to the vertical offset profile, Morton et al. (2002:Figure 12) did a time analysis of data from two benchmarks at Valentine, Louisiana. They compared data from leveling surveys made in 1955, 1965 and 1982. They found that the rates of vertical displacement increased substantially during the second interval, as follows:

Benchmark	Epoch 1 (1955 – 1965)	Epoch 2 (1965 – 1982)
AU1364	-0.30 mm/yr (-0.0001 ft/yr)	-2.56mm/yr (-0.0084 ft/yr)
AU1104	-3.09 mm/yr (-0.010 ft/yr)	-5.60mm/yr (-0.018 ft/yr)

Morton et al. (2002:769-772) correlated the accelerated rate of vertical movement with maximum rates of fluid production.¹⁷ It should be noted that the increase also corresponds with Epoch 2, the period of widespread increase in rates of relative sea level rise as determined from tide gauge records and reported by Ramsey and Moslow (1987), Penland et al. (1988), and others.

Bayou Petite Caillou Line

Figure 80 shows a profile of amounts and rates of vertical displacement of benchmarks along a line down Bayou Petite Caillou. As in the case of the Bayou Lafourche line, the data were derived from a line showing vertical displacement of benchmarks down the natural levee ridges of Bayou Petite Caillou from the Presquille Isle Bridge to Cocodrie, Louisiana published by Morton et al. (2002:Figure 13). The original data were from the NGS, and were adjusted by Morton et al. (2002). Morton et al. (2002) correlated two negative spikes on this line with the Lake Hatch and Golden Meadow Fault Zones. We have re-plotted the vertical displacement data and also calculated rates of vertical displacement for purposes of comparison.

Four faults were identified on the re-plotted profile and tentatively correlated with known subsurface faults (Lake Hatch, Boudreaux, Theriot, and Golden Meadow Fault Zones).

¹⁷ Specifically they investigated subsidence along segments of the Golden Meadow and Lake Hatch Faults with several individual oil and gas fields. They investigated formation pressure production and field pressure histories. They concluded that decreases in subsurface pore pressure associated with gas production were so large that subsurface faults were critically stressed and reactivated (Morton et al. 2002).

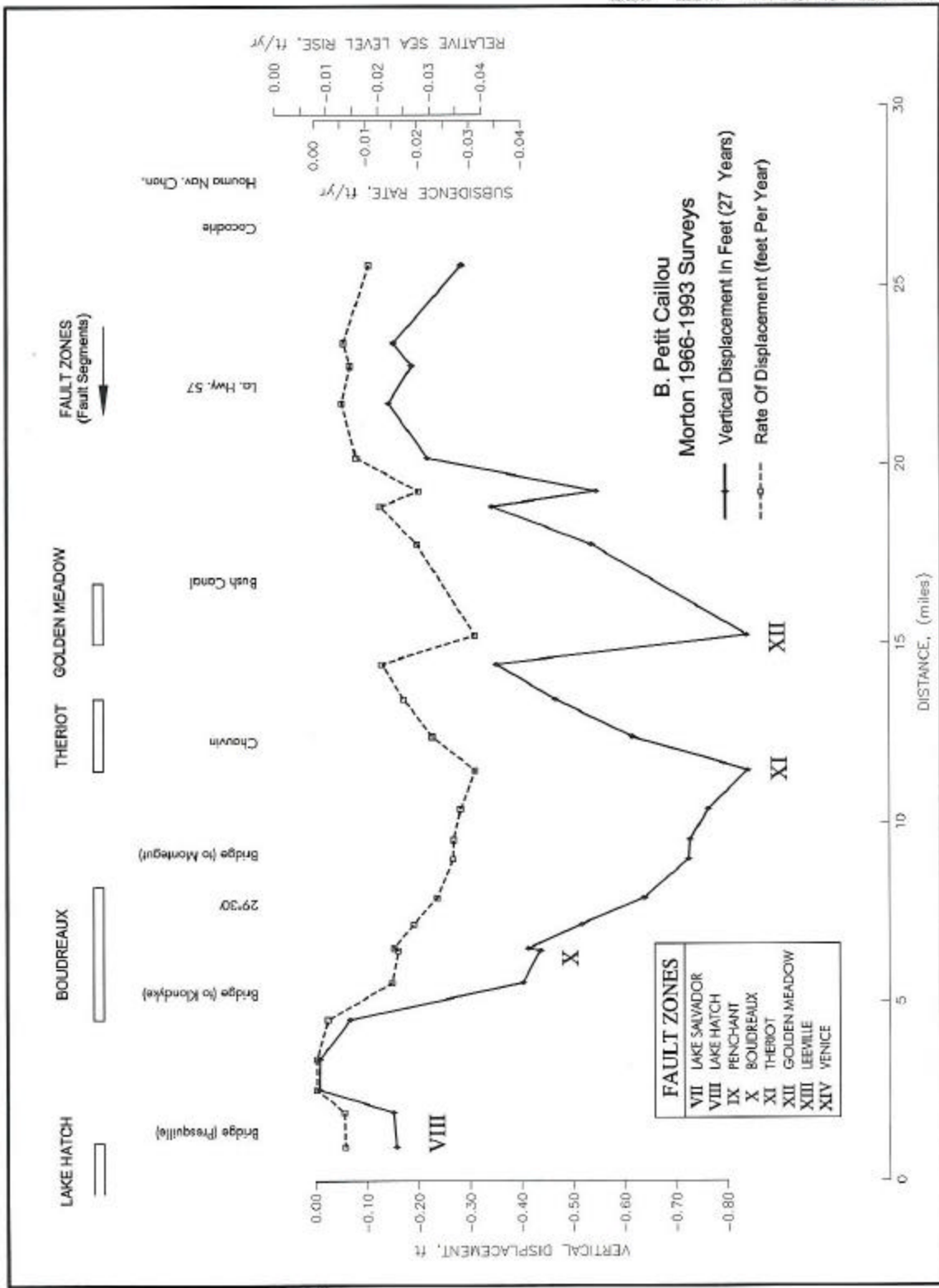


Figure 80. Profiles showing amount and rates of vertical displacement based on re - leveled benchmarks on a line along the natural levees of Bayou Petite Caillou from Presquille to Cocodrie, Louisiana. Data derived from profile by Morton et al. (2002). Original data from NGS. Fault correlations from this study.

There are one or possibly two additional negative spikes, but these do not correlate with known subsurface faults.

The average vertical displacement along the line for the 27-year period 1966 – 1993 was -0.403 ft (-122.834 mm) and the average rate of vertical displacement was -0.015 ft/yr (-4.572 mm/yr). The vertical displacement of the Theriot Fault and the Golden Meadow Fault was -0.82 and -0.837 ft (-249.936 and -255.118 mm,) respectively, and the rate of vertical displacement was -0.030 and -0.031 ft/yr (-9.144 and -9.449 mm/yr), respectively.

Comparison of Mississippi River, Bayou Lafourche and Bayou Petite Caillou Lines

Figure 81 shows a comparison of the vertical displacement along the three re-leveled benchmark lines studied. The time intervals for the three sections are unequal, but more representative of the Epoch 2 (1962 – 1982) than TheEpoch 1 (1947 - 1961). Figure 82 shows profiles of rate of vertical displacement and relative sea level rise. As can be seen from graphic presentation of the data, the amount and rates of displacement are internally consistent. They are also comparable to the values determined from tidal gauge records (Table 5). The amounts of vertical displacement are small, but the rates are relatively high.

Each of the three re-leveled lines crosses the Terrebonne Trough and the regional faults associated with it (See Figure 75). Direct comparisons of the three lines shown in Figures 81 and 82 indicate that the entire area within the trough has measurably subsided during modern decades. There appears to be generalized average displacement of the “floor” within the trough. In addition there are large negative spikes associated with faults. The amount of vertical displacement is greatest along the Mississippi River line and least along the Bayou Lafourche line.

Vertical Movement and Rates of Subsidence and Relative Sea Level Rise for Epoch 2

The rates of relative sea level rise derived from the tide gauge records, the re-leveled benchmarks and other sources are shown in reference to the tectonic framework in Figure 83. All rates shown are from Epoch 2 (1962-1982). The total amounts of vertical movement for Epoch 2 are shown in Figure 84.

Summary

The locations of benchmarks and tide gauges are distributed randomly in reference to the locations of faults. Relative sea level rise has been significantly less at tide gauges in Cedar Key, Florida; Pensacola, Florida; Biloxi, Mississippi; and Galveston, Texas than it has been at Houma, Louisiana and other gauges in Southeastern Louisiana. The average rate of sea level rise at Houma in Terrebonne Parish is four times the average rate for the Gulf of Mexico and five times the average rate for the U.S. Eastern seaboard (Penland et al. 1988:59).

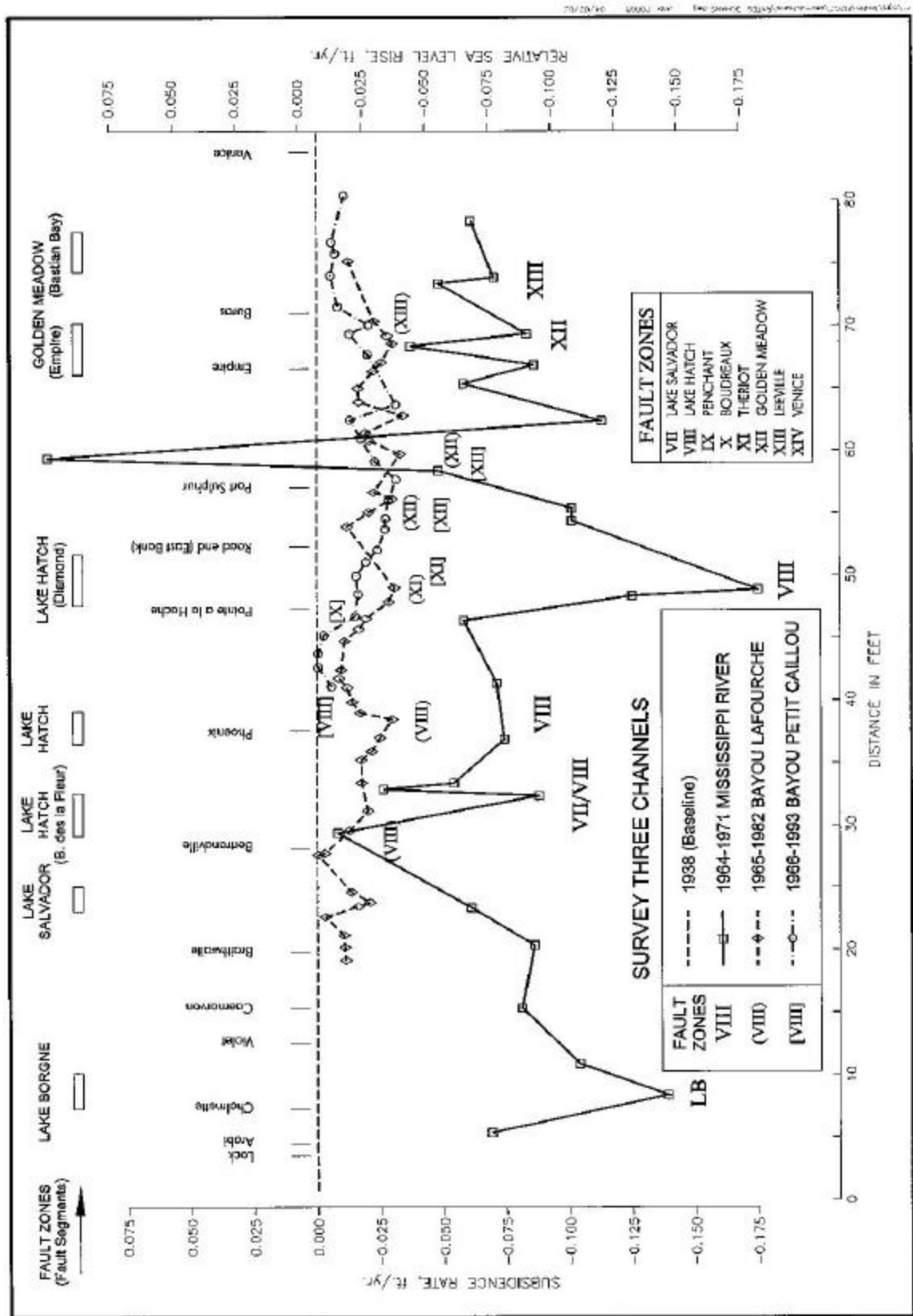


Figure 82. Comparison of rates of subsidence and RSL rise during Epoch 2 along the Mississippi River, Bayou Lafourche, and Bayou Petite Caillou lines. For sources see Figures 76, 77, 79 and 80.

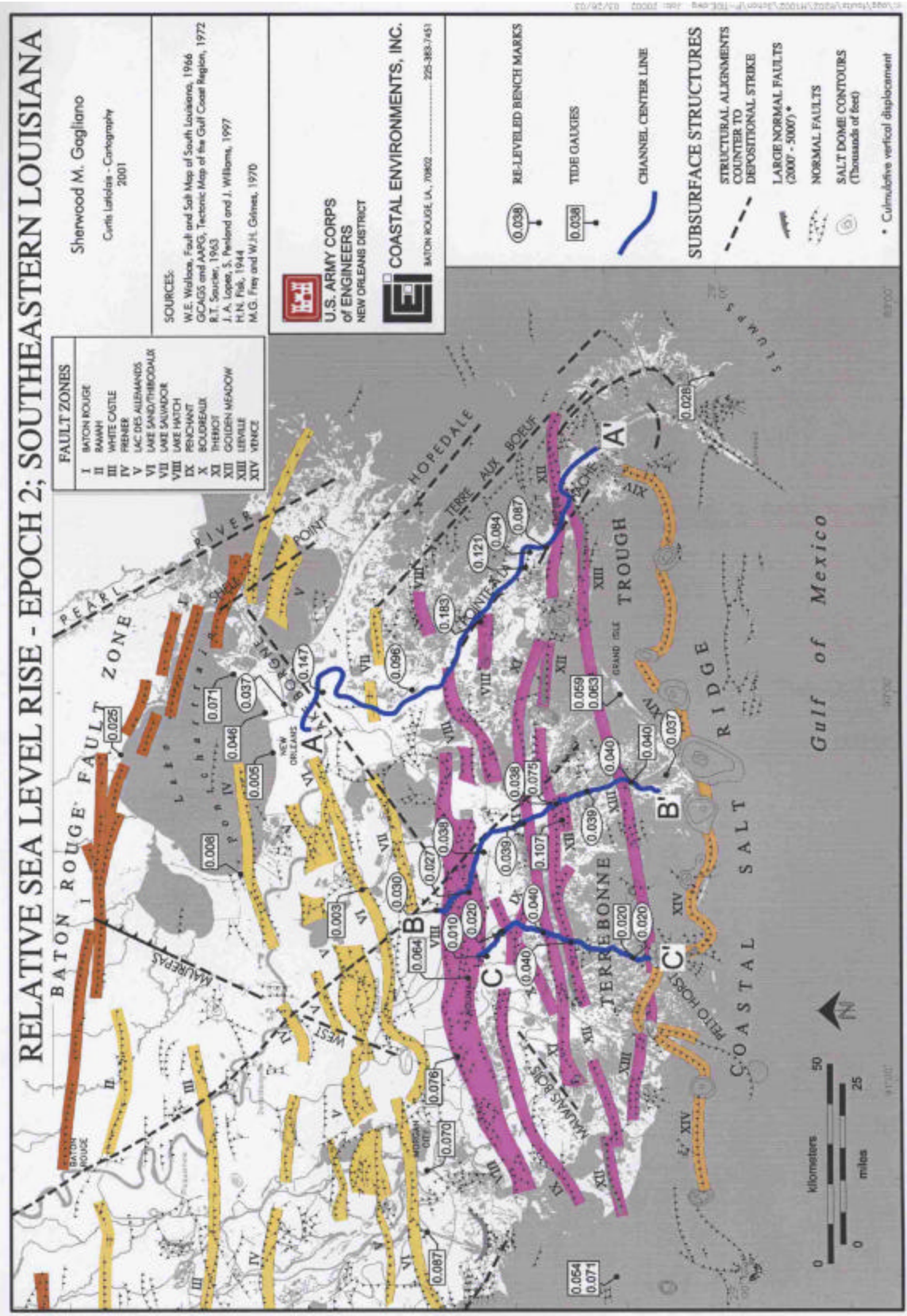


Figure 83. Rates of RSL rise (in ft/yr) from benchmark and tide gauge data for Epoch 2, 1962 - 1982.

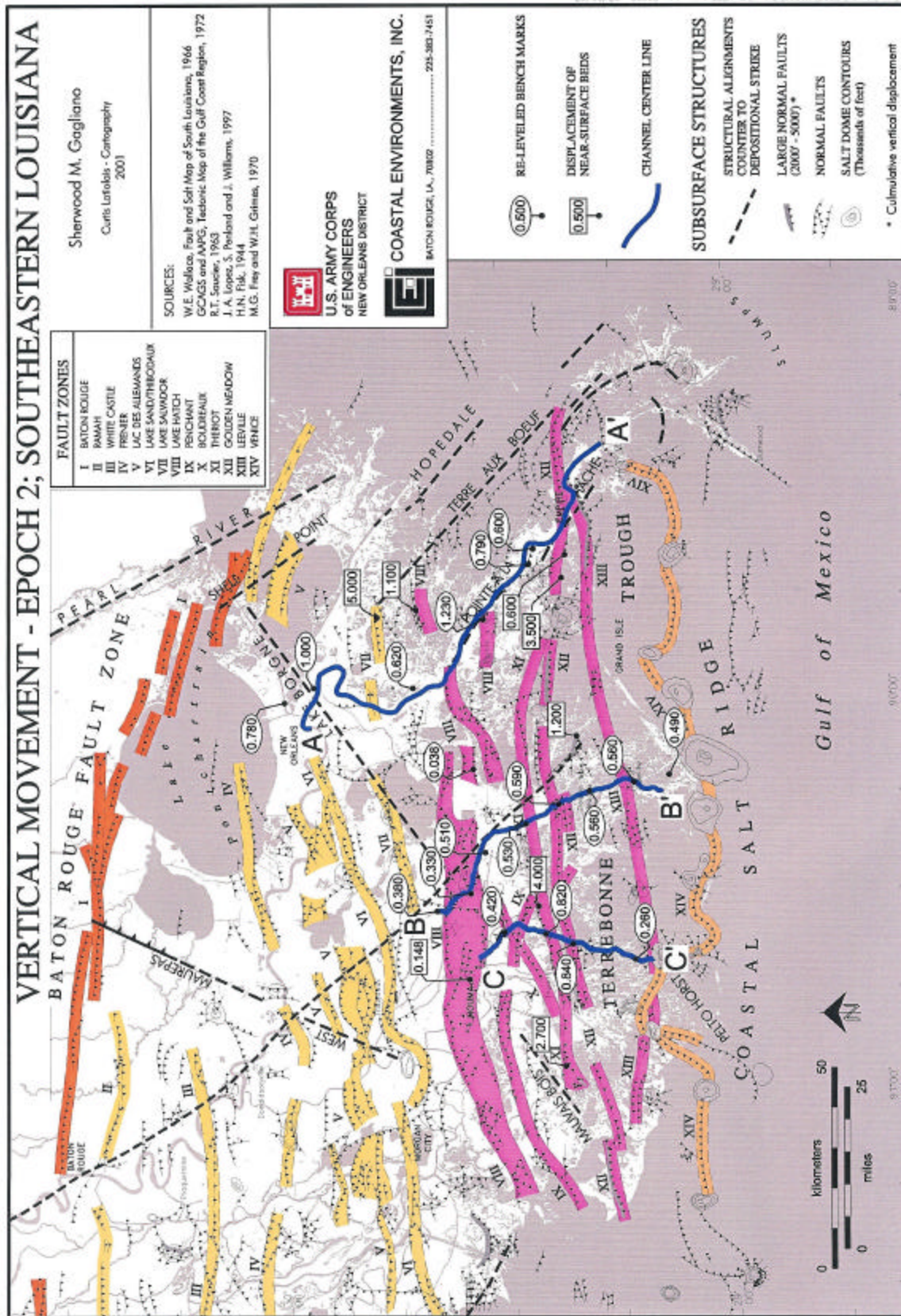


Figure 84. Vertical change in elevation (in ft) from benchmark and tide gauge data for Epoch 2, 1692 - 1982.

Shown in Table 6 are RSL rates from three key deltaic plain tide gauge stations and the Pensacola, Florida reference station. Rates are given for Epochs 1 and 2 as well as for the average of the total record. The Eugene Island and Grand Isle tide gauge stations are considered to be key stations by Penland et al. (1988). There are National Ocean Survey (NOS) and U.S. Army Corps of Engineers (USACE) stations at both locations.

Table 6. Rates of Relative RSL Rise for Three Key Deltaic Plain Tide Gauge Stations and the Pensacola, Florida Reference Station.

Average Rate RSL Rise		
Tide Gauge Station:	NOS	USACE
Pensacola, FL	0.23 cm/yr (0.007 ft/yr)	
Eugene Island, LA	1.19 cm/yr (0.039 ft/yr)	1.61 cm/yr (0.052 ft/yr)
Grand Isle, LA	1.03 cm/yr (0.034 ft/yr)	1.10 cm/yr (0.036 ft/yr)
Houma, LA		1.28 cm/yr (0.042 ft/yr)
Epoch 1 (1942-1962)		
Tide Gauge Station:	NOS	USACE
Pensacola, FL	0.05 cm/yr (0.002 ft/yr)	
Eugene Island, LA	0.95 cm/yr (0.031 ft/yr)	0.79 cm/yr (0.026 ft/yr)
Grand Isle, LA	0.30 cm/yr (0.010 ft/yr)	0.60 cm/yr (0.020 ft/yr)
Houma, LA		0.07 cm/yr (0.002 ft/yr)
Epoch 2 (1962-1982)		
Tide Gauge Station:	NOS	USACE
Pensacola, FL	0.46 cm/yr (0.015 ft/yr)	
Eugene Island, LA	2.17 cm/yr (0.071 ft/yr)	1.64 cm/yr (0.054 ft/yr)
Grand Isle, LA	1.92 cm/yr (0.063 ft/yr)	1.79 cm/yr (0.059 ft/yr)
Houma, LA		1.94 cm/yr (0.064 ft/yr)

Tide gauges operated by both the NOS and the USACE show an increase in rates of relative sea level rise (and rate of submergence) between Epoch 1 and Epoch 2. This same change in rate between the two epochs is found on tide gauge records from stations throughout Southeastern Louisiana, including, but not restricted to, Morgan City, Eugene Island, Greenwood, Houma, Grand Isle and Little Woods.

We have related tide gauge locations with known subsurface faults. Table 7 shows tide gauges that are in relatively close proximity to known subsurface faults.

Sasser et al. (2002) have re-examined the tide gauge records from Grand Isle for the period 1955 to 2000 and found that the rate of rise continues to increase for the interval 1982 – 2000. The average rate of relative sea level rise for the entire period of record was found to be 0.035 ft/yr (1.06 cm/yr).

Table 7. Correlation of Tide Gauge Stations with Fault Zones. The RSL Rise Rates for Epoch 2 Are Also Given for Each Station.

Tide Gauge Station	Fault	Epoch 2, RSL Rise Rate
Mandeville	I Baton Rouge	0.020 ft/yr (0.61 cm/yr)
Frenier	IV Frenier	0.023 ft/yr (0.70 cm/yr)
Little Woods	IV (?) Frenier (?)	0.071 ft/yr (2.16 cm/yr)
West End	Between IV & V Frenier & Lac Des Allemands	0.005 ft/yr (0.15 cm/yr)
South Point	V (?) Las Des Allemands	0.046 ft/yr (1.40 cm/yr)
Des Allemands	VI Lake Sand/Thibodaux	0.003 ft/yr (0.09 cm/yr)
Morgan City	VI Lake Sand/Thibodaux	0.070 ft/yr (2.13 cm/yr)
Calumette	VI Lake Sand/Thibodaux	0.087 ft/yr (2.65 cm/yr)
Houma	VIII Lake Hatch	0.064 ft/yr (1.95 cm/yr)
Greenwood	VIII Lake Hatch	0.076 ft/yr (2.32 cm/yr)
Eugene Island	XII Lake Salvador	0.054 ft/yr (1.65 cm/yr)
Eugene Island	XII Golden Meadow	0.071 ft/yr (2.16 cm/yr)
Catfish Lake	XII Golden Meadow	0.107 ft/yr (3.26 cm/yr)
Golden Meadow	XII Golden Meadow	0.075 ft/yr (2.29 cm/yr)
Cocodrie	N. of XIII Leeville	0.020 ft/yr (0.69 cm/yr)
Leeville	XIII Leeville	0.040 ft/yr (1.22 cm/yr)
Grand Isle	S. of XIII Leeville	0.050 ft/yr (1.52 cm/yr)
Grand Isle	S. of XIII Leeville	0.060 ft/yr (1.83 cm/yr)

*See Figure 6 for location of faults.

We have re-examined the tide gauge records from Grand Isle, Houma, and Little Woods and found that an abrupt change in corrected mean annual water level occurs in 1964.

Examination of changes of land elevation from re-leveling of benchmarks by the NGS at a number of locales shows an increase in the rate of subsidence between Epoch 1 and Epoch 2. Correlation of re-leveled bench marks whose records show change in RSL rise rates between Epochs 1 and 2 are given in Table 8.

Collectively, the above findings suggest that a major tectonic event occurred in the region in the 1960s, probably in 1964, that accelerated the rate of movement on a number of faults. Both the tide gauge and benchmark records show other vertical movement which appears to be related to individual faults before and after the 1960s regional event.

Aggradation versus Subsidence

During the early twentieth century, much of the movement of growth faults within the Upper Deltaic Plain appears to have been masked by aggradation resulting from river derived sediment deposition and accumulation of organic materials. Since the 1960s, surface traces of faults have become progressively more evident. This appears to be due largely to increased subsidence, but reduction of sediment supply and general breakdown of processes of accretion are also contributing factors.

Table 8. Correlation of Re-Leveled Benchmarks that Exhibit Changes in Rates of Relative Sea Level Rise Between Epoch 1 and 2 with Fault Zones and Segments. Rates of Relative Sea Level Rise for Epoch 2 Are Also Listed.

Benchmark (BM)	Fault	Epoch 2, RSL Rise
NASA-Michoud	VI Lake Sand/Thibodaux and/or Lake Borgne	0.036 ft/yr (1.10 cm/yr)
NASA-Michoud	VI Lake Sand/Thibodaux and/or Lake Borgne	0.034 ft/yr (1.04 cm/yr)
NASA-Michoud	VI Lake Sand/Thibodaux and/or Lake Borgne	0.042 ft/yr (1.25 cm/yr)
Valentine, B. Lafourche	VIII Lake Hatch	0.008 ft/yr (0.24 cm/yr)
Valentine, B. Lafourche	VIII Lake Hatch	0.018 ft/yr (0.55 cm/yr)
Miss. R. BM Line, at Chalmette	Lake Borgne	0.147 ft/yr (4.48 cm/yr)
Miss. R. BM Line, near Bertrandville	VII Lake Salvador VIII Lake Hatch (B. des la Fleur)	0.096 ft/yr (2.93 cm/yr)
Miss. R. BM Line, at Pt a la Hache	VIII Lake Hatch (Diamond)	0.183 ft/yr (5.58 cm/yr)
Miss. R. BM Line, S. of Pt Sulphur	N. of XII Golden Meadow	0.121 ft/yr (3.69 cm/yr)
Miss. R. BM Line, Empire	XII Golden Meadow (Empire)	0.084 ft/yr (2.56 cm/yr)
Miss. R. BM Line	XII Golden Meadow (Bastian Bay)	0.087 ft/yr (2.65 cm/yr)

Other Processes Contributing to Land Loss and Coastal Erosion

Negative feedback resulting from subsidence causes hydrological and water chemistry changes, which in turn accelerate wetland deterioration, land loss and erosion. Subsidence, whether due to compaction, faulting, or fluid withdrawal undermines the foundation of coastal lowlands by lowering land elevations, and thus, exposing wetlands, ridges, barrier islands and human infrastructures to the forces of the Gulf of Mexico that erode away the land.

Reduction of Overbank Flow and Sediment Supply

Construction of flood protection levees along the Mississippi River and closure of distributary channels have cut off virtually all over-bank flow into the estuarine basins of the deltaic plain (Gagliano et al. 1971, Gagliano and van Beek 1976, Reed 1995). The amount of sediment transported by the Mississippi River has decreased by 50 percent since 1953, due, primarily, to construction of five large dams on the upper Missouri River (Meade and Parker 1985). This in turn has reduced the river's capacity to fill the holes resulting from subsidence. Much of the land loss in the active Mississippi Delta can be attributed to this change.

Reduction of Organic Matter Build-up and Deterioration of Floating Marshes

Some swamp and marsh plants can adjust to subsidence and resulting increase in hydroperiod by elevating their root zone. This occurs where peat and other deposits accumulate and the plants maintain their position relative to the water level by constantly sprouting and seeding on the top of the accumulating deposits, or in the case of cypress trees, by sending out new lateral root networks. As long as subsidence rates do not exceed accretion rates of the swamp and marsh floor, the living surface survives. However, in many areas subsidence rates have exceeded aggradation rates (Nyman et al. 1990, Reed 1995).

Floating marshes represent another way in which vegetation responds to subsidence. By producing and maintaining a floating root mat, marsh plants are able to maintain their position relative to water level independent of the elevation of the firm substrate. Floating marshes require freshwater conditions, a firm skeletal framework (natural levees, cheniers, spoil banks, lake rims, etc.) and low water energy conditions (velocity, movements, etc.). Alteration of required conditions results in extensive breakup and loss of floating marsh mats (Sasser 1994).

Penland et al. (1988) compared rates of sediment accumulation with subsidence rates in the Terrebonne Basin (Terrebonne Deltaic Plain). They concluded that, "...wetland sedimentation rates lag behind the rates of RSL rise in Terrebonne Parish" (Figure 85). The relationship between wetland sedimentation and RSL rise controls deltaic plain land loss. When sedimentation rates exceed sea level rise rates, the delta plain aggrades and maintains its subaerial integrity. When sedimentation rates fall below sea level rise rates, land loss ensues. The mean modern (0 - 50 YBP) RSL rise rate of 4.20 ft/century (1.28 m/century) (based on the average rate recorded at the Houma USACE tide gauge station) exceeds the mean sedimentation rate for the Terrebonne coastal region of 0.0276 ft/yr (0.07cm/yr). Under these conditions, which have existed since the early 1960s, sedimentation cannot maintain the Terrebonne deltaic plain. The mean subsidence rate of 0.0048 ft/yr (0.012cm/yr) for 0 - 500 YBP, calculated from the radiocarbon data, indicates that wetland sedimentation rates were previously capable of maintaining the stability of the delta plain in the Terrebonne area (Penland et al. 1988). For a thorough review of the accretion process and its relationship to RSL rise, the reader is referred to Reed (1995).

Of the variety of damaging forces, marine tidal invasion and storms are responsible for removing a vast area of Louisiana's vulnerable coastal lowlands. Navigation canals such as the Gulf Intracoastal Waterway, the Mississippi River Gulf Outlet, and the Houma Navigation Canal, along with canals dredged for oil and gas extraction and transport have all disrupted hydrology, resulted in saltwater intrusion to fresh marshes, and caused extensive land loss through marine invasion of fresh marshes of the deltaic plain. Storms cause land loss not only because of the tremendous forces that they can wield on fragile wetlands, but also because the natural systems that once protected against extensive storm damage are presently in a state of near collapse. The protection offered by barrier islands is disappearing as the islands themselves disappear. The weakened condition of wetlands cannot stand up to, or recover from, intense storms and the storms accelerate

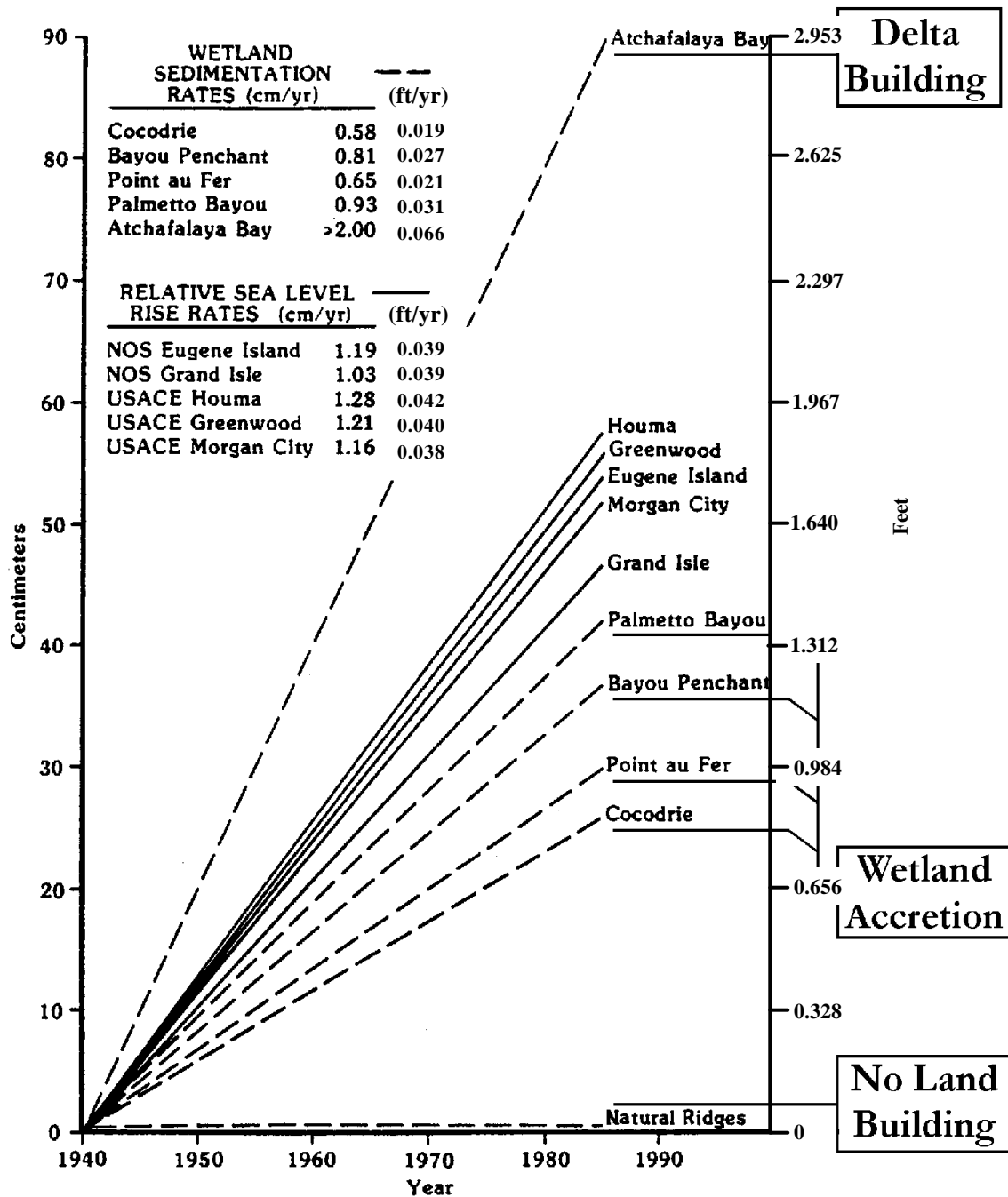


Figure 85. Comparison of RSL rise rates and wetland sedimentation rates for the Terrebonne Deltaic Plain area. Only in the Atchafalaya River Delta was land building up at rates higher than RSL rise. Wetland sedimentation rates are from DuLaune et al. (1985), and RSL rise rates are based on records from USACE and NGS tide gauges (adapted from Penland et al. 1988).

tidal intrusion, furthering tidal induced loss. In addition to inundation of the land by water, all the forces that cause land loss are exacerbated by the reduction of land elevation due to RSL rise.

Herbivory, the loss of marsh plants due particularly to intensive grazing by muskrat (*Ondatra zibethicus rivalicium*) and nutria (*Myocastor coypus*) and dredge and fill activities are also responsible for continued losses.

EFFECTS OF FAULTS

Fault movements alter both natural and manmade surface features in many ways. The following sections summarize findings regarding: 1) the effects of faulting on coastal lowlands including formation of brown marsh areas associated with saline marsh dieback, 2) reduction of elevation of barrier islands, ridges and fastlands, 3) overall land loss by fault zones, 4) relative fault hazard by zone and 5) the consideration of faults in coastal restoration and infrastructure project planning and implementation. The following discussion outlines where fault induced land loss has the strongest effects and what landforms are most severely impacted.

Effects on Wetlands

The areas of highest land loss in the Mississippi Deltaic Plain, almost all of which involve wetland loss, occur south of the Lake Hatch Fault Zone and appear to be associated with fault-related subsidence. Coastal wetlands are affected in several ways by fault movement. First, fault-related subsidence may change the slope over a broad area of fault deformation, which in turn changes the hydroperiod. Second, the invasion of higher salinity water and related sulfide formation kills the fresh and intermediate vegetation of which the living root mat is a part. In some instances, the fresh and intermediate plants are replaced by more salt-tolerant, species. Salt-tolerant plants, such as *Spartina alterniflora*, can only successfully colonize areas of mineral soils or firm peat substrate. Consequently, fresh floating marsh and fresh marsh with poorly consolidated organic substrate do not make the transition to brackish and saline marsh, but instead revert to unvegetated mud flats or open water. Third, if the skeletal framework of natural levee ridges and lake rims that hold the fresh and intermediate marsh together is reduced in elevation and breached by a fault event, a tidal pumping process quickly removes the fluid and semi-fluid soils and barren mudflats, where the freshwater plants have been killed by salt water, converting the marsh to ponds, lakes, and bays. The problem is exacerbated locally by canal networks, which accelerate marine tidal invasion.

All land surfaces are subject to reduction in elevation resulting from the combined effects of sea level rise and subsidence. But fault effects on vegetation in floating marshes are complex (Figures 86 and 87). Locally, rims may be left around eroding lakes and bays, but there are presently only a few small areas remaining in southeastern Louisiana where natural levee ridges are aggrading, such as in the lower Atchafalaya Delta. When the vertical dimension between the living root mat and the mineral sediment substrate becomes large, as is the case where a thick fluid or semi-fluid layer forms beneath the root mat, the mat becomes fragile and vulnerable to rupture and breakup during storm events and/or canal dredging.

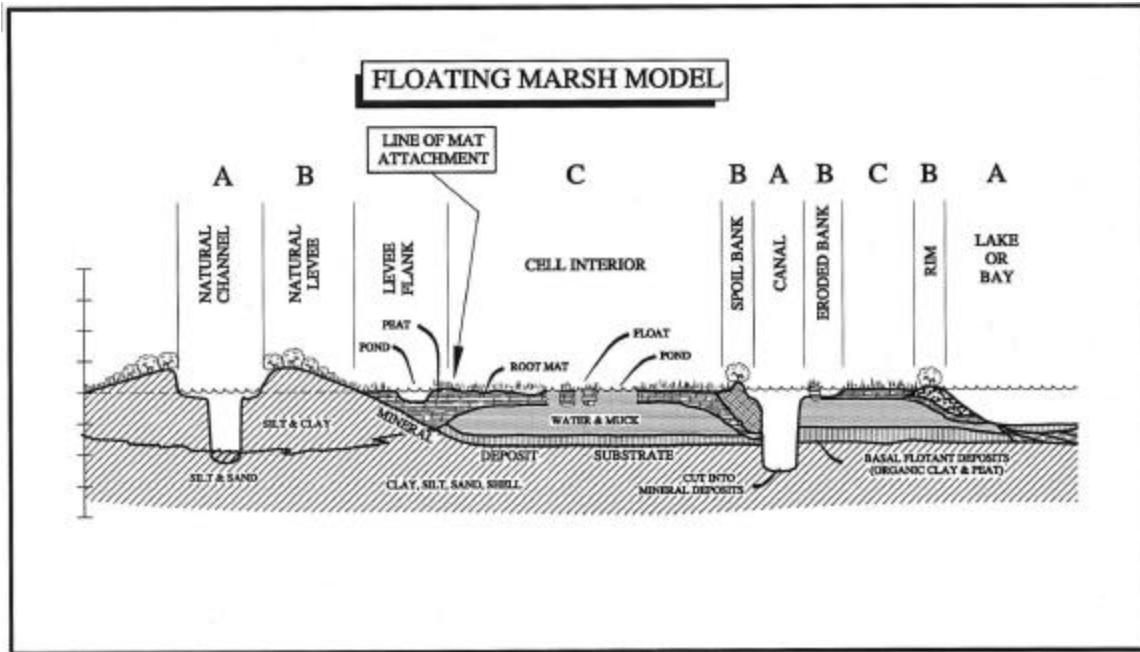


Figure 86. Idealized relationships between sedimentary units and vegetation in fresh marsh. (A - open water, B - ridges and rim and C - interior marsh).

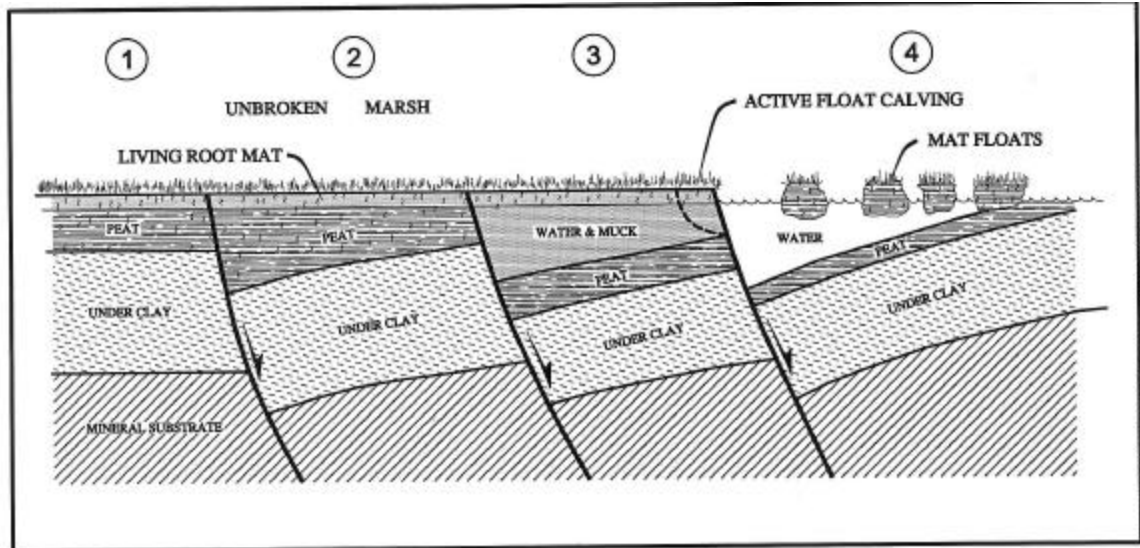


Figure 87. Diagrammatic section showing effects of fault movement on root mat and near-surface deposits.

Fresh and some intermediate marsh surfaces can build up through accretion and accumulation of organic materials and maintain a position above water with or without flotation of the root mat. Saline marsh vegetation, however, does not develop a floating mat and can only survive when directly rooted into a relatively firm substrate composed of mineral sediment or consolidated peat. Salt marsh may sustain a favorable elevation by the addition or accretion of some mineral sediment, usually clays, which may be derived from mudstreams, storm events and/or local erosion. When subsidence exceeds accretion in saltwater marshes, the vegetation dies. This usually occurs in the zone of deformation adjacent to the fault and broadly within interior marshes. Emergent salt marsh vegetation is found rooted on partially submerged natural levee segments, spoil banks and bay/lake rims.

The skeletal framework of the marsh may be ruptured and/or reduced in elevation by fault activity. This causes instability of the root mat and may result in hydrologic and water quality change.

Salt Marsh Dieback (Brown Marsh) and Stages of Fault Development

Severely stressed and broken saline marsh dominated by *Spartina alterniflora* was found at two of the case study sites on down-dropped fault blocks (Bayou Long and Lake Enfermer, (Figure 88). In addition, a brown marsh stage of dieback was identified on old aerial photographs on the down-dropped blocks of the Lower Madison Bay, Empire, and Bastian Bay Faults. Eyewitnesses confirm that the marsh condition recorded on the aerial photographs fits the definition of saline marsh dieback. The dieback stage precedes the appearance of open water on the down-dropped block. Results of this study raise the possibility that brine and gas may be introduced under the root mat, causing or contributing to mortality of the marsh grass.

Fault events were found to progress through stages and associated breakup areas exhibit sequential change in response to these stages (Figure 89). These stages include: 1) pre-fault event conditions, 2) wetland change, often including a “brown marsh” condition, 3) appearance of trace or scarp and 4) post-fault event changes related to secondary effects, which include hydrologic alterations of the tidal prism and the introduction of increased salinity into an unstable or incompatible plant community. Once the fault occurs, the existing plant community on the affected area of the downthrown block may become completely submerged, deteriorate, die, or adjust to the new elevation, slope and hydrology of the altered landscape. Faults usually become dormant and conditions in the breakup area stabilize; however, breakup may continue as a result of secondary effects.

Effects on Barrier Islands

Geomorphological evidence indicates that subsidence may be a major cause of barrier island deterioration along the Louisiana coast. With a limited sand budget, a reduction in the base level of the islands as a result of fault movement may initiate and accelerate deterioration. Estimates of the total area of the barrier islands around the perimeter of

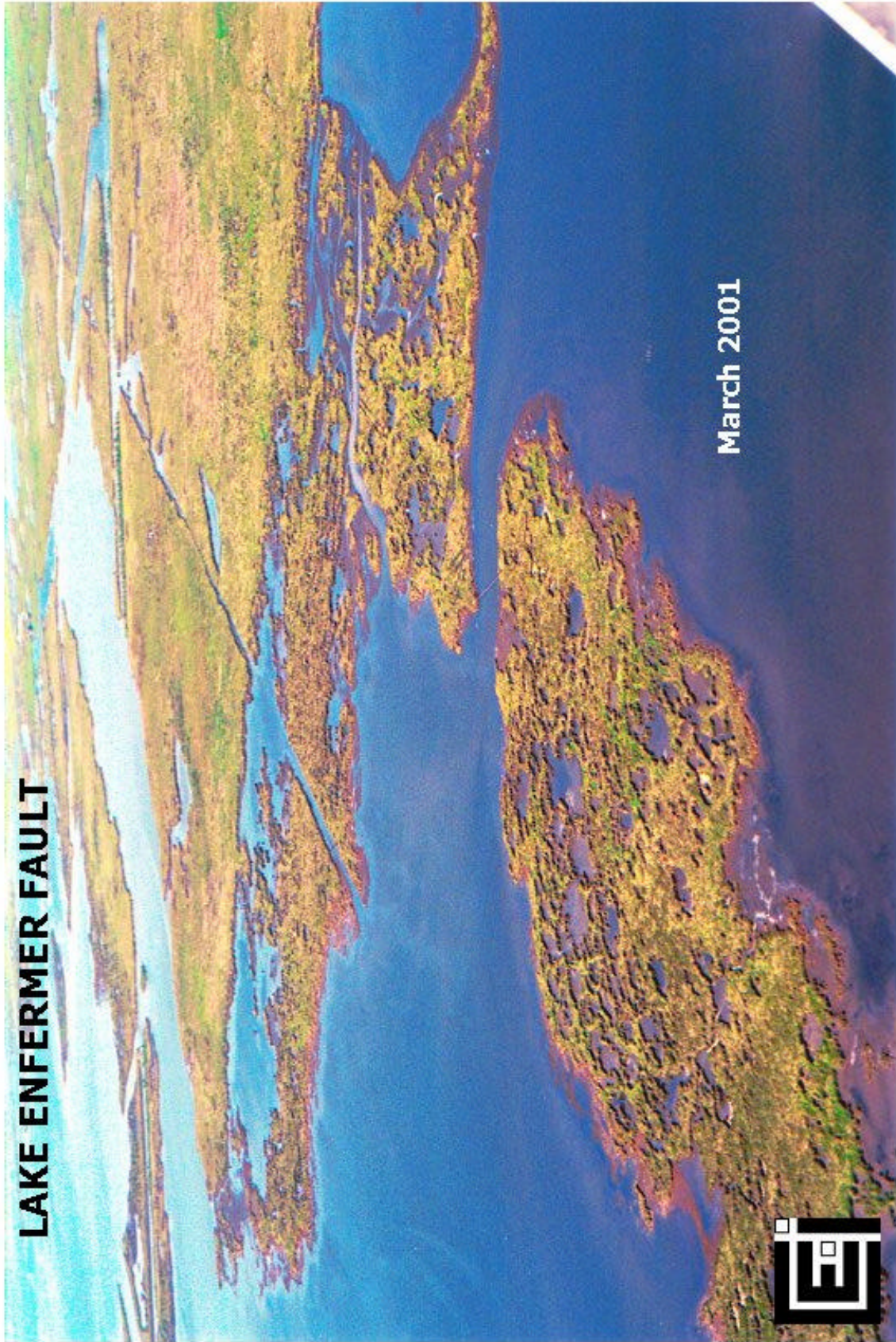


Figure 88. Aerial view of proposed Lake Enfermer Fault (BA - 15), looking north showing brown marsh on the down-dropped block. The distinctive fault scarp separates unbroken *Spartina alterniflora* marsh from partially submerged and broken *Spartina alterniflora* marsh (brown marsh). Photograph by S.M. Gagliano, March 2001.

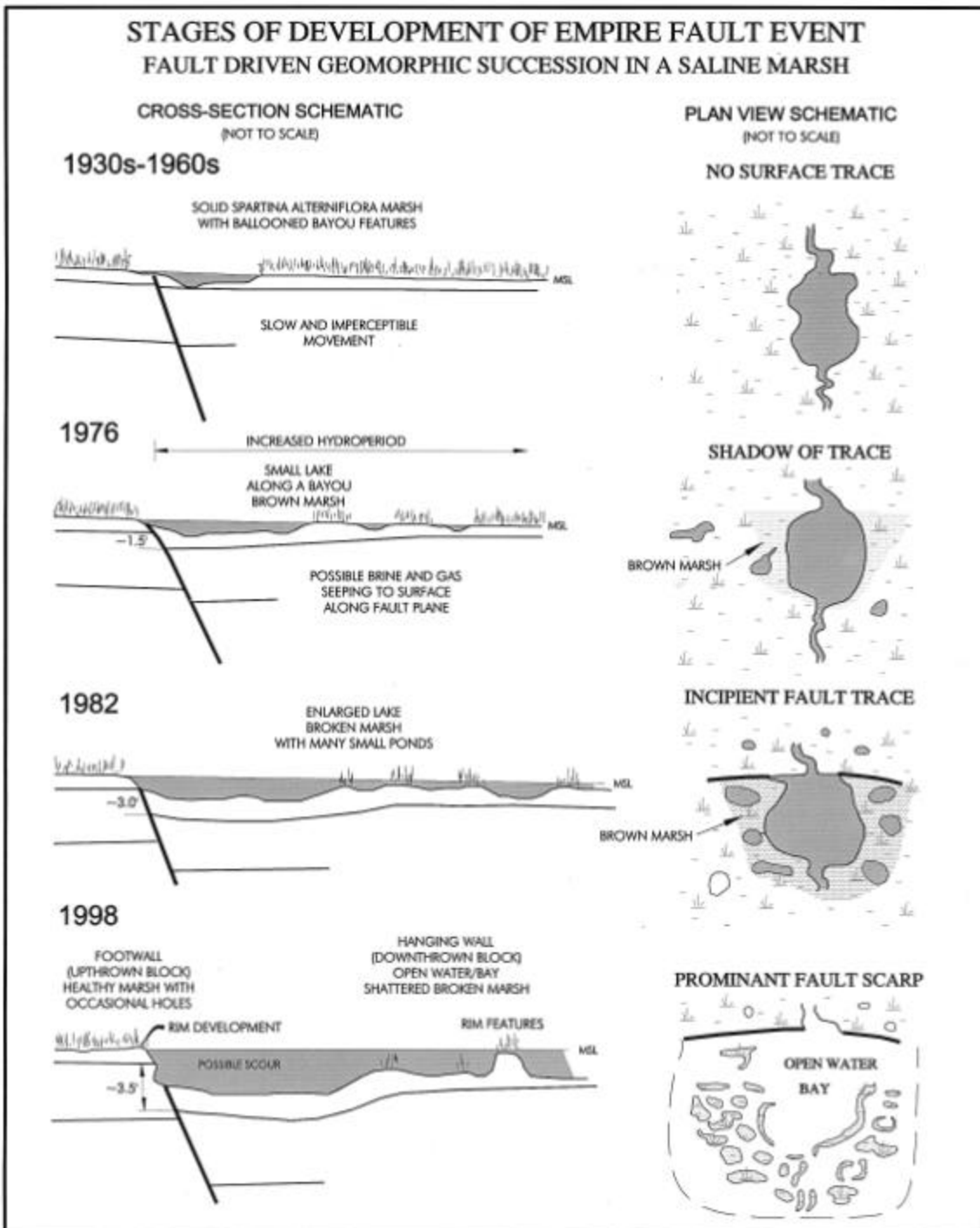


Figure 89. Stages of fault event in a saline marsh.

the deltaic plain have been made for five time intervals from pre-1890 through 1988 (Williams et al. 1992). These data show a stepped reduction in size through time punctuated by intervals of sharp reduction. The intervals of rapid reduction in size

correspond to the intervals of fault movement as determined in the present study. It should also be noted that the Chandelier Islands cross an eastern extension of the Baton Rouge Fault Zone. North of this fault line the islands have been relatively stable and sand washes back onto the beaches after hurricane impacts. South of the fault line the islands are deteriorating more rapidly and have progressively shifted toward the west (McBride and Byrnes 1997).

We have also found that complex sand beaches with multiple ridges and spits may form while still attached to distributary headlands. Fault events, as in the cases of Bastian Bay and Lake Pelto, may cause submergence of part of the headland, leaving the beach complex separated from the mainland as a barrier island.

Effects on Ridges and Fastlands

Ridges only aggrade or build up when they are being formed along the banks of distributaries or as active gulf beaches. Surface elevations of all relict natural levee ridges, relict beach ridges, man-made ridges, embankments, levees and fastlands become lower through time in response to fault-related subsidence, compaction and eustatic sea level rise.

By the very nature of the deltaic plain system there is a constant battle between processes that build land seaward (regression) and upward (aggradation) and those that cause submergence and erosion (transgression). These processes are well illustrated in a timeless sequence of drawings published by H. N. Fisk in 1960 (Figure 90). In the top section of the drawings, (Panel A), the distributary channel is shown when it is still receiving river flow with seasonal over-topping of its banks. There is a conspicuous difference between the relative elevation of the natural levee ridge and adjacent estuarine basin swamp and marsh surfaces in the condition where the distributary channel is receiving some river flow and overtopping of its banks during flood. The live oak on the natural levee and the fringing cypress swamp indicate that water conditions on and near the natural levee are predominately fresh. The buried natural levee and peat deposits indicate that aggradation (accretion) in the marsh has been able to keep pace with RSL rise.

Panel B of Figure 90 shows the effects of changing conditions. The channel fill indicates that the distributary has been essentially cut off from flow and sediment from the parent river. Aggradation of the natural levee by over-bank flooding is no longer taking place. The plant root mat is still maintaining its vertical elevation above mean water level (typically 1 to 1.5 ft [0.3 to 0.46 m]), but change in the width of the swamp zone at the expense of the brackish marsh zone indicates increasing saltwater intrusion.

Panel C of Figure 90 depicts a time when subsidence and marine invasion have become the dominant processes. All surface vestiges of the natural levee ridges are below mean water level and the oak and cypress trees, which cannot tolerate salt water, have died.

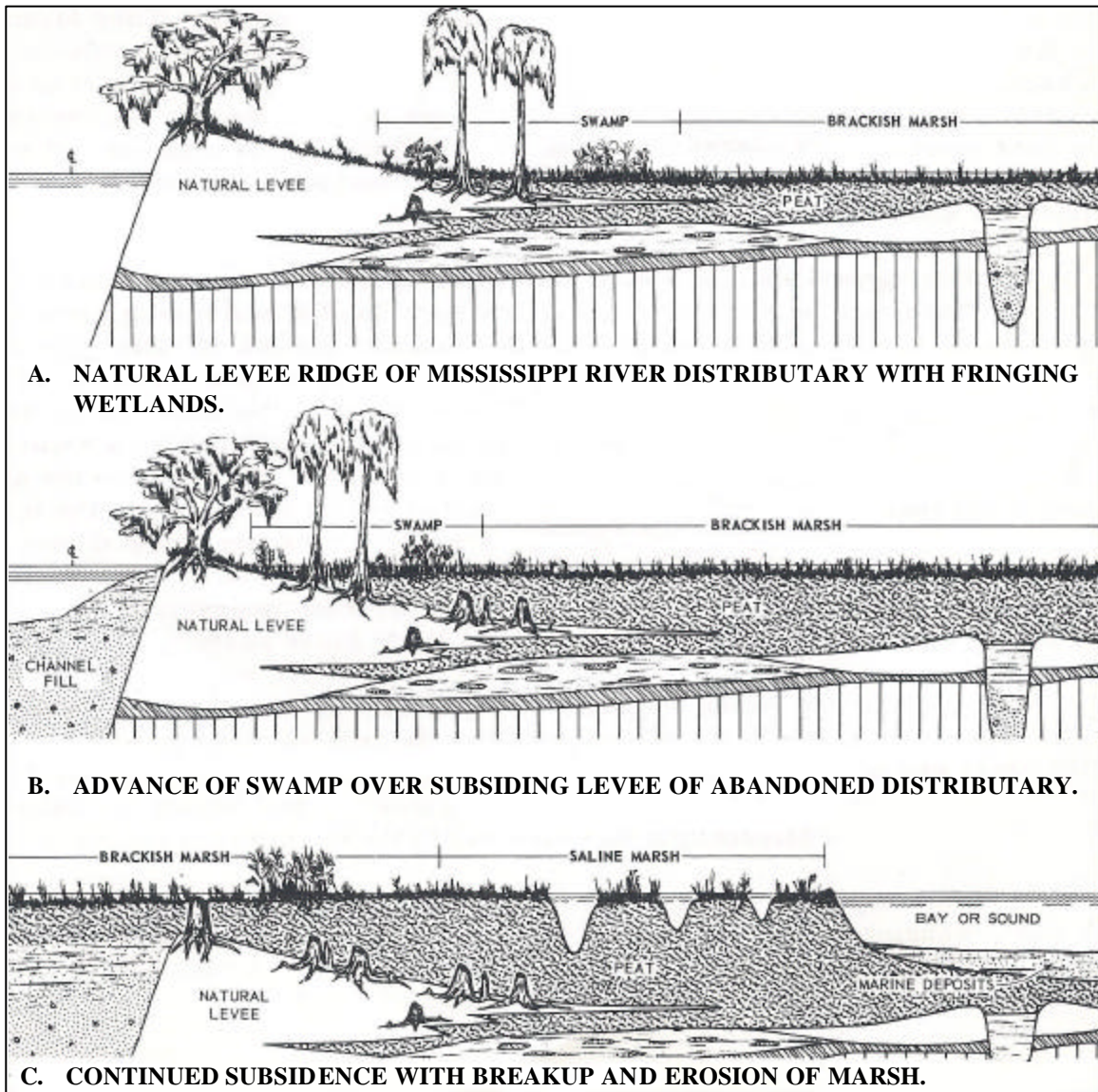


Figure 90. Effects of subsidence on natural levees and wetlands (modified from H.N. Fisk 1960).

The channel has been invaded by marsh and covered by a living root mat of brackish plants. The brackish marsh zone has shifted to a position that was formerly occupied by the channel and the freshwater natural levee and fringing swamp. The former brackish marsh has been replaced by saline marsh, much of which is broken and discontinuous, and by open bay or sound. The upper ends of the estuarine basins in many parts of the deltaic plain are characterized by conditions comparable to those depicted in Panel B of the Figure 90 and conditions in the Lower Deltaic Plain are comparable to those in Panel C.

Flood protection and drainage levees around fastlands prevent aggradation, and as a consequence all fastland areas within the deltaic plain are being reduced in elevation. The problem of reduction of land surface is exacerbated in forced drainage districts within fastlands where drained soils shrink and compact (Figure 91). Fastland levees are

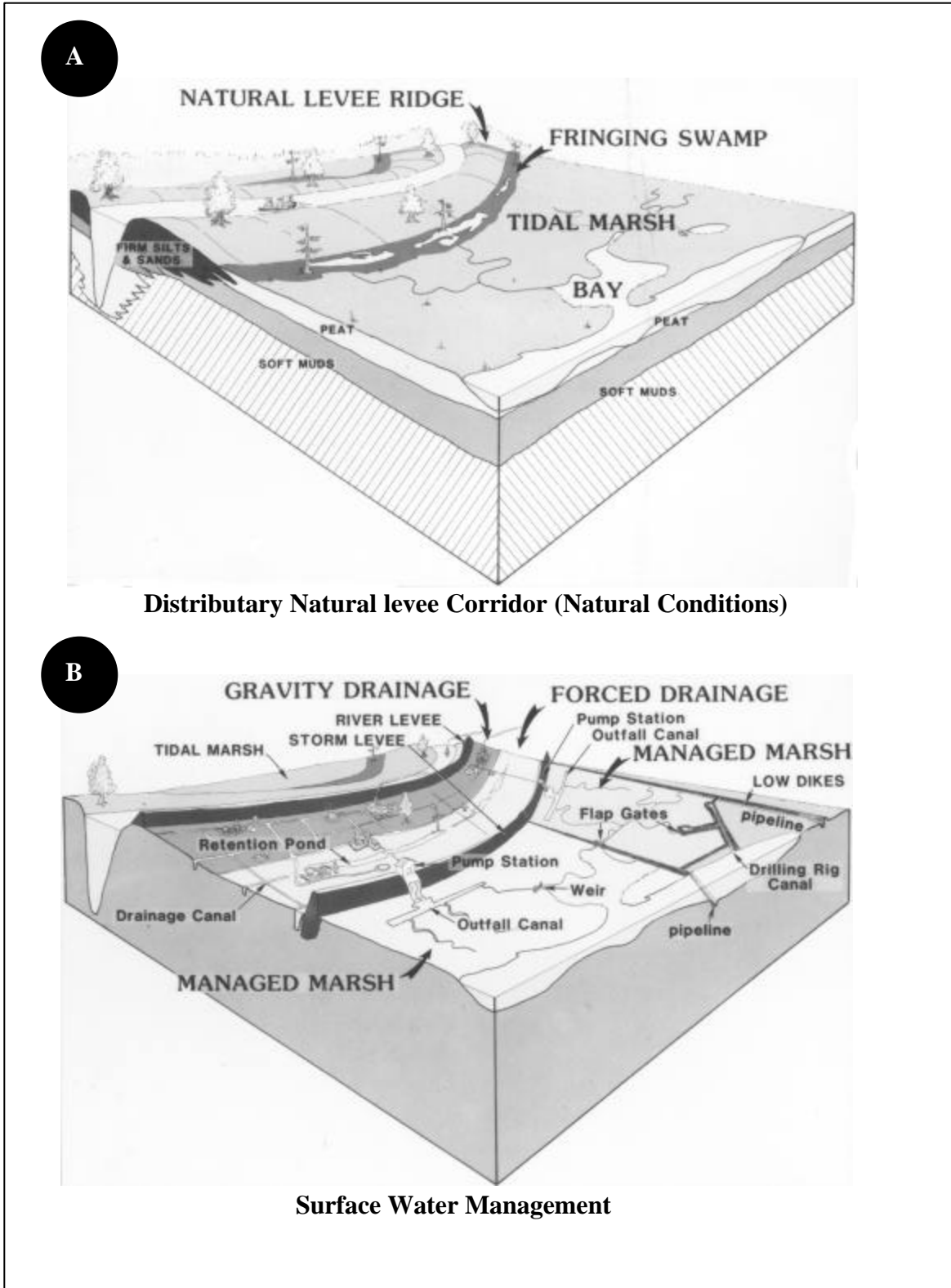


Figure 91. Effects of subsidence on ridgelands and fastlands. A. Distributary natural levee corridor, natural conditions. B. Subsided distributary natural levee corridor with forced drainage and storm protection levees (after Gagliano 1990).

constructed of earth and cannot withstand the marine erosive forces that are approaching many of them. Virtually all infrastructure along the coastal corridors is subject to sinking and erosion. Transcoastal corridors, which cross major fault zones, are critically affected by fault-induced subsidence. These corridors include: 1) the Mississippi River below New Orleans, 2) Bayou Lafourche - LA Hwy 1 and 3) the natural levee ridges and levees south of Houma.

ANALYSIS OF ZONES

The map entitled Southeastern Louisiana Fault Zones (Figure 92) delineates broad zones of related faults and was developed as a tool for analysis of the attributes of faults, for correlation with other processes and data and for evaluating effects on landforms and human infrastructure. Faults and related geological structures grouped by date of initial formation, trends and other characteristics provide the basis for delineation of nine zones identified as "A" through "I."¹⁸ It should be noted that some zones contain more than one fault trend.

Land Loss by Analysis Zones

Land loss data were analyzed for four periods between 1930 and 1990 and plotted on the zone map (Figure 93 and Table 9). The deltaic plain, within Fault Zones A through I, lost approximately 907 sq mi (2349 sq km) of land between 1930 and 1990. Land loss peaked in the Thibodaux, Lake Hatch and Golden Meadow Fault Zones in the 1956/58 – 1974 period. Land loss remained high in the Lake Hatch and Golden Meadow Fault Zones through the 1983-1990 period. Overall, the 60-year land loss rates were lowest for the period 1930-1956/58 and highest during the period 1956/58 – 1974.

The majority of the loss in the entire deltaic plain, 89.3 percent, occurred below the Thibodaux Fault in Zones D through I. Of this loss, 78 percent occurred below the Lake Hatch Fault in Zones E through I. Zone F, which includes the Golden Meadow and Leeville Fault Zones, accounts for 29.9 percent of the total loss.

Time-Rate Correlations

Research and data collection in the deltaic plain have produced a number of twentieth century data sets of rates of process and response change. Comparison of these changes sheds light on process-response relationships. The graphs in Figure 94 compare the following: A. decrease in area of deltaic plain barrier islands, B. land loss in the deltaic plain (1930 – 1990); and C. oil production in Louisiana (1900 – 1993). Tectonic events are also indicated. There are apparent correlations between decreasing area of barrier islands and fault events, land loss rates and fault events. As discussed in a previous

¹⁸ Please note that the term "fault zone" is used in two ways in this report. The band of fault traces associated with individual fault trends is referred to as a fault zone (See Figure 6). Fault zones as delineated on the map shown in Figure 92 are broader bands that may include multiple fault trends grouped on the basis of age and characteristics of the faults.

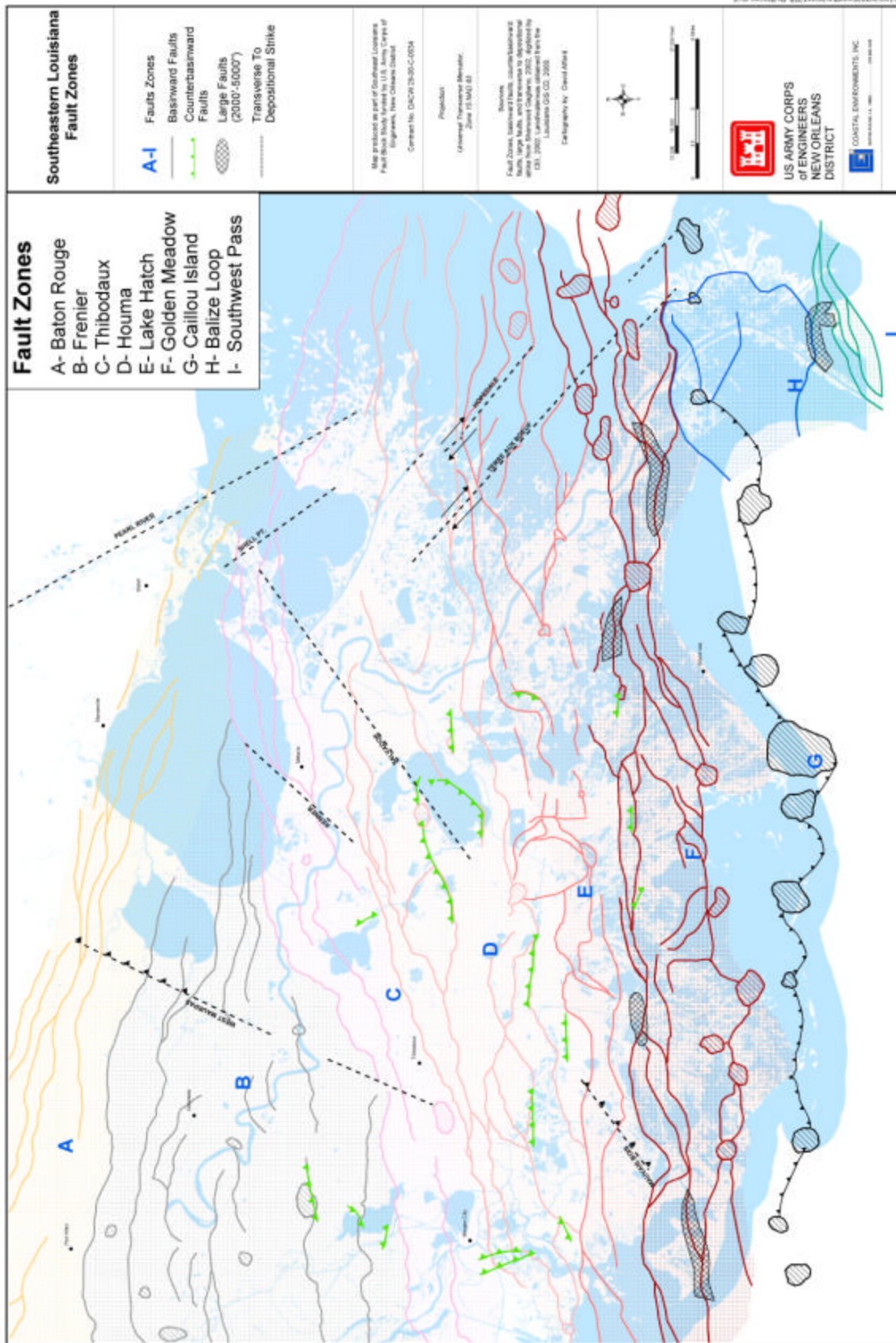


Figure 92. Fault zones in Southeastern Louisiana.

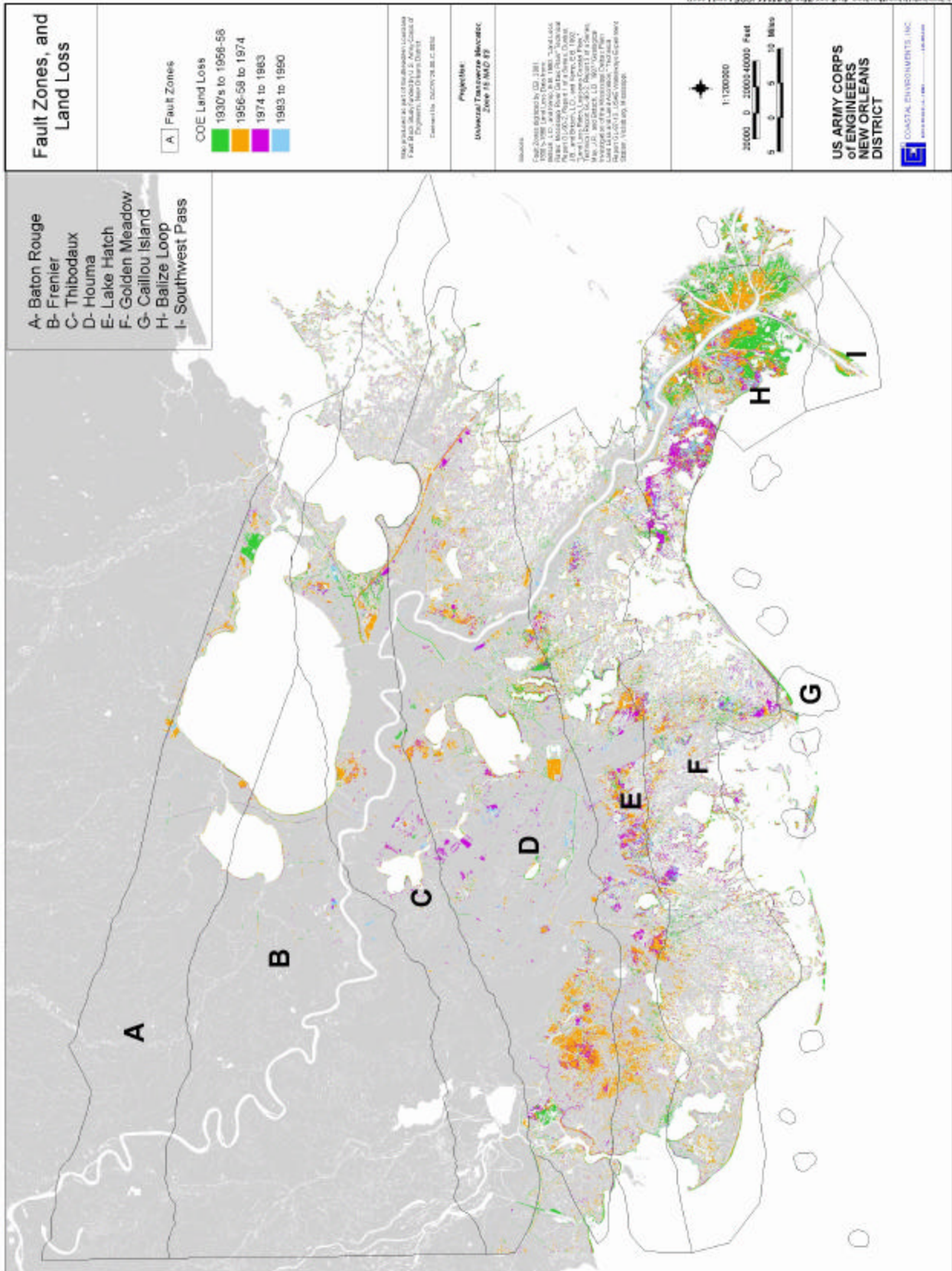


Figure 93. Fault zones and land loss.

Table 9. Area and Rate of Land Loss (sq mi/yr) by Fault Zones: 1930-1956/58, 1956/58-1974, 1974-1983 and 1983-1990 (after Britsch 2001).

Zone	1930-1956/58*		1956/58*-1974		1974-1983		1983-1990		1930-1990	
	Loss (sq mi)	Rate (sq mi/yr)	Loss (sq mi)	Rate (sq mi/yr)	Loss (sq mi)	Rate (sq mi/yr)	Loss (sq mi)	Rate (sq mi/yr)	Loss (sq mi)	Rate (sq mi/yr)
Zone A: Baton Rouge	11.1	0.41	10.0	0.58	3.6	0.40	2.3	0.32	27.0	0.45
Zone B: Frenier	2.1	0.08	2.6	0.15	1.2	0.13	1.2	0.17	7.1	0.12
Zone C: Thibodaux	18.7	0.69	25.3	1.48	12.5	1.38	6.3	0.90	62.8	1.05
Zone D: Houma	39.5	1.46	96.8	5.69	35.7	3.96	21.0	3.00	193.0	3.22
Zone E: Lake Hatch	34.7	1.28	81.8	4.81	40.4	4.48	28.2	4.02	185.0	3.08
Zone F: Golden Meadow	57.8	2.14	90.0	5.29	73.6	8.18	49.4	7.06	270.7	4.51
Zone G: Caillou Island	2.8	0.10	1.8	0.10	0.9	0.10	0.5	0.07	6.2	0.10
Zone H: Balize Loop	54.1	2.00	66.4	3.90	12.4	1.38	16.6	2.37	149.6	2.49
Zone I: Southwest Pass	2.7	0.10	2.1	0.12	0.2	0.02	0.2	0.02	5.2	0.09
Total Loss:	223.6	8.28	376.8	22.16	180.4	20.04	125.6	17.94	906.6	15.11

* Used 1957 to calculate rate of land loss

Bold numbers indicate highest land loss rate per time period and for all time periods.

section, Morton et al. (2002) have also correlated fault movement and land loss rates with oil and gas production in the Terrebonne Delta Plain, and postulate that fluid withdrawal is a major cause of subsidence, and may trigger fault movement.

Effects of Faults on Coastal Projects

An inventory was made of active and approved coastal restoration projects related to the CWPPRA and Louisiana coastal restoration programs (Tables 10 and 11). The locations of the project areas were plotted in reference to the fault zones as defined in this study (Figure 95). As might be expected, the projects cluster in areas of highest land loss and, consequently, are also in areas with the most active suspected fault movement. A higher resolution comparison was made of restoration and levee projects proposed for the Terrebonne deltaic plain area in reference to known faults (Figure 96).

An example of a coastal restoration project designed and constructed without recognition of a potential fault hazard is shown in Figure 97. The purpose of the project is to reduce shoreline erosion on the west side of Bayou Perot. The project consists of a riprap breakwater constructed parallel to the shoreline. The problem is that the breakwater is

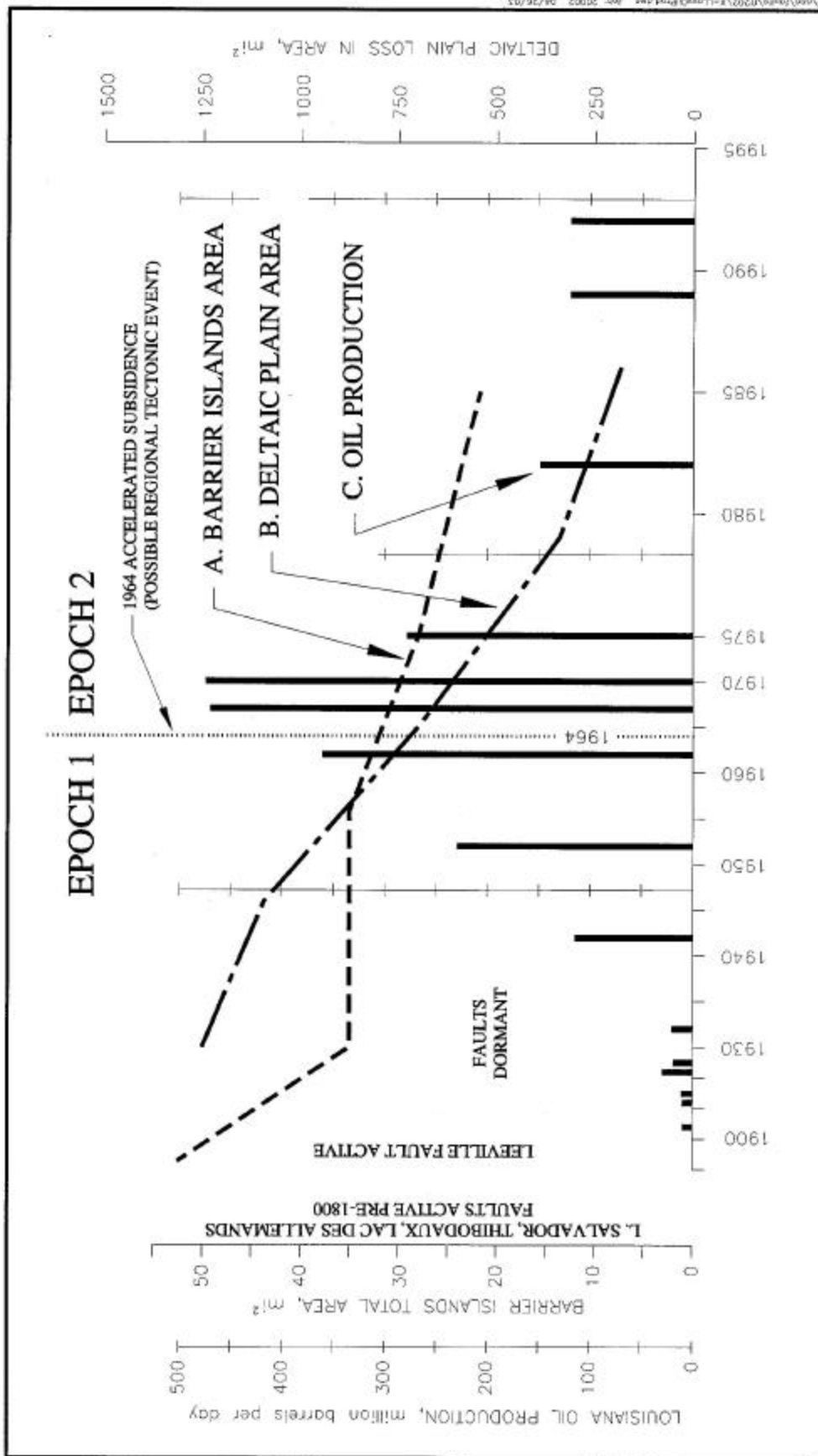


Figure 94. Comparison of rates of change of process indicators for: A. Total area of barrier islands; B. Area of deltaic plain; and, C. Louisiana oil production. The curves suggest possible relationships between fault events and loss of area of both the barrier islands and the deltaic plain. They also show that oil and gas production peaked during Epoch 2, when land loss and subsidence rates accelerated (barrier island measurements adapted from Williams et al. 1992, deltaic plain measurements adapted from Barras et al. 1994).

Table 10. Location of CWPPRA Projects in Relation to Fault Zones.

Map ID	Fed ID	State ID	Project Name	Sponsor	Project Type	Status	Basin	Year	Acres	Zone ID	Zone ID	Zone ID	Zone ID
1	BA-04c	BA-04c	West Pointe a la Hache Outfall Management	NRCS	OM	Active	BA	1993	16297	E			
2	XTE-67, XTE-45, XTE-67b	TE-25, TE-30	East Timbalier Island Restoration Phase 1 & 2	NMFS	BI	Active	TE	1993	754	G			
3	XPO-71	PO-19	MRGO Back Dike Marsh Protection	USACE	MM	No Monit.	PO	1993	880	D			
4	PPO-10	PO-17	Bavou Labranche Marsh Creation	USACE	DM	Active	PO	1991	435	C			
5	XPO-69	PO-22	Bavou Chevee Shoreline Protection	USACE	SP	Active	PO	1995	212	C			
6	TE-17	TE-17	Falgout Canal Plantings (Demo.)	NRCS	VP	Active	TE	1991	4	E			
7	XMR-12b	MR-10	Combination Dustpan and Cutterhead Maintenance Dredging (Demo.)	USACE	DM	No Date	MR	1996	4010	H			
8	FMR-03	MR-03	West Bay Sediment Diversion	USACE	SD	On Hold	MR	1991	12294	H			
9	PTE-27	TE-23	West Belle Pass Headland	USACE	DM/SP	Active	TE	1992	158	F			
10	XPO-52b, XPO-52a	PO-18, PO-16	Bayou Sauvage Refuge Restoration Phase 1 & 2	USFWS	HR	Active	PO	1992, 1991	10543	C			
11	TE-07f	TE-32	Introduction and Hydrologic Management Alternative B	USFWS	FD/HR	No Date	TE	1996	7848	E			
12	BA-15	BA-15	Lake Salvador Shore Protection (Demo.) Phase 1 & 2	NMFS	SP	Active	BA	1993	116	D			
13	XPO-74a	PO-25	Bayou Bienvenue Pump Station Diversion and Terracing	NMFS	HR/MC	No Date	PO	1998	2712	C			
14	PBS-01	BS-09	Upper Oak River Freshwater Siphon	NRCS	FD	No Date	BS	1998	4514	D			
15	PPO-38	PO-24	Hopedale Hydrologic Restoration	NMFS	HR	Active	PO	1998	4494	D			
16	PAT-02	AT-02	Atchafalaya Sediment Delivery	NMFS	SD/DM/MC	Active	AT	1992	2182	E			
17	BS-03a	BS-03a	Caernarvon Outfall Management	NRCS	OM	Active	BS	1992	19344	D			
18	PO-06	PO-06	Fritchie Marsh Restoration	NRCS	HR	Active	PO	1992	6217	A			
19	XAT-11	AT-04	Castille Pass Sediment Delivery	NMFS	MC/SNT	No Date	AT	1999	4791	E	F		
20	XPO-55a	PO-26	Opportunistic Use of Bonnet Carre Spillway	USACE	FD	No Date	PO	1999	14519	B	C		
21	PPO-07a	PO-28	La Branche Wetlands Terracing/Plantings	NMFS	SNT/SP/VP	No Date	PO	1999	4455	C			
22	PTE23, PTE-26a	TE-26	Lake Chapeau Sediment Input and Hydrologic Restoration	NMFS	HR/MC	Active	TE	1993	13827	F			
23	XAT-07	AT-03	Big Island Mining (Increment 1)	NMFS	SD/DM/MC	Active	AT	1992	2706	E			
24	BA-34	BA-34	Diversion to NW Barataria Basin	EPA	NA	No Date	BA	2000	5133	C			
25	TE-45	TE-45	Protection/Oyster Reef Demo. Project	USFWS	NA	No Date	TE	2000	3813	F			
26	BS-11	BS-11	Delta Management at Fort St Phillip	USFWS	NA	No Date	BS	2000	1351	F			
27	BS-10	BS-10	Delta Building at Fort St Phillip	USACE	NA	No Date	BS	2000	6826	F			
28	PMR-10	MR-09	Delta-Wide Crevasses	NMFS	SD	Active	MR	1996	66862	F	G	H	I
29	XMR-10	MR-06	Channel Armor Gap Crevasse	USACE	SD	Active	MR	1993	1566	H			
30	MR-13	MR-13	Bennys Bay	USACE	NA	No Date	MR	2000	24669	F	H		
31	XTE-45a	TE-40	Timbalier Island Dune/Marsh Restoration	EPA	BI/MC	No Date	TE	1999	119	G			
32	TE-18	TE-18	Timbalier Island Plantings (Demo.)	NRCS	VP	Active	TE	1991	2	G			
33	PTE-22, PTE-24	TE-22	Point au Fer Canal Plugs	NMFS	SP/HR	Active	TE	1992	5112	F			
34	PO-29, PO-30	PO-29, PO-30	Shore Protection/Marsh Creation in Lake Borene	EPA	NA	No Date	PO	2000	250	C	D		
35	PTE-26b	TE-28	Bradv Canal Hydrologic Restoration	NRCS	HR	Active	TE	1993	7510	E	F		
36	PTE-28	TE-39	South Lake Decade/Atchafalaya Freshwater Introduction	NRCS	HR	No Date	TE	1999	7343	F			
37	TE-44	TE-44	North Lake Mechant Landbridge	USFWS	NA	No Date	TE	2000	7781	E	F		
38	BA-32a	BA-29	Marsh Creation South of Leesville	EPA	MC	No Date	BA	1999	169	F			

Table 10. Concluded.

Map ID	Fed ID	State ID	Project Name	Sponsor	Project Type	Status	Basin	Year	Acres	Zone ID	Zone ID	Zone ID	Zone ID
39	PBA-35	BA-20	Jonathon Davis Wetland Protection	NRCS	HR/SP	Active	BA	1992	7368	D			
40	PTE-26j	TE-34	Penchant Basin Plan Without Shoreline Stabilization (Increment 1)	NRCS	HR	No Date	TE	1996	153267	D	E	F	
41	XTE-49	TE-10	Grand Bayou/GIWW Freshwater Diversion	USFWS	FD	Active	TE	1995	52833	D	E	F	
42	XTE-DEMC	TE-41	Mandalay Bank Protection Demonstration	USFWS	SP	No Date	TE	1999	512	D			
43	PBA-34i	BA-22	Bayou L'Ours Ridge Hydrologic Restoration Increment 1	NRCS	HR	No Date	BA	1994	26970	E	F		
44	BA-02	BA-02	GIWW To Clovelly Hydrologic Restoration	NRCS	HR	Active	BA	1991	15261	D	E		
45	TE-43	TE-43	GIWW Bank Restoration in Terrebonne	NRCS	NA	No Date	TE	2000	8154	D			
46	PBA-12b	BA-26	Barataria Bay Waterway East Dupre Cut Bank Protection	NRCS	SP	Active	BA	1996	2785	D	E		
47	BA-03c	BA-03c	Naomi Outfall Management	NRCS	OM	Active	BA	1995	24172	D	E		
48	PBA-12a	BA-23	Barataria Bank Waterway West Side Shoreline Protection	NRCS	SP	Active	BA	1994	1914	D	E		
49	PBA-48a	BA-24	Myrtle Grove Siphon	NMFS	FD	Active	BA	1995	16700	D	E		
50	BA-19, XBA-63ii	BA-19, BA-27b	Barataria Bay Waterway Marsh Creation, Barataria Bay Basin	USACE	MC	Active	BA	1991, 1997	2272	D	E	F	
51	XBA-63iii	BA-27c	Barataria Basin Landbridge Shore Protection Phase 3	NRCS	SP	Active	BA	1999	4873	D	E		
52	PBA-20	BA-25	Bayou Lafourche Siphon	EPA	FD	No Date	BA/TE	1995	58254	D	E	F	
53	BA-33	BA-33	Delta Building Diversion at Myrtle Grove	USACE	NA	No Date	BA	2000	423861	D	E	F	
54	XBA-01a	BA-30	East/West Grand Terre Islands Restoration	NMFS	BI/MC	No Date	BA	1999	1477	F			
55	XBA-01a-i	BA-28	Vegetative Planting of Grand Terre Island	NMFS	VP	Active	BA	1997	248	F			

BI	Barrier Island Restoration	OM	Outfall Management
DM	Beneficial Use of Dredged Material	NA	Not Applicable
FD	Freshwater Diversion	SD	Sediment Diversion
HR	Hydrological Restoration	SNT	Sediment and Nutrient Trapping
MC	Marsh Creation	SP	Shoreline Protection
MM	Marsh Management	VP	Vegetation Planting

located on the down-dropped block of an apparent active fault. The fault is a segment of the Lake Hatch Fault (See BA-5 and BA-19 in Figure 43). The fault appears to be active and is overlain by floating marsh. It is unlikely that the breakwater will be effective and it may become stranded in open water as the downthrown fault block becomes submerged. If this occurs the rocks may become a navigation hazard.

LAND LOSS ON LARGE FAULT BOUND BLOCKS

Figure 98 shows land loss on seven large fault-bound blocks in the deltaic plain for the period from 1930 through 1995. Block A falls within the Balize Depression and Block B is coincident with the Pelto Horst. Blocks C - F collectively overlie the Terrebonne Trough and Block G is most influenced by the Lake Hatch Fault Zone.

Table 11. Location of State Projects in Relation to Fault Zones.

Map ID	State ID	Project Name	Sponsor	Project Type	Status	Basin	Year	Acres	Zone ID	Zone ID
56	PO-15	Alligator Point Marsh Protection	DNR	DM	On Hold	PO	1991	11463	A	C
57	BA-05c	Baie de Chactas	DNR	SP	Active	BA	1991	409	D	
58	PO-02c	Bayou Chevee Wetland	DNR	SP	Active	PO	1990	1598	C	
59	BS-05	Bayou Lamoque Div. Outfall Mgt.	DNR	FD	On Hold	BS	1990	6488	E	
60	TE-08	Bayou Pelton Wetland	DNR	HR	On Hold	TE	1990	1236	E	
61	BS-01	Bohemia Div. Structure	DNR	FD	On Hold	BS	1990	5866	E	
62	PO-04	Bonnet Carre Freshwater Div.	DNR	FD	No Date	PO	NA	6898	C	
63	TE-09	Bully Camp Marsh Mgt.	DNR	MM	On Hold	TE	1991	701	E	
64	BS-03b	Caernarvon Div. Outfall	DNR	FD	On Hold	BS	1990	18155	D	
65	PO-08	Central Wetlands Pump Outfall	DNR	FD	Active	PO	1990	5762	C	
66	BA-17a, BA-17b	City Price - Happy Jack; Homeplace	DNR	FD	On Hold	BA	1991	8278	E	F
67	BA-07	Couba Island	DNR	SP	On Hold	BA	1990	509	D	
68	PO-11	Cutoff Bayou Marsh Mgt.	DNR	HR	On Hold	PO	1991	3787	C	
69	BA-10c, BA-10c	Davis Pond Div. Outfall Mgt.	DNR	FD	On Hold	BA	1991	25388	D	
70	TE-02	Falgout Canal Protection	DNR	MM	Active	TE	1991	7704	D	E
71	TE-21	Falgout Canal S. Wetland Creation	DNR	DM	On Hold	TE	NA	176	E	
72	TE-15	GIWW Levee Planting	DNR	VP	On Hold	TE	1991	58	D	
73	TE-05	Grand Bayou Wetland	DNR	MM	On Hold	TE	1990	26639	D	G
74	TE-07c	Grand Caillou	DNR	HR	On Hold	TE	1990	1787	E	
75	BA-12	Grand/Spanish Pass	DNR	FD	On Hold	BA	1991	5619	F	H
76	PO-14	Green Pt./Goose Point Marsh Rest.	DNR	HR	On Hold	PO	1991	5489	A	
77	BA-13	Hero Canal Div.	DNR	FD	On Hold	BA	1991	8374	D	
78	PO-03b	Labranche Shoreline Protection	DNR	SP	No Monit.	PO	1990	49	C	
79	PO-03a	Labranche Wetland	DNR	MM	On Hold	PO	1991	15736	C	
80	TE-07d, TE-07a	Lake Boudreaux Watershed	DNR	HR	On Hold	TE	1991	48536	D	E
81	BA-08	Lake Cataouatche Shore Protection	DNR	SP	On Hold	BA	1991	167	D	
82	BA-14	Little Lake Marsh Mgt.	DNR	MM	On Hold	BA	1991	3189	D	E
83	TE-07b	Lower Petit Caillou	DNR	HR	Active	TE	1990	3466	E	F
84	TE-01	Montegut Wetland	DNR	MM	Active	TE	1990	4122	E	
85	BA-03	Naomi (Lareussite) Freshwater Div. Siphon	DNR	FD	Active	BA	1990	13131	D	E
86	PO-07	North Shore Wetland	DNR	SNT	On Hold	PO	1990	3571	A	
87	MR-02a	Pass a Loutre Sediment Fence	DNR	SNT	On Hold	MR	1991	1180	H	
88	MR-05	Pass a Loutre Sediment Mining	DNR	SD	On Hold	MR	1993	134	H	
89	TE-14	Point Farm Refuge Planting	DNR	VP	Active	TE	1991	89	E	
90	TE-06	Point au Chien	DNR	MM	On Hold	TE	1990	4765	E	
91	BA-05b	Queen Bess	DNR	DM	Active	BA	1991	32	F	
92	BA-09	Salvador WMA Gulf Canal	DNR	SP/VP	On Hold	BA	1991	432	D	
93	BA-16	Segnette Wetland Protection	DNR	SP	Active	BA	1992	1374	D	
94	MR-01	Small Sediment Div.	DNR	SD	Active	MR	1990	4	F	H
95	TE-16	St. Louis Canal Wetland Rest.	DNR	DM	On Hold	TE	1991	45	D	
96	PO-13	Tangipahoa/Pontchartrain Shore Protection	DNR	SP	On Hold	PO	1991	578	A	
97	MR-04	Tiger Pass Creation	DNR	DM	On Hold	MR	1992	1001	H	
98	BA-11	Tiger/Red Pass Div. and Outfall Mgt.	DNR	FD	On Hold	BA	1991	1550	H	
99	PO-10	Turtle Cove Shore Protection	DNR	SP	Active	PO	1992	513	A	
100	BA-06	US 90 to GIWW	DNR	HR	On Hold	BA	1993	72392	D	
101	TE-03	Upper Bayou La Cache Wetland Protection	DNR	MM	Active	TE	1991	5044	E	F
102	PO-01	Violet Div. Siphon	DNR	FD	Active	PO	1990	1264	C	D
103	BS-06	Violet Freshwater Distribution	DNR	FD	No Monit.	BS	NA	3113	D	
104	PO-12	West Labranche Wetland Mgt.	DNR	MM	On Hold	PO	1991	4796	C	
105	BA-04	West Pointe a la Hache	DNR	FD	Active	BA	1990	16297	E	

- | | | | |
|----|------------------------------------|-----|--------------------------------|
| BI | Barrier Island Restoration | OM | Outfall Management |
| DM | Beneficial Use of Dredged Material | NA | Not Applicable |
| FD | Freshwater Diversion | SD | Sediment Diversion |
| HR | Hydrological Restoration | SNT | Sediment and Nutrient Trapping |
| MC | Marsh Creation | SP | Shoreline Protection |
| MM | Marsh Management | VP | Vegetation Planting |

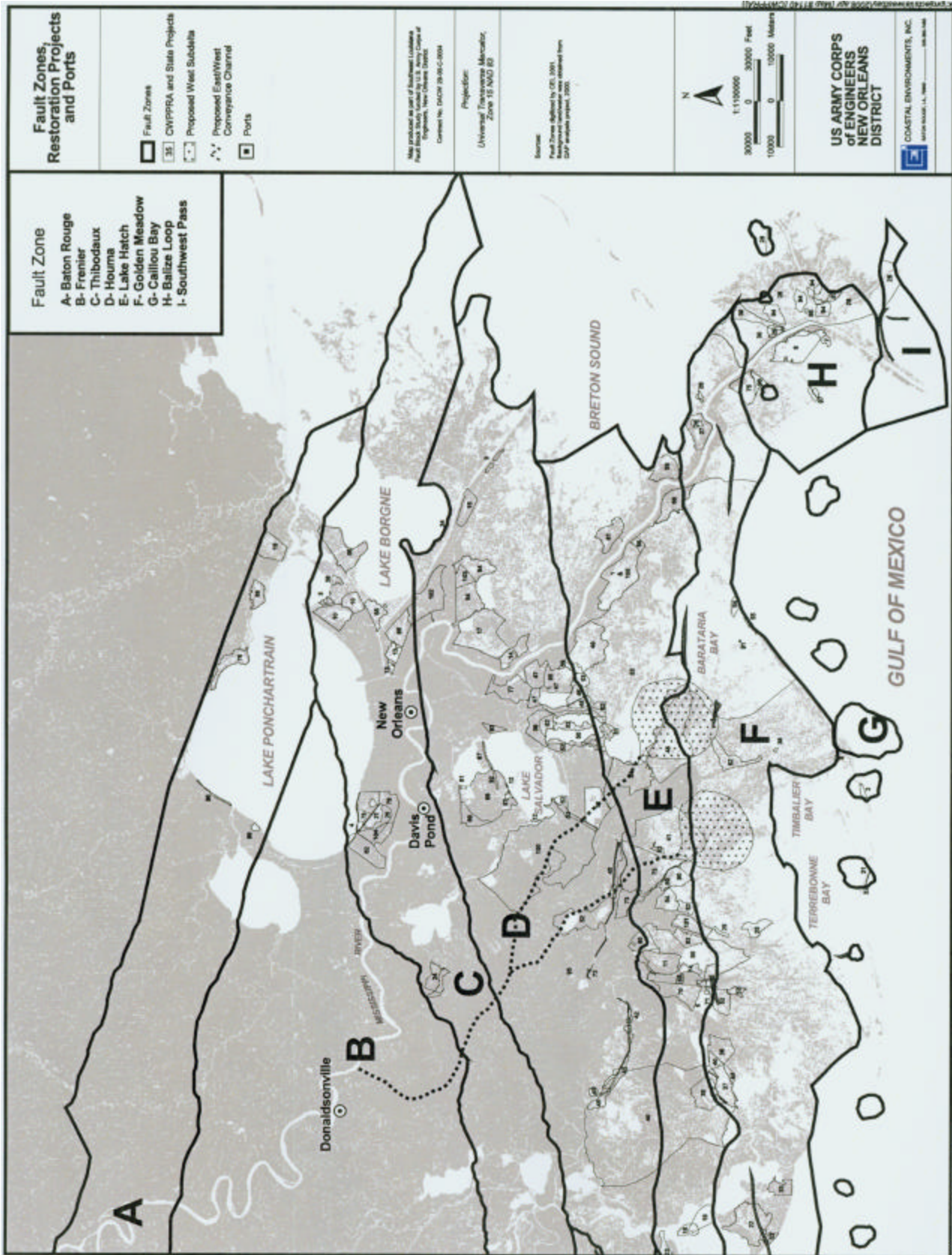


Figure 95. Map showing coastal restoration projects in reference to fault zones.

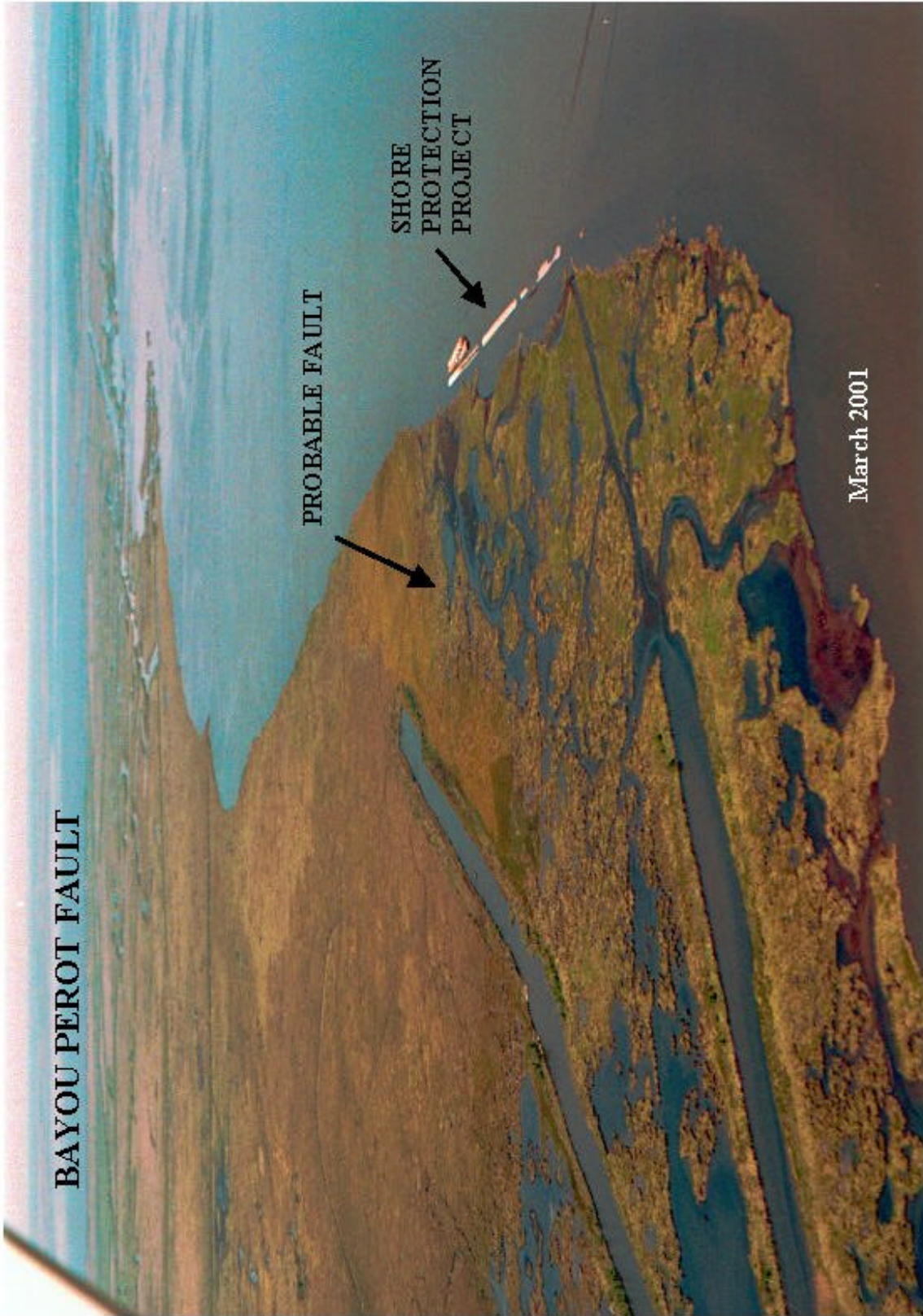


Figure 97. Shore protection feature built across a suspected active fault. Aerial view of proposed Bayou Perot Fault (BA - 5) looking north. On the north of the proposed fault is unbroken, brackish, floating marsh. On the down - dropped block the marsh is stressed and broken. A shore protection feature consisting of rip rap was under construction at the time the photograph was taken. Photograph by S.M. Gagliano March 2001.

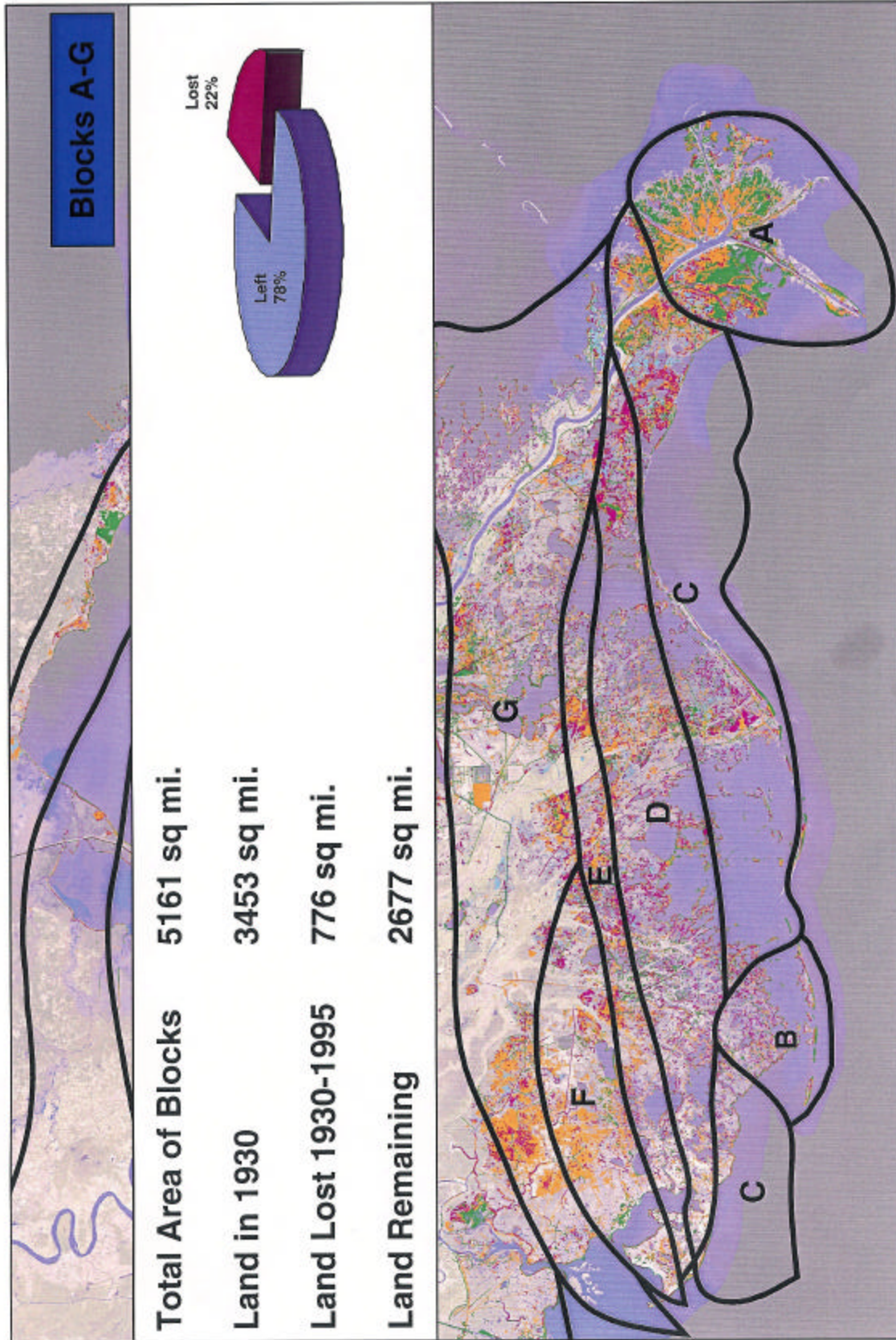


Figure 98. Land loss on mega-fault blocks: 1930 – 1995.

The total area of the blocks (land and water) is 5161 sq mi (13,366 sq km). Of this total, 3437 sq mi (8901 sq km) was land in 1930. By 1995, some 760 sq mi (1968 sq km) had reverted to open water and 2677 sq mi (6933 sq km) remained.¹⁹ The loss in this area accounts for approximately 48 percent of the total land loss in coastal Louisiana and approximately 63 percent of the total loss in the deltaic plain during this interval (see Figure 2). Furthermore, most of this loss has occurred since 1960. This is one measure of the magnitude of the landscape change that has resulted from movement of the major regional faults during modern decades. It should also be noted that the land loss resulting from nineteenth century movement along the Leeville Fault Zone is not included in these totals. The land loss rates in this area remain high, indicating either that the faults remain active and/or the secondary effects of fault movement are still unfolding.

FINDINGS AND RECOMMENDATIONS

Results and findings of the study include the following:

1. Regional faults and zones of faults have been delineated and a framework of faulting has been established to which landform change in Southeastern Louisiana can be linked.
2. Known and suspected surface faults have been correlated to known subsurface faults and related to the regional tectonic framework. Geomorphic signatures have been identified, classified and used to delineate surface faults. Surface indicators of fault activity (vegetation change, leakage of brine water and gas seeps along faults) have been investigated.
3. Evidence of modern, historic and prehistoric fault events along specific fault segments and trends has been presented. Evidence found in this study indicates that the Golden Meadow, Theriot, Leeville and Venice Faults were active throughout the Pleistocene Period and have also been active during prehistoric, historic and modern times.
4. Vertical and lateral movements along faults present geological hazards. Natural and man-made features crossing active faults are subject to short-term movement (up to 3.5 ft [1.07 m] within two years has been documented). Small movements along the Baton Rouge Fault are known to cause cracking of building foundations as well as structural damage to bridges and roads.

¹⁹ There are differences in land loss measurements made in conjunction with the maps shown in Figures 93 and 98. This is attributed largely to the differences in the intervals during which the land loss was measured.

5. Faults also alter slope and may cause submergence of lowlands. The study has further established and evaluated the relationship of faults to local and regional land loss patterns. Small increments of vertical displacement along faults in the low-lying coastal landscape may result in large areas of submergence and land loss.

Findings of the study indicate that submergence of lowlands on the surface of fault-bound blocks is a cause of land loss in the Louisiana Deltaic Plain. To date, the efforts to restore coastal Louisiana have been viewed largely as a fight against edge erosion, a lateral process. In reality, in submerged areas, the bottom is falling out as a result of a vertical process. If the coast is to be stabilized and moved toward a sustainable condition this fundamental difference must be taken into consideration.

6. Data from tide gauge records and re-leveled benchmarks have been analyzed to determine amount, rates and time of occurrence of vertical movement at specific locations, which have been correlated with fault segments and fault zones. Collectively, the data suggest that a major tectonic event occurred in Southeastern Louisiana in the 1960s, probably in 1964, that accelerated the movement on a number of faults. Both the tide gauge and re-leveled benchmark records show other vertical movements, which appear to be related to individual faults before and after the 1960s regional event.
7. Other processes that may contribute to subsidence and land loss include compaction, dewatering and fluid withdrawal. When oil, gas and produced water are removed localized subsidence and fault movement may occur. Geological fault movement, compaction and fluid withdrawal are inter-related processes contributing to subsidence. Compaction, consolidation and diagenesis of Holocene sediments also contribute to the overall subsidence rate. Adjustments to vertical changes resulting from these processes appear to take place along fault lines.
8. Faulting is an underrated natural hazard in the region. Geological faulting is ongoing and largely beyond human influence to control. Geological fault movement is relentless and irreversible. Faults and salt domes are permanent features of the region and some have remained periodically active for a 100 million years or more. This periodic activity will probably continue for tens of millions of years.
9. A tectonic framework has been established, and the parameters identified for further development of risk assessment procedures with regard to faults and human habitation, as well as maintenance of fish and wildlife habitats and other natural system values and functions.

An understanding of fault processes and their impact on the landscape is important for engineering planning and design of coastal restoration that will be most effective. Until

recently the relationship between geological faulting and coastal land loss had been largely neglected by researchers, and by the coastal restoration community.

The matching of projected surface traces of known subsurface faults with surface fault traces in the coastal wetlands, however, moves “fault induced subsidence” from the realm of a hypothesis to reality. Surface expressions of faults do exist, their appearance and growth can be found and measured on aerial photographs, and vertical displacement can be measured directly from surface features (natural and man-made) and displacement of near-surface and subsurface beds.

REFERENCES CITED

- Adams, R. L. 1997. “Microbasin Analysis of South Louisiana: An Exploration Model, or Hutton and Lyell Were Wrong!” *Transactions of the Gulf Coast Association of Geological Societies*; 47: 1-12.
- Aminzadeh, F. and D. Connolly. 2002. “Looking for Gas Chimneys.” *AAPG Explorer*, Dec. 2002: 20-21.
- Barras, J. A., P. E. Bourgeois, and L. R. Handley. 1994. *Landloss in Coastal Louisiana 1956-90*. National Biological Survey, National Wetlands Research Center.
- Britsch, L. D. 2000. Digital File of Total Land Loss 1930s to 1990. Derived from Britsch, L. D. and J. B. Dunbar. 1996. *Land Loss in Coastal Louisiana*. Tech. Rept. GL-90-2. Dept. of the Army, U.S. Army Engineers, Waterways Experiment Station, Vicksburg, MS and U.S. Army Engineer District, New Orleans, LA. 7 maps.
- Britsch, L. D. 2001. Personal communication regarding data on thickness of Holocene deposits.
- Britsch, L. D. and E. B. Kemp, III. 1990. *Land Loss Rates: Mississippi River Deltaic Plain*, Tech. Rept. GL-90-2. Vicksburg, MS: Geotechnical Laboratory, Department of the Army, Waterways Experiment Station.
- Britsch, L. D. and J. B. Dunbar. 1996. *Land Loss in Coastal Louisiana*, Tech. Rept. GL-90-2. Vicksburg, MS: U.S. Army Engineers Waterways Experiment Station, and New Orleans, LA U.S. Army Engineers District. A series of 1:125,000 scale maps.
- Britsch, L. D., J. B. Dunbar, and E. B. Kemp, III. 1991. “Determination of Land Loss Rates in Coastal Louisiana.” *Transactions of the Gulf Coast Association of Geological Societies* 41: 56-57.
- Burdeau, C. 2002a. “Quake’s Energy Tosses LA Boats.” Baton Rouge, LA: *The Advocate*. 4 November 2002, sec. A, p. 10.
- Burdeau, C. 2002b. “Alaska Earthquake Makes Waves in Louisiana.” New Orleans, LA: *The Times-Picayune*, 4 November 2002, sec. A, p. 2.

- Central United States Earthquake Consortium. 2002
http://www.cusec.org/s_zones/nmsz/nmsz_home.html
- Chabreck, R. H. and G. Linscombe. 1978. Vegetative Type Map of the Louisiana Coastal Marshes. Baton Rouge, LA: Louisiana Wildlife and Fisheries Commission.
- Chabreck, R. H. and G. Linscombe. 1988. Vegetative Type Map of the Louisiana Coastal Marshes. Baton Rouge, LA: Louisiana Wildlife and Fisheries Commission.
- Chabreck, R. H., T. Joanen and A. W. Palmisano. 1968. Vegetative Type Map of the Louisiana Coastal Marshes. New Orleans, LA: Louisiana Wildlife and Fisheries Commission.
- Chief of Engineers, U.S. Army Corps of Engineers. 1952. *Annual Report to Congress of the Chief of Engineers, U. S. Army Corps of Engineers.*
- Coleman, J. M. 1976. *Deltas: Processes of Deposition and Models for Exploration.* Champaign, IL: Continuing Education Publication Co.
- Coleman, J. M., D. B. Prior and L. E. Garrison. 1980. "Subaqueous Sediment Instabilities in the Offshore Mississippi River Delta." Section I. *In: L. R. Handley, Compiler. Environmental Information on Hurricanes, Deep Water Technology, and Mississippi Delta Mudslides in the Gulf of Mexico.* New Orleans, LA: U.S. Department of the Interior, Bureau of Land Management, BLM Open File Report 80-02.
- Curtis, D. M., and E. B. Picou, Jr. 1978. "Gulf Coast Cenozoic: A Model for the Application of Stratigraphic Concepts to Exploration on Passive Margins." *Transactions of the Gulf Coast Association of Geological Societies* 28: 103 – 120.
- Diegel, F. A., J. F. Karlo, D. C. Schuster, R. C. Shoup, and P. R. Tauvers. 1995. "Cenozoic Structural Evolution and Tectono-Stratigraphic Framework of the Northern Gulf Coast Continental Margin." *In: M. P. A. Jackson, D. G. Roberts, and S. Snelson, eds. Salt Tectonics: A Global Perspective, American Association of Petroleum Geologists Memoir No. 65:* 109-151.
- DeLaune, R. D., J. A. Nyman and W. H. Patrick, Jr. 1994. "Peat Collapse, Ponding and Wetland Loss in a Rapidly Submerging Coastal Marsh." *Journal of Coastal Research* 19: 4: 1021-30.
- Dunbar, J. B., L. D. Britsch, and E. B. Kemp, III. 1992. *Land Loss Rates, Report 3, Louisiana Coastal Plain.* Tech. Rept. GL-90-2. Vicksburg, MS: U.S. Army Engineers Waterways Experiment Station.
- Fails, T. G. 1985. "Intimate Relationships-Growth Faulting and Diapirism in South Louisiana." abstract. *American Association of Petroleum Geologists Bulletin* 69: 254.

- Fails, T. G. 1990. "Variation in Salt Dome Faulting, Coastal Salt Basin." *Transactions of the Gulf Coast Association of Geological Societies* 40: 181-194.
- Fails, T. G. 1992. "Variation in Diapiric Structure Development and Productivity, Northern Gulf Coast Basin." *Transactions of the Gulf Coast Association of Geological Societies* 42: 135-150.
- Fails, T. G., G. D. O'Brien and J. A. Hartman. 1995. *Exploration and Exploitation of Coastal Salt Basin Diapiric Structures in the Lower Pliocene Through Eocene Trends: Geology and Techniques*. Houston Geological Society and the New Orleans Geological Society.
- Fisk, H. N. 1943. *Geological Investigation of Faulting at Vacherie, Louisiana*. Vicksburg, MS: U.S. Army Engineers Waterways Experiment Station.
- Fisk, H. N. 1944. *Geological Investigation of the Alluvial Valley of the Lower Mississippi River*. Vicksburg, MS: U. S. Army Corps of Engineers, Mississippi River Commission.
- Fisk, H. N. 1960. "Recent Mississippi River Sedimentation and Peat Accumulation." *Compte rendu du quatrieme congress pour l'avancement des etudes de stratigraphic et de geologie du Carbonifere*. Heerlen, The Netherlands: 187-199.
- Frazier, D. E. 1967. "Recent Deltaic Deposits of the Mississippi River: Their Development and Chronology." *Transactions of the Gulf Coast Association of Geological Societies* 17: 287-311.
- Frey M. G. and W. H. Grimes. 1970. "Bay Marchand-Timbalier Bay-Caillou Island Salt Complex, Louisiana." In M. T. Halbouty, ed. *Geology of Giant Petroleum Fields. American Association of Petroleum Geologists Memoir 14*: 277-291.
- Gagliano, S. M. 1979. *A Cultural Resources Survey of the Empire to the Gulf of Mexico Waterway*. Baton Rouge, LA: Coastal Environments, Inc. prepared for the New Orleans District Corps of Engineers.
- Gagliano, S. M. 1984. "Geoarchaeology of the Northern Gulf Shore." In: D. D. Davis, ed. *Perspectives of Gulf Coast Prehistory*. Gainesville, FL: University of Florida Press/Florida State Museum: 1-39.
- Gagliano, S. M. 1990. "Development Corridors in the Mississippi River Deltaic Plain." *Proceedings of the Association of State Floodplain Managers*. 14th Annual Conference. 11-15 June 1990. Asheville, NC.
- Gagliano, S. M. 1994. *An Environmental-Economic Blueprint for Restoring the Louisiana Coastal Zone: The State Plan*. Report of the Governor's Office of Coastal Activities, Science Advisory Panel Workshop. Baton Rouge, LA: The Governor's Office of Coastal Activities.

- Gagliano, S. M. 1999. "Faulting, Subsidence and Land Loss in Coastal Louisiana." *In: Louisiana Coastal Wetlands Conservation and Restoration Task Force and Wetlands Conservation and Restoration Authority. Coast 2050: Toward A Sustainable Coastal Louisiana, the Appendices, Appendix B-Technical Methods.* Baton Rouge, LA: Louisiana Department of Natural Resources: 21-72.
- Gagliano, S. M. 2000a. "Fault Movement and the 20th Century Transgression of the Mississippi River Deltaic Plain." abstract. *Proceedings of the American Association of Petroleum Geologists Annual Convention.* 16-19 April 2000. New Orleans: A51.
- Gagliano, S. M. 2000b. "Salt Marsh Die-Back and Fault Induced Subsidence in Coastal Louisiana: An Interim Report." Paper presented at the *Brown Marsh Conference* in Baton Rouge, LA. 18 August 2000.
- Gagliano, S. M. and D. W. Roberts. 1990. *Restoration and Conservation of the Terrebonne Parish, Louisiana Coastal Area.* Baton Rouge, LA: Coastal Environments, Inc.
- Gagliano, S. M., and J. L. van Beek. 1970. *Geological and Geomorphic Aspects of Deltaic Processes, Mississippi Delta System.* Hydrologic and Geologic Studies of Coastal Louisiana, Report 1. Baton Rouge, LA: Coastal Resources Unit, Center for Wetland Resources, Louisiana State University.
- Gagliano, S. M. and J. L. van Beek. 1973. "New Era for Mudlumps." *Water Spectrum.* Department of the Army, Corps of Engineers 5: 1: 25-31.
- Gagliano, S. M., K. J. Meyer-Arendt and K. M. Wicker. 1981. "Land Loss in the Mississippi River Deltaic Plain." *Transactions of the Gulf Coast Association of Geological Societies* 31: 295-300.
- Gagliano, S. M., K. M. Wicker, and K. Wiltenmuth. 2003. *Geological Characterization of Potential Receiving Areas for the Central and Eastern Terrebonne Basin Freshwater Delivery Project.* Baton Rouge, LA: Louisiana Department of Natural Resources.
- Gagliano, S. M. and R. A. Weinstein. 1979. "The Buras Mounds: A Lower Mississippi River Delta Mound Group, Plaquemines Parish, Louisiana." *In: Gagliano, S. M. 1979. A Cultural Resources Survey of the Empire to the Gulf of Mexico Waterway.* Baton Rouge, LA: Coastal Environments, Inc., prepared for the New Orleans District, Corps of Engineers.
- Hebert, Pete. Camp Owner and Sportsman, Bayou Farrand, Plaquemines Parish, Louisiana. Interview by Ed Fike, 13 August 2001.
- Holdahl, S. R. and N. L. Morrison. 1974. "Regional Investigations of Vertical Crustal Movement in the U.S. Using Precise Re-Levelings and Mareograph Data." *Technolphysics* 23: 373-390.

<http://www.cityofseattle.net/projectimpact/pages/piooverview/regionalhazzards/tsunami.htm>. 14 June 2002.

Humphris, C. C., Jr. 1979. "Salt Movement on Continental Slope, Northern Gulf of Mexico." *American Association of Petroleum Geologists Bulletin*; 63: 782-798.

Ingram, R. J. 1991. "Salt Tectonics." In: D. Goldthwaite, ed. *An Introduction to Gulf Coast Geology*. New Orleans, LA: New Orleans Geological Society: 31-60.

Kattenhorn, S. A. and D. D. Pollard. 2002. "Integrating 3-D Seismic Data, Field Analogs, and Mechanical Models in the Analysis of Segmented Normal Faults in the Wytch Farm Oil Field, Southern England, United Kingdom." *American Association of Petroleum Geologists Bulletin* 85: 7: 1183-1210.

Kolb, C. R., F. L. Smith, and R. C. Silva. 1975. *Pleistocene Sediments of the New Orleans-Lake Pontchartrain Area*. Technical Report S-75-6, Vicksburg, MS: Soils and Pavement Laboratory, U.S. Army Engineers Waterways Experiment Station.

Kolb, C. R. and J. R. Van Lopik. 1958. *Geology of the Mississippi River Deltaic Plain, Southeastern Louisiana*. Technical Report No. 3-483. Vicksburg, MS: U.S. Army Engineers Waterways Experiment Station.

Kuecher, G. J. "Geologic Framework and Consolidation Settlement Potential of the Lafourche Delta, Topstratum Valley Fill: Implications for Wetland Loss in Terrebonne and Lafourche Parishes, Louisiana." Ph.D. diss., Louisiana State University, Baton Rouge, 1994.

Kuecher, G. J., H. H. Roberts, M. D. Thompson, and I. Matthews. 2001. "Evidence of Active Growth Faulting in the Terrebonne Delta Plain, South Louisiana: Implications for Wetland Loss and the Vertical Migration of Petroleum." *Environmental Geosciences*; 8: 2: 77-94.

Kupfer, D. H. 1963. "Structure of Salt in Gulf Coast Salt Domes." In: *First Symposium on Salt*. Northern Ohio Geological Society: 104 – 123.

Kupfer, D. H. 1976. "Shear Zones in the Gulf Coast Salt Delineate Spines of Movement." *Transactions of the Gulf Coast Association of Geological Societies* 24: 197-209.

Kupfer, D. H. 1980. "Problems Associated With Anomalous Zones in Louisiana Salt Stocks, USA." In: A. H. Coogan, and L. Hauber, eds. *Fifth Symposium on Salt*, Northern Ohio Geological Society; 1: 119-134.

Kupfer, D. H. 1989. "Internal Kinematics of Salt Diapers: Discussion." *American Association of Petroleum Geologist Bulletin*: 73: 939-945.

- Lacaffine, J. 1964. "Earthquake's Effect Here is Explained." *Baton Rouge Morning Advocate*, 28 March 1964.
- Liro, L. M., 1992. "Distribution of Shallow Salt Structures, Lower Slope of the Northern Gulf of Mexico, USA." *Marine and Petroleum Geology* 9: 405-411.
- Lopez, J. A. 1991. "Origin of Lake Pontchartrain and the 1987 Irish Bayou Earthquake." *Gulf Coast Section of the Society of Economic Paleontologists and Mineralogists Foundation, 12th Annual Research Conference*: 103-110.
- Lopez, J. A., S. Penland and J. Williams. 1997. "Confirmation of Active Geologic Faults in Lake Pontchartrain in Southeast Louisiana." *Transactions of the Gulf Coast Association of Geological Societies, 47th Annual Convention*; 47: 299-303.
- Louisiana Coastal Wetlands Conservation and Restoration Task Force. 1993. *Coastal Wetlands Planning, Protection and Restoration Act: Louisiana Coastal Wetland Restoration Plan*. Baton Rouge, LA: Louisiana Department of Natural Resources,
- Louisiana Coastal Wetlands Conservation and Restoration Task Force and Wetlands Conservation and Restoration Authority. 1998. *Coast 2050: Toward A Sustainable Coastal Louisiana*. Baton Rouge, LA: Louisiana Department of Natural Resources.
- Louisiana Geographical Information System Computer Disk (LA GIS CD). 2000. A Digital Map of the State. Baton Rouge, LA: Louisiana State University, Department of Geography and Anthropology.
- Louisiana Geological Survey. 2001. *Earthquakes in Louisiana*. Public Information Series No. 7. Baton Rouge, LA: Louisiana Geological Survey.
- Martin, R. G. 1978. "Northern and Eastern Gulf of Mexico Continental Margin-Stratigraphic and Structural Framework." In A. H. Bouma and Others, eds. *Framework, Facies and Oil-Trapping Characteristics of the Upper Continental Margin*. Tulsa, OK: American Association of Petroleum Geologists. *Studies in Geology*. 7: 21-42.
- Martin, R. G. 1980. Distribution of Salt Structures in the Gulf of Mexico – Map and Descriptive Text: USGS Misc. Field Studies. Map Mf-1213.
- Martinez, J. D. 1971. "Environmental Significance of Salt." *American Association of Petroleum Geologists Bulletin* 55: 810-825.
- Martinez, J. D. 1991. "Salt Domes." *American Scientist* 79: 420-431.
- Martinez, J. D. and R. L. Thomas, eds. 1977. *Salt Dome Utilization and Environmental Considerations. Symposium Proceedings*. Baton Rouge, LA: Institute of Environmental Studies, Louisiana State University.

- McBride, B. C. 1998. "The Evolution of Allchthonous Salt along a Megaregional Profile Across the Northern Gulf of Mexico Basin." *American Association of Petroleum Geologists Bulletin* 82: 1037-1055.
- McBride, R. A. and M. R. Byrnes. 1997. "Regional Variations in Shore Response along Barrier Island Systems of the Mississippi River Delta Plain: Historical Change and Future Prediction." *Journal of Coastal Research* 13: 3: 628-653.
- McIntire, W. G. 1958. *Prehistoric Indian Settlements of the Changing Mississippi River Delta*. Coastal Studies Series, No.1. Baton Rouge, LA: Louisiana State University Press.
- Meade, R. H. 1995. "Setting: Geology, Hydrology, Sediments and Engineering of the Mississippi River." In: R. H. Meade, ed. *Contaminants in the Mississippi River 1987-1992*. U.S. Geological Survey Circular: Nov. 1133: 13-30.
- Meloy, D. U. and R. K. Zimmerman. 1997. *Potential Seismic Risk Associated With Louisiana Wrench Faulting*. Baton Rouge, LA: Louisiana Geological Survey. Open-File Series No. 97-01.
- Meyerhoff A. A. 1968. "Geology of Natural Gas in South Louisiana." In: Beebe, B. W. and Curtis, B., eds. *Natural Gases of North America American Association of Petroleum Geologists Memoir* 9: 376-581.
- Mississippi River Commission (MRC). 1913. Index Chart of the Mississippi River from the Mouth of the Ohio River to the Gulf of Mexico. Chart to Accompany the Mississippi River Commission Report Dated Nov. 21, 1913 on the Separation of the Red and Atchafalaya Rivers from the Mississippi River. House Doc. No. 841, 63rd Cong., 2nd Session.
- Morgan, J. P. 1961. "Genesis and Paleontology of the Mississippi River Mudlumps, Pt. I: Mudlumps at the Mouths of the Mississippi River." *Louisiana Department of Conservation, Geological Bulletin*: 35: 1-116. (Written 1951, Published 1961.)
- Morgan, J. P., J. M. Coleman, and S. M. Gagliano. 1963. *Mudlumps at the Mouth of South Pass, Mississippi River: Sedimentology, Paleontology, Structure, Origin and Relation to Deltaic Process*. Louisiana State University Studies, Coastal Series Number 10. Baton Rouge, LA: Louisiana State University.
- Morgan, J. P., J. M. Coleman, and S. M. Gagliano. 1968. "Mudlumps: Diapiric Structures in Mississippi Delta Sediments." In *Diapirism and Diapirs. American Association of Petroleum Geologists Memoir* No. 8: 145-161.
- Morton, R. A., N. A. Busteri, and M. Dennis Krobin. 2002. "Subsidence Rates and Associated Wetland Loss in South-Central Louisiana." *Transactions of the Gulf Coast Association of Geological Societies* 52: 767-778.

- Morton, R. A., N. A. Purcell, and R. Peterson. 2001a. "Field Evidence of Subsidence and Faulting Induced by Hydrocarbon Production in Coastal Southeast Texas." *Transactions of the Gulf Coast Association of Geological Societies* 51: 239-248.
- Morton, R. A., N. A. Purcell, and R. Peterson. 2001b. *Shallow Stratigraphic Evidence of Subsidence and Faulting Induced by Hydrocarbon Production in Coastal Southeast Texas*. Open File Report 01-274. St. Petersburg, FL: U. S. Geological Survey, Center for Coastal and Regional Marine Studies.
- Murray, G. E. 1960. "Geologic Framework of Gulf Coastal Province of United States." In: F. P. Shepard, F. B. Phleger, and T. H. Van Andel, eds. *Recent Sediments, Northwest Gulf of Mexico*. Tulsa, OK: American Association of Petroleum Geologists.
- Murray, G. E. 1961. *Geology of the Atlantic and Gulf Coastal Province of North America*. New York: Harper and Brothers Publishers.
- Nakashima, L. D. and L. M. Loudon. 1988. *Water Level Change, Sea Level Rise, Subsidence, and Coastal Structures in Louisiana*. Technical Report prepared for Engineering Research Center, U.S. Army Corps of Engineers, Vicksburg, MS. Baton Rouge, LA: Louisiana Geological Survey, Louisiana State University.
- Nyman, J. A., R. D. DeLaune, and W. H. Patrick, Jr. 1990. "Wetland Soil Information in the Rapidly Subsiding Mississippi River Deltaic Plain: Mineral and Organic Matter Relationships." *Estuarine Coastal and Shelf Science* 31: 57-69.
- O'Neil, T. 1949. *The Muskrat in the Louisiana Coastal Marshes: A Study of the Ecological, Geological, Biological, Tidal, and Climatic Factors Governing the Production and Management of the Muskrat Industry in Louisiana*. New Orleans, LA: Louisiana Department of Wildlife and Fisheries.
- Peel, F. J., C. J. H. Travis, and J. R. Hossack. 1995. "Genetic Structural Provinces and Salt Tectonics of the Cenozoic Offshore U.S. Gulf of Mexico: A Preliminary Analysis." In: M. P. A. Jackson, D. G. Roberts and S. Snelson, eds. *Salt Tectonics, A Global Perspective*. American Association of Petroleum Geologists Memoir 65: 153-175.
- Penland, S., A. Beall, and J. Kindinger, eds. 2001. *Environmental Atlas of the Lake Pontchartrain Basin*. U.S. Geological Survey Open-File Report 02-206. New Orleans, LA: prepared by Lake Pontchartrain Basin Foundation, University of New Orleans, U.S. Geological Survey, and U.S. Environmental Protection Agency.
- Penland, S., I. A. Mendelssohn, L. Wayne, and D. Britsch. 1996a. *Natural and Human Causes of Land Loss in Coastal Louisiana*. Summary of 29 May 1996 Workshop, Louisiana State University, Baton Rouge, LA. Sponsored by the Gas Research Institute, Argonne National Laboratory, U. S. Army Corps of Engineers and U.S. Geological Survey. Coastal Studies Institute and Wetland Biogeochemistry institute, Louisiana State University.

- Penland, S., I. A. Mendelssohn, L. Wayne, D. Britsch, M. R. Bynes, D. Reed, P. Wildey, S. J. Williams, and T. Williams. 1996b. *Natural and Human Causes of Land Loss in Coastal Louisiana*. Summary of 29 May 1996 Workshop, Louisiana State University, Baton Rouge, LA. Sponsored by the Gas Research Institute, Argonne National Laboratory, U.S. Army Corps of Engineers and U.S. Geological Survey. Published in conjunction with the 29 May 1996 Workshop, Louisiana State University. Portfolio of Maps entitled *Louisiana Coastal Land Loss Study*.
- Penland, S., K. E. Ramsey, R. A. McBride, J. T. Mestayer, and K. A. Westphal. 1988. *Relative Sea Level Rise and Delta Plain Development in the Terrebonne Parish Region*. Coastal Geology Tech. Rept. No. 4. Baton Rouge, LA: Louisiana Geological Survey.
- Penland, S., K. E. Ramsey, R. A. McBride, T. F. Moslow and K. A. Westphal. 1989. *Relative Sea Level Rise and Subsidence in Louisiana and the Gulf of Mexico*. Coastal Geology Tech. Rept. No. 3. Baton Rouge, LA: Louisiana Geological Survey.
- Penland, S., H. R. Roberts, A. Bailey, G. J. Kuecher, J. N. Suhayda, P. C. Connor, and K. E. Ramsey. 1994. "Geological Framework, Processes, and Rates of Subsidence in the Mississippi River Delta Plain." In: H. R. Roberts, Proj. Coord. Final Report *Critical Physical Processes of Wetland Loss 1988-1994*. Baton Rouge, LA: Louisiana State University. Funded by the U.S. Geological Survey: 7.1.1 – 7.1.51
- Pickford, P. J. and Other Seminar Participants. Compilers. N.D. Salt Tectonics Structural Geology Seminar. Seminar Notes. Presented by R. J. Ingram.
- Ramsey, K. E., and T. F. Moslow. 1987. "A Numerical Analysis of Subsidence and Sea Level Rise In Louisiana." In N. C. Kraus, ed. *Coastal Sediments '87: Proceedings of a Specialty Conference on Advances in Understanding of Coastal Sediment Processes*. New Orleans, LA. 12-14 May 1987. New York City, NY: American Society of Civil Engineers: 1673-1688.
- Reed, D. J., ed. 1995. *Status and Trends of Hydrologic Modification, Reduction in Sediment Availability, and Habitat Loss/Modification in the Barataria-Terrebonne Estuarine System*. BTNEP Publ. No. 20. Thibodaux, LA: Barataria-Terrebonne National Estuary Program.
- Roberts, H. H. 1985. *A Study of Sedimentation and Subsidence in the South-Central Coastal Plain of Louisiana*. Baton Rouge, LA: Coastal Studies Institute, Louisiana State University, prepared for New Orleans District, U.S. Army Corps of Engineers.
- Russell, R. J. 1940. "Quaternary History of Louisiana." *Bulletin of the Geological Society of America* 51: 1199-1234.
- Sabaté, R. W. 1968. "Pleistocene Oil and Gas in Louisiana." *Transactions of the Gulf Coast Association of Geological Societies* 18: 373-386.

- Salvador, A. 1987. "Late Triassic-Jurassic Paleogeography and Origin of Gulf of Mexico Basin." *American Association of Petroleum Geologists Bulletin* 71: 419-451.
- Salvador, A., ed. 1991. The Gulf of Mexico Basin. Geology of North America. Vol. J. Plate 2. *Geological Society of America Journal*.
- Sasser, C. E. 1994. *Vegetation Dynamics in Relation to Nutrients in Floating Marshes in Louisiana, USA*. Baton Rouge, LA: Center for Coastal, Energy, and Environmental Resources, Louisiana State University.
- Sasser, C. E., D. E. Evers, D. A. Fuller, J. G. Gosselink, R. Kesel, D. J. Reed, E. M. Swenson, and J. A. Nyman. 1995. "Vignette Studies: Local Case Studies of Wetland Loss." In: D. J. Reed, ed. *Status and Trends of Hydrologic Modification, Reduction in Sediment Availability, and Habitat Loss/Modification in the Barataria-Terrebonne Estuarine System*. BTNEP Publ. No. 20. Thibodaux, LA: Barataria-Terrebonne National Estuary Program.
- Saucier, R. T. 1963. *Recent Geomorphic History of the Pontchartrain Basin*. Coastal Studies Series No. 9. Baton Rouge, LA: Louisiana State University.
- Saucier, R. T. 1994. *Geomorphology and Quaternary Geologic History of the Lower Mississippi Valley*. vol. 1. Vicksburg, MS: U.S. Army Engineers Waterways Experiment Station.
- Spearing, D. 1995. *Roadside Geology of Louisiana*. Missoula, MN: Mountain Press Publishing Co.
- Stevenson, D. A. and R. P. McCulloh. 2001. *Earthquakes in Louisiana*. Louisiana Geological Survey, Public Information Series No. 7, Jun. 2001
- Stover, C. W., B. G. Reagor, and S. T. Algermissen. 1979. Seismicity Map of the State of Louisiana, Scale 1:1,000,000, Map Mf-1081a, U.S. Geological Survey.
- Stover, S. C., S. Ge, P. Weimer, and B. C. McBride. 2001. "The Effects of Salt Evolution, Structural Development, and Fault Propagation on Late Mesozoic-Cenezoic Oil Migration: A Two-Dimensional Fluid-Flow Study along a Megaregional Profile in the Northern Gulf of Mexico Basin." *American Association of Petroleum Geologists Bulletin* 85: 11.
- Stuart, E. 2002. "Stay Or Go? Island Residents Debate Relocation". Houma, LA: *The Courier*, 18 June 2002, sec. A, pp. 1, 9.
- Tectonic Map Committee, Gulf Coast Association of Petroleum Geologists, compilers and eds. 1972. Tectonic Map of the Gulf Coast Region, U.S.A. Published by Gulf Coast Association of Petroleum Geologists and American Association of Petroleum Geologists. Scale 1:1,000,000.

- The Times-Picayune. 2002. "America's Wetlands". Editorial, *The Times Picayune*, 27 August 2002, sec. B. p.4. New Orleans, LA.
- Troutman, A. 1956. *The Oil and Gas Fields of Southeast Louisiana*. Houston, TX: Five Star Oil Report, Inc.
- U.S. Geological Survey. 19 June 2002. National Earthquake Information Center
http://neic.usgs.gov/neis/eqlists/usa/1930_10_19.html
- U.S. Geological Survey. 20 June 2002. National Earthquake Information Center
http://neic.usgs.gov/neis/bulletin/neic_fnbk.html plates
- U.S. Geological Survey. 19 June 2002. Earthquake History of Louisiana.
http://neic.usgs.gov/neis/states/louisiana/louisiana_history.html)
- U.S. Geological Survey, National Wetlands Research Center, Baton Rouge Project Office. (USGS, NWRs, BRPO). 1996a. Digital Files of 1956 and 1978 Habitat Maps Digitized from 7.5-Min Habitat Maps. prepared by Wicker et al. 1980. The Mississippi Deltaic Plain Region Habitat Mapping Study. Slidell, LA: U.S. Fish and Wildlife Service. FWS/OBS-79/07.
- U.S. Geological Survey, National Wetlands Research Center, Baton Rouge Project Office. 1996b. Digital Files of 1988/90 Habitat Maps Digitized from 7.5-Min Habitat Maps prepared by National Wetlands Inventory. 1988. St. Petersburg, FL.
- U.S. Geological Survey, National Wetlands Research Center, Lafayette. 2001. Louisiana Coastal Marshes-Vegetation Type Maps: 1949, 1968, 1978, 1988, 1997, and 2001. Lafayette, LA: Digital Data.
- Uzee, P. D., ed. 1985. *The Lafourche Country: The People and the Land*. Lafayette LA: Center for Louisiana Studies, University of Southwestern Louisiana.
- van Beek, J. L., P. C. Howard, K. J. Meyer-Arendt, and S. M. Gagliano. 1986. *Long-Term Management and Protection of Plaquemines Parish*. Baton Rouge, LA: Coastal Environments, Inc.
- Wallace, W. E., Jr. 1957. Fault Map of South Louisiana. *Transactions of the Gulf Coast Association of Geological Societies* 7: 240.
- Wallace, W. E., Jr. 1962. Fault Map of South Louisiana. *Transactions of the Gulf Coast Association of Geological Societies* 12: 194.
- Wallace, W. E., Jr. 1966. Fault and Salt Dome Map of South Louisiana. Published by the Gulf Coast Association of Geological Societies.
- Weinstein, R. A. and S. M. Gagliano. 1985. "The Shifting Deltaic Coast of the Lafourche Country and Its Prehistoric Settlement." In P. D. Uzee, ed. *The Lafourche Country: The People and the Land*. Lafayette, LA: Center for Louisiana Studies, University of Southwestern Louisiana, Lafayette.

- West, D. B. 1989. "Model for Salt Deformation on Deep Margin of Central Gulf of Mexico Basin." *American Association of Petroleum Geologists Bulletin* 3: 12: 1472-1482.
- White, W. A. and R. A. Morton. 1997. Wetland Losses Related to Fault Movement and Hydrocarbon Production, Southeastern Texas Coast: *Journal of Coastal Research* 13: 1305-1320.
- White, W. A. and T. A. Tremblay. 1995. Submergence of Wetlands as a Result of Human-Induced Subsidence and Faulting Along the Upper Texas Gulf Coast. *Journal of Coastal Research* 11: 3: 788-807.
- Wigley, T. M. and C. S. B. Raper. 1992. Implications for Climate and Sea Level of Revised IPCC Emission Scenarios. *Nature* 357: 293-300.
- Williams, S. J., S. Penland and A. H. Sallenger, Jr., eds. 1992. *Louisiana Barrier Island Erosion Study: Atlas of Shoreline Changes in Louisiana from 1853 to 1989*. Prepared by the U.S. Geological Survey in cooperation with the Louisiana Geological Survey.
- Winker, C. D. 1982. "Clastic Shelf Margins of the Post-Comanchean Gulf of Mexico: Implications for Deep-Water Sedimentation." Gulf Coast Section, *Society of Economic Paleontologists and Mineralogists, 5th Annual. Research Conference: Program and Abstracts*: 109-117.
- Worzel, J. L., and J. S. Watkins. 1973. "Evolution of the Northern Gulf Coast Deducted from Geophysical Data." *Transactions of the Gulf Coast Association of Geological Societies* 23: 84-91.
- Zilkoski, D. B., and S. M. Reese, Jr. 1986. *Subsidence in the Vicinity of New Orleans as Indicated by Analysis of Geodetic Leveling Data*. NOAA Technical Report NOS 120 NGS 38. U.S. Department of Commerce, National Oceanic and Atmospheric Administration, National Ocean Service: 61.

APPENDIX A. PREVIOUS RESEARCH

This study builds upon a foundation of more than 100 years of geological research conducted in the region. The century long exploration for, and production of oil and gas in the Gulf Coast Salt Basin has produced a vast amount of published and unpublished information regarding the geology of this basin. The Gulf Basin is one of the most intensely explored and most thoroughly known geological provinces on earth. Fewer publications pertain to surface effects of faults, but this topic has not been completely ignored. The list of contributors is long; however, the following works were found to be particularly relevant to the present study.

R. L. Adams (1997) investigated the relationships among the basement, salt bodies and decollement surfaces and the listric character of growth faults. He developed a section through the basin based on deep seismic, gravity and well data.

Louis D. Britsch, Joseph B. Dunbar and E. Burton Kemp, III collaborated to provide definitive data documenting sequential land loss in coastal Louisiana for four time periods between the 1930s and 1990 (Britsch and Kemp 1990; Britsch and Dunbar 1996; Britsch, Dunbar and Kemp 1991). Britsch and Kemp have developed contour maps of the depth to the Pleistocene Holocene contact. Britsch was also an active participant in the classification, mapping and measurement of the causes of land loss in coastal Louisiana with Penland and other colleagues (Penland et al. 1996a, 1996b).

James M. Coleman and his colleagues have been active in neotectonic studies in the vicinity of distributary outlets. He was also a participant in mudlump research (Morgan 1968) which produced a model for clay diapirs induced by distributary mouth sediment loading and later studies of sea floor slumps, faults and related phenomena in the area of the Mississippi River delta front (Coleman 1980).

Doris M. Curtis and Ed B. Picou (1978) developed and described a fundamental model for the northern Gulf region concerning the relationship between pods of deltaic sediment (depocenters) and growth faults.

Thomas G. Fails (1985, 1990, 1992 and Fails, O'Brien and Hartman 1995) has been a master researcher and synthesizer of salt and fault movement in the Gulf Coast Salt Basin.

Harold N. Fisk (1943, 1944), in his still monumental work on the geology and geomorphology of the Mississippi River Valley, placed considerable emphasis on the role of tectonics in directing the course of rivers and creating and shaping lakes. He investigated fault and fracture patterns, topographic expressions of faulting, isostatic adjustment and provided one of the few documentations of a fault event in the region.

Sherwood M. Gagliano, and his colleague Johannes L. van Beek first identified and quantified the land loss problem in coastal Louisiana in 1970 and developed the methodology for its study (Gagliano and van Beek 1970; Gagliano, Meyer-Arendt, and Wicker 1981). Gagliano was also a participant in mudlump research (Morgan, Coleman,

and. Gagliano, 1968; Gagliano and van Beek 1973). More recently, Gagliano has studied the relationship among faulting, subsidence and land loss in coastal Louisiana that provides a framework for the present study (Gagliano 1994, 1999, 2000a and 2000b).

Charles R. Kolb and Jack L. van Lopik (1958) investigated the nature of sediments in the Holocene section of coastal Louisiana and the role of compaction and faulting. C. R. Kolb, F. L. Smith and R. C. Silva (1975) identified Pleistocene and Holocene faults under Lake Pontchartrain using data derived from borings and high-resolution imagery.

Donald H. Kupfer (1963, 1976, 1980, 1989) made major contributions to the nature of salt movement within domes of the Gulf Coast Salt Basin and even larger contributions to teaching structural geology to several generations of Louisiana State University geology students.

Gerald J. Kuecher (1994) and his co-authors (Kuecher et al. 2001) made breakthrough contributions in establishing relationships between movement along the Golden Meadow and Lake Hatch regional growth faults in the coastal zone and land loss. They used seismic data to verify the tie between apparent surface fault scarps and subsurface fault planes and also presented evidence for upward saltwater movement along South Louisiana faults.

John A. Lopez and his co-authors documented neotectonic fault activity along the extension of the Baton Rouge Fault Zone in the Lake Pontchartrain area (Lopez 1991; Lopez et al. 1997) using measurements on bridge displacement, high-resolution seismic data, and historic earthquake reports.

Joseph D. Martinez (1971, 1977, 1991) devoted much of his professional career to the study of salt and salt domes. He published widely on the environmental significance of salt and the nature and utilization of salt domes.

B. C. McBride (1998) developed a megaregional cross-section through the Gulf Coast Salt Basin extending from the Louisiana–Mississippi state boundary to the Abyssal Plain. The section was constructed from seismic data and deep well borings and is a true image of the stratification and structure within the basin. S. C. Stover et al. (2001) have used this section to unpeel the depositional and structural history of the basin and to model the movement of salt.

James P. Morgan (1951, 1961) conducted the first definitive work on mudlumps at the outlets of the Mississippi River. With his students, he further evaluated the folds, faults and mud/gas vents that are associated with mudlump development (Morgan et al. 1963, 1968).

Robert Morton is the director of a U.S. Geological Survey project that was conducted concurrently with the present study. Morton and his colleagues have reported field evidence of faulting induced by hydrocarbon production in coastal southeast Texas (Morton et al. 2001a and 2001b). The Morton led team also has developed apparent correlations between oil and gas production in individual fields in the Terrebonne delta area of south Louisiana and subsidence and land loss (Morton et al. 2002).

Grover Murray was a great synthesizer of the stratigraphy and structural geology of the Gulf Coast Region. He provided easy to understand maps and cross-sections of the Gulf Coast Salt Basin (Murray 1960, 1961).

F. J. Peele and his colleagues identified and defined linked structural systems and driving processes in the northern Gulf. They showed that the extensional zone of the Eastern Province underlies southeastern Louisiana (Peele et al. 1995).

Shea Penland and his students and associates have been at the forefront of research into the relationships between subsidence and land loss in coastal Louisiana. Their early work on RSL rise and delta development (Penland et al. 1988; Penland et al. 1989) used tide gauge measurements, sequential measurement of benchmarkss and radiocarbon dates of buried organic material to investigate the components of RSL rise and established that rates of sea level rise varied in time and space across the Northern Gulf Coast Region, and in South Louisiana, in particular. This work established an apparent cause and effect relationship between RSL rise and coastal wetland loss and identified submergence as a contributing factor to a large part of land loss. In another phase of research, Penland and associates (Penland et al. 1996a; Penland et al. 1996b) classified, mapped and measured natural and human causes of land loss in coastal Louisiana. An important conclusion of their research was that 56 percent of the total land loss in the Deltaic Plain was due to submergence of land. An examination of their maps and tables reveals that 49 to 53 percent of this submergence may be related to fault related subsidence.

Robert W. Sabaté (1968) compiled a contour map of the base of the Pleistocene in South Louisiana and identified faults and salt domes that were active across this well defined contact. His work demonstrated the continuity of fault and salt dome movement during the Pleistocene period, the most active faults and salt domes and the amount of cumulative displacement on some faults since the Pleistocene.

Roger T. Saucier was the successor of Harold Fisk as the dean of Mississippi River Valley Quaternary geology research. In his early work on the geomorphology of the Pontchartrain Basin, Saucier (1963) elaborated on the structural control of landforms that had been proposed by Fisk. Saucier's (1994) comprehensive update of Mississippi River Valley geology and geomorphology further emphasizes the strong relationship between structure and landforms and summarizes research related to the evidence for surface effects of faulting.

Darwin Spearing (1995) wrote a very authoritative, yet readable, understandable and accessible book on the *Roadside Geology of Louisiana*. He explains the geological history and processes, including fault and salt movement, operating in coastal Louisiana in simplified terms and with simplified drawings.

W. E. Wallace, Jr. (1957, 1962, 1966) used subsurface fault and salt dome data from individual surveys, wells and oil and gas fields and information from a host of petroleum geologists to construct the *Fault and Salt Dome Map of South Louisiana*. He is identified as editor of the map. The map was "peer reviewed" by members of the New Orleans Geological Society. Copies of the original 1966 map were reproduced in limited quantity

at a scale of 1:250,000. Although additional faults and salt domes have been found and mapped since the 1966 edition was published, Wallace's map has proven to be an accurate and basic tool for the study of tectonic features of South Louisiana.

W. A. White and T. A. Tremblay (1995) demonstrated the relationship between the submergence of wetlands and resultant land loss and fault-induced subsidence resulting from fluid withdrawal along the Upper Texas Gulf Coast.